Damping of Electromechanical Oscillations Using Power System Stabilizers

Prepared by: Shaheen Sooleman Ahmed

Prepared for: The Department of Electrical and Electronic Engineering, University of Cape Town, South Africa

Supervisor: Professor Alexander Petroianu

15 April 1995

Thesis prepared in fulfillment of the requirements for the Degree of Ph.D. in Electrical and Electronic Engineering, Power Systems.

Acknowledgments

I wish to acknowledge the contribution of the following people to the research effort reported in the thesis:

- Professor Alex Petroianu for his guidance, support and patience throughout the long years of undergraduate and postgraduate research.

- Associate Professor Martin Braae for his valuable suggestions and criticisms throughout the Ph.D. research.

- Professor Edmund Handschin and his colleagues at the University of Dortmund for the assistance during my visit.

- Professor Chen-Ching Liu from the University of Washington, Seattle for his guidance and assistance during my stay as a visiting scholar.

- My family and friends for their constant encouragement and support.

Terms of Reference

This thesis originated from low frequency electromechanical oscillations experienced on the Eskom network in the mid 1980's. The weakly damped oscillations were especially pronounced during the peak loading periods but occurred even under light loading conditions. However, the oscillation frequencies of the electromechanical modes changed substantially as the loading conditions changed.

The University of Cape Town (UCT) was approached to investigate the origin of these oscillations as well as to develop techniques for damping the oscillations over a wide range of operating conditions. The idea proposed by Eskom was to investigate the possibility of detuning of the Automatic Voltage Regulators (AVR) for enhancing the small signal stability margin. However, in the early stages of the research, we found that detuning the AVR significantly deteriorates the transient stability margin of the Eskom network. Consequently, the research progressed to an investigation of supplementary excitation control using Power System Stabilizers (PSS). The results of the research on the use of PSS are contained in this thesis.

The Ph.D. thesis was commissioned by Professor Alexander Petroianu of the Department of Electrical Engineering, UCT in March 1992. His specific instructions were:

(1) To address the problems associated with the damping of electromechanical oscillations using PSS, namely determining the optimal locations of the PSS, determination of the control structure of the PSS and the design of robust PSS.

(2) To develop theoretical foundations for addressing these problems. In this respect much of the value of the thesis should lie in the theoretical development. The focus of the thesis should not be detailed implementation of the methods developed. As such, the methods developed in the thesis should form a sound foundation for more detailed investigation and implementation in the future.

(3) To attempt to formulate the advances of modern control theory in a power systems framework. In doing so, the value of using advanced control techniques for control of power system can be assessed.

Synopsis

This thesis deals with the damping of electromechanical oscillations using Power System Stabilizers (PSS). The thesis focuses on three problems associated with the damping of these oscillations, namely the determination of the optimal locations of the PSS, the determination of the best control structure of the PSS and the design of robust PSS.

We develop two new methods for determining the optimal locations of the PSS. These two methods are based on Total Modified Coupling Factors (TMC) and optimization by Simulated Annealing (SA). The TMC is a measure of the damping influence of each machine pair on several power system modes. The TMC incorporates the effect of the performance and the type of excitation system of the generator. The method based on TMC is tested on a nine-bus benchmark network. In the method based on SA, we formulate the PSS placement problem as a discrete nonlinear optimization problem. The objective function corresponds to the damping of the electromechanical modes of the system. In this method, the placement is performed simultaneously for all PSS. Using SA, we obtain a placement scheme which guarantees that the undesired poles can be controlled with finite control energy. As a result of the optimization formulation, the method based on SA is computationally more intensive than the method based on TMC. We demonstrate the method based on SA on two networks namely, a seven-bus network and a 35-bus equivalent of the Eskom network.

The problem of determining the control structure for damping of the electromechanical oscillations is composed of three aspects namely, the *type of feedback*, the *type of signal* and the *type of control.*

The *type of feedback* investigates the use of State Feedback and Output Feedback. We present a new method of determining the parameters of a fixed structure PSS by transforming the Dynamic Output Feedback problem into a Static Output Feedback problem.

The *type of signal* refers to the determination of the best output signals that are to be used for damping of the electromechanical oscillations. We develop two new methods for determining the best output signals. These methods are based on two measures of the contribution of the electromechanical oscillations to the outputs. The first measure, the *Centralized Modal Observer Measure (CMOM),* is based on the (centralized) observability of the electromechanical modes. The *CMOM* requires only the calculation of right and left eigenvectors and is therefore not computationally intensive. However, the *CMOM* does not take into account the existence of fixed modes in a system under decentralized control. The second measure, the *Decentralized Modal Observer Measure (DMOM),* takes into account the existence of decentralized fixed modes. The DMOM is based on the (decentralized) observability of the electromechanical modes. The methods based on CMOM and DMOM are tested on a seven-bus benchmark network.

The *type of control* investigates the use of centralized, decentralized and hierarchical control for damping of the electromechanical oscillations. We develop a new approach for designing decentralized controllers. For this approach, we derive new sufficient conditions for ensuring that the system under decentralized control is globally stable. In addition, we present a novel approach for the hierarchical control of power systems. For this approach, we derive new sufficient conditions for ensuring that the time-varying power system remains globally stable. We also propose that these conditions be incorporated in the dynamic security assessment of the power system.

The problem of designing robust PSS is addressed using two approaches. In the first approach, we develop methods of designing robust supplementary excitation controllers with structures which are different from the those of existing PSS. In the second approach, we develop methods to obtain robust tuning procedures for the existing PSS.

In the *first approach,* we describe a new procedure for designing suboptimal H_∞-based controllers for damping electromechanical oscillations. The stability of the interconnected power system is ensured by incorporating global stability constraints in the design procedure. These constraints are used in a new two-stage method for designing decentralized controllers.

In order to ensure low order controllers, the method of balanced truncation is used to reduce the order of the open loop plant. We make use of an existing Dynamic Output Feedback Ricatti-based method to synthesize the H_∞ controllers. We apply a bilinear transformation to improve the damping of the electromechanical oscillations. The design procedure is tested on a nine-bus benchmark network.

In the *second approach,* we address the problem of determining the parameters of fixed structure PSS. We propose two new methods to obtain the parameters of the PSS namely, *tuning the PSS using numerical optimization* and *tuning the PSS using Static Output Feedback.* The tuning by numerical optimization uses Sequential Quadratic Programming (SQP) to obtain the parameters of the PSS. The tuning by Static Output Feedback uses an existing Static Output Feedback control algorithm to obtain the static gain matrix. The method of tuning by numerical optimization is tested on a SMIB system.

We recommend that, for future work, the design of robust PSS using an H_2 objective function with an H_∞ constraint be investigated.

Table of Contents

List of Illustrations

Chapter 3

Chapter 4

Chapter 5

Appendix A

Appendix B

Appendix C

Appendix F

Appendix G

Appendix H

List of Tables

Appendix F

Appendix G

Appendix H

Nomenclature

The following is a list of the main symbols and acronyms used in the thesis. The symbols have been appropriately defined where they were used to denote different concepts.

ΔP_{acc}	Accelerating Power Deviation
ARE	Algebraic Ricatti Equation
AVR	Automatic Voltage Regulator(s)
$card(\cdot)$	Cardinality of $(\cdot)$
$CMOM$	Centralized Modal Observer Measure
$\mathbf{C}$	Complex Field
$CS(i)$	Configuration set element i
CPSS	Conventional Power System Stabilizer(s)
P	Controllability Grammian
$\xi(A,B)$	Controllability matrix of the pair (A,B)
C_{ij}	Coupling Factor between machines i and j
$T_{d0}^{'}$	d-axis transient open circuit time constant
$T_{d0}^{''}$	d-axis subtransient open circuit time constant
$DMOM$	Decentralized Modal Observer Measure
$\det(\cdot)$	Determinant of $(\cdot)$
$diag[k_1 \quad \ldots \quad k_n]$	Diagonal matrix with $k_1,\ldots.k_n$ on diagonal
$\lambda(\cdot)$	Eigenvalues of $(\cdot)$
ΔP_{el}	Electrical power deviation
Eskom	Electricity Supply Commission (South Africa)
$E[\cdot]$	Expectation value of $[\cdot]$
P_{mech}	Generator Mechanical Power
ΔV_{ref}	Generator reference voltage deviation
ΔV_T	Generator terminal Voltage deviation
$H_\infty(\cdot)$	H infinity norm of the system $(\cdot)$

σ^H	Hankel singular values
I	Identity matrix
$\|\cdot\|_\infty$	Infinity norm
$\bigcap_k (\cdot)$	Intersection of $(\cdot)$ of k
LTI	Linear time-invariant
s	Laplace operator $\frac{d}{dt}$
X_l	Leakage reactance
$V(x)$	Lyapunov Function
D	Machine damping
H	Machine inertia
$\Delta\delta$	Machine rotor angle deviation
S(1.0)	Machine Saturation at 1.0 p.u. voltage
S(1.2)	Machine Saturation at 1.2 p.u. voltage
$\Delta\omega$	Machine speed deviation
MIMO	Multi-input, multi-output
J	Objective Function
Q	Observability Grammian
$\vartheta(A,C)$	Observability matrix of the pair (A,C)
$\|\cdot\|_p$	p-norm
PF_i	Penalty Factor of Machine i
PSS/E	Power System Simulator for Engineers
PSS	Power System Stabilizer(s)
p.u.	per unit
T''_{q0}	q-axis subtransient open circuit time constant
R	Real Field
$\mathrm{Re}(\cdot)$	Real part of the complex number $(\cdot)$
RMS	Root Mean Square
$\mathrm{Im}(\cdot)$	Imgaginary part of the complex number $(\cdot)$
SQP	Sequential Quadratic Programming

SA	Simulated Annealing
SISO	Single-input, single-output
SMIB	Single machine infinite bus
$\sigma(\cdot)$	Singular values of $(\cdot)$
$\rho(\cdot)$	Spectral radius of $(\cdot)$
$\sup_x(\cdot)$	Supremum of $(\cdot)$ over x
TC_{ij}	Total Coupling Factor between machines i and j
TMC	Total Modified Coupling Factors
X_q''	Unsataurated q-axis subtransient reactance
X_d	Unsaturated d-axis synchronous reactance
X_d'	Unsaturated d-axis transient reactance
X_d''	Unsaturated d-axis subtransient reactance
X_q	Unsaturated q-axis synchronous time constant

Preliminaries

In this section, we present definitions and brief descriptions of concepts that will be required in the thesis. Some of the material in this section may be unfamiliar to power systems engineers since it is in the domain of the control theorist. Nevertheless, these concepts form the foundations of the methods developed in subsequent chapters and are essential for understanding of the thesis. For more details, the references at the end of the section should be consulted.

The following is an outline of the *Preliminaries*:

A. State Space Description [1]

Consider a linear time invariant system (LTI) system of finite dimension with multiple inputs and multiple outputs.

Assume that the system is under centralized control i.e. all the control signals are available for feedback to a single controller. The state space description of the system can be expressed as follows:

$$\begin{aligned} \dot{x} &= Ax + Bu \\ y &= Cx + Du \end{aligned} \tag{A1}$$

where:

$x \in R^n$ are the system states, $u \in R^m$ are the system inputs, $y \in R^p$ are the system outputs and A, B, C and D are constant matrices of appropriate dimensions.

Assume that the system is under decentralized control i.e. only local control signals are available to each controller. The state space description of the system can be expressed as follows:

$$S \triangleq \{S_i\} \triangleq \left\{ \begin{aligned} \dot{x}_i &= A_{ii}x_i + \sum_{j=i}^{m} A_{ij}x_j + B_i u_i \\ y_i &= C_i x + D_i u_i \end{aligned} \right\} \tag{A2}$$

or equivalently,

$$S \triangleq \{S_i\} \triangleq \left\{ \begin{aligned} \dot{x}_i &= A_i x + B_i u_i \\ y_i &= C_i x + D_i u_i \end{aligned} \right\} \tag{A3}$$

where:

$x_i \in R^{n_i}$ and $u_i \in R^{m_i}$ are the state and input vectors respectively corresponding to subsystem S_i of system S

x is the state vector of system S

$y_i \in R^{p_i}$ is the output vector

$A_{ii} \in R^{n_i \times n_i}$ is the square diagonal block i of the nominal plant A matrix, which relates $\dot{x}_i$ to x_i

$A_{ij} \in R^{n_j \times n_j}$ is the off-diagonal block (i,j) of the nominal plant A matrix, which relates $\dot{x}_i$ to x_j

$B_i \in R^{n_i \times m_i}$ is the input coefficient vector

$C_i \in R^{p_i \times n_i}$ is a constant matrix relating system output y_i to states x

$D_i \in R^{p_i \times m_i}$ is the direct feedthrough term relating output y_i to input u_i

n_i is the number of states in vector x_i and $\sum_{i=1}^{m} n_i = n$

p_i is the number of outputs of subsystem S_i

m_i is the number of inputs of subsystem S_i

Next we discuss some properties of the systems described by these state space equations.

B. Eigenstructure [1]

Eigenstructure refers to the properties of the system associated with its eigenvalues and eigenvectors. The eigenvalues of A are the roots of the characteristic polynomial $\det(sI - A)$. Let $\lambda_i = \sigma_i + j\omega_i$ be an eigenvalue of A. If $\mathrm{Re}(\lambda_i) > 0$ for any $i = 1,\ldots n$, the system is unstable. If $\mathrm{Re}(\lambda_i) < 0$ for all $i = 1,\ldots n$, the system is said to be asymptotically stable. The system is marginally stable if $\mathrm{Re}(\lambda_i) = 0$ for any $i = 1,\ldots n$. The damping ζ_i of eigenvalue λ_i is defined as:

$$\zeta_i = \frac{-\sigma_i}{\sqrt{\sigma_i^2 + \omega_i^2}}. \qquad \text{(B1)}$$

The nonzero vector v_i such that $Av_i = \lambda_i v_i$ is called the right eigenvector of mode λ_i. The right eigenvector v_i gives the relative activity of the states when λ_i is excited. The left eigenvector of λ_i is defined as the nonzero vector w_i such that $w_i^T A = \lambda_i w_i^T$. The left eigenvector weighs the contribution of the state variables in mode λ_i. The left and right eigenvectors can be used for determining which state variables contribute most to a particular mode. The problem in using these vectors individually for determining state contribution to the mode is that the elements of eigenvectors are dependent on units and scaling.

In order to solve this problem, the Participation Matrix P is defined as follows:

$$P = \begin{bmatrix} p_1 & p_2 & \cdots & p_n \end{bmatrix} \tag{B2}$$

where

$$p_h = \begin{bmatrix} v_{1h}w_{h1} \\ v_{2h}w_{h2} \\ \vdots \\ v_{nh}w_{hn} \end{bmatrix}$$

v_{kh} is the k*th* element of the right eigenvector v_h

w_{hk} is the k*th* element of the left eigenvector w_h

$v_{kh}\, w_{hk}$ is the participation factor

p_h is the participation vector corresponding to mode h

h is the mode of interest

The participation factor combines the right and left eigenvector to obtain a scale-free measure of the relative participation of each state to the associated mode.

C. Transmission Zeros [2]

The transmission zeros of a multi-input, multi-output system is defined as the complex frequencies z_i such that:

$$Rank\begin{bmatrix} z_i I - A & -B \\ C & D \end{bmatrix} < Min(n+m, n+p) \tag{C1}$$

For a square system i.e. number of inputs m equals the number of outputs p, the transmission zeros z_i can be determined from the following:

$$Det\begin{bmatrix} z_i I - A & -B \\ C & D \end{bmatrix} = 0. \tag{C2}$$

If $\mathrm{Re}(z_i) < 0$ then z_i is called a *minimum-phase zero.* Minimum-phase zeros pose no problems in control design.

If $\mathrm{Re}(z_i) \geq 0$ then z_i is called a *non-minimum-phase zero.* The control bandwidth (phase and gain margin) of the closed loop system is limited by non-minimum-phase zeros. This poses problems in control design.

D. Singular Value Decomposition [3]

Let $A \in \mathbf{C}^{m \times n}$ be a matrix. Then there always exists unitary matrices $U \in \mathbf{C}^{m \times m}$ and $V \in \mathbf{C}^{n \times n}$ such that:

$$A = U \sum V^H \tag{D1}$$

where:

$$\sum = \begin{bmatrix} \sigma_1 & 0 & \cdots & 0 & 0 & \cdots & 0 \\ 0 & \sigma_2 & \cdots & 0 & 0 & 0 & 0 \\ \vdots & \cdots & \cdots & \cdots & \cdots & \cdots & \vdots \\ 0 & 0 & \sigma_m & 0 & 0 & 0 & 0 \end{bmatrix} \text{ if } m \le n$$

or

$$\sum = \begin{bmatrix} \sigma_1 & 0 & \cdots & 0 \\ 0 & \sigma_2 & \cdots & 0 \\ \cdots & \cdots & \cdots & \\ 0 & 0 & \cdots & \sigma_n \\ 0 & 0 & \cdots & 0 \\ \cdots & \cdots & \cdots & \cdots \\ 0 & 0 & \cdots & 0 \end{bmatrix} \text{ if } n \le m$$

Let $U = \begin{bmatrix} u_1 & u_2 & \ldots & u_m \end{bmatrix}$ and $V = \begin{bmatrix} v_1 & v_2 & \ldots & v_n \end{bmatrix}$

We define the diagonal elements of $\sum$ are the singular values of A. The singular values are arranged in decreasing order i.e. $\sigma_1 \ge \sigma_2 \ge \ldots \sigma_p \ge 0$ where $p = \min(m,n)$. The minimum singular value gives a measure of how close the matrix is to singularity. The vectors u_i $(i = 1..m)$ and v_i $(i = 1..n)$ are the left and right singular vectors of A respectively.

E. System Controllability [1]

A system is controllable if it is possible to reach any state $x(t_f)$ at time t_f from an initial state x(0) using a control input function u(t) for $0 \le t \le t_f$. This is a property that relates the system inputs u(t) to the system states $x(t)$. A system is said to be stabilizable if all uncontrollable modes are stable.

We present three ways to check whether a system is controllable or not; namely *Controllability Matrix, Modal Decomposition* and *Controllability Grammian.*

E.1 Controllability Matrix

The system given by (A1) is said to be *completely controllable* or equivalently, the pair (A,B) is *completely controllable* if and only if the rank of the *controllability matrix* is n i.e.:

$$rank(\xi(A,B)) = n \qquad \text{(E1)}$$

where $\xi(A,B) = \begin{bmatrix} B & AB & A^2B & \cdots & A^{n-1}B \end{bmatrix}_{n \times nm}$ is the controllability matrix of the pair (A,B).

Thus we can check if a system is controllable or not by determining the rank of the controllability matrix. If the $rank(\xi(A,B)) = n$ then the system is completely controllable otherwise it is not completely controllable. If $rank(\xi(A,B)) = q, \quad q \le n$, then only a q-dimensional subspace of the system is completely controllable, the rest of the system being uncontrollable.

This method only provides information about whether a system is controllable or not. It does not provide information about which *modes* of the system are controllable or uncontrollable.

E.2 Modal Decomposition

The concepts of controllability can be formulated in the *modal canonical form.* In this form, the system described by (A1) can be expressed so that the transformed states are completely decoupled from each other. This can be achieved by applying a coordinate transformation to (A1) i.e.:

let $x = Tz$

where T is the matrix consisting of the eigenvectors

z is the vector of the transformed modal canonical coordinates.

Thus, in modal canonical form, system (A1) can be expressed as:

$$\begin{aligned} \dot{z} &= \Lambda z + T^{-1}Bu \\ y &= CTz + Du \end{aligned} \qquad \text{(E2)}$$

where:

$$\Lambda = diag[\lambda_1 \quad \lambda_2 \quad \cdots \quad \lambda_n]$$

Mode i is said to be uncontrollable if the i*th* row of $T^{-1}B$ denoted by $(T^{-1}B)_i$ is a row of zeros. Thus, using the method of modal decomposition, it is possible to determine directly which *modes* of the system are controllable or uncontrollable.

E.3 Controllability Grammian

The Controllability Grammian P for a stable system is defined as follows :

$$P = \int_0^{t_f} e^{At} BB^T e^{A^T t} dt \tag{E3}$$

where P is a symmetric positive semi-definite matrix. The matrix P satisfies the following steady-state Lyapunov matrix equation:

$$AP + PA^T + BB^T = 0. \tag{E4}$$

If $rank(P) = k$ then there are $(n-k)$ uncontrollable modes. However, it is not possible using this method, to determine directly which of the *modes* of the system are controllable or uncontrollable.

F. System Observability [1]

A system is observable if it is possible to determine the initial state $x(0)$ based on a set of measurements $y(t)$ for $0 \le t \le t_f$. This is a property that relates system outputs $y(t)$ to system states $x(t)$.

We present three ways to check whether a system is observable or not, namely *Observability Matrix, Modal Decomposition* and *Observability Grammian.*

F.1 Observability Matrix

The system given by (A1) is said to be *completely observable* or equivalently, the pair (A,C) is *completely observable* if and only if the rank of the *observability matrix* is n i.e.:

$$rank(\mathcal{O}(A,C)) = n \tag{F1}$$

where:

$\vartheta(A,C) = \left[C^T \;\; C^T A^T \;\; \left(CA^2\right)^T \;\; \cdots \;\; C^T\left(A^{n-1}\right)^T\right]^T_{n\times np}$ is the observability matrix of the pair (A,C).

Thus we can check if a system is observable or not by determining the rank of the observability matrix. If the $rank(\vartheta(A,C)) = n$ then the system is completely observable. If $rank(\vartheta(A,C)) = q$, $q \le n$, then only a q-dimensional subspace of the system is completely observable, the rest of the system being unobservable.

This method only provides information about whether a system is observable or not. It does not provide information about which *modes* of the system are observable or unobservable.

F.2 Modal Decomposition [2]

From the modal canonical form given by equation (E1), the output equation is expressed as:

$$y = CTz + Du \tag{F2}$$

It can be seen that mode j is unobservable if the jth column of the product CT is a column of zeros. Thus, using the method of modal decomposition, it is possible to determine directly which *modes* of the system are controllable or uncontrollable.

F.3 Observability Grammian

The Observability Grammian Q for a stable system is defined as follows :

$$Q = \int_0^{t_f} e^{A^T t} C^T C e^{At} dt \tag{F3}$$

where Q is a symmetric positive semi-definite matrix. The matrix Q satisfies the following steady-state Lyapunov matrix equation:

$$A^T Q + QA + C^T C = 0. \tag{F4}$$

If $rank(Q) = k$ then there are $(n-k)$ unobservable modes. However, it is not possible using the Observability Grammian, to determine directly which modes are unobservable.

If a system has no uncontrollable or unobservable modes then it is said to be *minimal.* On the other hand if a system has uncontrollable or unobservable modes, it is said to be *non-minimal.*

G. Fixed Modes [4]

In this section we define the concept of fixed modes for systems under centralized and decentralized control. The centralized fixed modes are equivalent to the uncontrollable modes of a system. Decentralized fixed modes are those modes which cannot be moved using decentralized control. Decentralized fixed modes may exist in a system which is completely controllable. We discuss these two concepts in more detail in the next section.

G.1 Centralized Fixed Modes

Suppose that the system given by (A1) is either not completely controllable or not completely observable. Then, no matter what feedback controller is connected to the system, the modes which are uncontrollable or unobservable in the open loop will remain unaffected by the feedback control. This means that the closed loop characteristic polynomial will have roots that are independent of the control. These roots identify the *centralized fixed modes* of the system. The *centralized fixed modes* are equivalent to the eigenvalues of the uncontrollable or unobservable part of the open loop system. If the centralized fixed modes are unstable, then it is not possible to stabilize the system by feedback control i.e. the system is said to be *not stabilizable.*

The *centralized fixed modes* λ^c_{fm} can formally be expressed as follows:

$$\lambda^c_{fm} = \bigcap_k \lambda(A + BkC) \text{ for all finite } k. \qquad \text{(H1)}$$

where $\lambda(\cdot)$ denotes the eigenvalues of $(\cdot)$

$\bigcap_k(\cdot)$ denotes the intersection of $(\cdot)$ over k

G.2 Decentralized Fixed Modes

Consider a finite dimensional LTI system which is completely controllable and completely observable i.e. it has no centralized fixed modes. In addition, assume that the feedback controllers are finite dimensional, LTI and restricted to be decentralized. The system under decentralized control can be described by equation (A2).

Since the system is completely observable and completely controllable, all the modes of the system can be freely controlled using centralized control.

Under decentralized control, only feedback signals available at the subsystem are used for control. The feedback signals of each subsystem may not have sufficient information about the entire system in order to fully control the system. Thus, some modes will remain unaffected by decentralized feedback control. Those modes which cannot be affected by decentralized control but can be affected by centralized control are called *decentralized fixed modes*. The set of decentralized fixed modes can be defined as:

$$\lambda^{d}_{fm} = \bigcap_{k \in \mathbb{K}} \lambda(A + \sum_{i=1}^{m} B_i k_i C_i) \qquad \text{(G1)}$$

where $\mathrm{K} = \left\{ K \,\middle|\, diag(k_1, k_2, \ldots, k_m), \quad k_i = R^{m_i \times p_i} \right\}$

A necessary and sufficient condition for the existence of decentralized fixed modes is that:

$$rank\,\xi^{d} < n - \alpha$$

where:

$$\xi^{d} = \begin{bmatrix} \lambda I - A & B_{i_1} & \cdots & B_{i_k} \\ C_{i_k+1} & 0 & \cdots & 0 \\ \vdots & \vdots & \ddots & \vdots \\ C_{i_m-1} & 0 & \cdots & 0 \end{bmatrix}$$

i_k is the k*th* input of subsystem *i*

i_m is the m*th* output of subsystem i

α is the rank deficit of matrix A

Thus, if the rank of the matrix ξ^{d} is less than n, the system contains decentralized fixed modes. If the rank of ξ^{d} is equal to n, then the system contains no decentralized fixed modes.

H Norms [5]

In the following section, we discuss three types of norms namely, vector norms, matrix norms and system norms.

H.1 Vector Norms

We define the p-norm of a vector as:

$$\|x\|_p = \left(\sum_{i=1}^{n} |x_i|^p \right)^{\frac{1}{p}} \tag{H1}$$

The infinity norm of a vector is defined as :

$$\|x\|_\infty = \max_i |x_i| \tag{H2}$$

H.2 Matrix Norms

The p norm of a matrix is defined in terms of vector norms as follows:

$$\|A\|_p = \sup_{x \in \mathbb{C}^n, x \neq 0} \frac{\|Ax\|_p}{\|x\|_p}, \quad A \in \mathbb{C}^{m \times n} \tag{H3}$$

Some useful p-norms are:

$\|A\|_1 = \max_j \sum_{i=1}^{m} |A_{ij}|$ (maximum column sum)

$\|A\|_2 = \sigma_{\max}(A)$ (maximum singular value)

The infinity norm of matrix A is defined as:

$$\|A\|_\infty = \max_i \sum_{j=1}^{n} |A_{ij}| \quad \text{(maximum row sum)} \tag{H4}$$

Let $A \in \mathbb{C}^{m \times n}$ $B \in \mathbb{C}^{n \times m}$. Some useful properties of matrix norms:

$$\|AB\|_p \leq \|A\|_p \|B\|_p$$

$$\max_{i,j} |A_{ij}| \leq \|A\|_2 \leq \sqrt{mn} \max_{i,j} |A_{ij}|$$

$$\|A\|_2 \leq \sqrt{\|A\|_1 \|A\|_\infty}$$

H.3 System Norms

Given a transfer function matrix $G(s) = C(sI - A)^{-1}B + D$ the H_∞ norm of G(s) denoted by $\|G(s)\|_\infty$ is defined as follows:

$$\|G(s)\|_\infty = \sup_\omega(\sigma_{max}(G(j\omega))) \tag{H5}$$

A physical interpretation of the H_∞ norm of G(s) can be given in terms of the RMS gain of the system as follows:

$$\int_0^{t_f} y^T(t)y(t)dt \le \|G(s)\|_\infty \int_0^{t_f} u^T(t)u(t)dt \qquad \text{for } t_f>0 \tag{H6}$$

As $t_f \to \infty$ the H_∞ norm is given by the following inequality:

$$\|G(s)\|_\infty \ge \frac{RMS(y(t))}{RMS(u(t))}. \tag{H7}$$

If $u(t) = u_0 \sin(\omega t)$ then: $\|G(s)\|_\infty = \frac{RMS(y(t))}{RMS(u(t))}$. (H8)

Thus, $\|G(s)\|_\infty$ is simply the RMS gain of the system.

I. State Space Computation of the H_∞ Norm [6]

Assume that matrix A has no purely imaginary eigenvalues and that the direct feedthrough term D is zero. In optimal H_∞ controller design, it is required that $\|G(s)\|_\infty < \gamma$ where γ is a robust stability margin. Given γ, the Hamiltonian matrix M_γ is defined as:

$$M_\gamma = \begin{bmatrix} A & \gamma^{-1}BB^T \\ -\gamma^{-1}C^TC & -A^T \end{bmatrix} \tag{I1}$$

The condition $\|G(s)\|_\infty < \gamma$ is satisfied if and only if M_γ has no purely imaginary eigenvalues.

Hence, we can determine whether $\|G(s)\|_\infty < \gamma$ is satisfied by calculating the eigenvalues of M_γ. If none of the eigenvalues of M_γ is purely imaginary, then the condition $\|G(s)\|_\infty < \gamma$ is satisfied. If any eigenvalue of M_γ is purely imaginary then the condition fails. However, calculating all the eigenvalues of M_γ is a computationally intensive procedure for very large systems.

Instead of performing the eigenvalue calculation, the condition that $\|G(s)\|_\infty < \gamma$ can be expressed in terms of a related Algebraic Riccati Equation (ARE) given by:

$$A^T X + XA + \gamma^{-1} XBB^T X + \gamma^{-1} C^T C = 0 \qquad \text{(I2)}$$

The matrix solution X of the ARE is positive definite if and only if M_γ has no imaginary eigenvalues. If the solution of the ARE is positive definite, then the condition $\|G(s)\|_\infty < \gamma$ is satisfied. Thus, we need to check only if the solution of X is positive definite.

The solution to the ARE can be found by computing a matrix T such that M_γ is in upper triangular form i.e.:

$$T^{-1} M_\gamma T = \begin{bmatrix} A_{11} & A_{12} \\ 0 & A_{22} \end{bmatrix} \qquad \text{(I3)}$$

where A_{11} is stable.

T is then partitioned as follows:

$$T = \begin{bmatrix} T_{11} & T_{12} \\ T_{21} & T_{22} \end{bmatrix}. \qquad \text{(I4)}$$

The solution to the ARE is then given by $X = T_{21} T_{11}^{-1}$.

J. Lyapunov Equations [7]

A general form of the Lyapunov algebraic matrix equation is given by $AX + XA^H = C$ where $A \in C^{n \times n}$.

The necessary and sufficient condition for the existence of a unique solution is that $\lambda_i(A) + \lambda_j(A) \neq 0$ for $i, j = 1, \ldots n$ which is automatically satisfied if A is stable.

Consider the following time-varying Lyapunov matrix differential equation:

$$\dot{X}(t) = AX(t) + X(t)A^T + BB^T$$
$$\text{with } X(0) = 0 \qquad \text{(J1)}$$

Then the solution of the matrix differential equation is given by:

$$X(t) = \int e^{A\tau} BB^T e^{A^T \tau} d\tau \qquad \text{(J2)}$$

If A is stable, the unique steady state solution $X_{ss} = \lim_{t\to\infty} X(t)$ must exist and satisfies the following steady state Lyapunov matrix equation:

$$AX_{ss} + X_{ss}A^T + BB^T = 0. \tag{J3}$$

K. Hankel Singular Values [6]

Consider an LTI system described by equation (A1). For this system the Observability and Controllability Grammians are not invariant under a coordinate transformation. If we let $x = Tz$ where T is nonsingular, then the controllability and observability Grammians in z coordinates are given by:

$$P' = T^{-1}PT^{-1} \tag{K1}$$

$$Q' = T^TQT \tag{K2}$$

respectively.

From equations (K1) and (K2), we can deduce that the eigenvalues of P' and Q' are not the same as those of P and Q. This means that a similarity transformation on system model alters the eigenvalues of the Grammians. On the other hand, the product $P'Q'$ and PQ are related through a similarity transformation T as follows:

$$P'Q' = (T^{-1}PT^{-T})(T^TQT) = T^{-1}PQT \tag{K3}$$

From equation (K3) we can deduce that the eigenvalues of the product PQ are invariant i.e.:

$$\lambda_i(PQ) = \lambda_i(P'Q') = \lambda_i(T^{-1}PQT), \quad (i = 1..n) \tag{K4}$$

We define the Hankel Singular Values σ_i^H as the square root of the eigenvalues of PQ i.e.:

$$\sigma_i^H = \sqrt{\lambda(PQ)} \tag{K5}$$

The Hankel Singular Values of (A,B,C,D) are invariant under coordinate transformations.

L. Balanced Realization [8]

For a minimal stable model of a system, there exists a coordinate transformation such that the Controllability Grammian and observability Grammian are equal and diagonal. The state space model of the transformed model is called a *balanced realization.* The transformation to a balanced realization is not unique. However, in the case where the system is minimal, T is unique except for a sign matrix (a diagonal matrix whose diagonal elements are either plus or minus one). The transformation T can be determined from a stable and minimal state space model (A,B,C,D) using the following equation:

$$T = \left[\sum^{-\frac{1}{4}} U^T R\right]^{-1} \qquad \text{(L1)}$$

where:

$R^T R = Q$ is the Choleski Factorization of Q

$U \sum U^T = RPR^T$

$U^T U = I$

P is the Controllability Grammian

Q is the Observability Grammian

$\sum^{\frac{1}{2}} = diag\left[\sigma_1^H, \sigma_2^H, \ldots, \sigma_n^H\right]$

$\sigma_1^H \geq \sigma_2^H \geq, \ldots, \geq \sigma_n^H \quad (i = 1..n)$ are the Hankel singular values

The Grammians P and Q are calculated from equations (E4) and (F4) respectively. The matrix R is solved using Choleski Factorization of Q. Once R is calculated, the matrix product RPR^T can be computed. The matrices U and $\sum$ are obtained from a singular value decomposition of RPR^T. The transformation T can then be computed using equation (L1).

M. Controller Canonical Form [1]

Consider the system described by (A1). The state space formulation can be expressed in *controller canonical form* by performing a coordinate transformation. Assume that the system is completely controllable i.e. the controllability matrix has rank n.

The characteristic polynomial $CP(s)$ is defined as follows:

$$CP(s) = \det(sI - A) = s^n + a_1 s^{n-1} + \ldots + a_{n-1} s + a_n \qquad \text{(M1)}$$

We define a matrix W which is obtained from the above characteristic polynomial as follows:

$$W = \begin{bmatrix} a_{n-1} & a_{n-2} & \cdots & a_1 & 1 \\ a_{n-2} & a_{n-3} & \cdots & 1 & 0 \\ \vdots & \vdots & & \vdots & \vdots \\ a_1 & 1 & \cdots & 0 & 0 \\ 1 & 0 & \cdots & 0 & 0 \end{bmatrix} \qquad \text{(M2)}$$

where the a_i's are coefficients of the characteristic polynomial.

We define a coordinate transformation T given by:

$$x = Tz \qquad \text{(M3)}$$

where $T = \xi W$

ξ is the controllability matrix $\xi = \begin{bmatrix} B & AB & A^2B & \cdots & A^{n-1}B \end{bmatrix}$

Applying this transformation to (A1) gives the following:

$$\begin{aligned} \dot{z} &= T^{-1}ATz + T^{-1}Bu \\ y &= CTz + Du \end{aligned} \qquad \text{(M4)}$$

where:

$$T^{-1}AT = \begin{bmatrix} 0 & 1 & 0 & \cdots & 0 \\ 0 & 0 & 1 & \cdots & 0 \\ \vdots & \vdots & \vdots & & \vdots \\ 0 & 0 & 0 & \cdots & 0 \\ -a_n & -a_{n-1} & -a_{n-2} & \cdots & -a_1 \end{bmatrix}$$

$$T^{-1}B = \begin{bmatrix} 0 \\ 0 \\ \vdots \\ 0 \\ 1 \end{bmatrix}$$

The system given by equation (M4) is in the controller canonical form. Note that T^{-1} exists only if the system is completely controllable.

N. Synthesis of H_2 and H_∞-Based Optimal Controllers [6]

In this section we present methods of obtaining controllers for problems with H_2 and H_∞ norm objective function. We focus on the methods which rely on solutions to Riccati equations.

The H_2 and H_∞ control problems can be formulated with the aid of the control system illustrated in Figure N1.

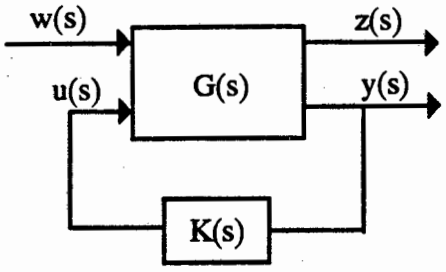

Figure N1: Block Diagram of a Standard Control Problem

The state space description of the control system in Figure N1 can be expressed as follows:

$$\begin{aligned} \dot{x}(t) &= Ax(t) + B_1 w(t) + B_2 u(t) \\ z(t) &= C_1 x(t) + D_{11} w(t) + D_{12} u(t) \\ y(t) &= C_2 x(t) + D_{21} w(t) + D_{22} u(t) \end{aligned} \qquad \text{(N1)}$$

where:

$w(t) \in R^{m_1}$ is the disturbance vector

$u(t) \in R^{m_2}$ is the control input vector

$z(t) \in R^{p_1}$ is the performance output vector

$y(t) \in R^{p_2}$ is the sensor output vector

$A, B_1, B_2, C_1, C_2, D_{11}, D_{12}, D_{21}$ and D_{22} are constant matrices of appropriate dimensions.

The design goal is to find a controller K(s) such that the closed loop is stable and that the influence of disturbance input w(t) to the performance outputs z(t) is minimized according to a system norm, for instance $\|T_{wz}\|_2$ (2-norm) or $\|T_{wz}\|_\infty$ (∞-norm). In the next section we describe a method of obtaining H_2-based controllers. Both State and Output Feedback

control problems are considered. Thereafter, we describe a method of obtaining H_∞-based controllers for both State and Output Feedback.

N.1 Synthesis of H_2 Optimal Controller

The problem is to determine a controller that minimizes the performance index. For the deterministic case (i.e. no noise) with random initial conditions the following objective function is sleeted as follows:

$$J = \int_0^\infty z^T(t)z(t)dt = \int_0^\infty [y^T(t)Qy(t) + u^T(t)Ru(t)]dt \qquad \text{(N2)}$$

where:

$$z(t) = \begin{bmatrix} Q^{\frac{1}{2}}y(t) \\ R^{\frac{1}{2}}u(t) \end{bmatrix} = \begin{bmatrix} Q^{\frac{1}{2}}C' \\ 0 \end{bmatrix} x(t) + \begin{bmatrix} Q^{\frac{1}{2}}D' \\ R^{\frac{1}{2}} \end{bmatrix} u(t)$$

or

$$C_1 = \begin{bmatrix} Q^{\frac{1}{2}}C' \\ 0 \end{bmatrix}, \quad D_{11} = 0 \text{ and } D_{12} = \begin{bmatrix} Q^{\frac{1}{2}}D' \\ R^{\frac{1}{2}} \end{bmatrix}$$

Q is a symmetric positive semi-definite matrix

R is a symmetric positive definite matrix.

If white noise is taken into account, the objective function takes the following form:

$$J = \lim_{t\to\infty} E[z^T(t)z(t)] = \lim_{t\to\infty} \int_0^\infty [y_p^T(t)Qy(t) + u^T(t)Ru(t)]dt \qquad \text{(N3)}$$

The H_2 controller can be obtained from State Feedback or Output Feedback. In the next sections, we present a method of synthesizing the H_2-based controllers for State Feedback. Thereafter, we present a method of synthesizing the Output Feedback controllers.

N.1.1 Synthesis of State Feedback H_2 Optimal Controllers

In the case of State Feedback, the measurement output vector is the state vector x(t) i.e. $y(t) = x(t)$. This means that in equation (O1), we set $C_2 = I_{n\times n}$ (identity) and $D_{21} = D_{22} = 0$.

The optimal State Feedback controller K can be found from the following feedback control law:

$$u(t) = -Kx(t) = -R'^{-1}(D'^{T}QC' + B_2^{T}S)x(t) \tag{N4}$$

where:

$R' = R + D'^{T}QD'$

S satisfies the following Ricatti equation

$A'^{T}S + SA' - SB_2R'^{-1}B_2^{T}S + C'^{T}QC' - C'^{T}QD'R'^{-1}D'^{T}QC' = 0$

$A' = A - B_2R'^{-1}D'^{T}QC'$

Thus, the controller for State Feedback can be expressed as a constant gain matrix K.

N.1.2 Synthesis of Output Feedback H_2 Optimal Controllers

The Output Feedback H_2 optimal control is called Linear Quadratic Gaussian Control (LQG). The noise is modeled as sensor noise and process noise. The disturbance vector w(t) and coefficient matrices B_1 and D_{21} are partitioned as follows:

$$w(t) = \begin{bmatrix} w_1(t) & \text{(process noise)} \\ w_2(t) & \text{(sensor noise)} \end{bmatrix} \tag{N5}$$

$$B_1 = \begin{bmatrix} \Gamma & 0 \end{bmatrix} \tag{N6}$$

$$D_{21} = \begin{bmatrix} 0 & I \end{bmatrix} \tag{N7}$$

where I is the identity matrix.

The sensor noise w_2 is modeled as zero-mean Gaussian white noise with covariance $E[w_2(t+\tau)w_2^{T}(t) = V_0\delta(\tau)$. The process noise is modeled in the partition $w_1(t)$ as zero-mean Gaussian white noise with covariance $E[w_1(t+\tau)w_1^{T}(t)] = W_0\delta(\tau)$. We assume that the process and sensor noise are uncorrelated i.e. $E[w_1(t)w_2^{T}(\tau)] = 0$.

The measurement output vector is then given by $y(t) = C_2x(t) + w_2(t)$.

The optimal LQG controller K(s) has the following LTI state space description:

$$\dot{\hat{x}}(t) = A\hat{x}(t) + B_2u(t) + H[y(t) - C_1z(t) - D_{22}u(t)$$
$$u(t) = -R'^{-1}(D'^T QC' + B_2^T S)\hat{x}(t) \quad \text{(N8)}$$

where:

$H = -PC_2^TV_0^{-1}$

P satisfies the Ricatti equation $AP + PA^T - PC_2^TV_0^{-1}C_2P + \Gamma W_0\Gamma^T = 0$

$\hat{x}$ is the vector of controller states.

N.2 Synthesis of H_∞ Optimal Controller

When we are dealing with the synthesis of H_∞-based controllers, we are concerned with ensuring that the H_∞-norm of the closed loop transfer function matrix T_{zw} is less than a specified bound say γ, i.e.

$$\|T_{zw}\|_\infty < \gamma \quad \text{(N9)}$$

As in the case of synthesizing H_2 controllers, the H_∞ controller can be synthesized using State or Output Feedback control. In the next sections we present the methods of obtaining the controllers using State and Output Feedback respectively.

N.2.1 Synthesis of State Feedback H_∞ Optimal Controllers

As in the case of H_2 State Feedback, the measurement output vector for H_∞ State Feedback is the state vector x(t) i.e. $y(t) = x(t)$. This means that in equation (N1), we set $C_2 = I_{n\times n}$ (identity) and $D_{21} = D_{22} = 0$. Furthermore, we assume that the white noise entering the system, does so through filters i.e. $D_{11} = 0$. This allows us to express the performance output vector z(t) as follows:

$$z(t) = C_1x(t) + D_{12}u(t) \quad \text{(N10)}$$

The existence of a stabilizing controller which satisfies the condition in equation (N10) is based on the existence of a positive semi-definite matrix P. This matrix P satisfies a matrix inequality together with two rank conditions. These conditions are expressed in the following lemma:

Lemma N1: Assume that the system (A, B_2, C_1, D_{12}) has no invariant zeros on the imaginary axis. Then the following statements are equivalent:

(1) There is a State Feedback gain matrix K such that $\|T_{zw}\|_\infty < \gamma$ and the closed-loop system is stable i.e. $\mathrm{Re}(\lambda(A + B_2K)) < 0$.

(2) There exist a real symmetric positive definite solution P to the matrix inequality $F_\gamma(P) \geq 0$ at the given value of γ such that the following to rank conditions are satisfied:

$$(2.1)\ rank(F_\gamma(P)) = normrank(G_{zu}(s)) \qquad (N11)$$

$$(2.2)\ rank\begin{bmatrix} L_\gamma(P) \\ F_\gamma(P) \end{bmatrix} = n + normrank(G_{zu}) \qquad (N12)$$

where:

$$G_{zu}(s) = C_1(sI - A)^{-1}B_2 + D_{12}$$

$$F_\gamma(P) = \begin{bmatrix} A^TP + PA + \gamma^{-2}PB_1B_1^TP + C_1^TC_1 & PB_2 + C_1^TD_{12} \\ B_2^TP + D_{12}^TC_1 & D_{12}^TD_{12} \end{bmatrix}_{(n+m_2)\times(n+m_2)}$$

$$L_\gamma(P,s) = \begin{bmatrix} sI_{n\times n} - A - \gamma^{-2}B_1B_1^TP & -B_2 \end{bmatrix}_{n\times(n+m_2)}$$

We can find a stabilizing State Feedback controller from the following control law:

$$u(t) = Kx(t) = -(D_{12}^TD_{12})^{-1}(B_2^TP + D_{12}^TC_1)x(t) \qquad (N13)$$

where:

P satisfies the following algebraic matrix Ricatti equation:

$$A^TP + PA + \gamma^{-2}PB_1B_1^TP + C_1^TC_1 - (PB_2 + C_1^TD_{12})(D_{12}^TD_{12})^{-1}(B_2^TP + D_{12}^TC_1) = 0 \qquad (N14)$$

The Hamiltonian matrix that corresponds to the solution of the Ricatti equation can be expressed as follows:

$$H(\gamma) = \begin{bmatrix} A - B_2(D_{12}^TD_{12})^{-1}D_{12}^TC_1 & \gamma^{-2}B_1B_1^T - B_2(D_{12}^TD_{12})^{-1}B_2^T \\ -C_1^T[I - D_{12}(D_{12}^TD_{12})^{-1}D_{12}^T]C_1 & -[A - B_2(D_{12}^TD_{12})^{-1}D_{12}^TC_1]^T \end{bmatrix} \qquad (N15)$$

The solution satisfying the Ricatti equation must produce a *stable* matrix $A + \gamma^{-2}B_1B_1^TP - B_2(D_{12}^TD_{12})^{-1}(B_2^TP + D_{12}^TC_1)$. This is equivalent to the condition that the Hamiltonian matrix does not have eigenvalues on the imaginary axis.

We next outline a procedure for the determination of a stabilizing State-Feedback law that results in $\|T_{zw}(s)\|_\infty < \gamma$. Firstly, construct the Hamiltonian matrix given by equation (N15) and check if it has eigenvalues on the imaginary axis. If it has eigenvalues on the imaginary axis, then we cannot find a state feedback controller that meets the required specifications. If possible, relax the constraint $\|T_{zw}(s)\|_\infty < \gamma$ by gradually increasing the value of γ until the Hamiltonian does not contain any imaginary axis eigenvalues. Secondly, solve the Ricatti equation given by equation (N14) for symmetric positive semi-definite matrix P. Finally, evaluate the required controller gain matrix K using equation (N13).

N.2.2 Synthesis of Output Feedback H_∞ Optimal Controllers

In the case of Output Feedback H_∞ controllers, we assume that $y(t) = C_2x(t) + D_{21}w(t)$ or $D_{22} = 0$. Furthermore, we assume that the performance output $z(t) = C_1x(t) + D_{12}u(t)$ or $D_{11} = 0$.

The existence of a stabilizing solution using Output Feedback is based on the existence of two positive semi-definite matrices P and Q. These matrices must satisfy two matrix inequality conditions and several rank conditions. Furthermore, the condition that $PQ < \gamma^2$ must be satisfied. These conditions are expressed in the following Lemma:

Lemma N2: Assume that the systems (A, B_2, C_1, D_{12}) and (A, B_1, C_2, D_{21}) have no invariant zeros on the imaginary axis. Then the following statements are equivalent:

(1) There exist an LTI, finite dimensional dynamic compensator K(s) such that the closed loop system is internally stable and has H_∞ norm $\|T_{zw}\|_\infty < \gamma$.

(2) There exist positive semi-definite solutions P and Q of the inequality $F_\gamma(P) \geq 0$ and $G_\gamma(Q) \geq 0$ such that the following conditions are met:

(2.1) $\rho(PQ) < \gamma^2$

(2.2) $rank(F_\gamma(P)) = normrank(G_{zu}(s))$

(2.3) $rank(G_\gamma(Q)) = normrank(G_{yw}(s))$

$$(2.4)\ rank\begin{bmatrix} L_\gamma(P,s) \\ F_\gamma(P) \end{bmatrix} = n + normrank(G_{zu}(s))$$

$$(2.5)\ rank\begin{bmatrix} M_\gamma(Q,s) & G_\gamma(Q) \end{bmatrix} = n + normrank(G_{yw}(s))$$

where:

$$F_\gamma(P) = \begin{bmatrix} A^TP + PA + \gamma^{-2}PB_1B_1^TP + C_1^TC_1 & PB_2 + C_1^TD_{12} \\ B_2^TP + D_{12}^TC_1 & D_{12}^TD_{12} \end{bmatrix} \quad (N16)$$

$$G_\gamma(P) = \begin{bmatrix} AQ + QA^T + \gamma^{-2}QC_1^TC_1Q + B_1B_1^T & QC_2^T + B_1D_{21}^T \\ C_2Q + D_{21}B_1^T & D_{21}D_{21}^T \end{bmatrix} \quad (N17)$$

$$L_\gamma(P,s) = \begin{bmatrix} sI_{n\times n} - A - \gamma^{-2}B_1B_1^TP & -B_2 \end{bmatrix}_{n\times(n+m_2)} \quad (N18)$$

$$M_\gamma(Q,s) = \begin{bmatrix} sI - A - \gamma^{-2}QC_1^TC_1 \\ -C_2 \end{bmatrix} \quad (N19)$$

$\rho(PQ)$ is the spectral radius of PQ. (N20)

Matrix Q satisfies the following Ricatti equation:

$$AQ + PA^T + \gamma^{-2}QC_1^TC_1Q + B_1B_1^T - (QC_2^T + B_1D_{21}^T)(D_{21}D_{21}^T)^{-1}(C_2Q + D_{21}B_1^T) = 0 \quad (N21)$$

The state space description of the Output Feedback H_∞ controller is given by the following:

$$\begin{aligned} \dot{x}_c(t) &= A_cx_c(t) + B_cy(t) \\ u(t) &= C_cx_c(t) \end{aligned} \quad (N22)$$

where:

$$C_c = K$$

$$B_c = -(I - \gamma^{-2}QP)^{-1}H$$

$$A_c = A + B_2C_c - B_cC_2 - (I - \gamma^{-2}QP)^{-1}\gamma^{-2}X$$

$$X = QC_c^TB_2^TP + QC_c^TD_{12}^T(C_1 + D_{12}C_c) + QY + (I - \gamma^{-2}QP)(B_cD_{21} - B_1)B_1^TP$$

$$Y = -(PA_{cl} + A_{cl}^TP + C_{cl}^TC_{cl} + \gamma^{-2}PB_1B_1^TP) > 0$$

$$H = -(QC_2^T + B_1D_{21}^T)(D_{21}D_{21}^T)^{-1}$$

We define a Hamiltonian matrix $G(\gamma)$ corresponding to the matrix Q as follows:

$$G(\gamma) = \begin{bmatrix} A^T - C_2^T(D_{21}D_{21}^T)^{-1}D_{21}^TB_1^T & \gamma^{-2}C_1^TC_1 - C_2^T(D_{21}D_{21}^T)^{-1}C_2 \\ -B_1[I - D_{21}^T(D_{21}D_{21}^T)^{-1}D_{21}]B_1^T & -[A^T - C_2^T(D_{21}D_{21}^T)^{-1}D_{21}B_1^T]^T \end{bmatrix} \quad (N23)$$

We next outline a procedure for the determination of a stabilizing Output-Feedback law that results in $\|T_{zw}(s)\|_\infty < \gamma$. The procedure is composed of four stages which are described as follows:

Stage 1

Construct the Hamiltonian matrix $H(\gamma)$ given by equation (N15) and check if it has eigenvalues on the imaginary axis. If it has eigenvalues on the imaginary axis, then we cannot find an Output Feedback controller that meets the required specifications. If possible, relax the constraint $\|T_{zw}(s)\|_\infty < \gamma$ by gradually increasing the value of γ until the Hamiltonian does not contain any imaginary axis eigenvalues. Next, solve the Ricatti equation given by equation (N14) for symmetric positive semi-definite matrix P. Evaluate the required controller gain matrix K using equation (N13).

Stage 2

Construct the Hamiltonian matrix $G(\gamma)$ given by equation (N23) and check if it has eigenvalues on the imaginary axis. If it has eigenvalues on the imaginary axis, then we cannot find an Output Feedback controller that meets the required γ specification. If possible, relax the constraint $\|T_{zw}(s)\|_\infty < \gamma$ by gradually increasing the value of γ until the Hamiltonian does not contain any imaginary axis eigenvalues. Next, solve the Ricatti equation given by equation (N21) for symmetric positive semi-definite matrix P. Evaluate the required gain matrix H using the following:

$$H = -(QC_2^T + B_1 D_{21}^T)(D_{21} D_{21}^T)^{-1} \qquad \text{(N24)}$$

Stage 3

Once P and Q have been calculated check whether $\rho(PQ) < \gamma^2$. If this condition is not satisfied then relax the constraint $\|T_{zw}(s)\|_\infty < \gamma$ by gradually increasing the value of γ. If the condition cannot be satisfied with a satisfactory value for γ, then an output feedback controller cannot be found.

Stage 4

Evaluate the controller state matrices A_c, B_c, C_c ($D_c = 0$ for a strictly proper controller).

O. Strongly Stabilizable [9]

In this section, we state a necessary and sufficient conditions for stabilizing an LTI multivariable system with a stable single variable controller.

Consider an LTI plant that is completely controllable and completely observable. Let the distinct zeros of $G(s)$ in $\mathrm{Re}(s) \geq 0$ (including zeros at infinity) be denoted by $z_1, z_2, \ldots z_l$. Let the total number of real poles of $G(s)$ to the right of z_i (each counted to its multiplicity), be denoted by v_i, $i = 1,2,\ldots l$. Then we can state the following Lemma:

Lemma O1: The plant $G(s)$ is strongly stabilizable if and only if the integers $v_1, v_2, \ldots v_l$ are either *all* even or *all* odd.

From the *Lemma O1* we can state that if $G(s)$ is strictly proper ($G(\infty) = 0$), then $G(s)$ is strongly stabilizable if and only if every real zero of $G(s)$ in $\mathrm{Re}(s) \geq 0$ lies to the left of an even number of real poles of $G(s)$, the poles counted according to their multiplicities. This property of the pole-zero pattern of a system is called the *Parity Interlacing Principle (PIP).*

If we wish to find a dynamic controller $K(s)$ for the plant $G(s)$, the Parity Interlacing Principle determines whether it is possible to find a stable $K(s)$. There exist a stable $K(s)$ which stabilizes $G(s)$, if and only if $G(s)$ satisfies the PIP.

The PIP is relevant for systems which have both poles and zeros in the right half plane i.e. unstable, non-minimum phase systems. Thus, if we calculate the poles and zeros of the unstable non-minimum phase system, we can determine if it satisfies the PIP principle and consequently if it is possible to stabilize the system with a stable controller.

If the PIP is not satisfied, then we can find only unstable controllers which will stabilize the input-output response of the system. As a special case, an unstable controller can eliminate the

poles and non-minimum phase zeros by pole-zero cancellation. This means that the unstable poles in the open loop plant will be made unobservable by the non-minimum phase zero of the controller. Similarly, the unstable pole of the controller is made unobservable by the non-minimum phase zero of the plant. This means that even though the *input-output* response of the plant will be stable, the *internal* dynamics will be unstable.

In addition, since the plant is stabilized by pole-zero cancellation in the right half plane, the closed loop system will be stable for only the operating point for which it was designed. If the plant dynamics change, the poles and zeros will move apart, thus destabilizing the system. Therefore the closed loop system possesses very weak robustness properties.

P. Static Output Feedback [10]

In this section, we describe a procedure for determining the static gain matrix for a system under Output Feedback. The gain matrix is calculated by solving an H_∞ norm constraint problem.

Consider a system described by the following state space description:

$$\begin{aligned} \dot{x} &= Ax + B_1 w + B_2 u \\ u &= -\bar{K} y \\ y &= C_2 x \\ z &= C_1 x + D_1 u \end{aligned} \qquad \text{(P1)}$$

where $x \in R^n, u \in R^m, w \in R^l, y \in R^r, z \in R^q$.

Assume that the following conditions are met:

$$\begin{aligned} C_1^T D_1 &= 0 \\ D_1^T D_1 &> 0 \end{aligned} \qquad \text{(P2)}$$

Define Matrix $F \in R^{p \times p}$ as follows:

$$F = \begin{bmatrix} A & -B_2 \\ 0 & 0 \end{bmatrix} \tag{P3}$$

where $p = n + m$

The closed loop transfer function from w and z is given by the following:

$$T_{zw}(s) \overset{\Delta}{=} (C_1 - D_1 \overline{K} C_2)[sI - A_{cl}]^{-1} B_1 \tag{P4}$$

where $A_{cl} = A - B_2 \overline{K} C_2$

We wish to find an output feedback gain $\overline{K} \in R^{p \times m}$ such that the closed loop transfer function $T_{zw}(s)$ satisfies a pre-specified $\gamma > 0$ attenuation level i.e. $\|T_{zw}(s)\|_\infty \leq \gamma$. We define the following:

$$G = \begin{bmatrix} 0 \\ I \end{bmatrix}_{p \times m} \tag{P5}$$

$$Q = \begin{bmatrix} B_1 B_1^T & 0 \\ 0 & 0 \end{bmatrix}_{p \times p} \tag{P6}$$

$$R = \begin{bmatrix} C_1^T & 0 \\ 0 & D_1^T D_1 \end{bmatrix}_{p \times p} \tag{P7}$$

The matrices G, Q and R are obtained from the open loop plant given by (P1)

We further define a convex function θ as follows:

$$\theta \overset{\Delta}{=} FW + WF^T + \gamma^{-2} WRW + Q \tag{P8}$$

where:

W is positive semi-definite symmetric matrix

Q is a positive definite matrix

$v^T \theta v$ is negative semi-definite

$v \in nullspace(G^T)$

We further define the space C_∞ as follows:

$$C_\infty \stackrel{\Delta}{=} \left\{ W = W^T \geq 0 \ : \ v^T \theta v \leq 0 \ : \ \forall v \in nullspace(G^T) \right\} \tag{P9}$$

We partition the matrix W as follows:

$$W = \begin{bmatrix} W_1 & W_2 \\ W_2^T & W_3 \end{bmatrix} \tag{P10}$$

where:

$W_1 \in R^{n \times n}$, $W_2 \in R^{n \times m}$ and $W_3 \in R^{m \times m}$

W_1 is positive definite

Lemma P1: The system described by (Q1) is stabilizable by a constant gain output feedback *if and only if* the following conditions exist.

$$(1)\ T \stackrel{\Delta}{=} \begin{bmatrix} C_2 \\ E^T \end{bmatrix} \in R^{n \times n} \text{ is of full rank} \tag{P11}$$

$$(2)\ C_\infty(E) \stackrel{\Delta}{=} C_\infty \cap \left\{ W : \begin{bmatrix} C_2 & 0 \\ 0 & I \end{bmatrix} \begin{bmatrix} W_1 & W_2 \\ W_2^T & W_3 \end{bmatrix} \begin{bmatrix} E \\ 0 \end{bmatrix} = 0 \right\} \neq 0 \tag{P12}$$

Thus, if we can find a matrix E such that these two conditions are satisfied, then the controller gain matrix is given by:

$$K = \overline{K} C_2 = W_2^T C_2^T (C_2 W_1 C_2^T)^{-1} C_2 \tag{P13}$$

The closed loop of the system is given by:

$$A_{cl} = A - B_2 W_2^T C_2^T (C_2 W_1 C_2^T)^{-1} C_2 \tag{P14}$$

Q. Sequential Quadratic Programming [11]

Consider an optimization problem of the following form:

$$\underset{x \in R^n}{\text{minimize}}\ f(x) \tag{Q1}$$

subject to the m constraints:

$$\begin{aligned} & g_i(x) = 0 \quad i = 1, \ldots, m_e \\ & g_i(x) \leq 0 \quad i = m_e, \ldots, m \\ & x_l \leq x \leq x_u \end{aligned} \tag{Q2}$$

where:

$f(x)$ is the nonlinear objective function

$g_i(x)$ are the nonlinear constraints

x_l and x_u are the upper and lower bounds on x

m_e is the number of equality constraints

The necessary conditions for optimality of the constrained optimization problem are the Kuhn-Tucker equations which can be stated as follows:

$$\nabla f(\bar{x}) + \sum_{i=1}^{m} \bar{\lambda}_i \nabla g_i(\bar{x}) = 0$$

$$\bar{\lambda}_i g_i(\bar{x}) = 0 \quad i = 1,\ldots,m_e \qquad \text{(Q3)}$$

$$\bar{\lambda}_i \geq 0 \quad i = m_e + 1,\ldots,m$$

where:

$\bar{x}$ is the optimal solution

$\bar{\lambda}_i$ are the Lagrange multipliers at the optimal solution

We define the Lagrangian function $L(x,\lambda)$ as follows:

$$L(x,\lambda) = f(x) + \sum_{i=1}^{m} \lambda_i g_i(x) \qquad \text{(Q4)}$$

In Sequential Quadratic Programming (SQP) we obtain a second order approximation of the Lagrangian function $L(x,\lambda)$ and solve the following Quadratic Programming (QP) sub-problem.

$$\underset{x \in R^n}{\text{minimize}} \quad \frac{1}{2} d^T H_k d + \nabla f(x_k)^T d \qquad \text{(Q5)}$$

subject to the linear constraints:

$$\nabla g_i(x)^T d + g_i(x) = 0 \quad i = 1,\ldots,m_e \qquad \text{(Q6)}$$

$$\nabla g_i(x)^T d + g_i(x) \leq 0 \quad i = m_e + 1,\ldots,m$$

where:

k represents the k*th* iteration

d is the search direction

H_k is the positive definite approximation of the Hessian matrix of the Lagrangian function

Thus, SQP is composed of two loops, a minor loop which involves the solution of a QP problem and a major loop which involves the sequential formulation of QP subproblems.

Minor Loop

The solution of the QP sub-problem (minor loop) is obtained by using standard QP algorithms such as the projection method. The solution of the QP sub-problem is used to form an update as follows:

$$x_{k+1} = x_k + \alpha_k d_k \tag{Q7}$$

where α_k is obtained by a line search procedure.

Major Loop

At each iteration of the major loop, the Hessian matrix is updated using the BFGS method as follows:

$$H_{k+1} = H_k + \frac{q_k q_k^T}{q_k^T s_k} - \frac{H_k^T H_k}{s_k^T H_k s_k} \tag{Q8}$$

where:

$$s_k = x_{k+1} - x_k$$

$$q_k = \nabla f(x_{k+1}) + \sum_{i=1}^{m} \lambda_i \nabla g_i(x)_{k+1} - \left(\nabla f(x_k) + \sum_{i=1}^{m} \lambda_i \nabla g_i(x)_k \right)$$

References

[1] Kailath T., *Linear Systems*, Prentice-Hall, 1980.

[2] Chen C. T., *Linear Systems Theory and Design,* Holt, Rhinehart and Winston, 1984.

[3] Beauregard T., *Introduction to Linear Algebra,* Prentice-Hall, 1980.

[4] Anderson B. D., Clements D. J., *"Algebraic Characterization of Fixed Modes in Decentralized Control", Automatica,* Vol. 17, No. 5, pp. 703-712.

[5] Boyd S., Barret C., *Linear Controller Design: Limits of Performance*, Prentice-Hall, 1991.

[6] Green M., Limebeer D., *Linear Robust Control,* Prentice-Hall, 1993.

[7] Zinober A. S., *Lecture Notes in Control and Information Science*: *Variable Structure and Lyapunov Control,* Springer-Verlag, 1993.

[8] Dongarra J. J., Moler C. B., Bunch J. R., *Linpack User's Guide*, SIAM Philadelphia.

[9] Youla D. C., Bongiorno, et. al., "Single-Loop Feedback-Stabilization of Linear Multivariable Dynamical Plants", *Automatica,* Vol. 10, 1974, pp. 159-173.

[10] Peres P. L., "H_∞ Robust Control By Static Output Feedback", *Proceedings of the American Control Conference*, San Francisco, California, June 1993.

[11] Fletcher R., *Practical Methods of Optimization,* Vol. 1 and Vol. 2, John Wiley and Sons, 1980.

[12] Ly U. L, *Linear Multivariable Control,* Department of Aeronautics and Astronautics, University of Washington (Seattle), Lecture notes, 1993.

Chapter 1

Introduction

1.1 Statement of the Problem

This thesis deals with the damping of electromechanical oscillations using Power System Stabilizers (PSS). Three aspects are addressed, namely the determination of the optimal locations of the PSS, the determination of the control structure of the PSS and the design of robust PSS.

In the following sections, we give a brief overview of the concept of power system stability. A time-scale decomposition of power system dynamics based on the type of disturbances is presented. Thereafter, the evolution of the small signal stability problem and the need for PSS are described. The characteristics of a power system are then discussed. Finally, the outline of the thesis is presented.

1.2 Power System Stability

Power system stability is broadly defined as the condition of a power system that enables it to remain in a state of operating equilibrium and to settle to a possibly new state of operating equilibrium (in finite time) after being subjected to a finite disturbance. *Power system instability* is defined as the condition of a power system under which *power system stability* is not satisfied.

In order for a power system to maintain stability, it must be able to withstand disturbances that perturb the system from its operating point. The dynamics of the power system resulting from these disturbances can conveniently be decomposed according to the time-scale of the dynamics and the type of disturbance.

Figure 1.1 illustrates the decomposition of power system dynamics based on the time-scale of the dynamics and the type of disturbance.

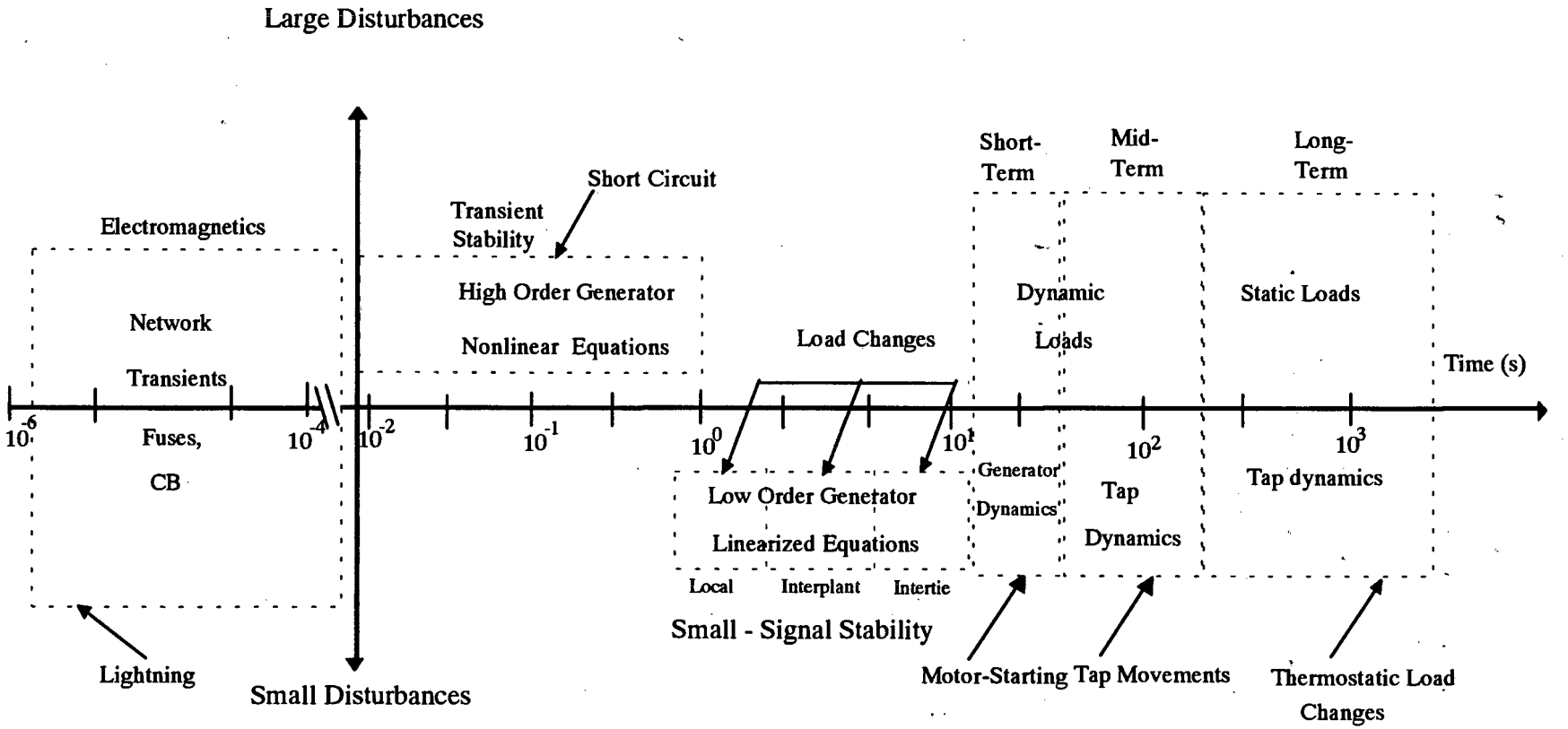

Figure 1.1: Decomposition of Power System Dynamics Based on the Time-Scale of the Dynamics and the Type of Disturbance

In the period of microseconds to milliseconds, the dynamics are relevant to the *electromagnetic* time-frame of the power system. In order to study the effects of the disturbances in this time-frame, detailed modeling of the network transients, transmission line insulation properties, switching of circuit breakers, dynamics of fuses etc. are required.

The stability of the power system in the time-frame greater than 10^{-2} seconds can be divided into two types, namely *synchronous stability* and *voltage stability*. Synchronous stability refers to the dynamics of the rotor angles of the generators while voltage stability is related to the dynamics of the loads.

In the period 10^{-2} to 1 second, the dynamics are relevant to the *transient stability* of the power system. The disturbances that are considered are large disturbances such as short circuits. Due to the magnitude of the disturbances, the nonlinear behavior of the power system needs to be modeled. In addition, the generators need to be modeled to include the effects of the damper windings on the dynamics following the disturbance.

In the period 1 to 10 seconds, the disturbances are relevant to the *small signal stability* of the power system. The disturbances that are considered here are small disturbances such as load changes. Since these disturbances perturb the system in a small region around the operating point, we use the linearized model of the power system [2]. In addition, the generators need not be modeled with high accuracy since the time constants associated with the damper windings are shorter than the small signal stability time-frame [3].

The study of small signal stability can be decomposed into the study of three types of oscillations, namely *interplant oscillations, local oscillations* and *inter-area oscillations*. Each of these has a characteristic range of oscillation frequencies. The *interplant oscillations* occur in the frequency range between 2 to 3 hertz. These oscillations result from the exchange of power between generating units that are electrically close to each other. The *local oscillations* occur in the frequency range between 0.8 to 2 hertz. These oscillations result from the exchange of power from a single machine to an electrically strong network. The *inter-area*

oscillations occur in the frequency range 0.1 to 0.8 Hertz. These oscillations result from the exchange of power from one group of machines to another group of machines via a tie-line.

The study of the power system dynamics that involves both transient stability and small signal stability is referred to as synchronous stability or rotor angle stability. A power system is said to be synchronously stable if after a disturbance the rotor angles of the machines reach a new equilibrium point in finite time.

Voltage stability can be conveniently divided into three areas namely, short-term, mid-term and long-term voltage stability. Short-term voltage stability involves disturbances such as motor starting. Mid-term voltage stability involves disturbances such as tap movements and the complex behavior of dynamic loads. Long term voltage stability involves disturbances that can last over several hours. These disturbances include thermostatic loads and changes in the static component of loads. Note that this decomposition does not fully capture the complex dynamics associated with voltage stability which is not yet completely understood [4].

This thesis focuses on the area of small signal stability. This means that we use the linearized system of equations to develop a procedure for enhancing the damping of electromechanical oscillations using PSS.

1.3 Evolution of the Small Signal Stability Problem

Modern electric power systems are large scale interconnected systems that can stretch across entire continents. For this reason, power systems are regarded as among the largest and most complex systems ever created by humans [6]. Despite the accuracy of these grandiose accolades, the origin of modern interconnected power systems is rather humble. The first complete commercial power system was built by Thomas Edison in the early 1880's and consisted of a d.c. generator, a cable, fuses and loads. The loads consisted mainly of incandescent lamps which behaved like constant impedance loads.

Since the generator was d.c. and the loads were constant impedance loads, the first power system did not present any synchronous stability problems. However, the d.c. generator was soon replaced by a.c generators elsewhere in the world [4]. The power systems which consisted of an a.c. generator connected to a constant impedance load did not present any synchronous stability problems. However, with the introduction of electric motors as loads in the mid 1880's, the problem of synchronous stability began. These loads can behave like constant power loads which change the angle difference between the sending end and receiving end voltages. Thus the problem of small signal stability arose.

The demand for electricity increased substantially in the early 1890's. The a.c. systems could deliver power at high voltages over longer distances while keeping the transmission losses and voltage drops to acceptable levels. The widespread acceptance of a.c. systems encouraged the growth of an electric grid (instead of a single generation center) supplying all the distributed loads. This meant that several distributed generating centers were interconnected via transmission lines to serve the distributed loads. Some of the advantages offered by the electric grid are [5,6]:

- It allows the generating centers to be located close to the source of energy
- It increases the reliability of the system
- It permits the construction of larger and more economical generating units
- It permits reduced reserve requirements by sharing of capacity between areas
- It permits capacity savings from time-zone differences and random diversity of loads
- It facilitates the transmission of off-peak energy
- It provides flexibility to meet unforeseen emergency demands
- It allows some generating centers to be located in areas where the environmental impact can be controlled

Despite all these advantages, the development of an electric grid makes the power system more difficult to monitor and control. Complex communication networks are required to transmit information about the power system from remote sources. Furthermore, the electric grid

compounds the problem of maintaining synchronous stability since it requires coordinated control of the angular difference between the generating centers.

Recent advances in the manufacturing industry, have resulted in the sizes of generators decreasing and the reactances of the generators increasing significantly [4]. In addition, for economic reasons, the power systems are increasingly being operated closer to the maximum power transfer limits. These factors have further aggravated the problem of maintaining synchronous stability in power systems.

In longitudinal power systems, such as the Eskom grid, the problem of maintaining synchronous stability is especially acute. In these networks, the equivalent reactance between two remote generating centers is very high. This reduces the maximum transfer capability between the two centers thus deteriorating the synchronous stability of the system.

In order to maintain the voltage profile of power systems, high speed automatic voltage regulators (AVR) were introduced. By controlling the excitation current of the generator, the high gain AVR ensures fast recovery of the generator terminal voltage. The primary function of the AVR is to maintain the voltage profile of the power system. By maintaining the voltage profile of the power system during a disturbance, the AVR maintains the maximum power transfer limit between two generating centers. Thus, the AVR have the secondary effect of improving the synchronous stability of the system. By increasing the gain of the AVR, the synchronous stability of the system can be enhanced [1].

It was soon discovered however, that the AVR did not present a satisfactory solution to the problem of maintaining the synchronous stability. In the seminal work by De Mello and Concordia [1], the deleterious effect of the high gain AVR were outlined. The AVR, while improving the transient stability margin of the system, deteriorates the small signal stability margin. By increasing the gain of the AVR, the damping of the electromechanical modes is reduced thus resulting in sustained low frequency oscillations.

It became clear that the problem of maintaining both transient stability and small signal stability involved satisfying two constraints namely, high AVR gains for improving the *transient stability* and low AVR gains for improving the *small signal stability* of the system. The authors in [1] suggested that, instead of detuning the high gain AVR, supplementary signals in the voltage control loop should be introduced to improve the damping of the system. These supplementary signals would provide a torque component in phase with the rotor speed thus enhancing the damping of the electromechanical oscillations. Thus the concept of Power System Stabilizers (PSS) was introduced. Since then, PSS have been implemented on power systems with varying success [4]

Figure 1.2 illustrates the block diagram of a second order Conventional Power System Stabilizer (CPSS). The lead-lag circuit of the PSS is required for phase compensation at the electromechanical frequency. The washout term is used to attenuate the influence of the PSS at low frequencies.

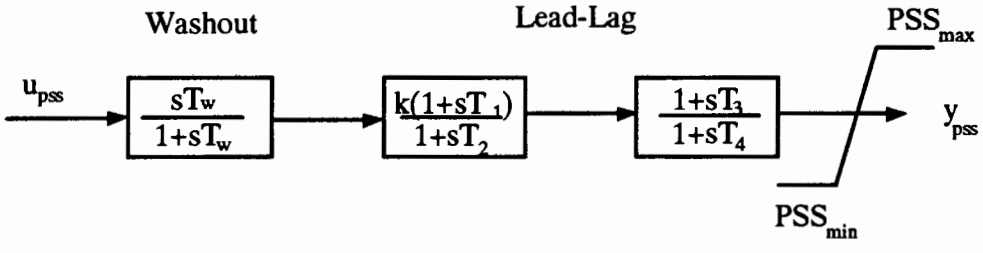

Figure 1.2: Structure of a Second Order Conventional PSS

Figure 1.3 illustrates the implementation of PSS in the two principal control loops of a generator control system.

The transfer function $G_{11}(s)$ represents the open loop response of the terminal voltage ΔV_T due to step in the reference voltage ΔV_{ref}. The transfer function $G_{12}(s)$ represents the open loop response of the electrical power ΔP_{el} due to step in the reference voltage ΔV_{ref}. The transfer function $G_{21}(s)$ represents the open loop response of the terminal voltage ΔV_T due

to step in the mechanical power ΔP_{mech}. The transfer function $G_{22}(s)$ represents the open loop response of the electrical power ΔP_{el} due to step in the mechanical power ΔP_{mech}.

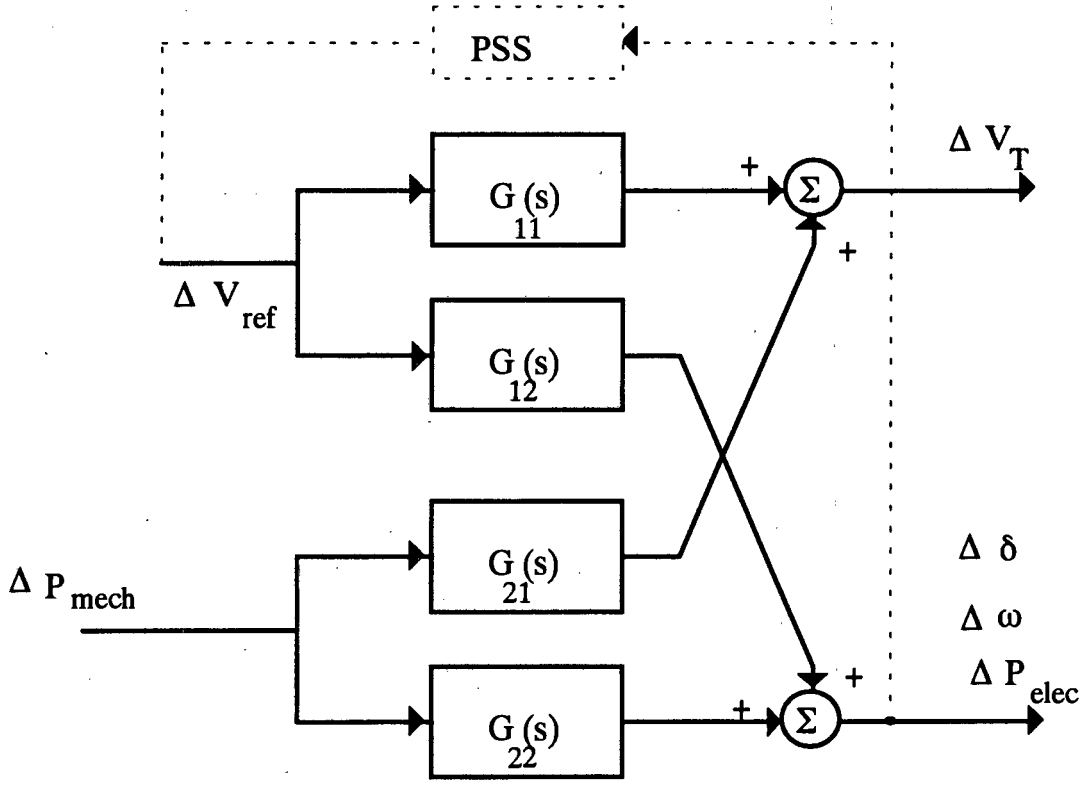

Figure 1.3: Implementation of PSS in the two Principal Control Loops of a Generator Control System

Figure 1.4 illustrates the typical responses of ΔV_T and ΔP_{el} due to a step in ΔV_{ref}. These responses were obtained using the Power System Simulator for Engineers (PSS/E). The response of ΔP_{el} is weakly damped with the oscillations persisting after eight seconds.

The aim in this thesis is to damp the oscillations in ΔP_{el} by using PSS. The PSS for each generator is connected between an output variable such $\Delta\delta, \Delta\omega$ and ΔP_{el} and the input ΔV_{ref}. The desired closed loop response of the system is such that the oscillations in ΔP_{el} must be well damped. Thus, we wish to control the damping of the power loop by means of control through the voltage loop.

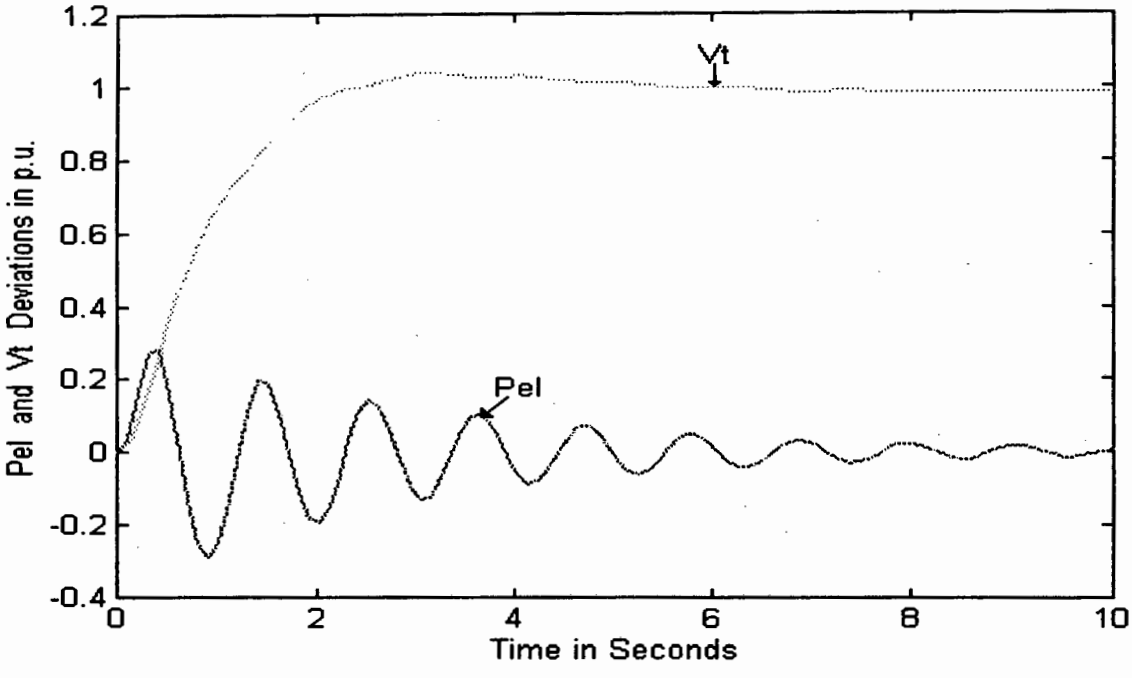

Figure 1.4: Step Responses of ΔV_T and ΔP_{el} for a Step in ΔV_{ref}

1.4 Characteristics of Power Systems

In this section, we outline the main characteristics of power systems. In doing so, we can determine the extent of modeling that is required as well as the nature of the control that needs to be employed. The characteristics of a power system are as follows:

- *Large Scale System* - In the transmission of electrical energy from the generation centres to the load centres, the electrical grid can cover millions of square kilometres. In addition, power systems are becoming even larger due to the interconnection of neighbouring power systems. This makes it necessary to transmit signals for monitoring and control over long distances. Furthermore, the full mathematical model of the power system is typically composed of several thousand states. The methods developed in Chapter 2, Chapter 3 and Chapter 4 take into account the large-scale nature of the power system.

- *Decentralized System:* Due to the large-scale nature of the power system, the control needs to be decentralized. Decentralized control reduces the cost and complexity of transmitting the signals over long distances. Furthermore, the reliability of the power system is increased by having several decentralized controllers instead of a single centralized controller. Decentralized control is however, a weaker form of control than centralized control. *Fixed modes* may exist in systems under decentralized control making these modes uncontrollable. An important focus of the thesis is to develop methods that take into account the decentralized nature of the power system. The methods developed in Chapter 2, Chapter 3 and Chapter 4 emphasise the decentralized nature of the power system.

- *Nonlinear System*: The power system is highly nonlinear due to nonlinear loads, saturation effects, limits on controllers, etc. For the study of disturbances that perturb the system far from the operating point, the nonlinearities of the power system need to be considered. On the other hand, when the disturbances perturb the system in a neighborhood of the operating point, the nonlinearities can be neglected [2]. In this thesis, we consider the linearized state space model of the power system. However, in Appendix C we incorporate an upper bound on the nonlinearities of the system when determining a robust stability margin.

- *Time Varying:* The power system is constantly changing with time due to variations in loads, switching of lines, changes in generator scheduling, settings of control devices, etc. In Chapter 2 and Chapter 3, we model the power system as a linear time-invariant (LTI) system. In Chapter 4, we incorporate an upper bound on the *time varying* perturbations of the system when determining a robust stability margin.

- *Uncertain System:* Due to limitations on the number of measurements that are performed, the full state vector of a power system can only be estimated. Furthermore, due to uncertainty in parameter values of the power system, only an approximate model can be obtained. We model these uncertainties as perturbations to the power system model. In

Chapter 4, we consider two types of perturbations, namely structured and unstructured perturbations in the determination of a robust stability margin.

- *Disturbed System:* The power system is subjected to two classes of disturbances, namely Gaussian white noise disturbances and finite energy disturbances. The Gaussian white noise can take the form of process noise or sensor noise. In this thesis, we do not consider the influence of Gaussian white noise on the power system. In synthesizing H_∞-based controllers we take into account disturbances that are finite energy signals.

- *Expanding System*: The power system is constantly expanding due to increases in demand for electricity. This expansion can be incremental such as in the addition of a single power station or it could be more substantial such as when one large power system is interconnected with another. Thus, in designing controllers for an expanding system, we should ensure that the system is able to absorb such expansion. In this thesis, we do not consider the power system as an expanding system.

Based on the outline of the characteristics of a power system, it is evident that a complete model of the power system is very complex. To obtain an accurate model incorporating all or most of these characteristics, would be a daunting task. Despite the complexities of the modeling problem, accurate models of power system components have been developed largely from physical laws. These include generator models, excitation system models, transmission line models, transformer models, etc. These models are widely accepted in industry for the analysis and design of power systems [4,8].

At this stage it is useful to identify two different approaches to modeling of a system for the design of a controller.

The first approach is to place great emphasis on obtaining an accurate model of the system. The model is obtained from direct measurements of the system parameters and states as well as from physical laws. Once an accurate model of the system has been obtained, the design of the

control is relatively simple. The emphasis is thus placed on the *model* accuracy at the expense of the *controller*. Methods such as model reference adaptive control, internal model control, inverse model control, etc. are examples of this approach.

The second approach is based on the viewpoint that imperfections in the model are not critical in design of the control system, since feedback reduces the effect of uncertainty. Instead of refining the model of the system, the emphasis is placed on developing a feedback design methodology that would yield a robust control system i.e. the controller is designed so that uncertainties in the model can be absorbed. The emphasis is thus placed on the *controller*, at the expense of the *model* of the system. Robust control methods such as H_∞ control is an example of this approach.

In this thesis, we recognize that successful treatment of the modeling problem requires a combination of the abovementioned viewpoints. In this respect, we use well-established existing models of the power system components to construct a *nominal* model of the power system. We obtain this *nominal* model from simulation software (such as PSS/E). In order to take into account inaccuracies in this model of the power system, we design controllers for robust closed loop performance. For instance, in designing supplementary excitation controllers, we model each generator with a high order (sixth order) model.. We use this model to synthesize controllers that maximize the robustness of the closed loop system. In this way, we ensure that the requirements for modeling the power system are not excessive while absorbing the unmodeled dynamics of the power system.

1.5 Outline of Thesis

The thesis is divided into six chapters. Each chapter is meant to be treated as a self-contained unit. In this respect, each chapter has its own *Reference* section. Each of these chapters contains the minimum results which are required for understanding the chapter.

The results in each chapter are supplemented with appendices at the end of the thesis. These appendices contain information that is required for detailed analysis of the contribution of each chapter. The appendices also deal with miscellaneous aspects that are relevant to all chapters in the thesis.

We now provide a brief outline of the thesis.

In *Chapter 2*, we address the problem of determining the optimal locations of the PSS. We provide a review of existing methods for determining the optimal PSS locations. We introduce two new methods for the determination of the optimal PSS locations. These two methods are based on Total Modified Coupling Factors (TMC) and optimization by Simulated Annealing (SA). Both of these methods have significant advantages over the existing PSS placement methods.

The TMC is a measure of the damping influence of each machine pair on several power system modes. The TMC incorporates an exciter penalty factor in order to take into account the effect of the performance and the type of excitation system. The method based on TMC is tested on a nine-bus benchmark network.

In the method based on SA, we formulate the placement problem as a discrete nonlinear optimization problem. The objective function in the optimization problem is the minimum damping of the electromechanical modes. In this method, the PSS placement is performed simultaneously for all the PSS. In addition, only generators with acceptable excitation systems are included in the optimization search space, thus ensuring that the performance and the type of exciter is taken into account. Using the method based on SA, a placement scheme is

obtained which guarantees that the undesired poles can be controlled with the available finite control energy. Since we use a discrete nonlinear optimization formulation, the nonlinear nature of the placement problem is taken into account. However, as a result of the nonlinear formulation, the method is computationally more intensive than the method based on TMC. The method of SA is tested on two networks namely, a seven-bus network and a 35-bus equivalent of the Eskom network.

In *Chapter 3,* we address the problem of determining the control structure of PSS. Three aspects of the control structure are addressed, namely the *type of feedback*, the *type of signal* and the *type of control* that is to be used for damping electromechanical oscillations.

The *type of feedback* refers to whether State Feedback or Output Feedback is to be used. When using State Feedback, all the state variables need to be measured. This makes State Feedback impractical. The use of Output Feedback requires only the output variables as feedback signals. For this reason, we use Output Feedback for damping electromechanical oscillations. However, Output Feedback requires that the controller be a dynamic controller. The order of the Dynamic Output Feedback controller is excessively high. In order to overcome this problem we present a new method of obtaining Output Feedback controllers of fixed structure. This is achieved by transforming the Dynamic Output Feedback problem into a Static Output Feedback problem. In this way, the synthesis of the Output Feedback PSS becomes a problem of tuning the parameters of existing PSS.

The *type of signal* refers to the determination of the best output signals that are to be used for damping of the electromechanical oscillations. We present two new methods for determining the best output signals. These methods are based on two measures of the contribution of the electromechanical oscillations to the outputs. The first measure, the *Centralized Modal Observer Measure (CMOM),* is based on the centralized observability of the electromechanical modes. The *CMOM* is not computationally intensive since it requires only the calculation of the right and left eigenvectors. However, the *CMOM* does not take into account the existence of fixed modes in a system under decentralized control. The second measure, the *Decentralized*

Modal Observer Measure (DMOM) takes into account the existence of decentralized fixed modes. The DMOM is based on the decentralized observability of the electromechanical modes. The CMOM and DMOM are tested on a seven-bus benchmark network.

The third aspect of the control structure that is addressed is whether centralized, decentralized or hierarchical control is to be used. Centralized controllers are controllers that make use of local control signals as well as control signals from remote sources in order to effect control. Decentralized controllers make use of only locally measured signals. Hierarchical controllers combine the concepts of decentralized and centralized control. We develop a new approach for designing decentralized controllers. For this approach, we derive new sufficient conditions for ensuring that the system under decentralized control is globally stable. In addition, we present a new approach for hierarchical control of power systems. For this approach, we derive new sufficient conditions for ensuring that the time-varying power system remains globally stable. We also propose that these conditions be incorporated in the dynamic security assessment of the power system.

In *Chapters 4* and *5* we address the problem of designing robust PSS for damping the electromechanical oscillations. Chapter 4 focuses on synthesizing H_∞-based controllers with structures which are different from those of existing PSS. On the other hand, Chapter 5 focuses on the determination of the parameters of existing PSS.

In *Chapter 4*, we describe a new procedure for designing suboptimal decentralized H_∞-based controllers for damping electromechanical oscillations. The global stability of the interconnected power system is ensured by incorporating the sufficient conditions (derived in *Chapter 3*) in the design procedure. These sufficient conditions are used in a new two-stage method for designing decentralized controllers.

In order to evaluate the robustness of the H_∞-based controllers, we introduce a Lyapunov-based robust stability margin. We use this margin to compare the robustness of three

controllers, namely CPSS, optimal H_∞ and suboptimal H_∞ controllers. In order to ensure low order controllers, the method of balanced truncation is used to reduce the order of the open loop plant. The model reduction technique is applied to the generator subsystems which ensures that the order of the controllers is less than that of the open loop subsystems. We make use of an existing Dynamic Output Feedback Ricatti-based method to synthesize the H_∞-based controllers. The chapter discusses the major shortcomings of the standard optimal H_∞ control algorithms as applied to power systems and presents techniques for overcoming these. We apply a bilinear transformation to the model of each generator subsystem in order to improve the damping of the electromechanical oscillations. The design procedure is tested on nine-bus benchmark network.

In *Chapter 5* we address the problem of determining the parameters of fixed structure PSS. The aim of this chapter is the robust tuning of existing PSS rather than the design of new supplementary excitation controllers. We propose two new methods to obtain the parameters of the CPSS, namely, *PSS tuning using numerical optimization* and *PSS tuning using Static Output Feedback.* The tuning by numerical optimization uses Sequential Quadratic Programming (SQP) to obtain the parameters of the PSS. The tuning by Static Output Feedback uses an existing Static Output Feedback control algorithm. The method of tuning by numerical optimization is tested on a SMIB system.

Chapter 6 concludes the thesis. The chapter presents an overview of the thesis and discusses the contributions and shortcomings of the methods proposed in the thesis. The chapter ends with suggestions for future work.

Appendix A discusses numerical problems associated with the linearized state space formulation of the power system. It is demonstrated that the state space description is ill-conditioned for eigenvalue calculation. Due to limitations of finite precision arithmetic, the ill-conditioned eigenvalues are calculated to be unstable even though the power system may be stable. We present two methods of addressing this problem The first method is an existing method and is based on selecting one machine in the network as a reference machine.

However, information about the absolute machine speed is lost by selecting one machine as a reference. The second method is a new method which adjusts the ill-conditioned state space description by making use of a bilinear transformation.

Appendix B presents the procedure of obtaining the controller canonical form for first order and second order lead-lag circuits. The controller canonical form is used in transforming the Dynamic Output Feedback problem into a Static Output Feedback Problem. Appendix B is relevant to Section 3.2.3 and Section 5.2.1.

Appendix C has mainly theoretical value. We present a classification of the linear and nonlinear perturbations that can affect power systems as well as a novel procedure for obtaining upper bounds on perturbations. We also present new derivations of robust stability margins using the Lyapunov stability criteria. The concepts which are developed in *Appendix C* are used in Section 4.3.2.3 where the robust stability margins of different controllers are compared.

Appendix D provides new sufficient conditions for ensuring global stability of an interconnected system while incorporating the influence of time-varying perturbations. The results of *Appendix D* are used in Section 3.4.3 for developing a conceptual hierarchical control scheme.

Appendix E presents the state space models of the nine-bus system. The nine-bus system is used in Section 2.4 and Section 4.4.

Appendix F presents the details of the model reduction technique described in Section 4.3.3. The network that is used in the model reduction is the nine-bus system described in *Appendix E*.

Appendix G presents the state space models of the seven-bus system. The seven-bus system is used in Section 2.6 and Section 3.3.3.

Appendix H presents the details of the optimal H_∞ and suboptimal H_∞ controllers for the nine-bus system used in Section 4.4.

Appendix I presents the state space models of the single machine infinite bus (SMIB) system which is used in Section 5.2.

References

[1] De Mello F., Concordia C., "Concepts of Synchronous Stability as Affected by Excitation Control" *IEEE Trans. on Power Apparatus and Systems*, Vol. PAS-88, pp.316-329, 1969.

[2] Anderson P.M., Fouad A., *Power System Control and Stability*. Vol. 1 , Iowa State University Press, Iowa, 1977.

[3] Yu Y. N., *Electric Power System Dynamics*, 1980.

[4] Kundur P., *Power System Stability and Control*, Prentice-Hall, 1993.

[5] Elgerd O. I., *Electric Energy Systems Theory*, Tata McGraw-Hill, New Delhi, India, 1983.

[6] M. Akke, *Power System Stabilizers in Multimachine Systems*, Licentiate Dissertation, Lund Institute of Technology, 1989.

[7] Elliasson B., *Damping of Power Oscillations in Large Power Systems*, Ph.D. Dissertation, Lund Institute of Technology, 1990.

[8] IEEE Task Force on Definitions and Procedures, "Current Usage and Suggested Practice in Power System Stability Simulations for Synchronous Machines." *IEEE Trans. on Energy Conversion*, Vol. EC-1, No. 1, pp.77-92, 1986.

Chapter 2

Determination of the Optimal Locations of Power System Stabilizers

2.1. Introduction

This chapter deals with the determination of the optimal locations of Power System Stabilizers (PSS) for damping electromechanical oscillations in power systems. We present two new methods for determining the optimal locations. The first method is based on the eigenstructure of the power system and uses the concept of Total Modified Coupling Factors (TMC). The second method is based on a discrete nonlinear programming formulation of the placement problem and uses the method of Simulated Annealing (SA).

Power System Stabilizers are decentralized controllers. This means that only local signals are used in the feedback path for control of the weakly damped modes. The local signals are state variables or output variables of the generator at which the PSS is placed. The control signals from other generators are not included in the feedback path of the decentralized PSS because of the prohibitive cost of on-line information exchange.

For damping electromechanical oscillations, PSS may be placed on several generators in a power system. Some of these generators contribute more to the damping of the electromechanical modes than others. The generators which contribute the most to the damping are the optimal locations for the placement of the PSS.

The most widely used method for determining the optimal locations of PSS is based on Participation Factors [1,2,3]. The Participation Factors are calculated using the right and left eigenvectors corresponding to the electromechanical mode. Participation Factors are scale-free measures of the sensitivity of the mode to each state. The procedure of calculating Participation Factors is provided in Section B of *Preliminaries*.

The use of Participation Factors for the optimal placement of PSS does have some shortcomings. Firstly, the method can only be used for damping a single electromechanical mode at a time. If we wish to determine the optimal location of the PSS for simultaneous damping of several modes, Participation Factors cannot be used [4].

Secondly, the method based on Participation Factors does not take into account the *performance* of the excitation systems and the *type of exciter* present on the generators. Due to factors such as ageing and wear of the excitation systems, the performance of exciters may deteriorate significantly. Placing a PSS on an exciter with a sluggish transient performance, will significantly reduce the effectiveness of the PSS for damping oscillations. In addition, some exciter types (such as a.c. exciters) are less suitable for placement of PSS than other types (such as d.c. exciters). The method based on Participation Factors completely ignores these two aspects of the generator excitation system. In fact, by using Participation Factors, it is possible to obtain a placement scheme which includes generators with excitation systems that have unsatisfactory transient performance or even generators with a.c. exciters [4].

Thirdly, the method of Participation Factors can only be used for placement of *one PSS at a time* [3]. This means that the interactions between generator control systems are ignored in the placement problem. If several PSS need to be placed in a tightly connected power system, the interactions between generator control systems cannot be ignored.

Fourthly, using Participation Factors for optimal placement of PSS does not guarantee that it will be possible to move the electromechanical modes using *finite control energy*. It is possible that, by using Participation Factors, an 'optimal' placement scheme is obtained that would require excessive (possibly infinite) control energy. This is due to the fact that the Participation Factors do not consider the controllability of the electromechanical modes and the pattern of the poles and zeros of system. This problem is highlighted in [2] where the authors use Participation Factors to optimally place the PSS one at a time. As a result of the existence of non-minimum-phase (right-half-plane) zeros, the network could not be stabilized with the PSS placed at the generators corresponding to the maximum

Participation Factors. Instead of using Participation Factors, the authors obtained the optimal locations of the PSS by trial and error.

Finally, the use of Participation Factors does not take into account the *nonlinear nature* of the placement problem. The nonlinear nature is illustrated by investigating the trajectory of the electromechanical mode damping when the PSS location is changed from one generator to another. By changing the location of the PSS, the damping factor of the electromechanical mode changes in a nonlinear manner, despite the fact that a linearized state space description of the power system is used. Up to now, this nonlinear behavior of the mode damping has been ignored in PSS placement.

In order to address some of these problem, we have developed the concept of Total Modified Coupling Factors (TMC) for the optimal placement of the PSS. The TMC is a measure of the damping influence of the PSS on all power system modes of interest. In addition, by incorporating an exciter penalty factor, TMC includes the effect of the performance and type of excitation system. As such, the TMC addresses the first two problems associated with the use of Participation Factors for placement of PSS.

In order to address all five problems associated with Participation Factors, we present a method based on discrete nonlinear optimization. The solution of the optimization problem is obtained by means of the method of Simulated Annealing. The placement is performed simultaneously for *all* PSS. In addition, only generators with acceptable excitation systems are included in the optimization search space thus ensuring that the performance and type of exciter is taken into account. Using the method of Simulated Annealing, a placement scheme is obtained which guarantees that the undesired poles can be controlled with the available control energy. Finally, since the placement problem is formulated as a discrete nonlinear optimization problem (with maximization of electromechanical mode damping as the objective), the nonlinear nature of the problem is taken into account. However, as a result of the nonlinear problem formulation, the method is computationally more intensive than the method based on TMC.

Figure 2.1 illustrates the case studies that are performed in this chapter.

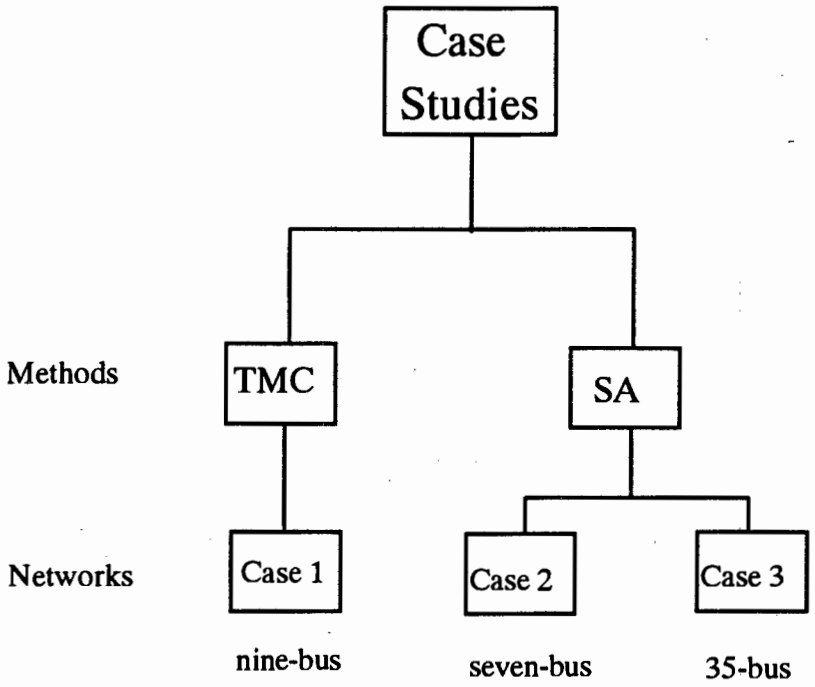

Figure 2.1: Representation of the Case Studies in Chapter 2

The method based on TMC was investigated on the nine-bus system described in *Appendix E* (Case 1). The method based on Simulated Annealing was investigated on two networks. The first network (Case 2) on which Simulated Annealing was applied, is the seven-bus system described *in Appendix G*. This system was chosen in order to compare the Simulated Annealing method with the Participation Factor method. The second network on which Simulated Annealing is applied, is a 35-bus equivalent of the South African grid (Case 3). The results for the three networks are presented and conclusions are drawn.

2.2. Mathematical Description of the Problem

Consider an n-dimensional interconnected power system consisting of m generator subsystems. The linearized state space equations of the power system can be expressed as follows:

$$S \triangleq \{S_i\} \triangleq \begin{Bmatrix} \dot{x}_i = (A_{ii})x_i + \sum_{j=i}^{m}(A_{ij})x_j + B_i u_i \\ y_i = C_i x + D_i u_i \end{Bmatrix} \tag{2.1}$$

where all the variables are defined in (A2) of the *Preliminaries.*

Assume that the plant is proper i.e. $D_i = 0$.

Consider feedback control of subsystem S_i with a controller of the following form:

$$K_i(s) = \frac{k_i(1+sT_{i1})^{n_c}}{(1+sT_{i2})^{n_c}}$$

where:

k_i, T_{i1}, T_{i2} are parameters of the controller K_i

n_c is the order of the controller

The state space description of the controller can be expressed as follows:

$$\begin{aligned} \dot{z}_i &= E_{ii}z_i + F_i w_i \\ v_i &= G_i z_i + H_i w_i \end{aligned} \tag{2.2}$$

where:

$z_i \in R^{n_c}$ is the vector of states of controller K_i

$w_i \in R^{m_c}$ is the vector of inputs of controller K_i

$v_i \in R^{p_c}$ is the vector of outputs of controller K_i

p_c is the number of outputs of the controller

E_{ii}, F_i, G_i, H_i are constant matrices of appropriate dimensions

The closed loop system can be obtained using the following equations:

$$\begin{aligned} y_i &= w_i = C_i x \\ u_i &= v_i = G_i z_i + H_i w_i \end{aligned} \tag{2.3}$$

The closed loop state equation then becomes:

$$S^{cl} = \left\{S_i^{cl}\right\} = \begin{bmatrix} \dot{x}_i \\ \dot{z}_i \end{bmatrix} = \begin{bmatrix} A_{ii} & B_i G_i \\ F_i C_i & E_{ii} \end{bmatrix} \begin{bmatrix} x_i \\ z_i \end{bmatrix} + \begin{bmatrix} \sum_{j \neq i} A_{ij} x_j \\ 0 \end{bmatrix} \tag{2.4}$$

Equation (2.4) gives the closed loop state coefficient matrix of the interconnected system when the *ith* generator subsystem has been fitted with a PSS. The damping of the electromechanical eigenvalues of the state coefficient matrix indicates the effectiveness of placing a PSS at the *ith* generator subsystem. If generator subsystem *j* is selected for PSS placement, the state coefficient matrix will change resulting in a different damping of the electromechanical mode.

Assume that the number of PSS that we wish to place is α. We define $G = \{1,2,\ldots m\}$ as a set containing all m generator subsystem numbers i.e. element *i* in *G* refers to the *ith* subsystem. We can construct a set β which consists of all possible combinations of α elements from the set *G* i.e.:

$$\beta = \left\{\beta_i \subset \{1,\ldots m\},\ \ card(\beta_i) = \alpha\right\},\ card(\beta) = \frac{m!}{\alpha!(m-\alpha)!} \tag{2.5}$$

where:

β_i is the *ith* element in the set β

$card\{\cdot\}$ refers to the cardinality of $\{\cdot\}$ (number of elements in the set $\{\cdot\}$)

Thus β_i is a set containing α elements. These elements correspond to generator subsystem locations. We refer to the space which is composed of the elements of β as the configuration space.

The problem that we wish to address in this paper is to find the optimal locations of PSS. This means that we need to find the set β_i which correspond to the optimal locations of the PSS. The optimal locations of the PSS are the generator subsystems at which the damping of electromechanical modes are maximized.

The two methods that we propose to determine the optimal locations, require different information about the generator control systems. In the TMC method, only the open loop

generator control system is used. No information about the PSS is required. However, using the method of Simulated Annealing, more information about the generator control system is required. In addition to the open loop generator control system, *nominal* parameters of the PSS are required for each generator control system. These PSS are tested on candidate generator subsystems in order to determine the effectiveness of the location as a site for a PSS. The *nominal* PSS parameters which are required by the method of Simulated Annealing are calculated from standard phase compensation design methods [2]. Once the optimal locations of the PSS with nominal parameters are obtained, the methods described in Chapter 4 and Chapter 5 can be used to refine the tuning of the PSS parameters.

We next present the method of Total Modified Coupling Factors and the method of Simulated Annealing.

2.3 Optimal Placement of PSS Using Total Modified Coupling Factors

In this section, we present a technique for the optimal placement of PSS using Total Modified Coupling Factors (TMC). In order to present the method based on TMC, we need to describe the concepts of Participation Factors and Total Coupling Factors.

In the next section, we describe the method of PSS placement based on Participation Factors. We then introduce the concepts of Total Coupling Factors and Total Modified Coupling Factors.

2.3.1 Participation Factors

Participation Factors provide a scale-free measure of the relative participation of each state to a particular mode. In the PSS placement problem, we are interested in investigating the relative participation of each state to the weakly damped electromechanical oscillations. Thus, we construct the Participation Vector (p_h) corresponding to the electromechanical mode (h) of interest i.e.

$$p_h = \begin{bmatrix} v_{1h} w_{h1} \\ v_{2h} w_{h2} \\ \vdots \\ v_{nh} w_{hn} \end{bmatrix} \tag{2.6}$$

where:

v_{kh} is the k*th* element of the right eigenvector v_i

w_{hk} is the k*th* element of the left eigenvector w_i

h is the electromechanical mode of interest

The Participation Vector provides information about which generators contribute the most to the damping of the electromechanical oscillation. The elements of the Participation Vector correspond to the states of the system. The structure of the Participation Vector is illustrated by the following equation:

$$p_h = \begin{bmatrix} Gen_{1h} \\ Gen_{2h} \\ \vdots \\ Gen_{mh} \end{bmatrix} \tag{2.7}$$

where Gen_{ih} is the block vector of Participation Vector elements corresponding to the states of the i*th* generator for mode h.

The elements of the Participation Vector which are of interest are those m elements that correspond to the rotor speed deviations $\Delta\omega_i$, $i = 1,...m$ for m generator subsystems. The elements which corresponds to $\Delta\omega_i$, are proportional to the amount of damping torque in the system. Thus, we can select the optimal location of the PSS as the generator subsystem which corresponds to the maximum $\Delta\omega$ element of the Participation Vector.

The Participation Factors as defined in (2.6) are calculated for a particular mode only; usually the most weakly damped electromechanical mode. This means that the Participation Factors do not take into account the effect of the PSS placement on *all* power system modes. Therefore, if we wish to determine the optimal locations of PSS for damping several modes, the method of Participation Factors cannot be used.

Due to factors such as ageing and wear of the excitation systems, the performance of the exciters may deteriorate significantly. These factors affect the performance of a PSS placed on the generator. Furthermore, certain types of exciters, such as d.c. exciters, are more suitable for PSS placement than others. For instance, generators equipped with static exciters are better for PSS placement than a.c. exciters. The Participation Factors ignores these aspects of the generator excitation system at which the PSS is to be placed.

In order to address these problems, we have developed a new method of PSS placement which takes into account the effect of a PSS on several modes as well as incorporating the effect of the type and performance of the excitation system. The method makes use of Total Modified Coupling Factors (TMC). The development of the TMC for optimal PSS placement is our main contribution in this section.

2.3.2 Total Coupling Factors

In this section, we develop a method which incorporates the effect of the PSS placement on several modes. In order to do this, we need to introduce the concept of Coupling Factors.

Coupling Factors are defined as follows:

$$C_{ij} = \frac{v_{ih} w_{ih} v_{jh} w_{jh}}{M_i M_j} = \frac{P_{ih} P_{jh}}{M_i M_j} \qquad (2.8)$$

where:

v_{ih} and w_{ih} are the right and left eigenvector elements respectively of mode h corresponding to the *ith* generator

M_i is the inertia of the *ith* generator

P_{ih} is the element of Participation Factor of mode *h* corresponding to generator i.

Note that C_{ij} are defined in terms of a generator pair *i* and *j*. The Coupling Factors multiply the Participation Factors of the *ith* generator with the Participation Factor of the *jth*. This product is inversely weighted with the product of the generator inertias M_i and M_j. Thus, the coupling factor C_{ij}, weighs the influence of stabilisers over generators *i* and *j* under excitation of mode *h*.

In order to incorporate the effect of the stabilizers over several power system modes, we introduce the concept of Total Coupling Factors. Total Coupling Factors are defined as follows :

$$TC_{ij} = \sum_{h=1}^{r} C_{ij}(h) \qquad (2.9)$$

where r is the total number of modes of interest

Therefore, the Total Coupling Factors sum the influence of the PSS under simultaneous excitation of several modes in the power system. Thus, by using TMC we can determine the optimal location of the PSS to maximise the damping of several modes.

In the next section, we modify the Total Coupling Factors to incorporate the influence of the exciter on the placement of PSS.

2.3.3 Total Modified Coupling Factors

In order to take into account the influence of the performance and type of exciter, we introduce the concept of exciter Penalty Factor (PF) in the formulation of the Coupling Factors.. The Penalty Factor incorporates an engineering judgement of the effect that the excitation system will have on the performance of a PSS. The exact value of the Penalty Factor should be obtained from a practical knowledge of the excitation system.

The Coupling Factors C_{ij} are multiplied by the Penalty Factors of the generator pair i and j to give the Modified Coupling Factors MC_{ij} . The Modified Coupling Factors are defined as follows:

$$MC_{ij} = \frac{P_{ih} P_{jh} PF_i PF_j}{M_i M_j} \qquad (2.10)$$

where:

PF_i is the Penalty Factor corresponding to the i*th* generator

PF_j is the Penalty Factor corresponding to the j*th* generator

The Total Modified Coupling Factors (TMC) sum the Modified Coupling Factors over all power system modes of interest as follows:.

$$TMC_{ij} = \sum_{h=1}^{r} MC_{ij}(h) \tag{2.11}$$

The TMC thus provides a scale-free measure of the contribution of each state to all power system modes of interest, while taking into account the influence of the excitation system. Therefore, we select the maximum value of the TMC in order to obtain the optimal PSS location.

In the next section, we demonstrate the use of TMC on a benchmark network.

2.4 Case Study Using Total Modified Coupling Factors

Case 1

The power system used in this section is a nine bus, three generator system. *Appendix E* contains the network parameters and load flow data for Case 1. Each generator was modeled with a sixth order model. The transmission network was modeled with algebraic equations i.e. the stator transients were neglected. The loads were modeled as static loads. Compared to constant current and constant power loads, the constant impedance load provides results which are conservative. For this reason, all three loads were modeled as constant impedance loads. The full description of the network can be obtained from [5].

In order to investigate the effect of the type of exciter on the PSS placement problem, we assume that generator 1 has an a.c. exciter whereas generators 2 and 3 have static exciters.

Appendix E provides the state space model of the power system considered in Case 1. The model consists of 24 states. In order to eliminate the ill-conditioned eigenvalue, we select generator 1 as a reference (the procedure of eliminating the ill-conditioned eigenvalue is provided in *Appendix A*). Thus, we reduce the order of the state space model to 23. The reduced order model is also provided in *Appendix E* together with the eigenvalues and right and left eigenvectors.

We wish to improve the damping of all the weakly damped electromechanical modes while ensuring that no other modes are destabilized. For this purpose, we wish to place two PSS at the optimal locations. Note that we cannot use Participation Factors for determining the optimal locations since more than one mode needs to be controlled.

From Table E2, we deduce that two electromechanical modes are weakly damped namely, $\lambda_1 = -0.785 \pm 7.233i$ and $\lambda_2 = -1.276 \pm 12.086i$ with damping factors of 0.108 and 0.105 respectively. In addition, there exist a mode $\lambda_3 = -0.3490 \pm 0.4395i$ which has a real part close to the imaginary axis. Thus there is a danger that this mode will be destabilized by a PSS placement scheme. We consider these three modes as critical when determining the optimal location of the PSS.

Figures 2.2 to 2.4 illustrate the response of the terminal voltage V_T due to a step in the reference voltage V_{ref} for generator 1 to 3 respectively.

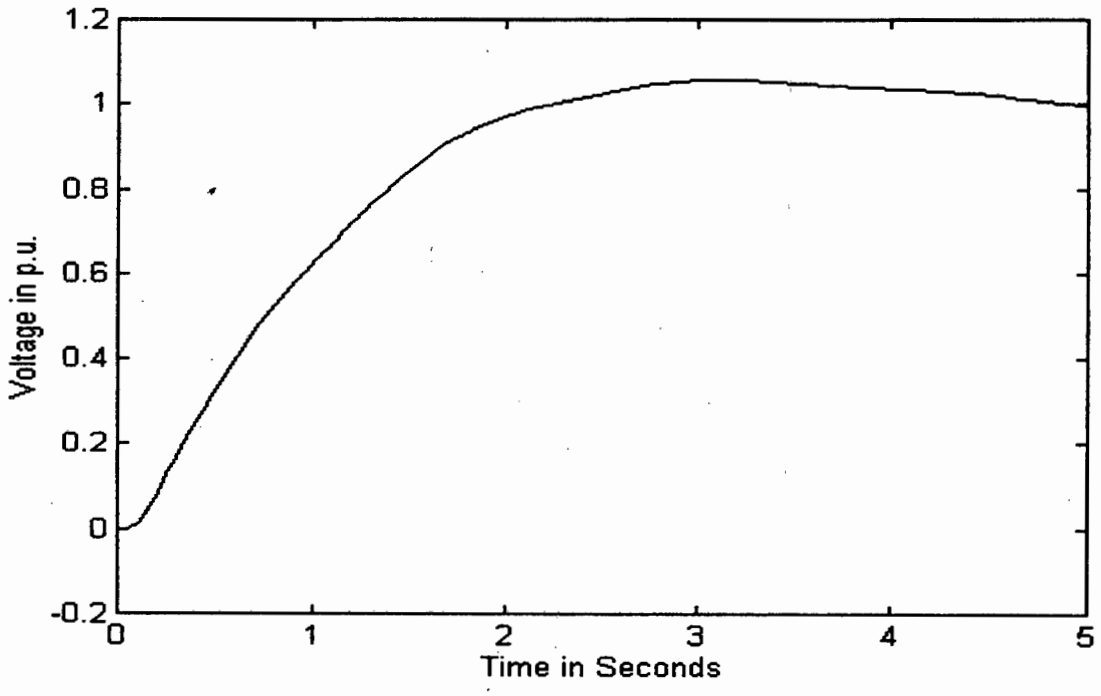

Figure 2.2: Response of Terminal Voltage at Generator 1 Due to a Step in the Reference Voltage

Figure 2.2 illustrates that the terminal voltage of generator 1 has a slow first order response reaching the set point after three seconds. This is due to the presence of a slow a.c. exciter on generator 1.

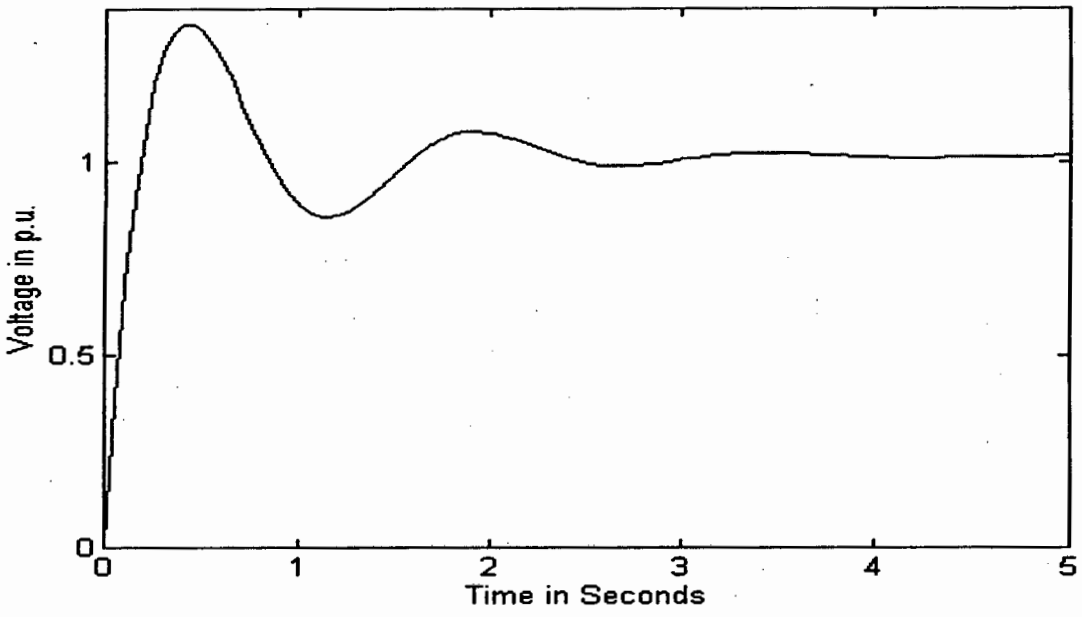

Figure 2.3: Response of Terminal Voltage at Generator 2 Due to a Step in the Reference Voltage

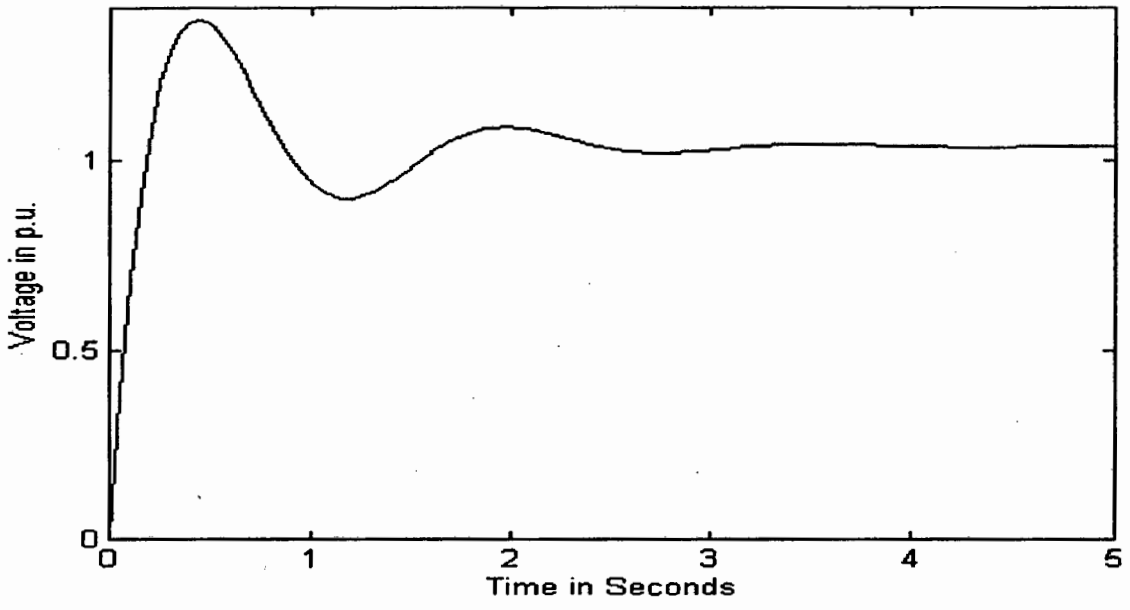

Figure 2.4: Response of Terminal Voltage at Generator 3 Due to a Step in the Reference Voltage

Figures 2.3 and 2.4 illustrate that the d.c. exciters on generators 2 and 3 result in fast second order responses of the terminal voltages.

Due to the poor performance of the excitation system of generator 1 as compared to generators 2 and 3, the penalty factor of the exciter on generator 1 was taken to be 0.5 (a.c. exciter) while the penalty factor for the exciters on generators 2 and 3 were taken to be equal to 1.0 (d.c. exciter). We wish to illustrate that the performance and type of the excitation system is critical in the determination of the optimal locations of the PSS.

From the right and left eigenvectors given in *Appendix E*, we calculate the Coupling Factors (C_{ij}) and Modified Coupling Factors using equation (2.8) and (2.10). These values are tabulated in Table 2.1.

Table 2.1 illustrates that the C_{ij} for mode 1 is the largest for generator pair 2 and 3 (0.445>0.016>0.003). This means that mode 1 is mainly due to the interaction between generators 2 and 3. Thus, for damping mode 1, we should place a PSS on either generator 2 or 3.

The value of C_{ij} for mode 2 is the largest for generator pair 1 and 2 (0.243>0.137>0.050). This means that mode 2 is mainly due to the interaction of generators 1 and 2 . Thus, for damping mode 2, we should place a PSS on either generator 1 or 2. However, since generator 1 is equipped with an a.c. exciter (with a penalty factor of 0.5), the Modified Coupling Factors give a more realistic indication of the best location of the PSS. The Modified Coupling factors indicate that, for damping mode 2, the best location of the PSS is either generator 2 or 3 (0.137>0.122 >0.025).

For damping mode 3, the Modified Coupling Factors indicate that the best location of the PSS is at either generator 2 or 3 (0.426>0.389>0.245). Thus, in order to damp mode 2 or mode 3, a PSS should be placed on either generator 2 or 3.
However, in determining the optimal PSS locations, we wish to maximise the damping effect on modes 1 and 2 while ensuring that mode 3 is not destabilised. Thus we have to investigate the Total Coupling Factors and Total Modified Coupling Factors.

Mode No	Generator Pair	C_{ij} $x10^{-3}$	PF	MC_{ij} $x10^{-3}$
1	1,2	0.003	0.500	0.002
1	1,3	0.016	0.500	0.008
1	2,3	0.445	1.000	0.445
2	1,2	0.243	0.500	0.122
2	1,3	0.050	0.500	0.025
2	2,3	0.137	1.000	0.137
3	1,2	0.777	0.500	0.389
3	1,3	0.491	0.500	0.245
3	2,3	0.426	1.000	0.426

Table 2.1: Values of Coupling Factors and Modified Coupling Factors

Generator No.	TC_{ij} $x10^{-3}$	TMC_{ij} $x10^{-3}$
1	1.580	0.790
2	2.030	1.519
3	1.564	1.286

Table 2.2: Values of Total Coupling Factors and Total Modified Coupling Factors

Table 2.2 provides the Total Coupling Factors (*TC*) and Total Modified Coupling Factors (*TMC*) corresponding to the three generators. Recall that we wish to place two PSS on the nine-bus system. Using the values of TMC from Table 2.2, we deduce that generator 2 is the most effective in controlling all three modes since the TMC is the greatest for generator 2 (1.519>1.286>0.790). The TMC also indicates that generator 3 is more effective in controlling the three modes than generator 1 (1.286>0.790). Thus, using the TMC, we conclude that the optimal locations for the two PSS are at generators 2 and 3.

On the other hand, if we use the values of TC, we obtain different 'optimal' locations for the two PSS. We wish to show that the locations provided by the TMC are the optimal locations for PSS placement as opposed to the locations provided by the TC.

From the TC values in Table 2.2, we deduce that generator 2 is the most effective in controlling all three modes since the TC is the greatest for generator 2 (2.030>1.580>1.564). The TC also indicates that generator 1 can control the three modes more effectively than generator 3 (1.580>1.564). This means that, by using TC, the 'optimal' locations of the two PSS are at generators 1 and 2.

However, we find that choosing generators 1 and 2 for placement of the two PSS is not optimal since the exciter on generator 1 is unable to provide adequate control of the three modes. This is illustrated in the simulation plots of Figures 2.5 and 2.6. Figure 2.5, illustrates the step response of the electrical power at generator 1 due to a step in the reference voltage V_{ref}, with the two PSS placed at generators 1 and 2 (from TC). The oscillations in the electrical power have a large overshoot (0.55 p.u.) and persists after 6 seconds. This is due to the poor performance of the excitation system on generator 1. Figure 2.6 illustrates the step response of the electrical power of generator 1 due to a step in V_{ref}, with the two PSS placed at generators 2 and 3 (from TMC). The oscillations in the power loop have an overshoot of 0.31 p.u. and a settling time of less than 4 seconds. Thus, the locations provided by the TMC result in an improved damping of the oscillations in comparison to the locations provided by the TC. These simulation plots verify that the method based on TMC provides the optimal locations of the PSS.

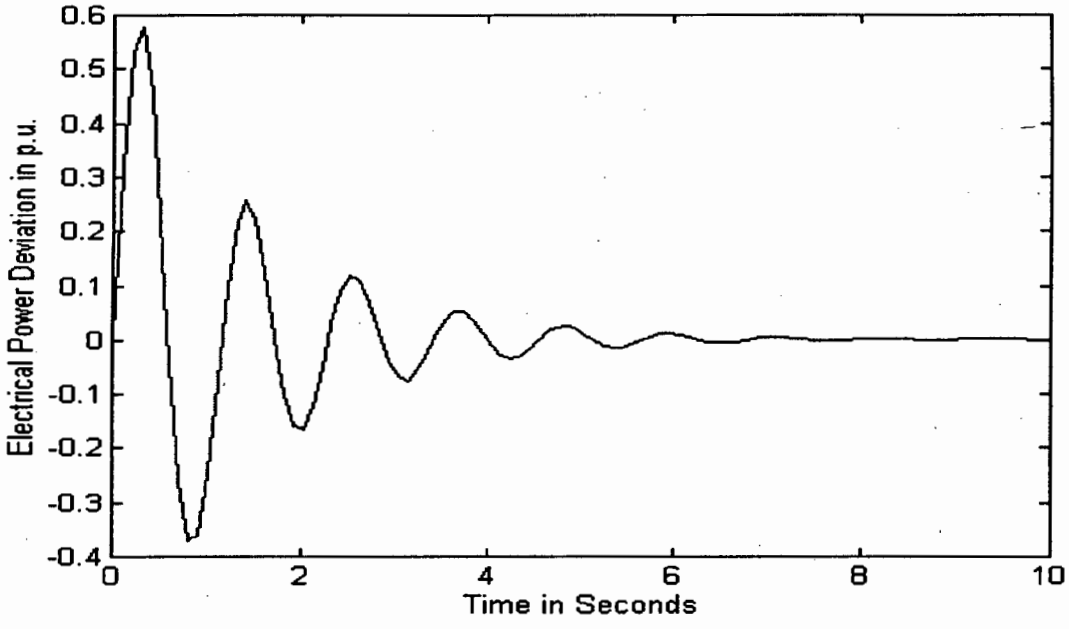

Figure 2.5: Response of Electrical Power at Generator 1 Due to a Step in V_{ref}

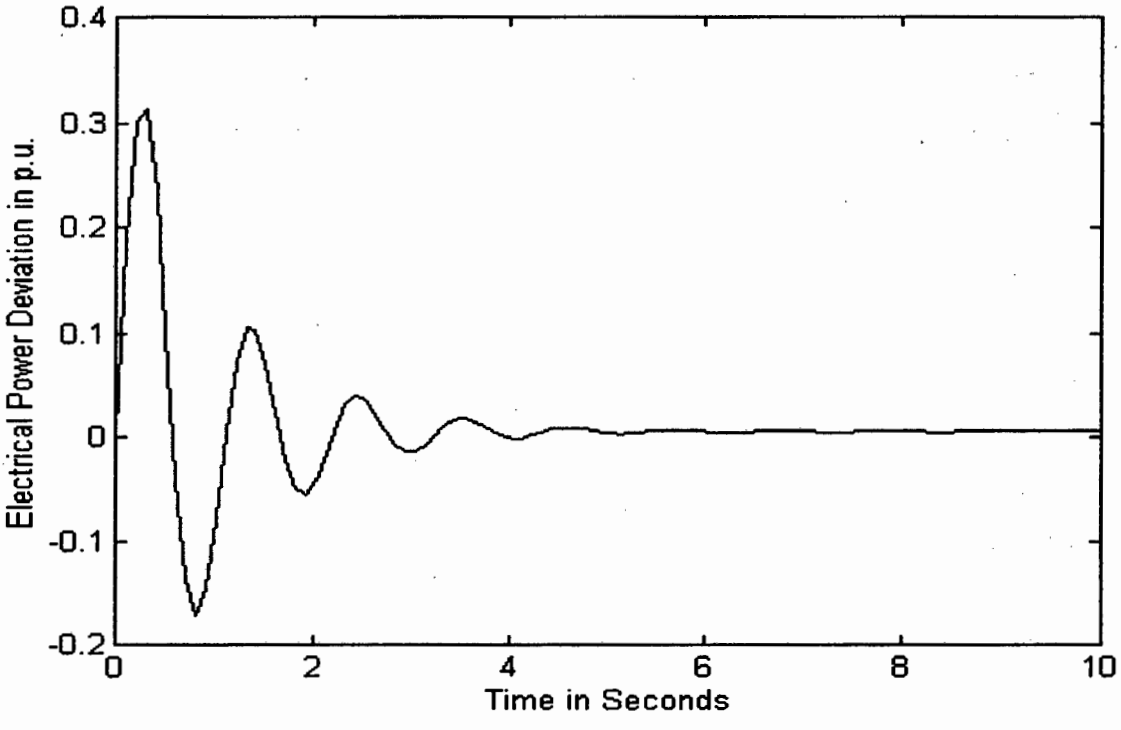

Figure 2.6: Response of Electrical Power at Generator 2 Due to a Step in V_{ref}

2.5 Optimal Placement of PSS Using Simulated Annealing

In this section, we present a new method of optimal PSS placement using Simulated Annealing.(SA). The section begins by providing a brief background to optimization by Simulated Annealing. Next, the PSS placement problem is formulated in the Simulated Annealing framework. Thereafter, the details of the Simulated Annealing algorithm is provided. The method used for calculating the nominal parameters of the PSS is then presented. Finally, the method of Simulated Annealing is applied to two test cases (Case 2 and Case 3) and the results are discussed.

2.5.1 Optimization by Simulated Annealing

Annealing is the physical process of heating up a solid to its melting point followed by cooling it down until it crystallizes into a state with a stable lattice structure. In the cooling process the stable lattice structure is formed by minimizing the lattice energy of the crystal.

Simulated annealing is a technique of combinatorial optimization which is based on the annealing process. As an optimization method, simulated annealing generates feasible solutions randomly and moves amongst these solutions using a strategy that has a high probability of leading to a global minimum.

Ever since its introduction in 1983, the simulated annealing algorithm has been applied to a large number of different combinatorial optimization problems. These include areas as diverse as operations research, VLSI design, programming code design, image processing and molecular physics [11]. In power systems it has been successfully applied to problems such as network reconfigurations, least cost distribution planning, optimal capacitor placement and unit commitment [9,10].

In the SA algorithm, all moves that reduce the objective function are accepted. Moves that increase the objective function are accepted with probability of $e^{-\Delta J/T}$ where ΔJ is the increase in the objective function and T is the temperature. Thus the acceptance criteria allows for moves that increase the objective function.

2.5.2 Simulated Annealing for PSS Placement

In this section, the PSS placement problem is formulated in the Simulated Annealing framework.

Figure 2.7 illustrates an arbitrary configuration of the system to be optimized. The zeros indicate that no PSS is at the generator while ones indicate that a PSS is being tested at this location. The numbers above the rectangle indicate the generator number .

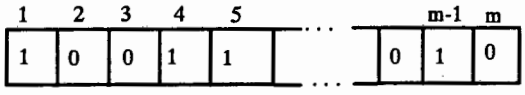

Figure 2.7: Arbitrary Configuration of the System Showing Trial Locations of PSS

An algorithm for PSS placement based on the simulated annealing technique requires the appropriate choice of the following aspects:

(a) A *configuration space* which is the set of allowable PSS placement configurations.
(b) A set of feasible moves or a *move set*
(c) A *cost function*
(d) A *cooling schedule*

Each of these will be briefly discussed in the following section.

2.5.2.1 Configuration Space (CS)

From Figure 2.7, we can deduce that, in order to define the configuration, it is necessary first to determine the number of PSS that need to be placed i.e. the number of ones in Figure 2.7.

In order to determine the minimum number of PSS that are required, we state and prove following Lemma:

Lemma 2.1: Assume that $(A_{ii}, B_i), (A_{ii}, C_i)$ *are completely controllable and observable respectively. The minimum (integral) number of decentralized controllers required to move p poles freely in the complex plane is given by:*

$$\alpha = \sup_{\mathbf{I}}(\theta = \frac{2p}{2q+1}) \tag{2.12a}$$

where α *is the integral number of controllers*

p is the number of poles that are to be moved

q is the order of each controller.

$\mathbf{I}$ *is the set of integers*

θ *is the possibly non-integral number of controllers*

Proof: Consider the n-dimensional interconnected power system given by equation (2.1). Furthermore consider decentralized controllers of the form $K_i(s) = \frac{k_i(1+sT_{i1})}{(1+sT_{i2})}$

The closed loop state space coefficient matrix is given by equation (2.4). The order of the closed loop is $\theta q + n_i g$ where g is the total number of generators. Since only p of these poles need to be assigned, we know that $p < \theta q + n_i g$. The full state space description of the system can be written as:

$$\begin{bmatrix} \dot{x} \\ \dot{z} \end{bmatrix} = [A] \begin{bmatrix} x \\ z \end{bmatrix} \tag{2.12b}$$

where $[A]$ contains the unknown parameters $k_1 \ldots k_q, T_{i1} \ldots T_{iq}$

Since p pole location are known, the following nonlinear system of equations results:

$$\begin{aligned} &\det(\lambda_i I - A) = 0 \\ &i = 1 \ldots p \\ &\lambda_i \in \mathbf{C} \end{aligned} \tag{2.13}$$

The system of equations described by (2.13) has *2p* equations with real coefficients. This system of equations can be solved using the Newton Raphson method. A necessary condition that the system can be solved is that the number of equations is equal to the

number of unknown parameters. This condition is a necessary condition for the Jacobian matrix to be nonsingular i.e.:

$$2p = (2q+1)\theta \tag{2.14}$$

This completes the proof.

Assume that $(A_{ii}, B_i), (A_{ii}, C_i)$ are stabilizable and reachable respectively. Then it is clear from the preceding discussion that the (integral) number of controllers required for *stabilizing* the system is given by:

$$\alpha = \sup_{\mathbf{I}}(\theta = \frac{2p_u}{2q+1}) \tag{2.15}$$

where p_u is the number of unstable poles.

It is thus necessary to determine the number of poles which need to be damped from which the number of PSS required to stabilize the system can be calculated.

The *configuration space* β is defined as the set of allowed network configurations over which the optimal system configuration is to be searched for. This would be all the generators on which it is feasible to place PSS. Only the generators which possess static exciters are thus included in the configuration space.

2.5.2.2 Move Set

When a change is applied to achieve a new system configuration, only one position of the PSS is altered i.e. both a zero and a one are changed in Figure 2.7. The placement or removal of a PSS would change the system A matrix and thus the resulting eigenvalues. Compound moves (moves that consider changing the location of more than one PSS at a time) are not considered due to the complexities in calculating the new system configuration.

2.5.2.3 Objective Function

The objective in the PSS placement problem is to *maximize* the damping of the electromechanical modes. Thus the objective function (which is to be maximized) for the optimal placement is defined as:

$$J = \min_i \left(\frac{-\sigma_i}{\sqrt{\sigma_i^2 + \omega_i^2}} \right), \quad i = 1,...m \tag{2.16}$$

where $\lambda_i = \sigma_i + j\omega_i$ denotes the i*th* eigenvalue

This is the computationally intensive part of the problem as the objective function for each new configuration has to be computed. Thus for each iteration, the electromechanical modes need to be calculated in order to construct the new value of the objective function.

2.5.2.4 Cooling Schedule

The temperature parameter T has to be gradually lowered to zero asymptotically according to predefined cooling schedule. A geometric cooling schedule is used i.e. $T_{t+1} = \gamma\ T_t$ where $0 < \gamma < 1$ is a control parameter. We selected the value of $\gamma = 0.95$. The initial temperature T_0 should be chosen high so that the initial stabilizers are randomly placed. The final temperature T_f has to be specified as a stopping criterion. The value of T_0 was selected as 100 and the final value T_f was chosen as 10. In the PSS placement problem, the temperature relates to the sensitivity of the damping with respect to the placement of a PSS at each generator subsystem. As such, the temperature is a variable which isolates the machines that are significantly involved in the most weakly damped electromechanical mode. In this way the temperature acts as a 'filter' for rejecting generators which are not involved in the weakly damped mode.

2.5.3 The Simulated Annealing Algorithm

The simulated annealing algorithm is illustrated in the flowchart of Figure 2.8.

The SA algorithm is composed of two loops; an outer temperature loop and an inner Monte Carlo loop. In the outer loop, the system to be optimized starts at a high temperature which implies that all the particles of the system move around freely. The temperature is then gradually lowered by the factor γ until the system 'freezes' at which point all the particles are virtually fixed. The system is said to be 'frozen' at the final temperature T_f. This frozen configuration will be close to the optimal configuration of the system. The temperature stop criterion is determined by the maximum number of temperature loop iterations I_M and the temperature decrement γ.

At each temperature, the *Monte Carlo algorithm* (inner loop) is used to simulate the system. The Monte Carlo loop allows the objective function to settle to a value at the fixed temperature. Each iteration in the Monte Carlo loop involves the selection of a move which alters the system from one configuration state to another. Moves are chosen as defined by the move set.

The acceptance criteria of the loop is dependent on whether the objective function is increased or decreased. If the new configuration causes a decrease in the value of the objective function, the new configuration is accepted. If however the value of the objective function is increased, the new configuration is accepted/rejected using the following procedure:

> *The Boltzmann factor $e^{-\Delta J/T}$ is first calculated and a random number r uniformly distributed in the interval [0,1] is then chosen. If $r < e^{-\Delta J/T}$, the uphill move is accepted; otherwise it is discarded and the configuration before this move is used for the next step. This means that the system will accept uphill moves with a reasonable probability as long as these moves do not increase the objective function more than the temperature increases the objective function.*

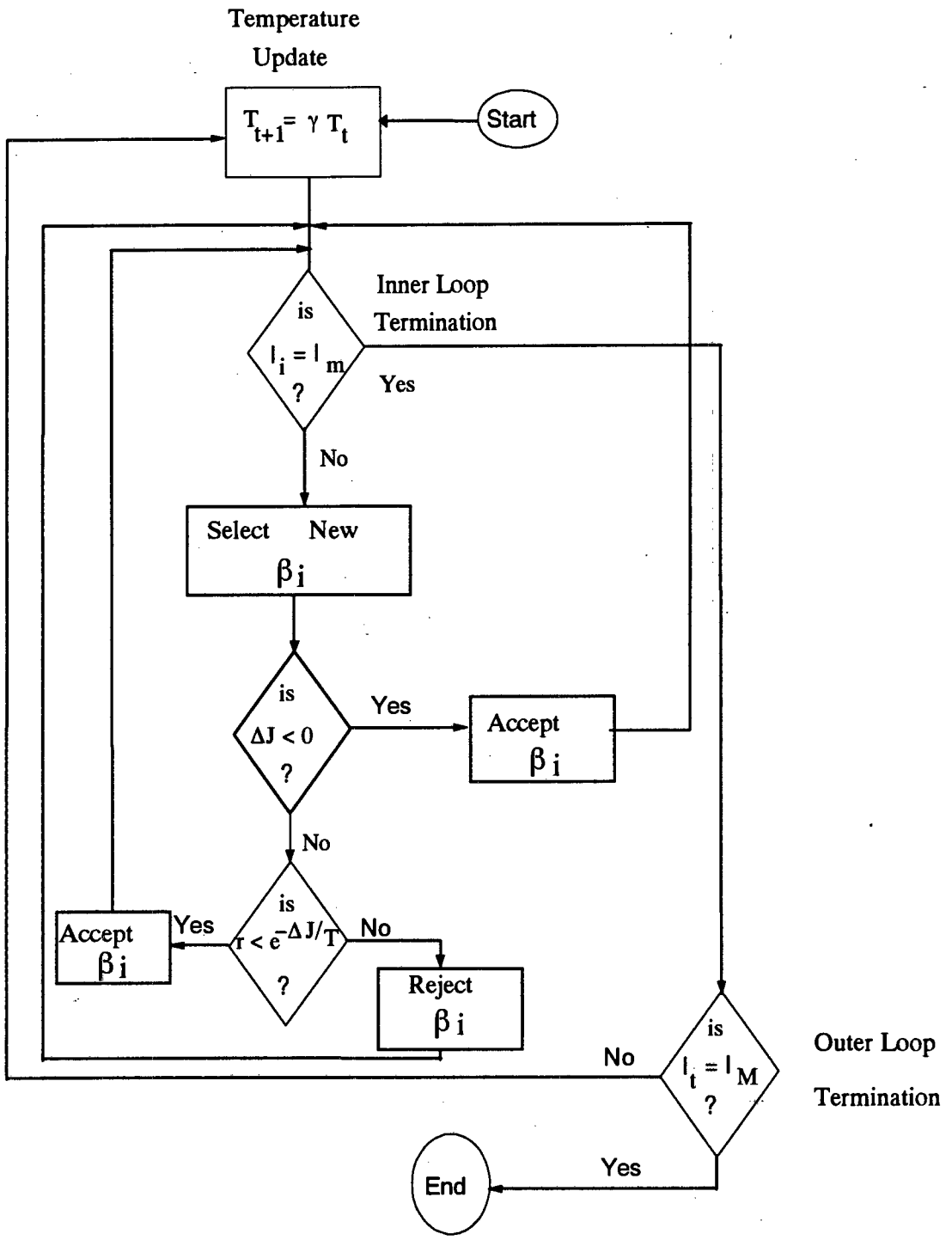

Figure 2.8: Flowchart of the Simulated Annealing Algorithm

Note that at very high temperatures, the SA algorithm accepts all moves and searches broadly in the configuration space. This means that even generators which have a small effect on the damping is selected i.e. the 'filter' acts as an all-pass filter. At very low temperatures, the algorithm only accepts downhill moves and behaves like a greedy search algorithm. Thus at low temperatures, only the generators that are critically involved in the most weakly damped mode are selected i.e. the 'filter' acts as a band-pass filter. It is due to the probabilistic selection rule that the process can always get out of local minimum (where it could get trapped) and proceed to the desired global minimum. The inner loop is terminated by specifying a maximum number of loop iterations I_m.

2.5.4 Calculating the Nominal PSS Parameters

At the end of section 2.2, we stated that the nominal parameters of the PSS are required. In this section we present the method that we have used in obtaining these parameters.

In order to obtain the parameters of the PSS, the transfer function of each generator control system has to be obtained. This model is obtained by a procedure of model reduction.

The reduced order model for generator i is obtained as follows. Consider the state space description of the system without control and output. In order to obtain the equivalent model for subsystem i, rearrange the A matrix so that the states corresponding to subsystem i appear first. This means that we divide the network into two sub-networks namely (1) *generator subsystem i* and (2) *the rest of the network.* Thus we can write the system as follows:

$$\dot{x} = \begin{bmatrix} A'_{i11} & \phi_i \\ \mu_i & \chi_i \end{bmatrix} \begin{bmatrix} x'_1 \\ x'_2 \end{bmatrix} \qquad (2.17)$$

where:

x'_1 is the vector of states belonging to generator subsystem i.

x'_2 is the vector of states belonging to the rest of the system.

$$\phi_i = \begin{bmatrix} A_{12} & \cdots & A_{1m} \end{bmatrix}$$

$$\mu_i = \begin{bmatrix} A_{21} & \cdots & A_{m1} \end{bmatrix}^T$$

$$\chi_i = \begin{bmatrix} A_{22} & \cdots & A_{2m} \\ \cdots & \cdots & \cdots \\ \cdots & \cdots & \cdots \\ A_{m2} & \cdots & A_{mm} \end{bmatrix}$$

In order to obtain the equivalent reduced model of the system, let all the states $\dot{x}_2 = 0$. This means that we only consider the dynamics of subsystem i while ignoring the dynamics of all the other generator subsystems. This is equivalent to reducing every generator in the rest of the system to an infinite bus.

Thus by algebraic rearrangement, the equivalent model of the generator can be obtained as follows:

$$\dot{x}_i' = (A_{i11}' - \phi_i[\chi_i]^{-1})x_i' \qquad (2.18)$$

This procedure is performed for all generator subsystems which results in m reduced models. Once the equivalent state space representations of each machine is obtained, single variable control theory can be used to calculate the nominal parameters of the PSS for each subsystem.

2.6 Case Studies Using Simulated Annealing

Two networks were used to investigate the effectiveness of using simulated annealing for optimal placement. The first network (Case 2) was a seven-bus four-generator network. The network configuration, network parameters and generator data are provided in *Appendix G*. Case 2 was chosen in order to demonstrate the advantages that the method of PSS placement using Simulated Annealing has over conventional methods. The second network (Case 3) was a 35-bus equivalent of the South African grid. This system consists of 65 transmission lines, 35 buses and 5 transformers. The aim of Case 3 was to investigate the computational feasibility of the proposed method on a large network. The results obtained for both networks will now be discussed:

Case 2

Appendix G gives the details of the seven-bus network used in Case 2. From Table G5 we note that the network has an unstable pair of eigenvalues ($\lambda = 0.54162 \pm j5.5296$) which is associated with the electromechanical oscillations. From Tables G6 and G7, we also note that the network has a pair of non-minimum-phase zeros for eight output signals. Thus, the open loop of the seven-bus network is an unstable, non-minimum phase system. This complicates the problem of damping the electromechanical modes since the right-half plane zero attracts the unstable pole under feedback control. In [7], it was demonstrated that by using participation factors, it is not possible to obtain an optimal placement scheme which stabilizes the system. We will demonstrate that, by using Simulated Annealing, we can obtain a placement scheme which stabilizes the system and maximizes the damping of the electromechanical modes.

In order to apply Simulated Annealing to the seven-bus system, we need to obtain the nominal parameters of PSS for each of the four generators. The nominal PSS parameters were obtained using phase-compensation tuning methods for the four generator subsystems as outlined in Section 2.5.4. We selected ΔQ_{el} as the feedback signal for all generators. In Chapter 3, we will demonstrate that ΔQ_{el} is in fact the best signal to use in this case. The nominal controller parameters are shown in Table 2.3.

Gen. No.	K	T_1	T_2
1	0.75	0.0080	0.53
2	0.80	0.0075	0.60
3	0.76	0.0072	0.55
4	0.70	0.0071	0.55

Table 2.3: Nominal PSS Parameters for Case 2

We wish to find an optimal placement scheme which stabilizes the network, i.e. we wish to move the two unstable poles into the left half plane. Using equation (2.15) two of the four possible PSS are to be placed in order to stabilize the system $(p_u = 2, \theta = \frac{4}{3}, \alpha = 2)$.

Using the method of simulated annealing, the PSS were placed at generators 3 and 4. The unstable eigenvalues was moved to a stable location at $\lambda = -0.356 \pm j5.861$.

Figure 2.9 to 2.12 illustrate the closed loop response with the two PSS placed at generators 3 and 4.

Figure 2.9 is a plot of the electrical power P_{el} of Generator 1 due to a step in the reference voltage Vref. We note that the system is stable but the oscillations are weakly damped and persist after 25 seconds. However, the damping can be further improved by finer adjustment of the parameters using the methods in Chapter 4 and Chapter 5.

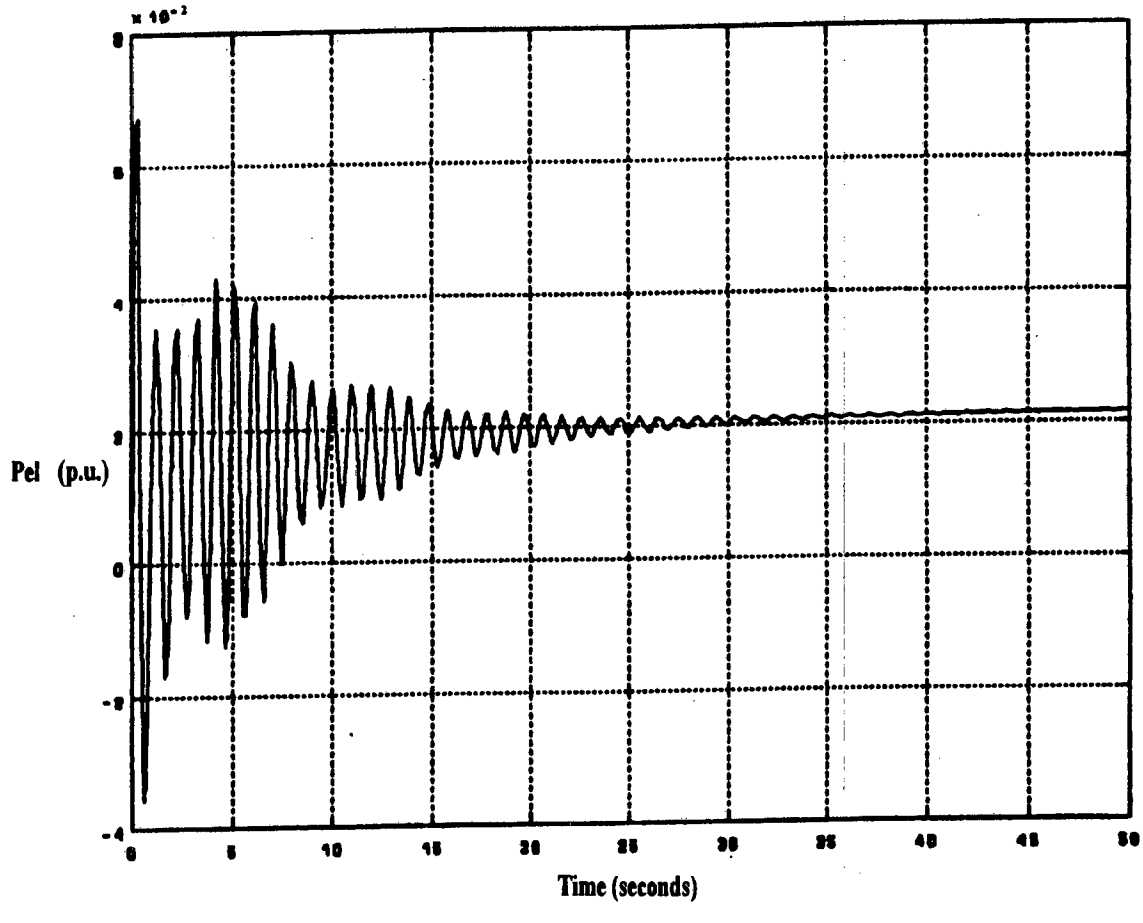

Figure 2.9: Plot of Electrical Power P_{el} of Generator 1 Due to a Step in the Reference Voltage V_{ref}

Figure 2.10 is a plot of the electrical power P_{el} of Generator 2 due to a step in the reference voltage V_{ref}. We note that the system is stable with the oscillations are persisting after 15 seconds. However, the damping can be further improved by finer adjustment of the parameters using the methods in Chapter 4 and Chapter 5.

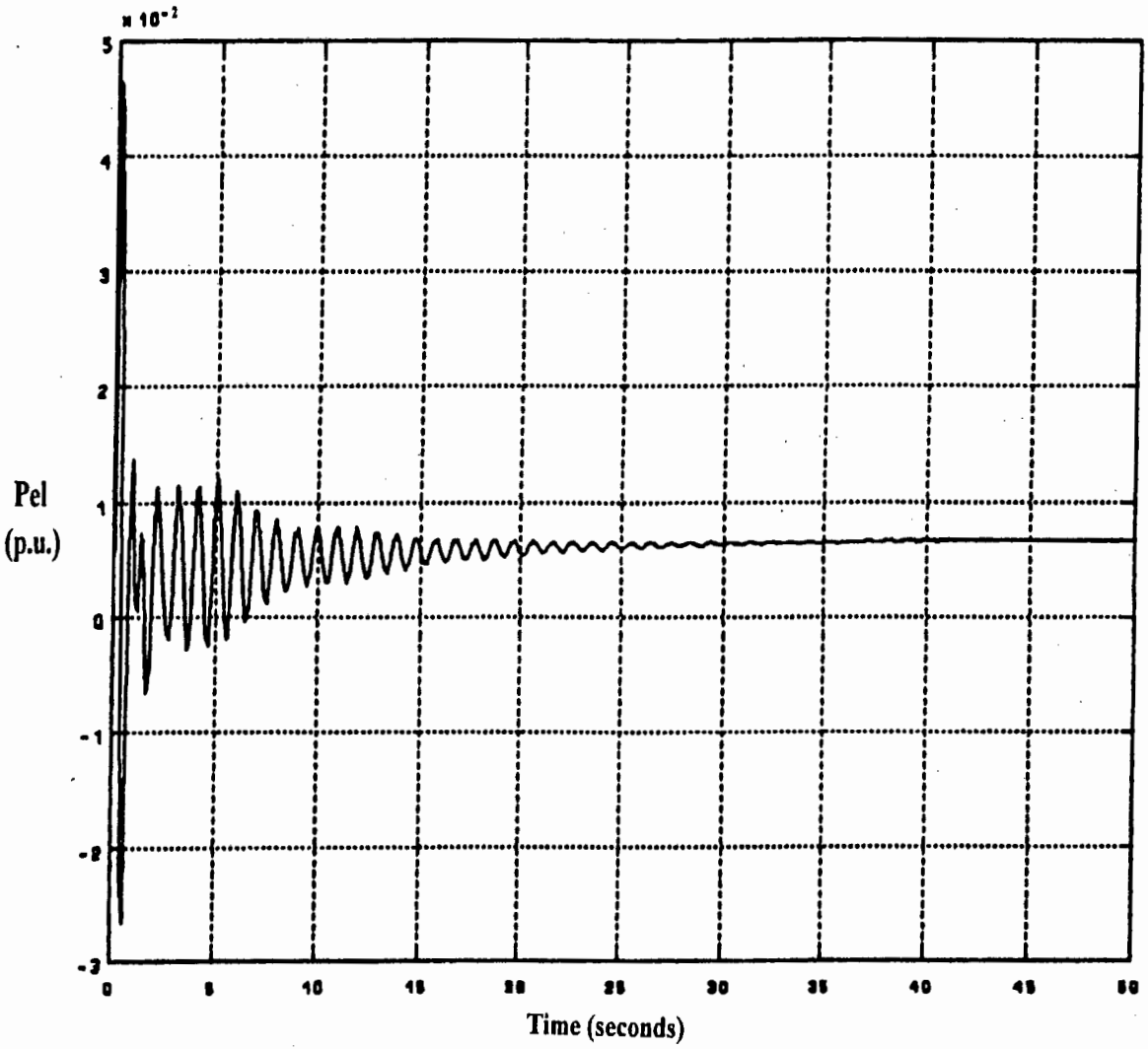

Figure 2.10: Plot of the Electrical Power P_{el} of Generator 2 Due to a Step in the Reference Voltage V_{ref}

Figure 2.11 is a plot of the electrical power P_{el} of Generator 3 due to a step in the reference voltage V_{ref}. We note that the system is stable with the oscillations are persisting after 15 seconds. However, the damping can be further improved by finer adjustment of the parameters using the methods in Chapter 4 and Chapter 5.

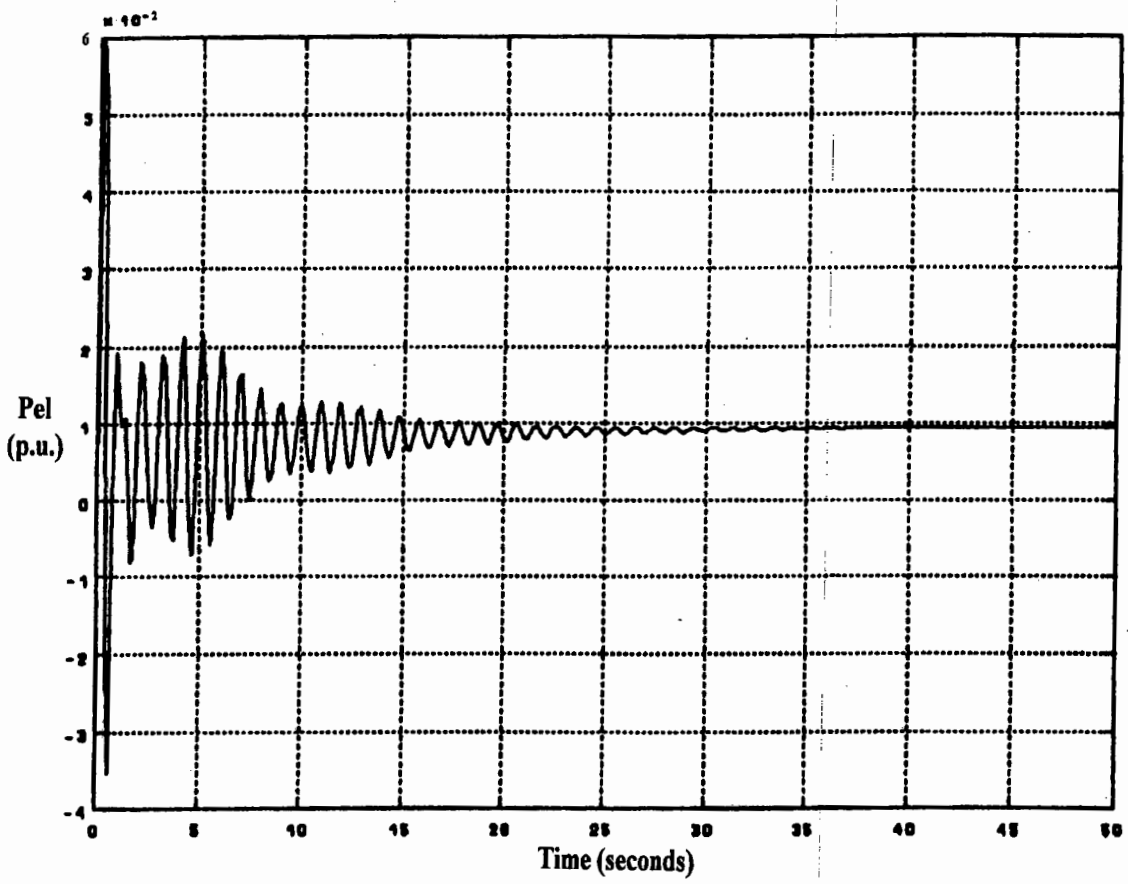

Figure 2.11: Plot of the Electrical Power P_{el} of Generator 3 Due to a Step in the Reference Voltage V_{ref}

Figure 2.12 is a plot of the electrical power P_{el} of Generator 4 due to a step in the reference voltage V_{ref}. We note that the system is stable with the oscillations are persisting after 20 seconds. However, the damping can be further improved by finer adjustment of the parameters using the methods in Chapter 4 and Chapter 5.

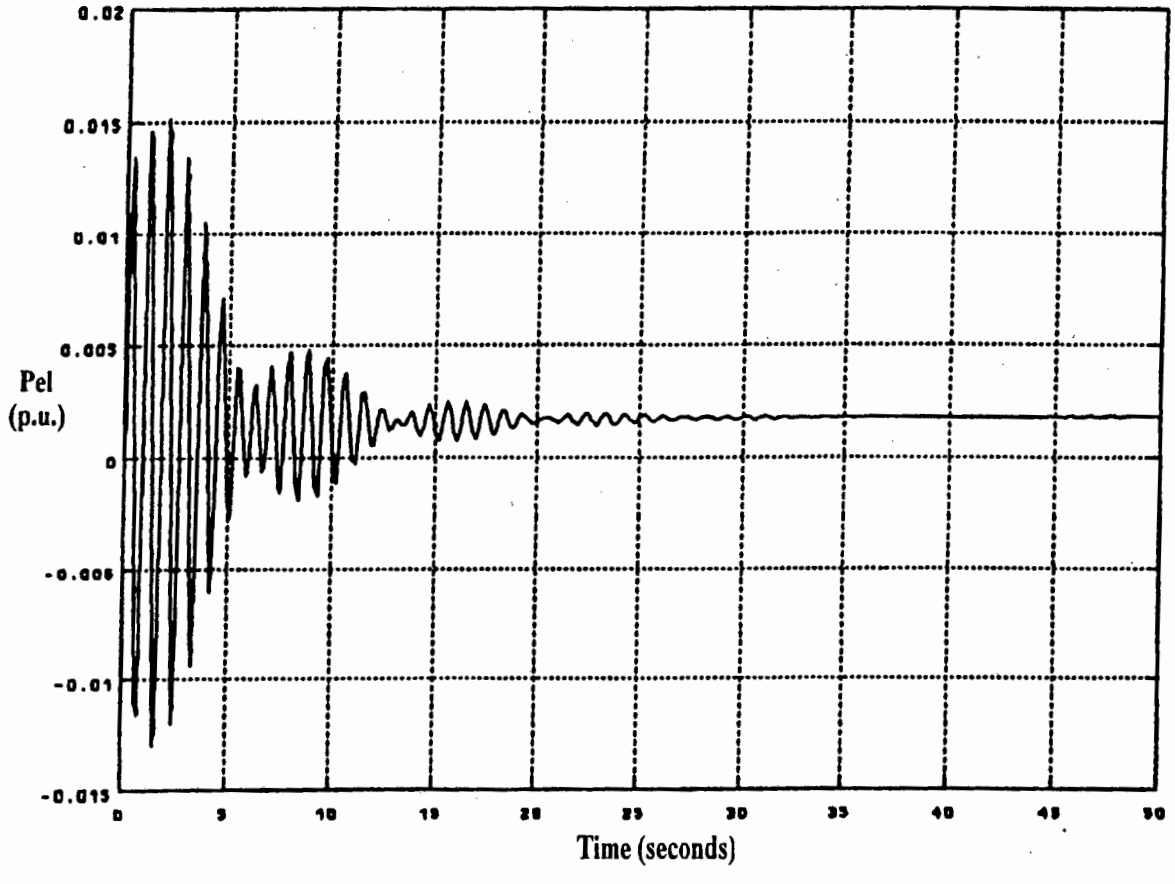

Figure 2.12: Plot of the Electrical Power P_{el} of Generator 4 Due to a Step in the Reference Voltage V_{ref}

In order to verify that the results obtained from SA are indeed the optimal locations for the PSS, we perform an exhaustive search for all possible locations. Since there are four generators in the system and we wish to place two PSS, there are six possible locations. From equation (2.5), we can obtain the configuration space $\beta = \{\beta_1, \beta_2, \beta_3, \beta_4, \beta_5, \beta_6\}$ where $\beta_1 = \{1, 2\}$, $\beta_2 = \{1, 3\}$, $\beta_3 = \{1, 4\}$, $\beta_4 = \{2, 3\}$, $\beta_5 = \{3, 4\}$ and $\beta_6 = \{2, 4\}$. Figure 2.13 illustrates the values of the objective function over the elements of set β. The pair of numbers above the X's indicate the generator pair which corresponds to the value of the objective function.

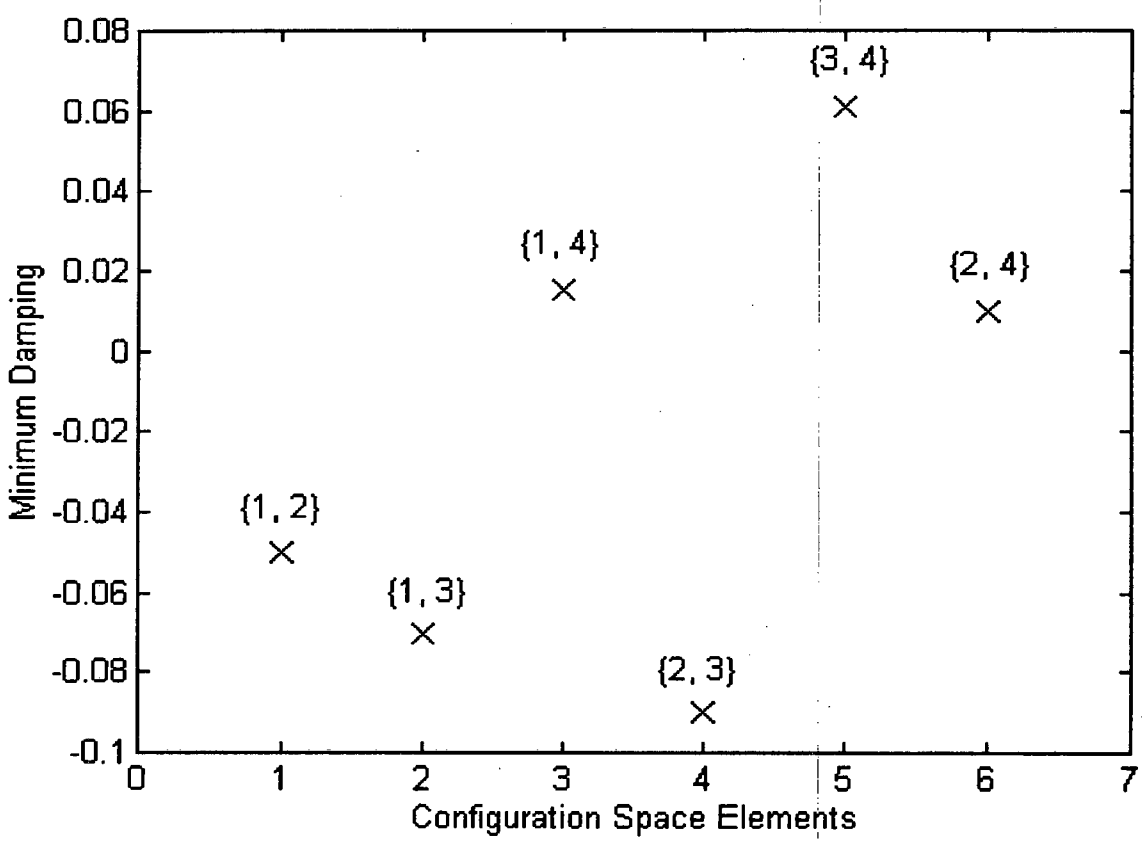

Figure 2.13: Values of Objective Function over the Elements in β

Figure 2.13 illustrates that the objective function is a nonlinear function over the elements of the configuration space β. From Figure 2.13 we can deduce that the optimal locations of the PSS is at generators 3 and 4 since the damping is maximized for these locations.

These locations correspond to the locations obtained from SA. Thus, the method based on SA provides the optimal solution.

Case 3

Figure 2.14 illustrates the open loop eigenvalue plot of the 35-bus, ten-machine system.

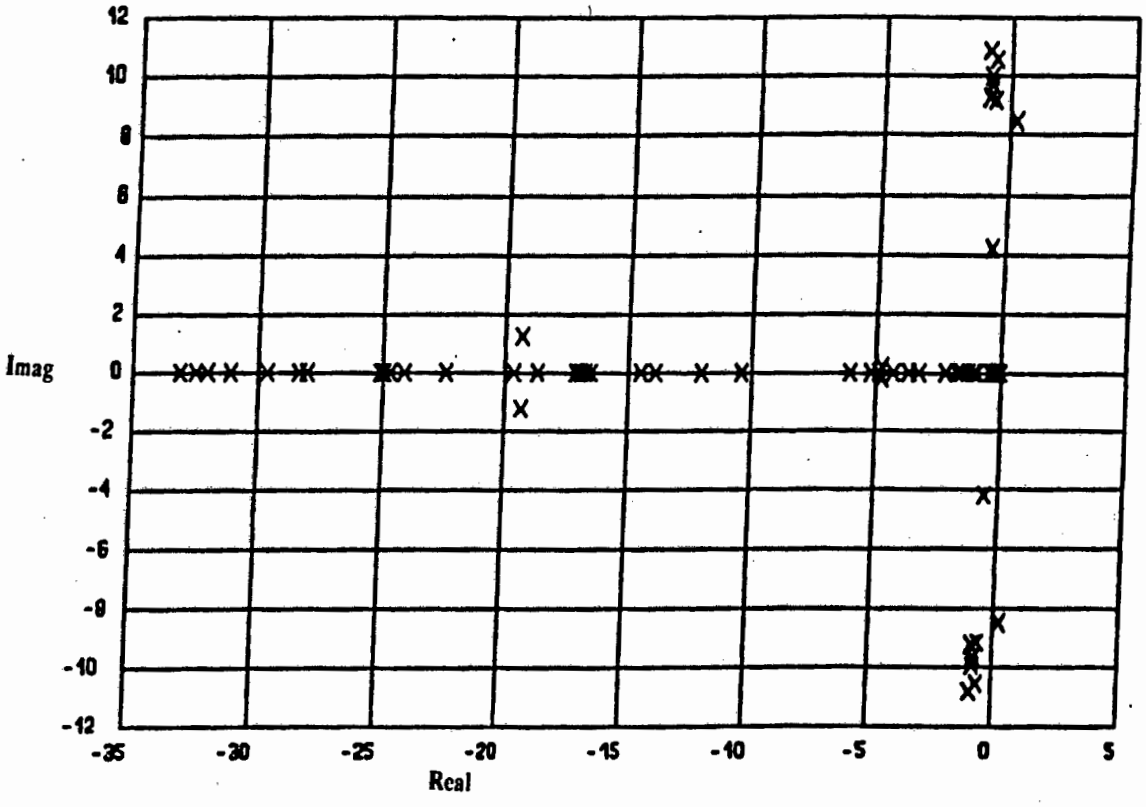

Figure 2.14: Eigenvalue Plot of the Open Loop of the 35-Bus System

From Figure 2.14 we note that one pair of eigenvalues ($\lambda = 0.354 \pm j9.378$) is in the right-half plane (unstable) and several others are weakly damped.

The nominal PSS parameters were obtained using phase-compensation tuning methods for the ten generator subsystems as outlined in Section 2.5.4. Table 2.4 gives the values of the nominal PSS parameters.

Gen. No.	K	T_1	T_2
140	4.3	0.135	0.05
165	1.76	0.295	0.07
170	7.89	0.393	0.03
190	5.67	0.233	0.04
195	0.43	0.126	0.08
200	0.67	0.205	0.06
205	2.34	0.435	0.05
220	4.1	0.123	0.04
1180	3.5	0.245	0.07
1325	0.45	0.200	0.08

Table 2.4: Nominal PSS Parameters for Case 3

Using equation (2.12a), we find that of the ten possible PSS, only five need to be placed $(p = 7, \theta = \frac{14}{3}, \alpha = 5)$. From equation 2.5 we know that the set β has 210 elements. Therefore it is not feasible to perform an exhaustive search for this network.

The SA algorithm was applied to this system and the locations were at generators 165, 195, 200, 205 and 220 (for propriety reasons, the details of these generator subsystems cannot be provided). The solution which was obtained required 65 iterations.

Figure 2.15 shows the closed loop eigenvalue plot of the system. It can be seen that the system has been stabilized with the PSS placed at the four generators.

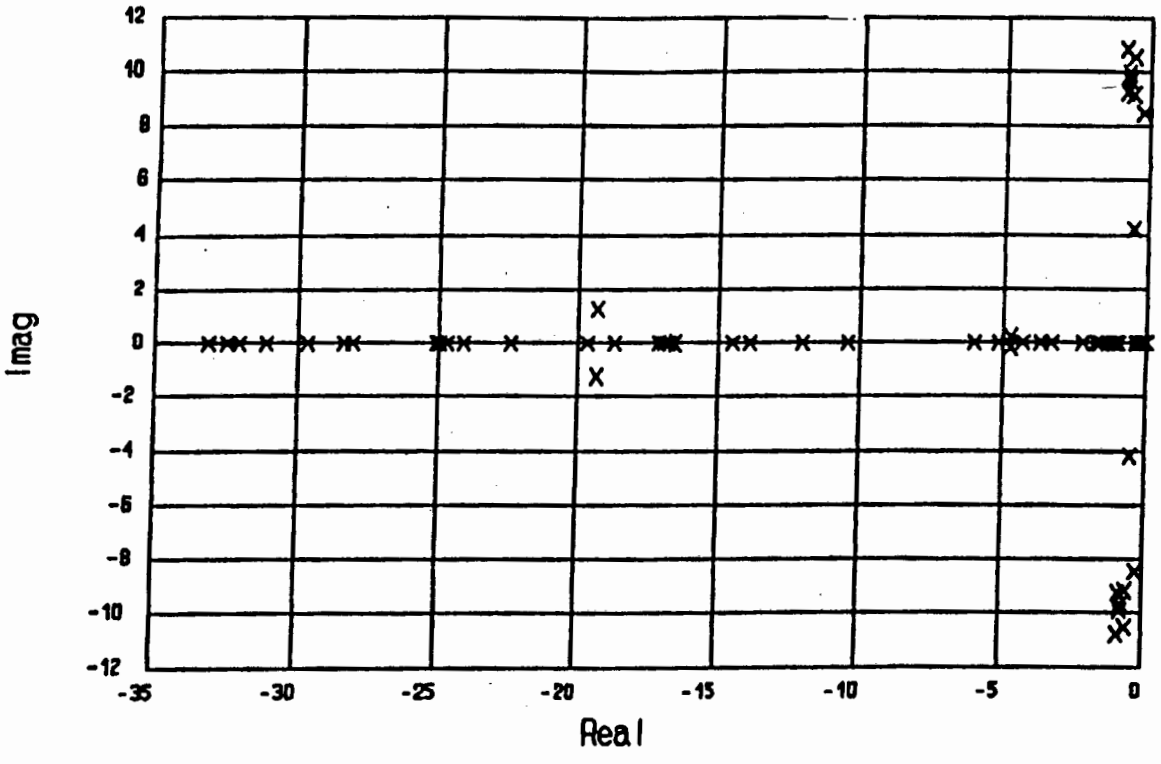

Figure 2.15: Closed Loop Eigenvalue Plot of 35-Bus System

Figures 2.16 to 2.19 are time domain simulation plots of the closed loop system. The plots illustrate the response of electrical power due to a step in the reference voltage for generators 165, 195, 205, and 220 respectively. From the simulations it can be deduced that the system is stabilized with the PSS at these locations. The system damping can be further enhanced by refined tuning of the controller parameters.

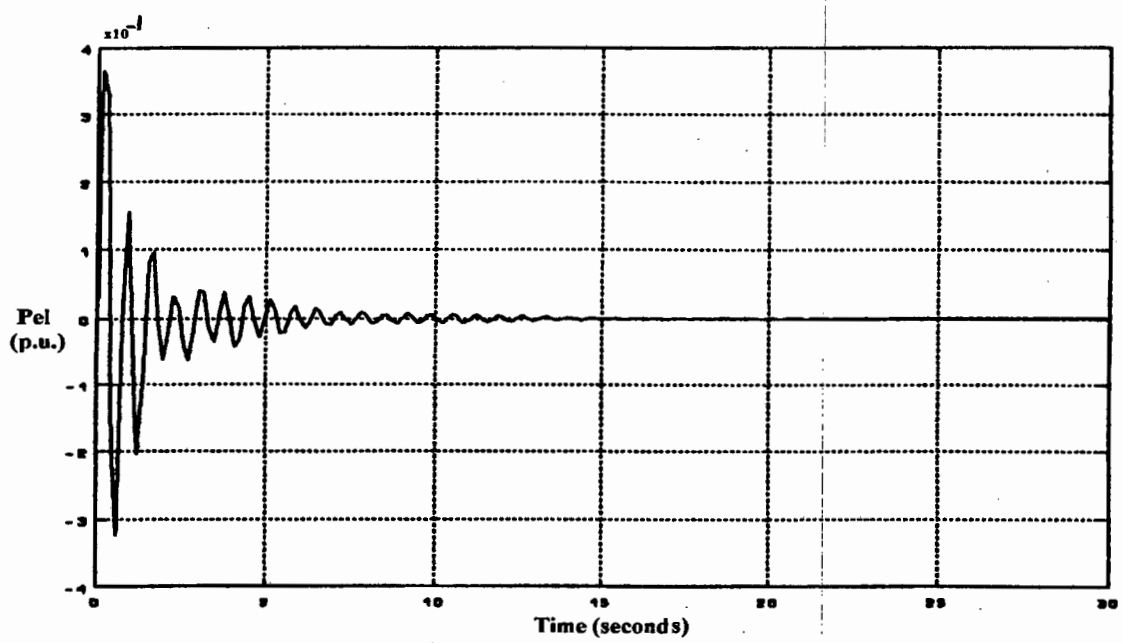

Figure 2.16: Response of Electrical Power of Generator 165 Due to a Step in the Reference Voltage

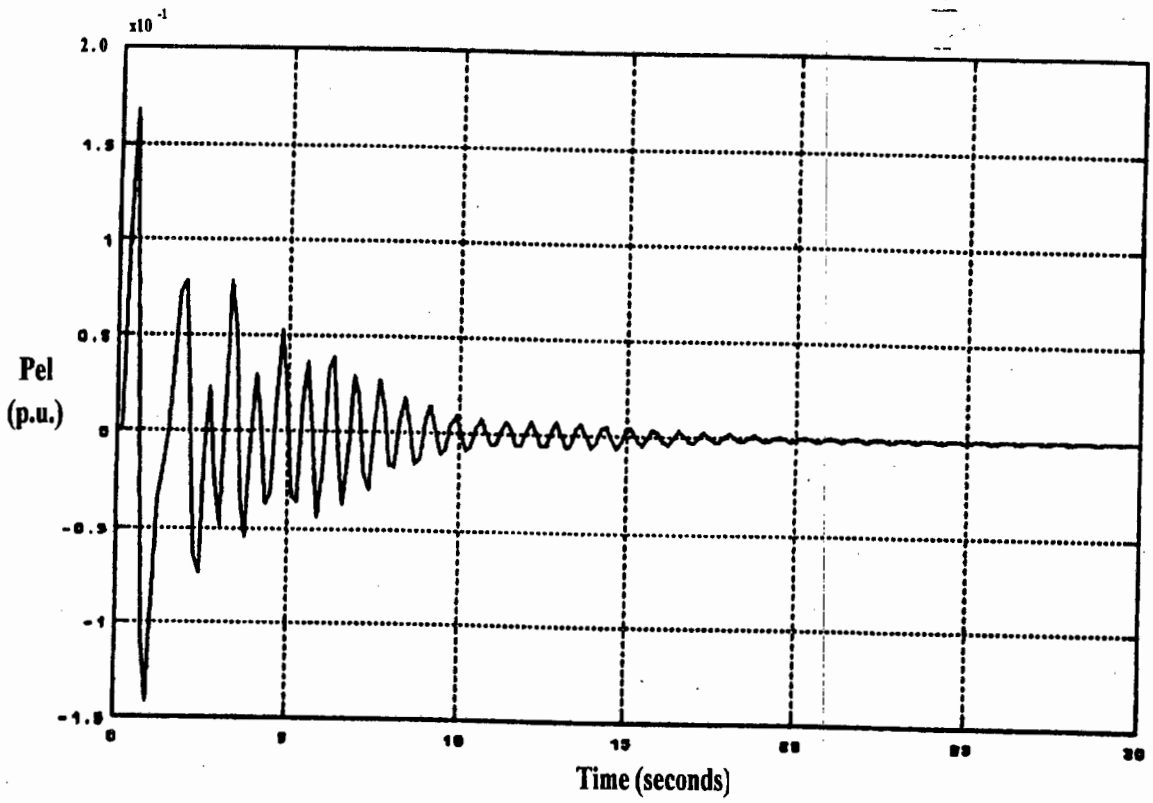

Figure 2.17: Response of Electrical Power Deviation of Generator 195 Due to a Step in the Reference Voltage

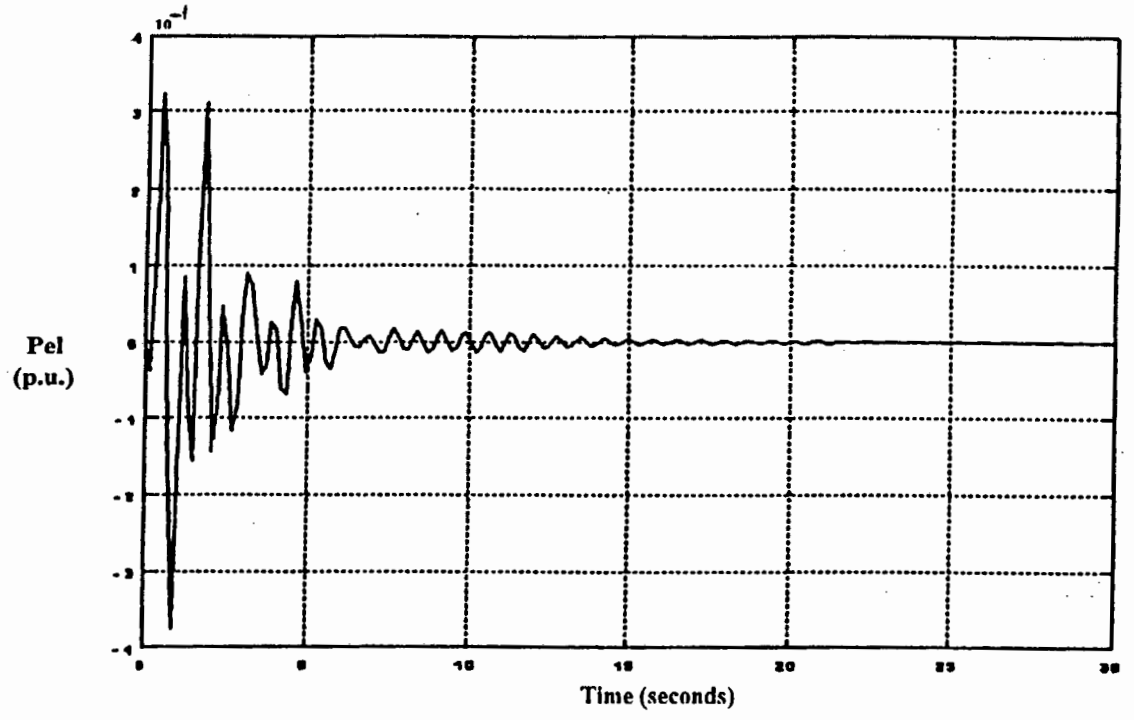

Figure 2.18: Response of Electrical Power Deviation of Generator 205 Due to a Step in the Reference Voltage

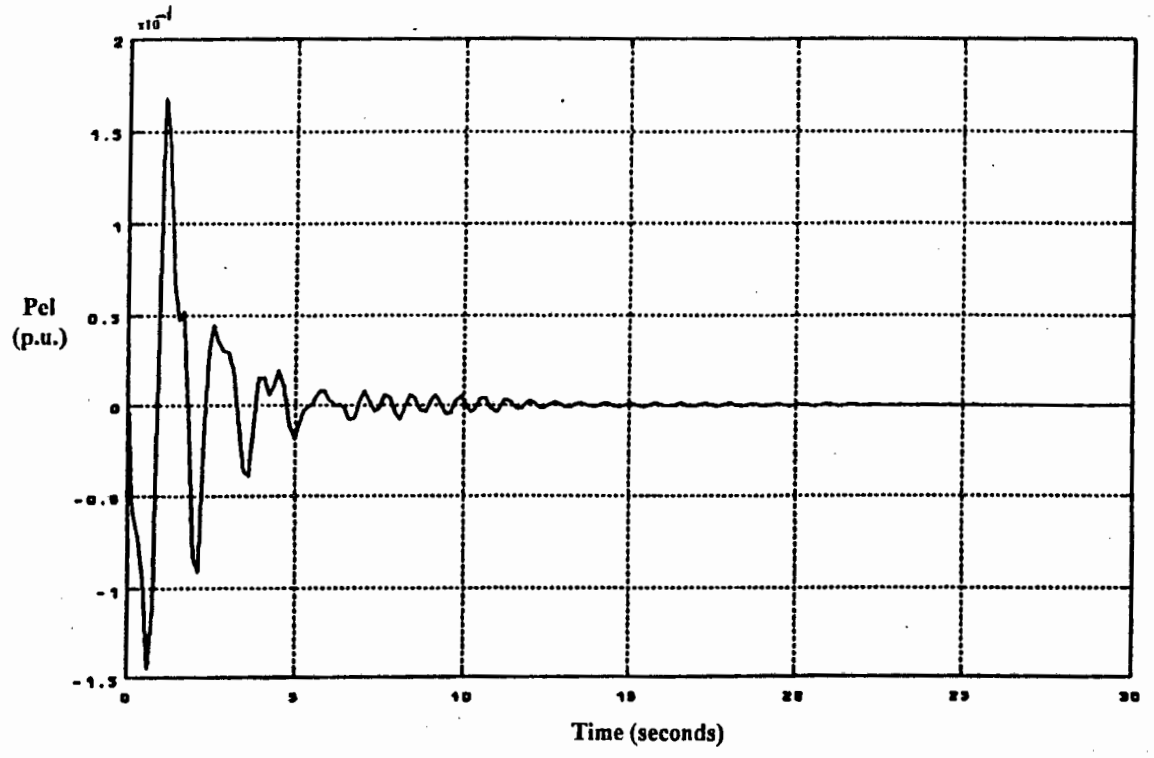

Figure 2.19: Response of Electrical Power Deviation of Generator 220 Due to a Step in the Reference Voltage

2.6 Conclusions

In this chapter, two methods for placement of PSS were presented. The first method was based on Total Modified Coupling Factors (TMC). The TMC is a measure of the damping influence of several PSS on all power system modes. The TMC takes into account the effect of one PSS on another. By incorporating an exciter penalty factor, TMC includes the effect of the performance and type of excitation system which is present on each generator being considered for placement.

The second method was based on formulating the PSS placement problem as a discrete nonlinear optimization problem. The solution of the optimization problem was obtained by means of the method of Simulated Annealing. The method of Simulated Annealing requires PSS with nominal parameters for determining the optimal locations of the PSS. The PSS placement is performed simultaneously for all PSS. Only generators with acceptable excitation systems are included in the optimization search space. Using the method of Simulated Annealing, a placement scheme is obtained which guarantees that the undesired poles can be controlled with the available finite control energy. Finally, since the placement problem is formulated as a discrete nonlinear optimization problem (with maximization of electromechanical mode damping as the objective), the nonlinear nature of the problem is taken into account. As a result of the nonlinear problem formulation however, the method based on Simulated Annealing is computationally more intensive than the method based on TMC.

References

[1] Hsu Y., Chen C, "Identification of Optimum Location for Stabiliser Application Using Participation Factors." *IEE Proc.*, Vol. 134, Pt. C, No 3, pp.238-234.

[2] Martins N., Lima L., "Eigenvalue and Frequency Domain Analysis of Small-Signal Electromechanical Stability Problems." *IEEE/PES Symp. on Eigenanalysis and Frequency Domain Methods for System Dynamic Performance.* pp.17-33,1989.

[3] Pagola F., Perez-Arriaga, et. al., "On Sensitivities, Residues and Participations. Applications to Oscillatory Stability Analysis and Control". *IEEE Trans. on Power Systems*, Vol. 4, No. 1, 1989.

[4] Ostojic D. "Identification of Optimum Site for Power System Stabiliser Applications." *IEE Proc.*, Vol 135, Pt. C, No. 5. pp.416-419, September 1988

[5] Anderson P., Fouad A., Power System Control and Stability, Iowa State University Press, Ames, Iowa, 1977.

[6] Arcidiacono V., et. al. "Evaluation and Improvement of Electromechanical Oscillation Damping by Means of Eigenvalue-Eigenvector Analysis. Practical Results in Central Peru Power System", *IEE Trans. on Power Apparatus and Systems*, Vol. PAS-99, pp.769-778, 1980.

[7] Chen C.L., Hsu Y. Y. " An Efficient Algorithm for the Design of Decentralized Output Feedback Power System Stabilizers", *IEEE Transactions on Power Systems*, Vol. 3, pp.999-1004, August 1988.

[8] Kirkpatrick S., Gelatt C.D., Vecchi M.P., "Optimization by Simulated Annealing", *Science*, Vol. 220, pp.671-680, May 1983.

[9] Zhuang F., Galiana F.D., "Unit Commitment by Simulated Annealing", *IEEE Transactions on Power Systems*, Vol. 5, pp.311-318, February 1990.

[10] Chiang HD, Jean-Jumeau R.M., "Optimal Network Reconfigurations in Distribution Systems: Part 1: A New Formulation and Solution Methodology", *IEEE Trans. on Power Delivery*, Vol. 5, pp. 1902-1908, Nov. 1990.

[11] Aarts E., Korst J., *Simulated Annealing and Boltzmann Machines*, John Wiley and Sons, New York, 1989.

[12] Ramsay B., Lesani H., "Co-ordinated Stabilisation of Power Systems Using Eigensensitivity Analysis", *Electric Power Research*, Vol. 18, pp.141-148, 1990.

[13] IEEE Working Group on Computer Modelling of Excitation Systems: IEEE Committee Report, Excitation System Models for Power System Stability Studies, *IEEE Transactions on Power Apparatus and Systems*, Vol. PAS-100, No. 2, February 1981.

Chapter 3

Determination of the Control Structure of Power System Stabilizers

3.1 Introduction

This chapter deals with the *control structure* of Power System Stabilizers (PSS) for damping electromechanical oscillations. Figure 3.1 illustrates the aspects of the control structure that are addressed in the chapter.

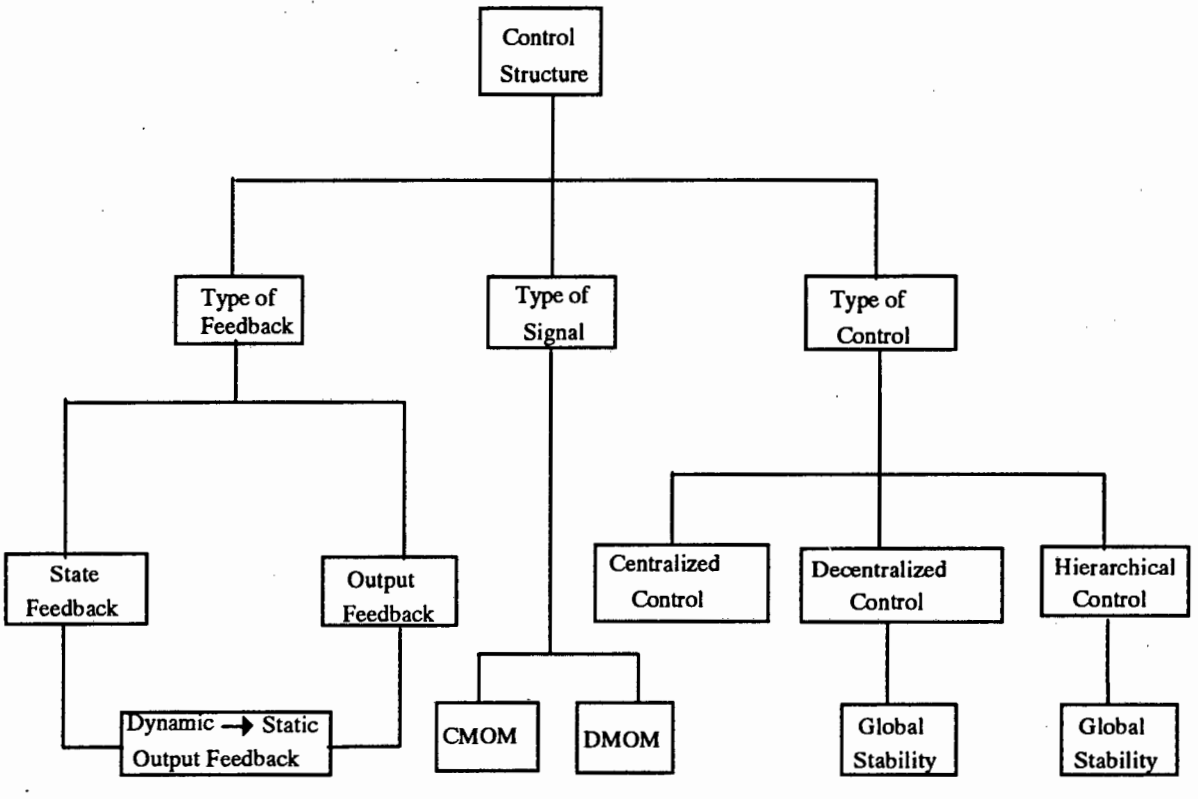

Figure 3.1: Aspects of the Control Structure which are addressed in Chapter 3

Figure 3.1 illustrates that three aspects of the control structure are addressed, namely the *type of feedback* ,the *type of signal* and the *type of control* used. The *type of feedback* refers to whether State Feedback or Output Feedback configuration is to be used. The *type of signal* refers to the selection of best feedback signals that are to be used for control. The type of control deals with the issue of whether centralized, decentralized or hierarchical control is to be used.

The type of feedback compares the use of State Feedback and Output feedback control. State Feedback requires measurement of all states for control [1]. It is possible though, that all states are not directly measurable. Furthermore, for large scale systems, the number of states is very large thus increasing the cost and complexity of the communication network. Output Feedback requires measurement of only output signals for control [1]. Thus, by using Output Feedback, the abovementioned problems associated with measurement of the control signals are eliminated. However, the controllers which are obtained from standard Output Feedback techniques are dynamic controllers of very high order; usually of the same order as the open loop plant [2]. This means that if PSS are designed using standard Dynamic Output Feedback techniques, the order of the PSS will be excessively high.

In this chapter, we present a method to ensure that the simple lead/lag structure of the Conventional Power System Stabilizers (CPSS) is retained while making use of output feedback control. This is achieved by transforming the Dynamic Output Feedback problem into a Static Output Feedback problem. Standard Static Output Feedback Methods can then be used to obtain the PSS parameters.

Once we have addressed the problem of the feedback type, the *best signal for feedback* needs to be determined. Typically, signals such as rotor speed deviation $\Delta\omega$, electrical power deviation (ΔP_e), accelerating power deviation (ΔP_{acc}) and bus frequency deviation Δf are used for damping of electromechanical oscillations. The state information contained in an output such as ΔP_{acc} is different from the state information contained in a signal such as $\Delta\omega$. It is therefore conceivable that one signal will be more effective than another in damping the electromechanical oscillation.

In the past, various studies have been conducted to determine the best signal for damping of the electromechanical oscillations. These studies have concluded that two signals namely ΔP_d and ΔP_{acc} are the best signals to be used for power system stabilisation [3,4]. These two signals stabilise the power systems with higher gain margins as compared to that of $\Delta\omega$. The PSS using $\Delta\omega$ as input signal, causes torsional oscillations which complicate the design of the PSS filters considerably. In the presence of rapid mechanical power swings, use of ΔP_d as stabilising signal results in undesirable voltage changes. For this reason, ΔP_{acc} is presently considered a better signal than ΔP_d for stabilisation [5].

In the past, the best signals were determined by testing all the available signals on benchmark networks. For each signal, a PSS is designed and the effect on the damping of the electromechanical oscillations was investigated [5]. This approach is computationally intensive. There is thus need for a improved method of selecting the best signal for feedback.

In order to analyse the effectiveness of the signals in stabilisation of the power system, it is important to perform a thorough analysis of the structure of its state space. In the past, stabilisation was performed exclusively on the basis of the location of poles. However, the location of the zeros is decisive in determining whether the poles can be moved effectively to the desired position. A zero located close to a pole will make the pole almost uncontrollable, whereas a zero in the right half plane will tend to destabilize the poles. It is therefore necessary to assess the effectiveness of each PSS signal based on both pole and zero locations.

In this chapter, we present two new methods of determining the best output signals for damping of electromechanical oscillations. These methods are based on two measures of the contribution of the electromechanical oscillations to the outputs. The first measure, the *Centralized Modal Observer Measure (CMOM),* is based on the observability of the electromechanical oscillations. The *CMOM* is not computationally intensive since it requires only the calculation of the right and left eigenvectors. However, the *CMOM* does not take into account the existence of fixed modes in a system under decentralized control. In order to take into account the existence of decentralized fixed modes, we develop the

second measure of the contribution of the electromechanical oscillation to the outputs, namely the *Decentralized Modal Observer Measure (DMOM)*. This measure is based on the observability of the system under decentralized control.

The final aspect of the control structure that is addressed in this chapter is whether centralized or decentralized control is to be used. Centralized controllers are controllers that make use of local control signals as well as control signals from remote sources in order to effect control. Decentralised controllers use locally measured signals such as $\Delta\omega^i, \Delta P_{el}^i, \Delta P_{acc}^i$, where i refers to the *ith* subsystem. No control signals from other subsystems are used to effect control. Hierarchical controllers combine the concepts of decentralized and centralized control.

The use of decentralized control presents problems related to the global stability of the interconnected system. Under decentralized control, the subsystems are stabilized with the local control i.e. controller k_i is designed so that subsystem i is stabilized. Thus, if all subsystems are under decentralized control, all the closed loop subsystems are stable. However, because of the interactions, the interconnected system may be unstable. This means that for a system under decentralized control, stabilizing the subsystems *does not* guarantee that the interconnected system is stable.

In this chapter, we address the problem of stabilizing the interconnected system using only decentralized control. We present sufficient conditions, based on *Lyapunov Stability Criterion*, which guarantee global stability of the interconnected system. These conditions restrict the selection of the decentralized controllers to only those controllers satisfying an H_∞-norm inequality constraint. The global stability of the interconnected system is guaranteed if controllers which satisfy the inequality constraints are selected. We use these conditions in a conceptual hierarchical control structure for stabilization of large power system.

The chapter begins by determining the type of feedback for damping of the electromechanical oscillations. The Dynamic Output Feedback problem is then converted into a Static Output Feedback problem. Thereafter, the problem of determining the best

feedback signal is addressed. The two new methods of selecting the best signals based on CMOM and DMOM are presented. Finally, the problem of determining whether centralized or decentralized control is to be used is addressed. The sufficient conditions for global stability of the interconnected system is derived and discussed. The use of this condition in a conceptual hierarchical control structure is discussed.

3.2 Type of Feedback

Consider an LTI invariant system described by:

$$\dot{x} = Ax + Bu$$
$$y = Cx + Du \tag{3.1}$$

There are two different forms that the feedback control can take, namely State Feedback or Output Feedback. In this section, we discuss some features of State and Output Feedback. Thereafter, we present a technique to transform an Output Feedback problem into a State Feedback problem.

3.2.1 State Feedback

Figure 3.2 presents the control configuration of State Feedback control.

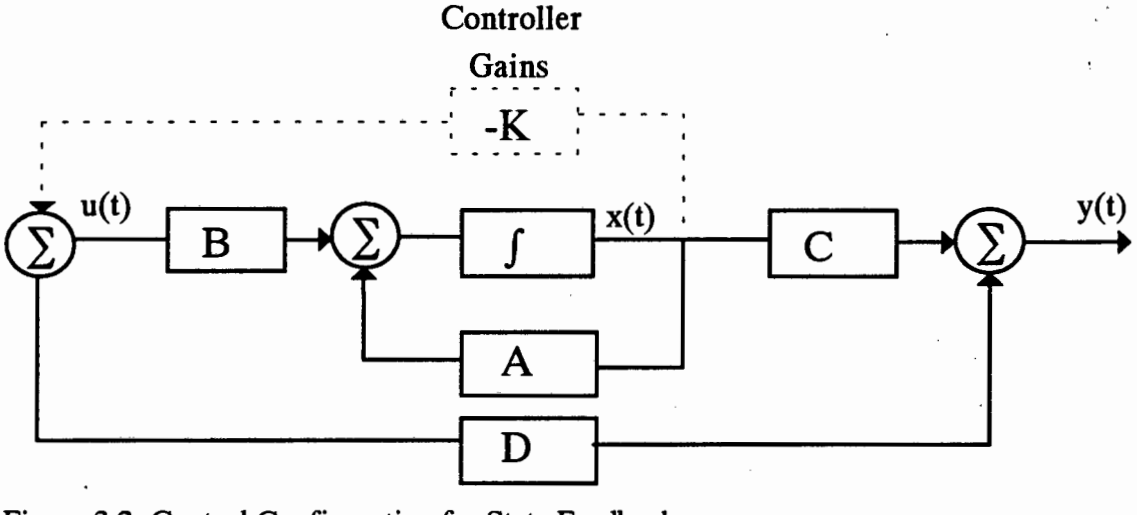

Figure 3.2: Control Configuration for State Feedback

Figure 3.2 illustrates that State Feedback controllers make use of all the states $x(t)$ of the system as feedback variables (dashed line in Figure 3.2) i.e.:

$$u = -Kx \tag{3.2}$$

where K is the matrix of constant controller gains

x is the vector of states.

u is the vector of inputs

By substituting equation (3.2) into equation (3.1), the closed loop system state equation can be expressed as follows:

$$\dot{x} = (A - BK)x \tag{3.3}$$

This is the *standard form* for the closed loop system under state feedback control.

There are two advantages of using state feedback control which are of particular interest in this thesis. Firstly, by using State Feedback control, all controllable modes of the system can be moved to arbitrary locations in the complex plane i.e. we have complete control of the controllable part of the system. This is due to the fact that the states contain complete information about the system and this information is fed back to the controller. Secondly, the calculation of the constant gain matrix K for State Feedback has become standard in control system design software. As a result, the design of feedback controllers using State Feedback has become a matter of routine.

The problem with using State Feedback control is that *all* the states of the system need to be measured. In large systems, the measurement of all the states becomes prohibitively expensive. Furthermore, not all the state variables are accessible for measurement as feedback signals. Thus the use of State Feedback for large systems becomes impractical. Instead of using State Feedback for large systems such as power systems, Output Feedback control is used.

3.2.2 Output Feedback

Figure 3.3 presents the configuration for Output Feedback control. Output Feedback controllers are controllers that make use of only the measurable outputs $y(t)$ of the system as feedback signals (the dotted lines in Figure 3.3). In the Laplace domain, the Output Feedback can be expressed as follows:

$$u(s) = -K(s)y(s) = -K(s)Cx(s) \tag{3.4}$$

where

$K(s)$ is the feedback matrix of transfer functions.

Comparison of equation (3.2) with equation (3.4) illustrates that the state feedback controller is a static controller (K is a constant matrix) whereas the output feedback controller is a dynamic controller (K(s) is a transfer functions matrix).

From equation (3.1), if $D = 0$, the equation for the *ith* output can be expressed as follows:

$$y_i = C_i x \qquad i = 1,\ldots p \tag{3.5}$$

where y_i denotes the *ith* output

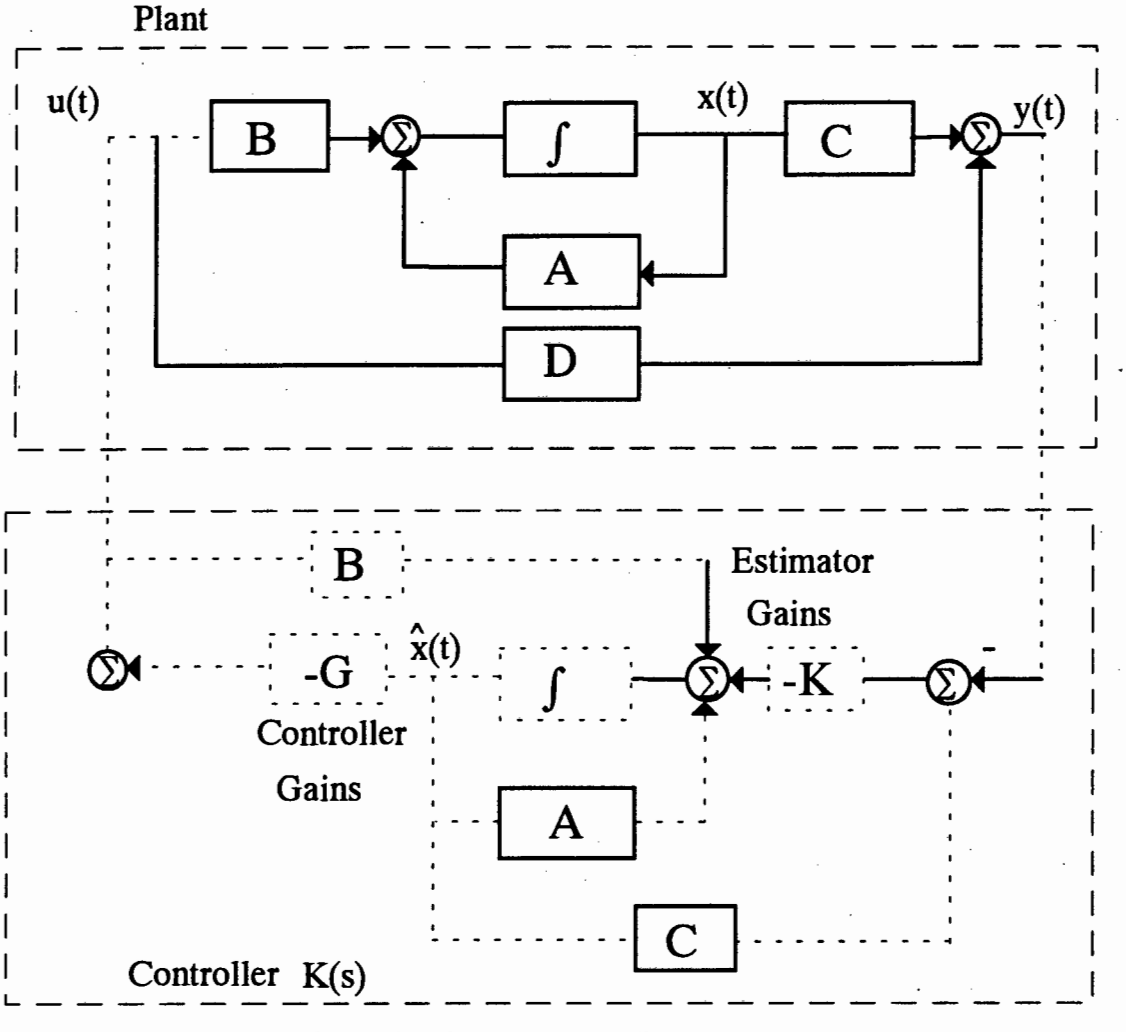

Figure 3.3: Control Configuration for Output Feedback

The main advantage of using Output Feedback control is that only measurable outputs need to be used as feedback signals. All the states need not be measured as in State feedback. Thus, for large scale systems, the cost of transmitting the control signals is greatly reduced.

The use of Output Feedback does however, have some serious shortcomings. The output signals y_i do not contain complete information of the system since only some states of the system contribute to the output. From equation (3.5) we know that the information contained in an output signal y_i is dependent on the row vector C_i. Therefore, since only partial information about the system is fed to the controller, Output Feedback control presents a weaker form of control as compared to State Feedback control.

From Figure 3.3 we can deduce that Output Feedback control requires the use of dynamic controllers (the integrator sign in the controller K(s)). These dynamic controllers are usually of the same order as that of the plant. This can be deduced from Figure 3.3 since matrix A of the plant is contained in the controller K(s). This order is typically too high for practical implementation. Therefore, if PSS are designed using Dynamic Output Feedback techniques, then the order of the PSS would be unacceptably high.

In the next section, we present a method of obtaining Output Feedback controllers of fixed structure. This method is based on transforming a Dynamic Output Feedback Problem into a Static Output Feedback problem.

3.2.3 Transforming Dynamic Output Feedback to Static Output Feedback

In this section, we present a method to obtain fixed structure Output Feedback controllers. This is achieved by transforming the Dynamic Output Feedback control problem into a Static Output Feedback control problem. In order to ensure that the structure of the controller remains fixed (e.g. lead/lag), the controller is augmented with the open loop plant. Once the problem has been converted into a Static Output Feedback problem, standard methods of constructing the gain matrix K can be used. The procedure of transforming a Dynamic Output Feedback problem into a Static Output Feedback problem will now be presented.

The state space description of the open loop plant given by equation (3.1). We wish to augment the controller dynamics with that of the open loop plant. In order to do this, we

need to find the state space description of the controller. We restrict the controller to be strictly proper i.e. the number of poles is strictly greater than the number of zeros.

The state space description of the *controller* can be expressed as follows:

$$\begin{aligned} \dot{z}_c &= Ez_c + Fu_c \\ y_c &= Gz_c \end{aligned} \tag{3.6}$$

where:

$z_c \in R^{nc}$ is the controller state vector

$y_c \in R^p$ is the controller outputs vector

$u_c \in R^p$ is the controller inputs vector

E, F, G are constant matrices of appropriate dimensions.

Figure 3.4 illustrated the block diagrams of the open loop plant and controller.

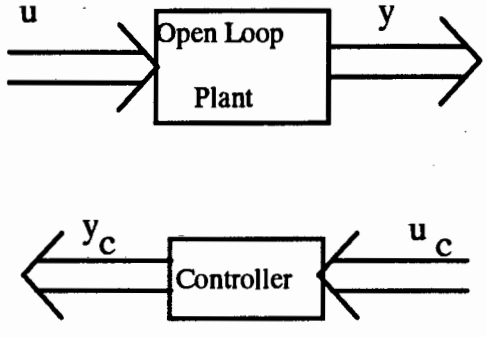

Figure 3.4: Block Diagrams of Open Loop Plant and Controller

We wish to transform the state space equations of the controller into the *controller canonical form* (see Section M of *Preliminaries*). The controller canonical form allows us to decompose the controller into a part that is completely known and another which contains the unknown parameters. Figure (3.5) illustrates this decomposition of the controller.

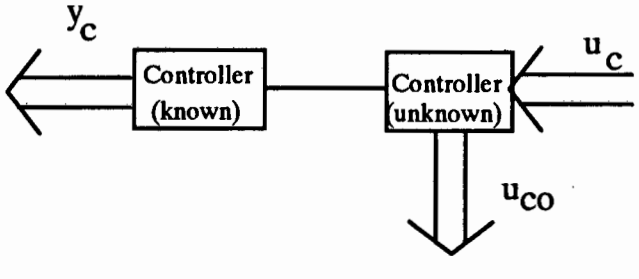

Figure 3.5: Decomposition of the Controller

The controller dynamics (in controller canonical form) is expressed as follows:

$$\begin{aligned} \dot{z} &= \left(P_c^0 - P_c N^0\right) z - N^0 u_c \\ y_c &= -Hz \end{aligned} \tag{3.7}$$

where:

z is the transformed controller state vector

$$P_c^0 = \text{Block Diag}\left[\mathrm{P}_1^0 \quad \cdots \quad P_p^0\right]$$

$$P_i^0 = \begin{bmatrix} 0 & 1 & 0 & \cdots & 0 & 0 \\ 0 & 0 & 1 & \cdots & 0 & 0 \\ & & & \vdots & & \\ 0 & 0 & 0 & \cdots & 0 & 1 \\ 0 & 0 & 0 & \cdots & 0 & 0 \end{bmatrix}_{v_i \times v_i}$$

$$N^0 = \text{Block Diag}\left[0 \quad \cdots \quad 0 \quad 1\right]^T_{v_i \times 1}, i = 1,\ldots,p$$

v_i is the controllability index of block i

Using Figure 3.5, we can rewrite equation (3.4) as follows:

$$\begin{aligned} \dot{z} &= P_c^0 z + N^0 u_{co} - N^0 u_c \\ u_{co} &= -P_c z \\ y_c &= -Hz \end{aligned} \tag{3.8}$$

where

u_{co} is a fictitious input of the unknown part of the controller.

The unknown parameters of the controller are contained in P_c and H. All the other matrices are known.

We wish to augment the controller dynamics with the dynamics of the open loop plant i.e. connect u_c to y ($u_c = y$). Thus we can rewrite the state space description of the controller in controller canonical form as follows:

$$\begin{aligned} \dot{z} &= P_c^0 z + N^0 u_{co} - N^0 y \\ u_c &= -P_c z \\ u &= -Hz \end{aligned} \tag{3.9}$$

The dynamics of the plant with the augmented controller are given by the following state space description:

$$\begin{aligned} \dot{x}' &= A'x' + B'u' \\ y' &= C'x' \end{aligned} \tag{3.10}$$

where:

$$x' = \begin{bmatrix} x \\ z \end{bmatrix},\ u' = \begin{bmatrix} u \\ u_{co} \end{bmatrix},\ y' = z$$

$$A' = \begin{bmatrix} A & 0 \\ -N^0 C & P_c^0 \end{bmatrix},$$

$$B' = \begin{bmatrix} B & 0 \\ -N^0 D & N^0 \end{bmatrix}$$

$$C' = \begin{bmatrix} 0 & I_{nc} \end{bmatrix}$$

$$D = \begin{bmatrix} 0 & 0 \\ 0 & 0 \end{bmatrix}$$

In order to find the closed loop system, we need to connect the output of augmented system to its input i.e.:

$$u' = -G'y' \tag{3.11}$$

where:

$$G' = \begin{bmatrix} H \\ P_c \end{bmatrix}$$

The state equation of the closed loop system is given by the following:

$$\dot{x}' = (A' - B'G'C')x' \tag{3.12}$$

By comparing equation (3.12) to equation (3.3) we can deduce that the closed loop dynamics of equation (3.6) is in the *standard State Feedback* form with $G'C' = K$. Since C' is obtained from the open loop plant and is therefore completey known, matrix G' contains the unknown controller parameters.

The controller transfer function K_{co} is then obtained from the following:

$$K_{co}(s) = H(sI - P_{co})^{-1}N^0 \tag{3.13}$$

where:

$$P_{co} = P_c^0 - N^0 P_c$$

Thus the Dynamic Output Feedback problem has been converted into a Static Output Feedback problem. The procedure to convert the Dynamic Output Feedback problem into a Static Feedback problem using a fixed structure dynamic controller is summarized in Figure 3.6.

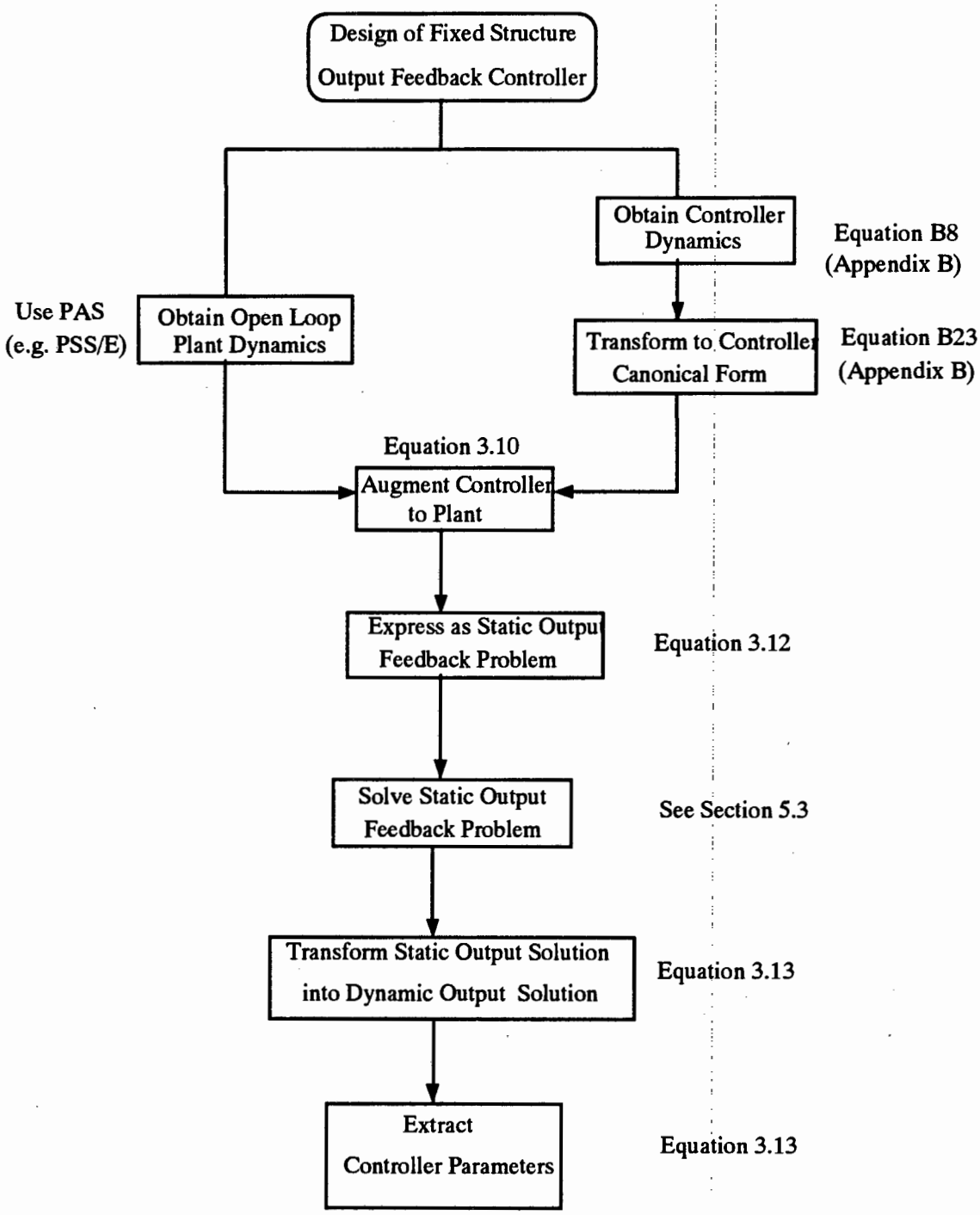

Figure 3.6: Procedure for Converting from a Dynamic Output Feedback Problem to a Static Output Feedback Problem.

This procedure can be used to obtain the parameters of a lead-lag PSS for damping electromechanical oscillations. The state space descriptions of the open loop plant and controller are first obtained using Power Application Software (PAS) such as PSS/E. The state space of the fixed structure controller is then transformed into the controller canonical form. The procedure for calculating the controller canonical form for a second order lead-lag is given in *Appendix B*. The controller with unknown parameters is then augmented to the open loop plant. Next, the closed loop system is expressed in the Static Output Feedback form. The constant Gain Matrix G is then calculated. From G the parameters of the controller is extracted resulting in a fixed structure Output Feedback controller.

3.3 Type of Signal

In this section, we develop methods to determine the best output signal to be used in the damping of the electromechanical oscillations. We present two new methods of determining the best output signal. These methods are based on two measures of the contribution of the electromechanical oscillation to the output signal. For an output to be effective as a control signal in supplementary excitation control, the electromechanical oscillations must be prominent in that signal. If the electromechanical oscillations are not prominent in the candidate output, then the output cannot be an effective control signal.

The first measure that we introduce is called the *Centralized Modal Observer Measure (CMOM)*. This measure is based on *centralized observability* of the electromechanical oscillations. The *CMOM* requires calculation of only the left and right eigenvectors corresponding to the electromechanical oscillations. No knowledge about the feedback structures of other subsystems are required. This method, although computationally very simple, does not take into account the existence of decentralized fixed modes in the system.

The second measure that we introduce is called the Decentralized Modal Observer Measure (*DMOM*) and it is based on the concept of *decentralized fixed modes*. The *DMOM* does require information about the feedback structures of the other subsystems in the interconnected system. As such, the *DMOM* takes into account the existence of decentralized fixed modes. Each of these measures will now be presented.

3.3.1 Centralized Modal Observer Measure (CMOM)

In this section we present the first method of determining the best output signal. This method is based on the concept of (centralized) observability of the electromechanical oscillations.

Consider an LTI system described by the following state space equations:

$$\begin{aligned} \dot{x} &= Ax + Bu \\ y &= Cx + Du \end{aligned} \tag{3.17}$$

Assume that matrix A has distinct eigenvalues. We can obtain the modal canonical form of the system by using the transformation $x = T\bar{z}$ where T is the nonsingular right eigenvector matrix and $\bar{z}$ is the vector of transformed states (see Section F2 of *Preliminaries*)

Then the system described by (3.17) can be expressed in the new set of coordinates $\bar{z}$ as follows:

$$\begin{aligned} \dot{\bar{z}} &= \bar{\Lambda}\bar{z} + \bar{\vartheta}u \\ y &= \Theta\bar{z} + Du \end{aligned} \tag{3.18}$$

where

$\bar{\Lambda} = T^{-1}AT$ is the diagonal matrix of eigenvalues

$\bar{\vartheta} = T^{-1}B$ is the modal controller matrix

$\bar{\Theta} = C \cdot T$ is the modal observer matrix

Since the matrix $\bar{\Lambda}$ is diagonal, the *ith* eigenvalue of A is dependent on only the *ith* element in the state vector $\bar{z}$. Thus the matrix $\bar{\Theta}$ gives a measure of the contribution of each mode to the output.

The matrix $\bar{\Theta} = C \cdot T$ is not unique since the eigenvector matrix T is not unique. For this reason, matrix $\bar{\Theta}$ does not provide a reliable means of determining the modal content of the output signals.

In order to overcome this difficulty, we use the left eigenvector matrix to scale the outputs in equation (3.18). Thus we define the scaled outputs y_s as follows:

$$y_s = \theta\bar{z} + Du \tag{3.19}$$

where:

$$\Theta = CW^T T$$

W is the left eigenvector matrix

We designate the matrix Θ as the *modal controller matrix.* The element Θ_{ij} denotes the *jth* element of the modal controller matrix corresponding to output i. If $\Theta_{ij} = 0$, then mode j is unobservable in output i. Figure 3.7 provides an interpretation of Θ_{ij}.

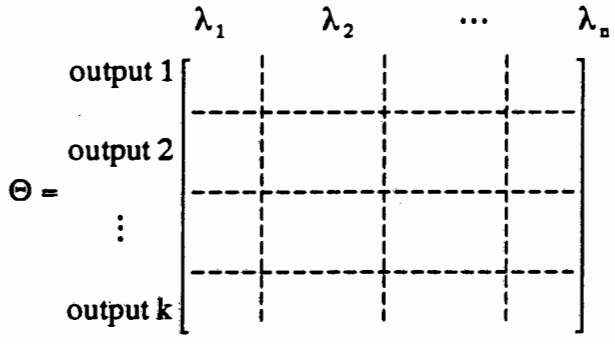

Figure 3.7: Interpretation of Θ

The rows of Θ correspond to the output signals whereas the columns correspond to the modes. Thus Θ_{ij} gives a measure of the contribution of mode i in output j. Since we are interested in damping the electromechanical modes, we select λ_i as corresponding to these modes.

We define the *Centralized Modal Observability Measure (CMOM) as follows*:

$$CMOM_j^i = \max_j(\|\Theta_{ij}\|_\infty) = \max_j(\sqrt{\sum_{j=1}^{n_k}|\Theta_{ij}|^2}) \tag{3.20}$$

where n_k is the number of output signals that are to be used

If only one output signal is to be used as a feedback signal, the *CMOM* reduces to the following:

$$CMOM_j^i = \max_j \left\| \Theta_{ij} \right\|_\infty \tag{3.21}$$

The *CMOM* assumes that the system is under centralized control. Thus we can use the CMOM as a measure of the effectiveness of an output signal if the system is under centralized control. Note that in order to calculate the best output signal using CMOM, we need to calculate only the electromechanical eigenvalues and the corresponding right and left eigenvectors. Due to its computational simplicity, we would like to use the CMOM for systems under decentralized control. However, it is important to note that the decentralized nature of the control is ignored in the CMOM. The most important consequence of this is that the possibility of fixed modes are not taken into account in the *CMOM*. Thus if a decentralized fixed mode does exist, the 'best' signal identified by the CMOM will be entirely ineffective in moving that mode.

In the next, we present the second measure of determining the best output signal for damping electromechanical oscillations. This measure takes into account the existence of fixed modes in systems under decentralized control.

3.3.2 Decentralized Modal Observer Measure

Consider an LTI system described by equation (3.1) and assume that the pairs $(A,B),(A,C)$ are controllable and observable respectively. Further assume that decentralized dynamic controllers are to be used.

Figure 3.8 illustrates the decentralized control system configuration for an interconnected system consisting of two subsystems.

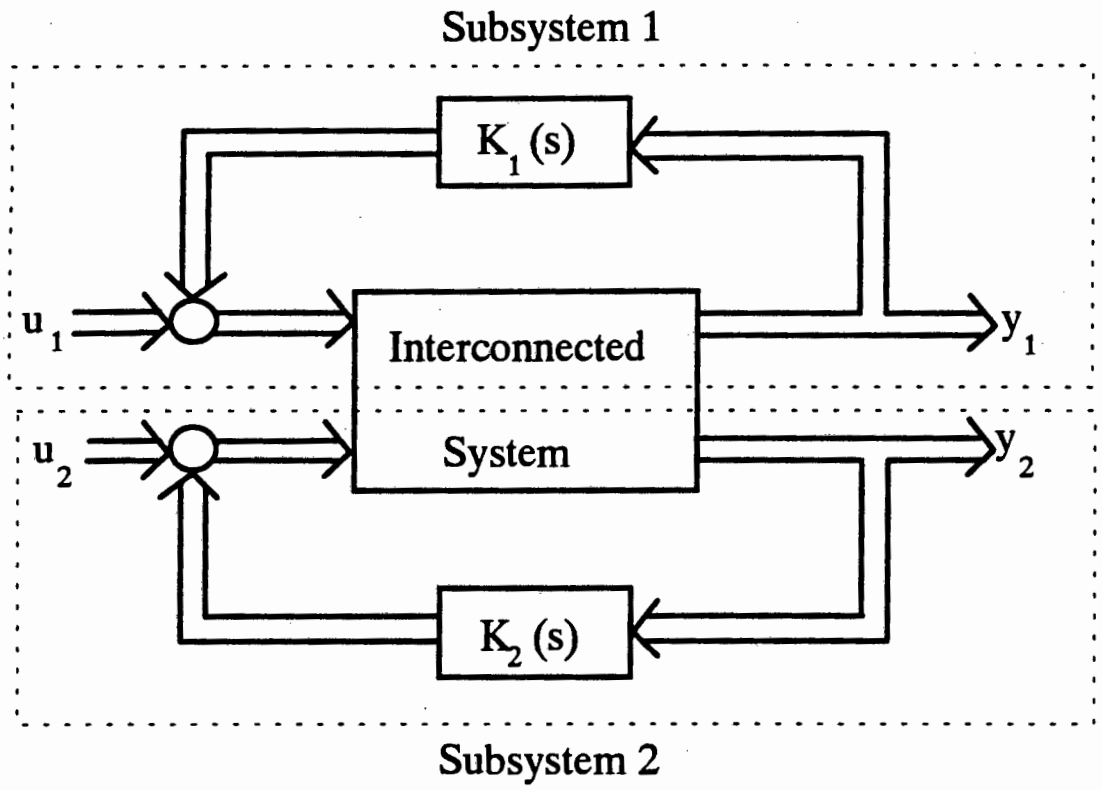

Figure 3.8: Decentralized Control System Configuration of an Interconnected System Consisting of Two Subsystems

For an interconnected system under decentralized control, there exists a decentralized fixed mode if and only if for some eigenvalue λ of A one of the following conditions apply (see Section G of *Preliminaries*):

$$rank(\vartheta_i) < n - \alpha \qquad (3.21)$$

for any $i = 1,...k$

where:

$$\vartheta_i = \begin{bmatrix} \lambda I - A & B_{i_1} & \cdots & B_{i_k} \\ C_{i_k+1} & 0 & \cdots & 0 \\ \vdots & \vdots & \ddots & \vdots \\ C_{i_m-1} & 0 & \cdots & 0 \end{bmatrix}$$

i_k is the k*th* input of subsystem i

i_m is the m*th* output of subsystem i

n is the number of rows/columns in A

α is the rank deficiency of A i.e. $\alpha = n - rank(A)$

We wish to use the condition in (3.21) to determine the best feedback signals for damping electromechanical oscillations.

Consider a power system with m generator subsystems. We define an index set $I = \{1,...,m\}$. We use the elements of I as indices to the subsystems. Set I can be partitioned into two disjoint subsets $I_1 = \{i_1,...i_k\}$ and $I_2 = \{i_{k+1},...i_m\}$. Since there are m elements in I, the number of such partitions equals $m!$. We define the set of all partitions as P. Thus each element in set P corresponds to a particular partitioning of set I.

Let the set v_i contain all the candidate output signals at subsystem i where the number of elements in v_i equals q_i i.e. we wish evaluate the effectiveness of q_i signals at the *ith* subsystem. The total number of candidate output signals in the system is given by $q = \sum_{i=1}^{m} q_i$.

We construct a set μ which contains combinations of elements in v_i with elements in v_j i.e. each element in μ is a set containing one element from each v_i. The number of elements in μ is $m \prod_{i=1}^{m-1} q_i$ where Π denotes the product of its arguments.

Using (3.21) we obtain $m!$ matrices for each element in μ. For each matrix, we calculate its singular values and extract $\sigma_{n-\alpha}$, the $(n-\alpha)$-est singular value. Thus, we obtain $m!$ values of $\sigma_{n-\alpha}$ for each element in μ. We extract the minimum $\sigma_{n-\alpha}$ from these $m!$ values. This value gives a measure of how observable the mode is in the output signals given by the element in μ. If the minimum $\sigma_{n-\alpha} = 0$, the mode is uncontrollable by decentralized control. We define the DMOM as follows:

$$DMOM_{\mu_i} = \min_{P} \sigma_{n-\alpha}\left(\vartheta_{p_i}^{\mu_i}\right) \tag{3.22}$$

where:

$p_i \in P$

$\mu_i \in \mu$

The best output signals μ_b is defined as the set of outputs which maximize the DMOM and is defined as follows:

$$\mu_b = \max_{\mu} DMOM_{\mu_i} \tag{3.23}$$

Let λ in equation (3.21) correspond to the weakly damped electromechanical oscillation. The singular values $\sigma_{n-\alpha}$ are then calculated for each ϑ. The output signal corresponding to the maximum $\sigma_{n-\alpha}$ is taken as the best signal for damping the electromechanical oscillations.

Note that in order to determine the best output signal, we need to calculate the singular values of $m!m\prod_{i=1}^{m-1} q_i$ matrices. For systems consisting of a large number of subsystems, this calculation becomes costly. However, for systems under decentralized control, the DMOM provides a reliable measure of the effectiveness of an output as a control signal. We demonstrate this in the next section.

It should be emphasised that the methods based on *CMOM* and *DMOM* are based only on the contribution of the electromechanical oscillations to the output signal. As such, these methods serve to provide a theoretical ranking of all the candidate output signals. They do not attempt to address practical issues relating to implementation of the control system. These practical issues may relate to measurement of the output signal, influence of unmodeled dynamics, filtering requirements etc. For instance, it is more difficult to measure the accelerating power signal than the speed and electrical power signals [3]. Furthermore, use of the speed signal or the electrical power signal may excite torsional oscillations or high frequency electrical oscillations respectively, thus necessitating complex filtering techniques [4]. Therefore, the ranking based on *CMOM* and *DMOM* should be used in conjunction with an analysis of the practical issues in determining the most appropriate feedback signal.

3.3.3 Case Study Using CMOM and DMOM

In this section, we apply the CMOM and DMOM to obtain the best signal for damping electromechanical oscillations. We demonstrate that for a system under decentralized control, the CMOM can provide unreliable results.

Appendix G provides the network diagram and eigenstructure of the seven-bus system. The system has a pair of unstable eigenvalues at $\lambda = 0.5416 \pm 5.5296i$ and a pair of non-minimum-phase zeros for control inputs at generators 3 and 4 (see Tables G6 and G7 in *Appendix G*).

We wish to apply the CMOM and DMOM to this network. In Chapter 2, we demonstrated that the optimal locations of the PSS for the seven-bus network was at generator 3 and generator 4. The output signals that we used to stabilize the system were Q_{el} at generator 3 and Q_{el} at generator 4. In this section, we demonstrate that these two signals are in fact the best signals for damping the electromechanical oscillations.

We select eight candidate outputs namely, P_{el}, Q_{el}, ω and V_T at generators 3 and 4.

Before applying the CMOM and DMOM, we determine whether the unstable mode is controllable with respect to the two input variables V_{ref} at generator 3 and V_{ref} at generator 4.

The product $T^{-1}B$ (where T is the right eigenvector matrix) is given in Table 3.1a. Since all elements in the matrix $T^{-1}B$ are non-zero, all modes in the system are controllable.

Eigenvalue No.	V_{ref} (Gen 3)	V_{ref} (Gen 4)
1	2.4312e+000- 6.1823e-014i	-3.0706e-001- 4.1689e-014i
2	3.3271e-001+ 3.8342e-014i	-4.2830e-001- 8.7550e-014i
3	-4.8398e+001- 1.9503e-013i	2.6078e+000- 1.0365e-013i
4	-2.9817e+002- 2.2670e-013i	-1.6578e+000+ 3.4139e-013i
5	1.2758e+001- 2.9013e+001i	2.3192e+000+ 4.7136e+000i
6	1.2758e+001+ 2.9013e+001i	2.3192e+000- 4.7136e+000i
7	4.4109e+002- 7.6285e-014i	-9.0316e+001+ 1.7616e-014i
8	4.2011e+000- 7.3767e-015i	5.4412e+002+ 7.9464e-014i
9	-4.9101e-001+ 1.7165e+000i	-5.0137e-002+ 1.8542e-001i
10	-4.9101e-001- 1.7165e+000i	-5.0137e-002- 1.8542e-001i
11	-4.5589e-001+ 2.7832e+000i	-2.0797e-002+ 9.3399e-002i
12	-4.5589e-001- 2.7832e+000i	-2.0797e-002- 9.3399e-002i
13	**-2.8136e-001+ 2.7051e+000i**	**2.3732e+001+ 8.0609e+000i**
14	**-2.8136e-001- 2.7051e+000i**	**2.3732e+001- 8.0609e+000i**
15	2.1660e+000- 5.3450e+000i	-2.3858e+000+ 4.5328e+000i
16	2.1660e+000+ 5.3450e+000i	-2.3858e+000- 4.5328e+000i
17	-1.6718e+002- 6.5302e+001i	-9.9119e+001- 5.9677e+001i
18	-1.6718e+002+ 6.5302e+001i	-9.9119e+001+ 5.9677e+001i
19	-4.3772e-002- 1.2018e-016i	-1.9399e-002- 1.2409e-015i
20	1.4676e+001- 2.4141e-015i	4.6631e-001- 1.8982e-014i
21	8.9579e+000+ 3.2826e-014i	-6.4662e+000- 4.6153e-014i
22	2.0138e+001+ 2.2011e-014i	3.6563e-001- 1.0061e-013i
23	6.1382e+000+ 1.2243e-014i	1.4124e+000- 1.3097e-015i
24	-1.2084e+002+ 7.5866e+000i	5.5948e+001+ 1.0838e+002i
25	-1.2084e+002- 7.5866e+000i	5.5948e+001- 1.0838e+002i
26	-9.3942e+001- 2.8224e-014i	2.6490e+002- 1.6844e-013i
27	1.8619e+001- 5.3854e+001i	-3.2122e+002- 1.4179e+002i
28	1.8619e+001+ 5.3854e+001i	-3.2122e+002+ 1.4179e+002i
29	-5.9535e+000+ 3.2991e-014i	-1.4386e+002+ 5.7586e-014i

Table 3.1a: Values of $T^{-1}B$ for V_{ref} at Generator 3 and Generator 4

In particular, the rows corresponding to the mode $\lambda = 0.5416 \pm 5.5296i$ (eigenvalues 13 and 14 which are highlighted in Table3.1a) are given in Table 3.1b.

Eigenvalue No.	V_{ref} (Gen 3)	V_{ref} (Gen 4)
13	-2.8136e-001+ 2.7051e+000i	2.3732e+001+ 8.0609e+000i
14	-2.8136e-001- 2.7051e+000i	2.3732e+001- 8.0609e+000i

Table 3.1b: Values of $T^{-1}B$ Corresponding to the Unstable Mode

All the elements in these two rows are non-zero, therefore the mode is controllable (if centralized control is used).

We now determine the best output signal to stabilize the system.

Calculating the CMOM

In calculating the CMOM, we need the right and left eigenvectors. From these, we can calculate the Participation Vector. The right eigenvector, left eigevector and Participation Vector associated with the unstable eigenvalue $\lambda = 0.5416 + 5.5296i$ are given in Table 3.2:

Right Eigenvector	Left Eigenvector	Participation Vector
7.4688e-003- 5.6854e-003i	1.9182e-005+ 1.3838e-003i	8.0108e-006+ 1.0226e-005i
-2.0630e-003- 9.8901e-003i	-1.8821e-004+ 7.6585e-005i	1.1457e-006+ 1.7034e-006i
-2.1688e-003+ 2.8005e-003i	1.6713e-005+ 9.3622e-005i	-2.9843e-007- 1.5624e-007i
-1.6908e-004+ 1.3312e-004i	2.5542e-002+ 2.0736e-002i	-7.0789e-006- 1.0602e-007i
8.7151e-002+ 4.3955e-002i	-2.6095e-004+ 4.0971e-004i	-4.0751e-005+ 2.4237e-005i
8.0776e-003- 7.2336e-003i	3.2747e-004+ 1.0661e-003i	1.0357e-005+ 6.2429e-006i
-2.9907e-003- 1.1397e-002i	-1.2825e-004+ 1.0179e-004i	1.5436e-006+ 1.1572e-006i
-2.6250e-003+ 3.5113e-003i	1.1925e-005+ 1.1616e-004i	-4.3917e-007- 2.6305e-007i
-1.8197e-004+ 1.2821e-004i	1.8635e-002+ 1.3014e-002i	-5.0595e-006+ 2.0987e-008i
8.6735e-002+ 4.4793e-002i	-1.5894e-004+ 2.9564e-004i	-2.7028e-005+ 1.8523e-005i
7.3061e-003- 4.7915e-003i	-2.6397e-005+ 1.3628e-003i	6.3368e-006+ 1.0083e-005i
-1.7811e-003- 8.7467e-003i	-2.0992e-004+ 8.3108e-005i	1.1008e-006+ 1.6881e-006i
-1.9182e-003+ 2.1513e-003i	3.0057e-005+ 4.8025e-005i	-1.6097e-007- 2.7461e-008i
-1.5264e-004+ 1.3900e-004i	2.8280e-002+ 2.0081e-002i	-7.1081e-006+ 8.6559e-007i
8.7657e-002+ 4.2884e-002i	-2.4738e-004+ 4.4830e-004i	-4.0909e-005+ 2.8688e-005i
5.5670e-003- 1.0222e-002i	1.8531e-002+ 4.5971e-003i	1.5015e-004- 1.6383e-004i
-1.1644e-002- 4.4775e-003i	7.1622e-004+ 2.5617e-003i	3.1308e-006- 3.3035e-005i
-6.6941e-004- 3.6788e-003i	-4.7150e-003+ 7.5231e-004i	5.9238e-006+ 1.6842e-005i
2.8545e-004+ 5.9794e-004i	-2.4264e-001- 6.9952e-001i	3.4901e-004- 3.4476e-004i
1.2155e-001+ 1.6336e-002i	9.8501e-003- 4.7415e-003i	1.2747e-003- 4.1540e-004i
3.4454e-003- 1.2031e-002i	1.1665e-002+ 2.6026e-003i	7.1501e-005- 1.3137e-004i
-2.0160e-002- 5.5732e-003i	4.3845e-004+ 1.3064e-003i	-1.5586e-006- 2.8781e-005i
-1.2080e-002+ 5.4880e-003i	5.4591e-003+ 1.0695e-003i	-7.1818e-005+ 1.7040e-005i
3.5041e-004- 1.2083e-003i	1.8773e-001+ 6.4270e-001i	8.4235e-004- 1.6274e-006i
2.0719e-001+ 1.9820e-001i	3.5559e-006+ 1.2516e-005i	-1.7439e-006+ 3.2980e-006i
2.5591e-001+ 2.0961e-001i	5.5783e-006+ 8.8785e-006i	-4.3347e-007+ 3.4413e-006i
1.8180e-001+ 1.9697e-001i	3.0907e-006+ 1.2436e-005i	-1.8877e-006+ 2.8696e-006i
5.0619e-001+ 1.7705e-001i	1.1807e-004- 2.3374e-006i	6.0182e-005+ 1.9722e-005i
6.2850e-001+ 9.2700e-002i	1.2117e-004- 3.2697e-005i	7.9184e-005- 9.3178e-006i

Table 3.2: Right Eigenvector, Left Eigenvector and Participation Vector Corresponding to the Unstable Mode

Multiplying matrix C with the participation vector gives the following values for Θ :

Generator No.	Output Signal	Θ
3	P_{el}	[1.0228e-003+ 3.7128e-004i
4	P_{el}	5.2397e-003- 2.7819e-003i
3	Q_{el}	4.3448e-004- 6.2011e-005i
4	Q_{el}	5.0317e-003- 2.2708e-003i
3	ω	-2.3508e-005+ 5.7375e-006i
4	ω	-1.2053e-004- 2.0936e-005i
3	V_T	-7.1081e-006+ 8.6559e-007i
4	V_T	3.4901e-004- 3.4476e-004i]

Table 3.3a: Values of Θ Corresponding to the Eight Output Signals

The magnitude of each element on Θ is given in Table 3.3b.

Generator No.	Output Signal	$\lvert\Theta\rvert$ =CMOM
3	P_{el}	**1.0881e-003**
4	P_{el}	**5.9324e-003**
3	Q_{el}	4.3888e-004
4	Q_{el}	5.5203e-003
3	ω	2.4198e-005
4	ω	1.2234e-004
3	V_T	7.1606e-006
4	V_T	4.9058e-004

Table 3.3b: Values of CMOM corresponding to the Eight Output Signals

The maximum element in $|\Theta|$ corresponding to machine 3 is 1.0881e-003. The maximum element corresponding to machine 4 is 5.9324e-003. These two elements correspond to P_{el} at machine 3 and P_{el} at machine 4 respectively. Therefore, using the CMOM, we select P_{el} at machine 3 and P_{el} at machine 4 as feedback signals.

In the next section, we demonstrate that the signals obtained from CMOM, are not the best signal for controlling the unstable electromechanical mode.

Calculating the DMOM

For the seven-bus system, the number of states $n = 29$ and the rank deficiency of matrix A is $\alpha = 0$. The index set $I = \{1,2\}$. The partition set P contains two element namely $\{\{i_1\} = \{1\}, \{i_2\} = \{2\}\}$ and $\{\{i_1\} = \{2\}, \{i_2 = 1\}\}$. The number of candidate output at subsystem 1 and 2 are $q_1 = q_2 = 4$. Therefore, we need to calculate the eight matrices $\vartheta_2^3, \vartheta_4^3, \vartheta_6^3, \vartheta_8^3, \vartheta_1^4, \vartheta_3^4, \vartheta_5^4, \vartheta_7^3$ corresponding to $\lambda = 0.5416 + 5.5296i$.

$$\vartheta_2^3 = \begin{bmatrix} \lambda I - A & B_3 \\ (C_2)^T & 0 \end{bmatrix}, \quad \vartheta_4^3 = \begin{bmatrix} \lambda I - A & B_3 \\ (C_4)^T & 0 \end{bmatrix}, \quad \vartheta_6^3 = \begin{bmatrix} \lambda I - A & B_3 \\ (C_6)^T & 0 \end{bmatrix}, \vartheta_8^3 = \begin{bmatrix} \lambda I - A & B_3 \\ (C_8)^T & 0 \end{bmatrix},$$

$$\vartheta_1^4 = \begin{bmatrix} \lambda I - A & B_4 \\ (C_1)^T & 0 \end{bmatrix}, \vartheta_3^4 = \begin{bmatrix} \lambda I - A & B_4 \\ (C_3)^T & 0 \end{bmatrix}, \vartheta_5^4 = \begin{bmatrix} \lambda I - A & B_4 \\ (C_5)^T & 0 \end{bmatrix}, \vartheta_7^4 = \begin{bmatrix} \lambda I - A & B_4 \\ (C_4^4)^T & 0 \end{bmatrix}$$

where:

B_3 corresponds to V_{ref} at generator 3

B_4 corresponds to V_{ref} at generator 4

$(C_1)^T$ corresponds to P_{el} at Generator 3

$(C_2)^T$ corresponds to P_{el} at Generator 4

$(C_3)^T$ corresponds to Q_{el} at Generator 3

$(C_4)^T$ corresponds to Q_{el} at Generator 4

$(C_5)^T$ corresponds to ω at Generator 3

$(C_6)^T$ corresponds to ω at Generator 4

$(C_7)^T$ corresponds to V_T at Generator 3

$(C_8)^T$ corresponds to V_T at Generator 4

The singular values of these matrices are given in Table 3.3a. The highlighted values in Table 3.4 correspond to the 29*th* singular values σ_{29}.

Generator 4 (P_{el})	Generator 4 (Q_{el})	Generator 4 (ω)	Generator 4 (V_T)	Generator 3 (P_{el})	Generator 3 (Q_{el})	Generator 3 (ω)	Generator 3 (V_T)
8.4302994e+002	8.4302994e+002	8.4302994e+002	8.4302997e+002	8.4303007e+002	8.4303007e+002	8.4303007e+002	8.4303010e+002
6.7469685e+002	6.7469644e+002	6.7469628e+002	6.7469627e+002	7.3670433e+002	7.3670444e+002	7.3670429e+002	7.3670429e+002
4.3742930e+002	4.3742412e+002	4.3742065e+002	4.3742017e+002	4.2477956e+002	4.2477876e+002	4.2477887e+002	4.2477867e+002
3.7707234e+002	3.7707234e+002	3.7707234e+002	3.7707235e+002	3.7707228e+002	3.7707227e+002	3.7707226e+002	3.7707321e+002
3.7707222e+002	3.7707222e+002	3.7707222e+002	3.7707222e+002	3.7707211e+002	3.7707211e+002	3.7707211e+002	3.7707212e+002
3.7706464e+002	3.7706464e+002	3.7706463e+002	3.7706562e+002	3.7707099e+002	3.7707099e+002	3.7707099e+002	3.7707103e+002
2.9307185e+002	2.9308909e+002	2.9307185e+002	2.9307179e+002	1.9395712e+002	1.9395984e+002	1.9395672e+002	1.9395671e+002
1.8231117e+002	1.8237093e+002	1.8230921e+002	1.8230920e+002	1.3359065e+002	1.3359120e+002	1.3359049e+002	1.3359048e+002
1.3152752e+002	1.3152735e+002	1.3152734e+002	1.3152734e+002	6.9497351e+001	6.9619691e+001	6.9437566e+001	6.9437525e+001
3.7990205e+001	3.7990128e+001	3.7990061e+001	3.7990061e+001	3.5646645e+001	3.4869699e+001	3.4869665e+001	3.4869665e+001
3.1163020e+001	3.1163003e+001	3.1163002e+001	3.1163002e+001	3.1166061e+001	3.1165910e+001	3.1165775e+001	3.1165775e+001
2.9512717e+001	2.9512344e+001	2.9512293e+001	2.9512293e+001	2.7101771e+001	2.7011650e+001	2.7011643e+001	2.7011643e+001
2.5901921e+001	2.5901692e+001	2.5901674e+001	2.5901674e+001	2.3248393e+001	2.3061526e+001	2.3061365e+001	2.3061365e+001
1.9380187e+001	1.9380410e+001	1.9380162e+001	1.9380162e+001	1.9406749e+001	1.9403950e+001	1.9403482e+001	1.9403482e+001
1.6522731e+001	1.6511202e+001	1.6498253e+001	1.6498253e+001	1.6882944e+001	1.6882923e+001	1.6882918e+001	1.6882918e+001
1.5856518e+001	1.5856714e+001	1.5845743e+001	1.5845743e+001	1.5844500e+001	1.5844388e+001	1.5844387e+001	1.5844387e+001
1.3397326e+001	1.3152836e+001	1.2983894e+001	1.2983894e+001	1.3300779e+001	1.3298459e+001	1.3298440e+001	1.3298440e+001
9.3577406e+000	9.2211668e+000	8.1621410e+000	8.1621413e+000	8.7582834e+000	8.7453309e+000	8.7450305e+000	8.7450305e+000
8.1359731e+000	8.1358137e+000	8.1021669e+000	8.1021669e+000	8.1302123e+000	8.1262345e+000	8.1262160e+000	8.1262162e+000
5.5634260e+000	5.5634003e+000	5.5633264e+000	5.5812739e+000	5.5634704e+000	5.5634702e+000	5.5634697e+000	5.5814091e+000
5.2782365e+000	5.2780480e+000	5.2779589e+000	5.2779623e+000	3.9618019e+000	3.9564526e+000	3.9549479e+000	3.9549515e+000
3.9566762e+000	3.5171865e+000	1.5934934e+000	1.5935118e+000	2.8221479e+000	2.6850337e+000	2.2181452e+000	2.2180145e+000
1.1104967e+000	1.1087715e+000	1.1021203e+000	1.1021193e+000	1.9467341e+000	1.4331616e+000	1.4050571e+000	1.4050533e+000
4.9484504e-001	4.8659110e-001	4.2553787e-001	4.2521278e-001	1.3860522e+000	1.0534950e+000	1.0471790e+000	1.0471555e+000
3.9288733e-001	4.0034243e-001	3.8424135e-001	3.8398378e-001	1.0466490e+000	3.6389410e-001	3.5742577e-001	3.5708388e-001
2.4997932e-001	1.6231247e-001	1.2662606e-001	1.2662277e-001	3.5218447e-001	1.4192806e-001	1.2628703e-001	1.2650736e-001
1.2645751e-001	1.2650429e-001	1.1753525e-001	1.1749593e-001	1.1650285e-001	1.1604744e-001	1.1517362e-001	1.1495370e-001
1.1741848e-001	1.1608690e-001	2.9362974e-002	1.4604612e-002	4.3129802e-002	5.5317097e-002	2.0149327e-002	2.1076870e-002
4.6614171e-003	**1.1476073e-002**	**9.9761264e-003**	**7.8359929e-004**	**3.1527148e-003**	**1.9077934e-002**	**1.1011921e-002**	**2.8507469e-003**
2.4419472e-004	2.6338148e-004	2.6307836e-004	2.3435191e-004	4.0482771e-004	2.3573112e-003	2.3485939e-003	1.8804424e-004

Table 3.4: Singular Values Corresponding to the Eight Candidate Outputs

We can guarantee that no fixed modes exist by selecting the output signals such that :

$rank(\vartheta_i^j) \geq n - \alpha$

where:

n is the number of states

α is the rank deficiency of the state coefficient matrix A

In this case $rank(A) = n$, therefore of α is zero.

Thus, we wish to choose the output signals which correspond to the ϑ_i^j with the rank closest to $n = 29$.

From equation 3.23, we know that the larger the value of σ_{29}, the more effective will be the corresponding signal for damping of the electromechanical oscillation. Conversely, the smaller the value of σ_{29} the less effective will be the corresponding signal for damping of the electromechanical oscillation. If $\sigma_{29} = 0$, then the corresponding signal will be ineffective for moving the electromechanical mode since it is a decentralized fixed mode.

If we select the signals obtained using CMOM (namely P_{el}) at generators 3 and 4, the singular values are $\sigma_{29} = 3.1527148e-003$ and $\sigma_{29} = 4.6614171e-003$ respectively.

The best output signals using DMOM are Q_{el} of generators 3 and 4. The corresponding singular values are $\sigma_{29} = 1.9077934e-002$ $\sigma_{29} = 1.1476073e-002$ respectively.

The values of σ_{29} for the signals corresponding to DMOM are greater than those for the signals corresponding to DMOM ($1.9077934e-002 > 3.1527148e-003$ and $1.1476073e-002 > 4.6614171e-003$). Thus the output signals given by DMOM are better than those given by the CMOM for damping of the electromechanical mode.

Generator No.	Output Signal	DMOM(ϑ_i^j)
3	P_{el}	3.1527148e-003
3	Q_{el}	**1.9077934e-002**
3	ω	1.1011921e-002
3	V_T	2.8507469e-003
4	P_{el}	4.6614171e-003
4	Q_{el}	**1.1476073e-002**
4	ω	9.9761264e-003
4	V_T	7.8359929e-004

Table 3.5: Values of DMOM Corresponding to the Eight Candidate Signals

In order to verify this, we compare the use of signals provided by CMOM and DMOM to stabilize the unstable electromechanical oscillations. In Section 2.5.5, we demonstrated that by using the signals obtained from DMOM (namely Q_{el}), the unstable mode $l = 0.5416 \pm 5.5296i$ was moved to the stable locations $\lambda = -0.356 \pm 5.861i$. However, by using the signals obtained from CMOM (namely P_{el}), we can only move the unstable eigenvalue to the location $\lambda = 0.0115 \pm 5.634i$. Thus, by using the P_{el} on generators 3 and 4 we are unable to stabilize the electromechanical mode. This illustrates that the CMOM can provide unreliable results for systems under decentralized control.

3.4 Type of Control

In this section, we briefly discuss the issues related to centralized and decentralized control for large scale systems. The term *large scale system* can refer to systems that cover a large area or systems that have a mathematical model of large dimension. Power systems are *large scale systems* in both respects since the electrical grid can stretch over thousands of kilometres and the dimension of the mathematical model is typically composed of several thousand states. In addition, power systems are becoming even larger due to power pooling. As a result of the large scale nature of power systems, the type of control (centralized or decentralized) needs to be investigated.

This section investigates issues related to the type of control for damping of electromechanical mode oscillations in power systems. The main advantages and disadvantages of centralized and decentralized control are outlined. The problem of ensuring global stability of the interconnected system under decentralised control is addressed. Sufficient conditions which guarantee global stability are presented.

3.4.1 Centralized Control

Figure 3.9 is a diagrammatic representation of a large scale system consisting of four subsystems under centralized control.

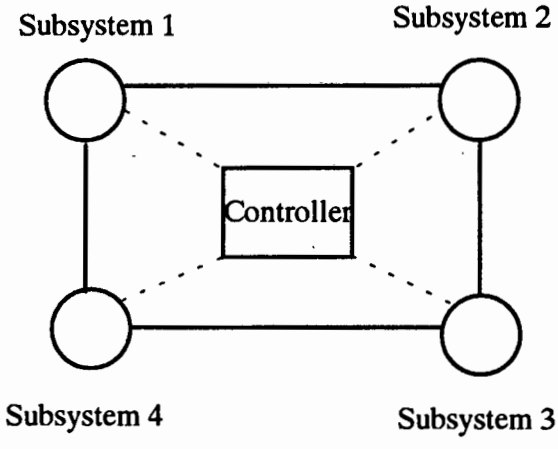

Figure 3.9: Diagrammatic Representation of a System Under Centralized Control

Centralized controllers make use of local control signals as well as control signals from remote sources in order to effect control. The main advantage of centralized control is that the controller receives information about all the subsystems of the network. Therefore, all the controllable modes of the system can be controlled.

The main problem with the implementation of centralised controllers for large scale systems is that the control signals need to be transmitted over long distances. The long distances result in delays in transmitting the control signals. Furthermore, the high cost of the communication network for transmitting the control signals from all subsystems make the use of centralized control impractical.

Advances in the area of signal communication is however making the use of centralized control more attractive. The increased speed of transmission would eliminate the delays associated with conventional communication networks. Therefore subsystems which are close to each other can be linked together via dedicated lines.

3.4.2 Decentralized Control

Figure 3.10 is a diagrammatic representation of a large scale system under decentralized control.

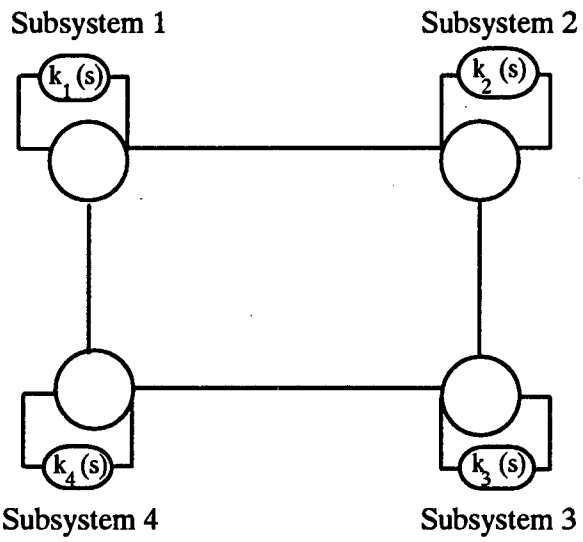

Figure 3.10: Diagrammatic Representation of a System Under Decentralized Control

Figure 3.10 illustrates that decentralized controllers make use of only local control signals in the feedback path. No information about other subsystems is used by the controllers. The main advantage of using decentralized control is related to transmission of control signals. Since only local signals are required in the feedback path, the delay in transmission of the signals and the cost of the communication network is greatly reduced.

The first problem associated with decentralized control is the possibility of the existence of decentralized fixed modes in the system. These fixed modes occur because the decentralised controller k_i uses control signals from subsystem i only and therefore it lacks information about the other subsystems. If these decentralized fixed modes do occur, they cannot be moved (in the complex plane) by LTI decentralised control [12].

The second problem associated with the use of decentralized control is related to *global stability* of the interconnected system. A system is said to be *globally stable* if all the eigenvalues of the state coefficient matrix has negative real parts. Under decentralized control, the subsystems are stabilized with the local control i.e. controller k_i is designed so that subsystem i is stabilized. Thus, if all subsystems are under decentralized control, all the closed loop *subsystems* are stable. However, even if all the subsystems are stable, the interconnected system may be globally unstable due to the interactions between subsystems. This means that for a system under decentralized control, stabilizing the subsystems does not guarantee that the interconnected system is stable. In the next section, we present a method to select decentralized controllers which guarantees the global stability of the interconnected system.

3.4.2.1 Global Stability of the Interconnected System

In this section we analyze the global stability aspects of the interconnected power system by taking into account the interactions between subsystems. We wish to select decentralized controllers that will absorb the interactions and ensure global stability.

Consider the System S described by equation (A2) in the Preliminaries. Assume that there is no control on System S i.e. $u_i = 0, \quad i = 1,\ldots,m$. Further assume that the initial conditions of the system is such that $x(0) = 0$. We designate the system with the assumptions as System T. The state equations for the interconnected system is then given by the following:

$$T \overset{\Delta}{=} \{T_i\} \overset{\Delta}{=} \left\{ \dot{x}_i = A_{ii}^0 x_i + + \sum_{\substack{j=1 \\ j \neq i}}^{m} A_{ij}^0 x_j \right\} \tag{3.24}$$

Equation (3.24) can be rewritten as follows:

$$T \overset{\Delta}{=} \{T_i\} \overset{\Delta}{=} \{\dot{x} = (A_{ii} + A_{ij})x\} \tag{3.25}$$

where:

$$A_{ii} = \begin{bmatrix} 0 & . & 0 & . & 0 \\ . & . & . & . & . \\ 0 & . & A_{ii} & . & 0 \\ . & . & . & . & . \\ 0 & . & 0 & . & 0 \end{bmatrix}_{n\times n}$$

$$A_{ij} = \begin{bmatrix} 0 & \dots & 0 & \dots & 0 \\ . & . & . & . & . \\ A_{i1}^0 & \dots & 0 & \dots & A_{im}^0 \\ . & . & . & . & . \\ 0 & \dots & 0 & \dots & 0 \end{bmatrix}_{n\times n}$$

$$x = \begin{bmatrix} x_i & \dots & x_m \end{bmatrix}$$

Assume that the uncoupled and unperturbed subsystems are asymptotically stable i.e. $\mathrm{Re}(\lambda_k(A_{ii}^0)) < 0, \quad k = 1,\dots,n$ for all k. If $\mathrm{Re}(\lambda_k(A_{ii}^0)) \geq 0$ for any k, then we apply feedback control in order to stabilize A_{ii}^0.

We can now state the following Lemma:

Lemma 3.1: *The interconnected system described by equation (3.24) is globally stabilizable by completely decentralized feedback if* $\sigma_{\max}(A_{ij}) \leq \dfrac{1}{\sigma_{\max}(P_{ii})}$ *for all* $i=1,..m$

where:

P_{ii} *is the solution to the Lyapunov equation* $(A_{ii}^0)P_{ii} + P_{ii}(A_{ii}^0)^T = -2Q_{ii}$.

Q_{ii} *is a positive semi-definite matrix*

$\sigma_{\max}$ *denotes the maximum singular value*

Proof:

Since A_{ii}^o is asymptotically stable, it satisfies the following steady state Lyapunov equation:

$$(A_{ii}^0)P_{ii} + P_{ii}(A_{ii}^0)^T = -2Q_{ii} \tag{3.26}$$

The solution to equation (18), P_{ii}, is a symmetric, positive semi-definite matrix i.e. $P_{ii}^T = P_{ii}$ and $x_i^T P_{ii} x_i > 0$. Matrix Q_i is positive definite i.e. $x_i^T Q_{ii} x > 0$.

We construct two matrices P_i and Q_i as follows:

$$P_i = \begin{bmatrix} 0 & \cdots & 0 \\ \vdots & [P_{ii}] & \vdots \\ 0 & \cdots & 0 \end{bmatrix}_{n \times n}$$

$$Q_i = \begin{bmatrix} 0 & \cdots & 0 \\ \vdots & [Q_{ii}] & \vdots \\ 0 & \cdots & 0 \end{bmatrix}_{n \times n}$$

Matrix P_i is symmetric, positive semi-definite and satisfies the following Lyapunov equation:

$$A_{ii}^T P_i + P_i A_{ii} = -2Q_i \tag{3.27}$$

Matrix Q_i is a positive semi-definite matrix

We can choose a Lyapunov function for subsystem i as:

$$V_i(x) = x^T P_i x \tag{3.28}$$

The system is stable where (a) $V_i(x)$ is positive semi-definite and (b) $\dot{V} \leq 0$.

(a) $V_i(x) = x^T P_i x$ is positive semi-definite for all x since P_i is positive semi-definite

Thus, to obtain the stability region we need to determine the region where:

$$\text{(b) } \dot{V}_i(x) = \dot{x}^T P_i x + x^T P_i \dot{x} \leq 0 \tag{3.29}$$

Substituting equation (3.25) into (3.29) we obtain the following:

$$\dot{V}_i(x) = \left((A_{ii} + A_{ij})x\right)^T P_i x + x^T P_i (A_{ii} + A_{ij})x$$

$$\dot{V}_i(x) = x^T (A_{ii})^T P_i x + x^T A_{ij}^T P_i x + x^T P_i (A_{ii})x + x^T P_i A_{ij} x$$

$$\dot{V}_i(x) = x^T \left((A_{ii})^T P_i + P_i A_{ii}\right)x + x^T \left(A_{ij}^T P_i + P_i A_{ij}\right)x \tag{3.30}$$

Substituting equation (3.27) into equation (3.30) gives the following:

$$\dot{V}_i(x) = x^T (-2Q_i)x + x^T (A_{ij}^T P_i + P_i A_{ij})x$$

For stability, we need $\dot{V}(x) \leq 0$ i.e.:

$$x^T(A_{ij}^T P_i + P_i A_{ij})x \le x^T(2Q_i)x \tag{3.31}$$

Since $(A_{ij}^T P_i)^T = P_i A_{ij}$ we can rewrite equation (3.31) as follows:

$$x^T P_i A_{ij}^T x + x^T (P_i A_{ij}^T)^T x \le x^T (2Q_i)x \tag{3.32}$$

Thus the matrix $(A_{ij}^T P_i + P_i A_{ij})$ is symmetric.

Thus we need to satisfy this inequality in order to guarantee stability.

Now consider the following inequality:

$$\sigma_{\max}(A_{ij}) \le \frac{\sigma_{\min}(Q_{ii})}{\sigma_{\max}(P_{ii})} \tag{3.33a}$$

$$\Rightarrow \sigma_{\max}(P_{ii})\sigma_{\max}(A_{ij}) \le \sigma_{\min}(Q_{ii}) \tag{3.33b}$$

We wish to show that the inequality in equation (3.33b) satisfies the condition for stability given in equation (3.32).

Since $\sigma_{\max}(P_{ii}A_{ij}) \le \sigma_{\max}(P_{ii})\sigma_{\max}(A_{ij})$

$$\Rightarrow \sigma_{\max}(P_{ii}A_{ij}) \le \sigma_{\min}(Q_{ii}) \tag{3.34}$$

We also know that the singular values of a matrix are the same as the singular values of its transpose. Thus, the following is true:

$$\sigma_{\max}(A_{ij}P_i) + \sigma_{\max}(P_i A_{ij}^T) = 2\sigma_{\max}(A_{ij}P_i) \tag{3.35}$$

From (3.34) and (3.35) we obtain the following:

$$\Rightarrow \sigma_{\max}(A_{ij}P_{ii} + P_{ii}A_{ij}^T) \le \sigma_{\min}(2Q_{ii}) \tag{3.36}$$

$$\Rightarrow \sigma_{\max}(A_{ij}P_{ii} + P_{ii}A_{ij}^T)x^T x \le \sigma_{\min}(2Q_{ii})x^T x \tag{3.37}$$

We know from Rayleigh's identity that, for a symmetric matrix $(A_{ij}P_{ii} + P_{ii}A_{ij}^T)$, the following:

$$x^T(A_{ij}P_{ii} + P_{ii}A_{ij}^T)x \le \sigma_{\max}(A_{ij}P_{ii} + P_{ii}A_{ij}^T)x^T x \tag{3.38}$$

Similarly,

$$x^T 2Q_{ii}x \ge \sigma_{\min}(Q_{ii})x^T x \tag{3.39}$$

Thus,

From (3.37), (3.38) and (3.39) we obtain the following result:

$$\Rightarrow x^T(A_{ij}P_{ii} + P_{ii}A_{ij}^T)x \leq x^T 2Q_{ii}x \tag{3.40}$$

Thus the condition for stability is satisfied. This means that the global system is stable if

$$\sigma_{\max}(A_{ij}) \leq \frac{\sigma_{\min}(Q_{ii})}{\sigma_{\max}(P_{ii})} \tag{3.41}$$

If we choose $Q_{ii} = I$ then equation (3.41) becomes:

$$\sigma_{\max}(A_{ij}) \leq \frac{1}{\sigma_{\max}(P_{ii})}$$

In alternative notation, the condition for stability can be expressed as follows:

$$\|A_{ij}\|_2 \leq \frac{1}{\|P_i\|_2}$$

This means that the subsystem i with all its interactions is stabilized. If all subsystems satisfy these conditions, the global system will be stable.

The conditions in *Lemma 3.1* provide us with a method of designing decentralized controllers which guarantee global stability of the interconnected system. This method is illustrated in Figure 3.11.

First, we obtain the models of the subsystem A_{ii}^0. Once these models have been obtained, we need to obtain information about the interactions A_{ij}^0. The only information about A_{ij}^0 that is required is an upper bound on the maximum singular value. This upper bound is much easier to obtain or to estimate than the exact model of A_{ij}^0. Once $\sigma_{\max}(A_{ij})$ has been obtained, the controller $k_i(s)$ for subsystem i is calculated. The closed loop state coefficient matrix of the system with $k_i(s)$ must satisfy the conditions of *Lemma 3.1*. If the condition is satisfied for the *ith* subsystem, the design procedure for this subsystem is complete. The same procedure is then applied to all other subsystem $i+1...m$. Since all the subsystems plus interactions are stabilized, this procedure guarantees global stability of the interconnected system.

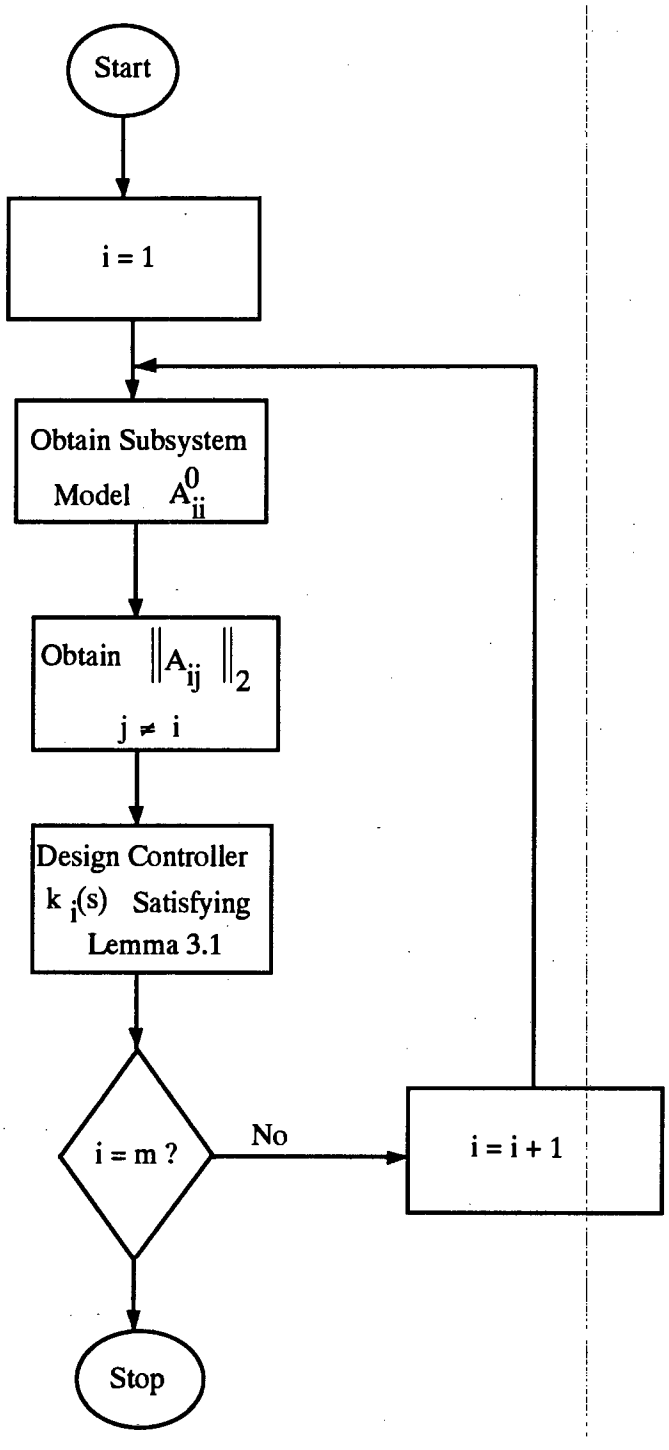

Figure 3.11: Procedure for Designing Decentralized Controllers which Guarantee Global Stability

The conditions specified in *Lemma 3.1* are only sufficient conditions. This means that the stability margins provided for the closed loop subsystems are conservative. The decentralized controllers that are obtained will therefore guarantee stability but will not be optimal.

It is important to note that the assumption that the subsystems A_{ii}^0 are all asymptotically stable, implies that all fixed modes in the system are stable. If any fixed mode in the system is unstable, then the assumption that A_{ii}^0 is stable cannot be satisfied.

Example 3.2

Consider a following state coefficient matrix:

$$A = \left[\begin{array}{cc:cc} -1.0000 & 0.1000 & a & 0 \\ 2.0000 & -2.0000 & 0 & 0 \\ \hdashline 0 & b & -0.5000 & 0 \\ 0 & 0 & 0 & -1.5000 \end{array}\right]$$

We wish to find values of a and b which would guarantee the stability of matrix A.

Matrix A can be considered as the state coefficient matrix of a system consisting of two subsystems with:

$$A_{11}^0 = \begin{bmatrix} -1 & 0.1 \\ 2 & -2 \end{bmatrix}, \quad A_{12}^0 = \begin{bmatrix} a & 0 \\ 0 & 0 \end{bmatrix}, \quad A_{21}^0 = \begin{bmatrix} 0 & b \\ 0 & 0 \end{bmatrix}, \quad A_{22}^0 = \begin{bmatrix} -0.5 & 0 \\ 0 & -1.5 \end{bmatrix}$$

The matrices A_{12}^0 and A_{21}^0 can be interpreted as the interactions between subsystems 1 and 2.

The eigenvalues of A_{11}^0 are -1.0000 and -2.0000 and the eigenvalues of A_{22}^0 are -0.5000 and -1.5000 i.e. matrices A_{11}^0 and A_{22}^0 are asymptotically stable. Thus we can find two symmetric, positive-definite matrices P_{11} and P_{22} satisfying the following Lyapunov equations:

$$(A_{11}^0)P_{11} + P_{11}(A_{11})^T = -2Q_{11}$$

$$(A_{22}^0)P_{22} + P_{22}(A_{22})^T = -2Q_{22}$$

We make use of Matlab™ to solve for P_{11} and P_{22} which is given by the following:

$$P_{11} = \begin{bmatrix} 1.0759 & 0.7593 \\ 0.7593 & 1.2593 \end{bmatrix}$$

$$P_{22} = \begin{bmatrix} 2.0000 & 0 \\ 0 & 0.6667 \end{bmatrix}$$

$$\sigma_{max}(P_{11}) = 1.9324$$

$$\sigma_{max}(P_{22}) = 2.0000$$

Therefore, we know that the system will be stable if the following two conditions hold:

$$\sigma_{max}(A_{12}) \leq 0.5175$$

$$\sigma_{max}(A_{21}) \leq 0.5000$$

where:

$$A_{12} = \left[\begin{array}{c:c} 0 & A_{12}^0 \\ \hdashline 0 & 0 \end{array}\right] = \left[\begin{array}{cc:cc} 0 & 0 & a & 0 \\ 0 & 0 & 0 & 0 \\ \hdashline 0 & 0 & 0 & 0 \\ 0 & 0 & 0 & 0 \end{array}\right]$$

$$A_{21} = \left[\begin{array}{cc} 0 & 0 \\ A_{21}^0 & 0 \end{array}\right] = \left[\begin{array}{cc:cc} 0 & 0 & 0 & 0 \\ 0 & 0 & 0 & 0 \\ \hdashline 0 & b & 0 & 0 \\ 0 & 0 & 0 & 0 \end{array}\right]$$

Therefore, by *Lemma 3.1*, if $|a| \leq 0.5175$ and $|b| \leq 0.5000$ we know that A will be stable. The eigenvalues of matrix A with $a = 0.5175$ and $b = 0.5$ are the following:

$$\lambda = \begin{bmatrix} -1.6828 + j0.1265 \\ -1.6828 - j0.1265 \\ -0.1343 \\ -1.5000 \end{bmatrix}$$

If $b = 1.0000$ then not all the conditions of *Lemma 3.1* are satisfied. In this case, we cannot say whether the system is stable or not since the conditions are only sufficient.. If we substitute $b = 1.000$ into A we obtain the following eigenvalues.

$$\lambda = \begin{bmatrix} -1.7696 + j0.5541 \\ -1.7696 - j0.554 \\ +0.0393 \\ -1.5000 \end{bmatrix}$$

Thus the system is unstable.

In order to show that these are not necessary conditions for stability, we let $a = 0.5200$. The eigenvalues of matrix A now becomes:

$$\lambda = \begin{bmatrix} -1.6834 + j0.1326 \\ -1.6834 - j0.1326 \\ -0.1333 \\ -1.5000 \end{bmatrix}$$

Thus, despite the fact that the conditions in *Lemma 3.1* are not satisfied if $a = 0.52$, matrix A is stable. This means that we can guarantee stability using the conditions in *Lemma 3.1*, but we cannot deduce anything about the instability of the system i.e. sufficient but not necessary conditions.

3.4.3 Hierarchical Control

The size of power systems is increasing rapidly due to the interconnection of power networks. This presents new challenges for the control of the system since the system that needs to be controlled may stretch over an entire continent. Figure 3.12 illustrates the hierarchical control that we envisage for large power systems.

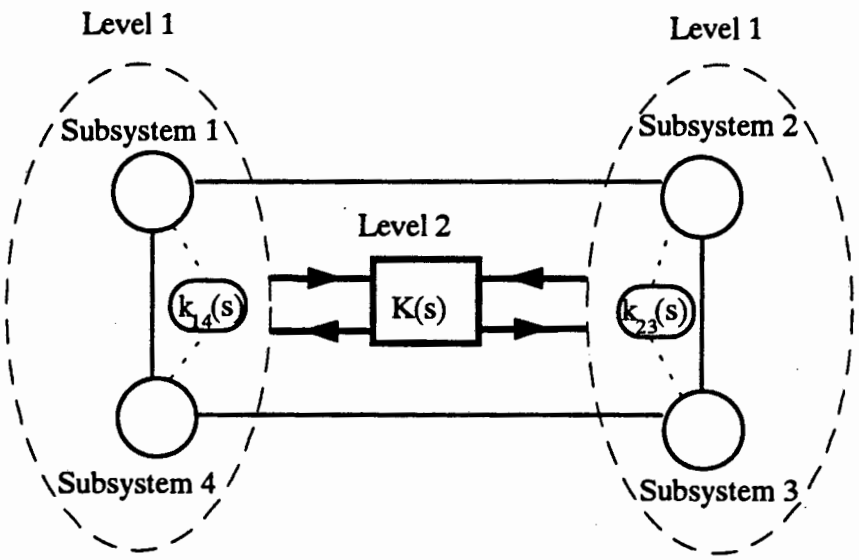

Figure 3.12: Diagrammatic Representation of a System Under Hierarchical Control

Assume that subsystems 1 and 4 are located closed to each other and that subsystem 2 is close to subsystem 3. The generator subsystems which are close to each other are collectively controlled by $k_{14}(s)$ and $k_{23}(s)$ respectively. This forms the first level of control. From the groups of generators the control signals are transmitted to the second

level controller. The Level 2 controller can transmit signals back to the first level controller by adjusting the parameters of the first level controller.

The strategy that we wish to employ for hierarchical control, depends on the operating states of the power system. Figure 3.13 illustrates the operating states and the transitions between these states [8].

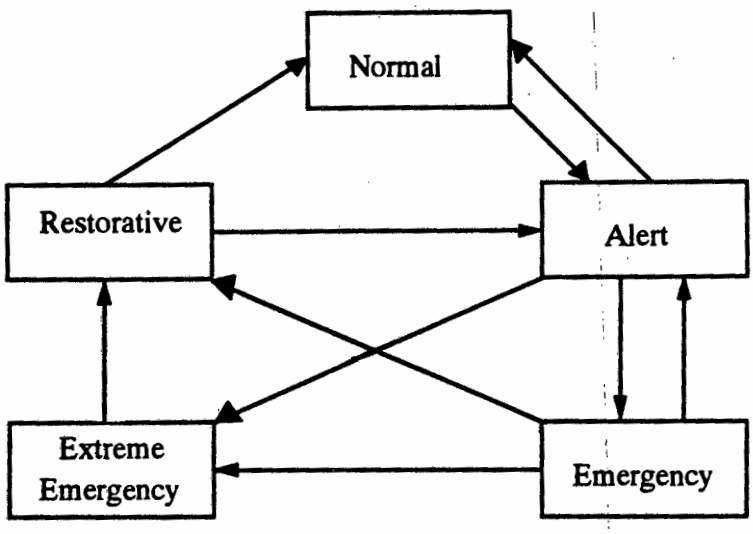

Figure 3.13: Operating States of a Power System and Transitions Between States

In the *normal state*, all steady state variables are within the normal range and there are no equipment violations. The system is in a secure state and is able to withstand any contingency without violating these constraints, If the security level falls below a certain level, the system enters the *alert state*. In this state, the variables are within the acceptable range and all constraints are satisfied. However, the steady state security of the system has deteriorated to such an extent, that a contingency may cause violations of constraints or equipment overload. Thus the system will move into an *emergency state*. If the contingency is particularly severe, the system will enter the state of extreme emergency. In the *restorative state* control action is taken to improve the steady state security of the system to the *normal* or *alert state*.

The above description of the operating states is provided in terms of steady state security analysis since all the violations and constraints are steady state quantities. In this section, we present a method of incorporating constraints for the dynamic security of the power system.

In *Appendix D*, we present conditions on the upper bound of time-varying perturbations such that stability of the system is guaranteed. The derivation of the sufficient conditions is the main contribution in this section of the thesis and can be stated as the following Lemma:

Lemma 3.2: *The interconnected system described by equation (D1) in Appendix D is globally stabilizable by completely decentralized feedback if the following conditions are met:*

$$\sigma_{\max}(A_{ij}^0) + \varepsilon_{ij}\sigma_{\max}(U_{ij}) + \varepsilon_{ii}\sigma_{\max}(U_{ii}) \le \frac{1}{\sigma_{\max}(P_{ii})} = \alpha_{ii}^t$$

for all i=1,..m (3.42)

where:

P_{ii} *is the solution to the Lyapunov equation* $(A_{ii}^0)P_{ii} + P_{ii}(A_{ii}^0)^T = -2Q_{ii}$

Q_{ii} *is a positive semi-definite matrix that we select*

$\sigma_{\max}$ *denotes the maximum singular value*

α_{ii}^t *is the global stability margin for the ith subsystem*

$A_{ij}^0, U_{ii}, U_{ij}, \varepsilon_{ij}$ and ε_{ii} are defined in *Appendix D*

Lemma 3.2 states that if the inequalities in (3.42) are satisfied for all subsystems, the system will be globally stable. We wish to use *Lemma 3.2* to control a time-varying plant.

Since we are dealing with a time-varying plant, the variables $A_{ij}^0, U_{ii}, U_{ij}, \varepsilon_{ij}, \varepsilon_{ii}, P_{ii}$ and α_i^t in (3.42) could change as the model of the plant changes. We wish to ensure that if the plant model changes, the system remains globally stable i.e. all the conditions in (3.42) are satisfied. Note that we cannot directly control the variables $A_{ij}^0, U_{ii}, U_{ij}, \varepsilon_{ij}, \varepsilon_{ii}$ since these are related to the perturbations (see *Appendix D*). However, we can directly control the variables P_{ii} and ε_i^t by adjusting the parameters of the controller on the *ith* subsystem. If we adjust the controller parameters of the *ith* subsystem such that the corresponding condition in (3.42) is satisfied, then the *ith* subsystem is stable. If this adjustment of the controller parameters is applied to all subsystems, we can ensure global stability of the

interconnected time-varying system. Using this approach, we can formulate a strategy for hierarchical control for the damping of electromechanical oscillations.

We regard variations in the operating states of the power system as time-varying perturbations (in *Appendix C* we categorise the different perturbations that a power system can be subjected to). Under *normal operating* conditions, the dynamics of the generator subsystems are regulated by the decentralized Level 1 controllers. The Level 2 controller receives information about the interactions between the subsystems but remains idle. The Level 2 controller monitors the upper bound on the interactions through on-line modelling. When the interactions between the subsystems increase to a value close to the margins given in (3.42), the global system may become unstable even though the local subsystems are stable. We regard this state as the *alert state* for dynamic security. Under the *alert state*, the Level 2 controller is activated. The Level 2 controller adjusts the parameters of the Level 1 controller in order to ensure that the system remains stable. The adjustments of the Level 1 controllers are performed using the stability margin given in *Appendix D*. Thus the system is moved from *alert state* to *normal state* by hierarchical control.

We propose therefore that the conditions that we have developed in *Lemma 3.2* be incorporated as constraints in dynamic security assessment. However, we emphasize that since the conditions in *Lemma 3.2* are only sufficient conditions, they provides a conservative bound on the dynamic security of the system.

3.5 Conclusions

This chapter deals with the *control structure* for damping electromechanical oscillations using Power System Stabilizers (PSS). Three aspects of the control structure are addressed, namely the *type of feedback*, the *type of signal* and *type of control.*

The *type of feedback* that was selected for damping of electromechanical oscillations was Dynamic Output Feedback. The Dynamic Output Feedback control problem was converted into a Static Output Feedback problem in order to ensure that a low order controller is obtained.

The selection of the *type of signal* for damping of the electromechanical mode oscillations was addressed using two methods. These two methods were based on two measures of the contribution of the electromechanical oscillation to the output signals. The first measure, the *Centralized Modal Observer Measure (CMOM)*, is based on a centralized observability of the electromechanical modes. The second measure, the *Decentralized Modal Observer Measure (DMOM)*, is based on the existence of decentralized fixed modes. The DMOM is a more realistic measure of the effectiveness of a signal for damping the electromechanical modes than the CMOM since it takes into account the decentralized nature of the control problem. However, the DMOM is computationally more intensive than CMOM.

The issues related to the *type of control* were addressed by investigating the problems associated with the use of centralized, decentralized and hierarchical control. Sufficient conditions for global stability of the interconnected system were derived for systems under decentralized control. These conditions place inequality constraints on the H_∞ norms of the closed loop subsystems. These constraints were incorporated in a conceptual hierarchical control structure for large power systems.

References

[1] Kailath T., *Linear Systems*, Prentice-Hall, 1980.

[2] Chen C. T., *Linear Systems Theory and Design*, Holt, Rhinehart and Winston, 1984.

[3] Bollinger K., Gu W., Norum E., "Accelerating Power Versus Electrical Power as Input Signal to PSS" *IEEE Trans. on Energy Conversion.* Vol. 6., No. 4, pp.620-626, December 1991.

[4] Handschin E., Wohlfahrt H., "Different Power System Stabilizer Properties Under Unified Short- and Mid-Term Aspects", *Presented at the IFAC Symposium on Power Systems, Modelling and Control Applications*, Brussels, September 1988.

[5] Martins N., Lima L., "Eigenvalue and Frequency Domain Analysis of Small-Signal Electromechanical Stability Problems." *IEEE/PES Symp. on Eigenanalysis and Frequency Domain Methods for System Dynamic Performance.* pp.17-33,1989.

[6] Chen C. L., Hsu Y. Y. " An Efficient Algorithm for the Design of Decentralized Output Feedback Power System Stabilizers", *IEEE Transactions on Power Systems*, Vol. 3, pp.999-1004, August 1988.

[7] Yu Y. N., *Electric Power System Dynamics*, Academic Press Inc., New York 1983.

[8] Anderson P., Fouad A., Power System Control and Stability, Iowa State University Press, Ames, Iowa, 1977.

[9] Davison E., "A Computational Method For Finding the Zeros of a Multivariable LTI System", *Automatica*, Vol. 6, pp.481-484, May 1970.

[10] Anderson B., Clements D., "Algebraic Characterization of Fixed Modes in Decentralized Control", *Automatica,* Vol. 17, No. 5, pp. 703-712,1981.

[11] Steinbuch M., Bosgra O., "Necessary Conditions for Static and Fixed Order Dynamic Mixed H_2 / H_∞ Optimal Control", *Proceedings of the American Control Conference*, pp.1137-1142, paper TA3 8:30, 1993.

[12] Wang S., Davidson E., "On the Stabilization of Decentralized Control Systems, *IEEE Transactions on Automatic Control*, AC-18,473.

[13] Chow J., Sanchez-Gasca J., "Pole-Placement Designs of Power System Stabilisers." *IEEE Transactions on Power Systems*, Vol. 4, No. 1, pp.271-277, February 1989.

[14] Fletcher R., *Practical Methods of Optimization*, Vol. 1 and Vol. 2, John Wiley and Sons, 1980.

Chapter 4

Design of Robust H_∞-Based Supplementary Excitation Controllers

4.1. Introduction

This chapter deals with the design of robust H_∞-based supplementary excitation controllers for damping electromechanical oscillations. The chapter focuses on the design of new controllers which will replace existing lead-lag PSS.

Generator excitation control systems consist of Automatic Voltage Regulators (AVR) for transient voltage regulation and Conventional Power System Stabilizers (CPSS) for damping of the electromechanical oscillations. The design of CPSS is based on classical linear systems theory and is therefore valid for only a small region about the operating point.

There have been several reports demonstrating the poor performance of CPSS under changing operating conditions of the power system. The CPSS can cause large overshoot in terminal voltage after the removal of a fault. In addition, under light loading conditions, CPSS can provide inadequate damping which results in sustained oscillations under even small disturbances [1,2,3]. This reflects a need for the design of control systems with robust performance with respect to changes in the parameters of the power system.

One method of addressing this need is to design controllers that minimize the sensitivity to changes in the model of the plant. This chapter makes use of modern linear control theory in the form of $H\infty$ optimal control to design robust excitation controllers.

Recently, there has been a growing interest in the application of $H\infty$ control to power systems. In [7] the authors use a state feedback $H\infty$ algorithm on a single machine infinite bus (SMIB) system. In [9] the voltage loop is coupled to the power loop for multi-input,

multi output (MIMO) H_∞ design and the closed loop performance is compared to that of Proportional Integral Differential (PID) controllers for a SMIB system. In [10], the author implements a Dynamic Output Feedback H_∞ algorithm on a SMIB power system. Up to now however, issues concerning weakly damped modes, decentralized control, robustness margins and global stability of power systems under H_∞ control have not been addressed.

In this chapter we present several contributions to the area of robust control of power systems. Firstly, we develop a new method for the design of completely decentralized H_∞ controllers . The method ensures stability of the interconnected multimachine power system by incorporating global stability constraints in the design procedure.

Secondly, we introduce a Lyapunov-based robust stability index in order to evaluate the robustness of the closed loop generator subsystems. This index is used to compare the robust margins of three controllers, namely CPSS, optimal H_∞ and suboptimal H_∞ controllers.

Thirdly, the method of balanced truncation is used to reduce the order of the open loop plant. The model reduction technique is applied to the generator subsystems which ensures that the order of the controllers is less than that of the open loop subsystems.

Fourthly, we use an existing Ricatti-based Dynamic Output Feedback H_∞ algorithm to synthesize the controllers.

Finally, the chapter discusses the major shortcomings of the standard optimal H_∞ control algorithms as applied to power systems and presents techniques for overcoming these. We compare the performance of three different types of controllers, namely CPSS, optimal H_∞ and suboptimal H_∞ over different operating conditions.

The chapter begins by providing a brief description of the control requirements of an interconnected power system with time-varying perturbations. The design strategy used in the chapter is then presented. Next, the design strategy is applied to a nine-bus benchmark network. We apply the standard *optimal* H_∞ method design controllers for the benchmark

network. The problems associated with this method are outlined and improvements in the form of *suboptimal* H_∞ controllers are presented. The time domain results are shown for different operating conditions. The performance of CPSS, optimal H_∞ and suboptimal H_∞ controllers are compared.

The results indicate that the system with the suboptimal H_∞ controllers has satisfactory performance under a wide range of operating conditions. Furthermore, the results demonstrate that the suboptimal H_∞ controllers possess superior robustness properties compared to that of the CPSS and optimal H_∞ controllers.

4.2 Problem Formulation

Consider an n-dimensional interconnected power system S consisting of m generator subsystems. The linearized state space equations can be expressed as follows:

$$S \triangleq \{S_i\} \triangleq \begin{Bmatrix} \dot{x}_i = \left(A_{ii}^0 + E_{ii}(t)\right)x_i + \sum_{j \neq i}^{m} (A_{ij}^0 + E_{ij}(t))x_j + B_i u_i \\ y_i = C_i x + D_i u_i \end{Bmatrix} \tag{4.1}$$

where:

$x_i \in R^{n_i}$ and $u_i \in R$ are the state and input vectors respectively corresponding to subsystem S_i

$x = [x_1 \quad \dots \quad x_m]$ is the state vector of S

$A_{ii}^0 \in R^{n_i \times n_i}$ is the square diagonal block i of the nominal plant A matrix relating $\dot{x}_i$ to x_i

$A_{ij}^0 \in R^{n_j \times n_j}$ is the off-diagonal interaction block *(i,j)* of the nominal plant A matrix relating $\dot{x}_i$ to x_j

$E_{ii}(t) \in R^{n_i \times n_i}$ is the linear time-varying perturbation matrix function relating $\dot{x}_i$ to x_i

$E_{ij}(t) \in R^{n_j \times n_j}$ is the linear time-varying interaction perturbation matrix function relating $\dot{x}_i$ to x_i

$B_i \in R^{n_i \times 1}$ is the constant input coefficient vector relating $\dot{x}_i$ to u_i

$C_i \in R^{p_i \times n_i}$ is the constant vector relating the output y_i to the state vector x

$D_i \in R$ is the direct feedthrough term relating the output y_i to the input u_i

n_i is the number of states in vector x_i and $\sum_{i=1}^{m} n_i = n$

System S describes the dynamics of the power system by taking into account (a) the decentralized nature of the power system (b) the interactions between subsystems and (c) the time-varying perturbations. These aspects reflect the essence of the power system model used for damping electromechanical oscillations. As such, system S represents the most general description of the power system that we deal with in this chapter.

By ignoring the interaction and/or perturbation terms in equation (4.1), S can be reduced to less general descriptions of the power system. We define two systems which are obtained from system S, namely systems R and V.

By ignoring the interactions $(A_{ij}^0 = 0)$ as well as the perturbations $(E_{ii} = E_{ij} = 0)$ in system S, we obtain *system R* which is defined as follows:

$$R \triangleq \{R_i\} \triangleq \begin{Bmatrix} \dot{x}_i = A_{ii}^0 x_i + B_i u_i \\ y_i = C_i x + D_i u_i \end{Bmatrix} \tag{4.2}$$

System R describes a fictitious power system where the subsystems are disconnected from each other i.e. there is no coupling between the generator subsystems $(A_{ij}^0 = 0)$. Furthermore, the power system operating point is fixed and time-invariant $(E_{ii} = E_{ij} = 0)$.

By ignoring only the interactions $(A_{ij}^0 = 0)$ in system S, we obtain *system V* which is defined as follows:

$$V = \{V_i\} = \{\dot{x}_i\} = \begin{Bmatrix} (A_{ii}^0 + E_{ii}(t))x_i(t) \\ y_i = C_i x + D_i u_i \end{Bmatrix} \tag{4.3}$$

System V describes a fictitious power system where the subsystems are disconnected from each other i.e. there is no coupling between the generator subsystems $(A_{ij}^0 = 0)$. The power system is not time-invariant since $E_{ii} \neq 0, E_{ij} \neq 0$.

Assume that (A_{ii}, B_i) is controllable and (A_{ii}, C_i) observable for all i. In this chapter, we wish to improve the damping of the power system given by S. In addition to improving the damping of S, the following *control requirements* must be met:

(1) *Decentralized Dynamic Output Feedback control* in order to reduce the communication of control signals
(2) *Global stability* of the interconnected system
(3) *Robust closed loop performance* in order to take into account changes in the plant dynamics
(4) *Low order controllers* in order to simplify the implementation
(5) *Satisfactory damping* of the closed loop in order to damp the electromechanical oscillations.

The following section will present a brief description of the design strategy employed in the chapter to meet these requirements.

4.3 Design Strategy

In this section we develop a design strategy to meet the requirements as listed in Section 4.2. First, we describe a new *two-stage decentralized control* approach. Stage one meets requirement (1) of the design strategy i.e. we design *decentralized controllers using dynamic Output Feedback.* Stage two meets requirement (2) of the design strategy i.e. we guarantee *global stability of the interconnected* system. Thereafter, we outline a method of obtaining controllers with robust closed loop performance thus addressing requirement (3). We also develop a new a robust stability margin for determining the robustness of a decentralized control system. Finally, we present a model reduction technique based on *balanced realization* in order to obtain low order controllers, thus satisfying requirement (4).

4.3.1 Design of Two-Stage Decentralized Control

In this section, we address requirement (1) of the design strategy i.e. that decentralized control is to be used. This means that no signals from remote subsystems can be used for control.

In the first stage of the design, the controllers are obtained for each subsystem as if these subsystems have no interactions ($A_{ij}^{0} = 0$) and are unperturbed ($E_{ii} = E_{ij} = 0$). Therefore, in the first stage of the controller design, we make use of system R.

The second stage of the design is concerned with ensuring global stability of the interconnected system i.e. we address requirement (2) of the design strategy. In this stage, the stability of the interconnected system is checked. If the controllers calculated in stage one result in a stable interconnected system, these controllers are accepted as feasible. However, if the controllers calculated in stage one result in an unstable interconnected system, these controllers are rejected. In this stage of the design, we require information about the interactions between subsystems. We do not consider the effect of the perturbations.

There are two major advantages of this new two-stage decentralized design approach. Firstly, since we are making use of only the subsystem equations R_i for the design of the decentralized controller k_i, the order of the open loop plant is low. The low order plant eases the computational burden in synthesizing each controller. Furthermore, a low order plant requires only a low order controller. Thus, by using the uncoupled, unperturbed subsystems for designing the controllers we reduce the computational requirements of the problem and we can obtain low order controllers.

Secondly, the two-stage decentralized design procedure eliminates the need for on-line exchange of information between subsystems in order to stabilize the interconnected system. The second stage of the design procedure guarantees global stability of the interconnected system despite the use of fully decentralized control. Therefore, in order to control system S, we do not need to transmit signals from other subsystems to the decentralized controllers.

For Dynamic Output Feedback control, the following feedback control law is used for subsystem R_i:

$$u_i = -k_i(s)y_i \tag{4.4}$$

The output signal y_i which used in the control of subsystem i can be chosen using the methods described in Section 3.4 i.e. CMOM and DMOM.

4.3.2 Obtaining Robust Controllers

In this section, we address the problem of synthesizing controllers which will ensure *robust performance of the closed loop.* We also develop a method of determining the robust stability margin of the control system.

4.3.2.1 Synthesizing Robust Controllers

In the first stage of the design procedure, we were required to obtain a controller for each subsystem. In this section, we outline a method to obtain a controller that ensures robust performance of the closed loop.

The decentralized controller $k_i(s)$ for the *ith* subsystem is obtained by using H_∞ control theory. We provide a brief description of the problem formulation in H_∞ control theory. (for clarity, subscripts and superscripts denoting subsystems will be omitted)

To formulate the problem of H_∞ design, the reduced order nominal plant is arranged as shown in Figure 4.1. The transfer functions $\Delta_A(s)$ and $\Delta_M(s)$ are the additive and multiplicative uncertainties respectively. Let $\Delta_A(s) = \Delta_M(s) = 0$:

We define three transfer functions:

$$S(s) = \frac{e}{u} = \frac{1}{1+G(s)K(s)} \tag{4.5}$$

$$R(s) = \frac{u_1}{u} = \frac{K(s)}{1+G(s)K(s)} = K(s)S(s) \tag{4.6}$$

$$T(s) = \frac{y}{u} = \frac{G(s)K(s)}{1+G(s)K(s)} = 1 - S(s) \tag{4.7}$$

where S(s), R(s) and T(s) are the Sensitivity, Related Additive Robustness and Complimentary Sensitivity Transfer Functions respectively.

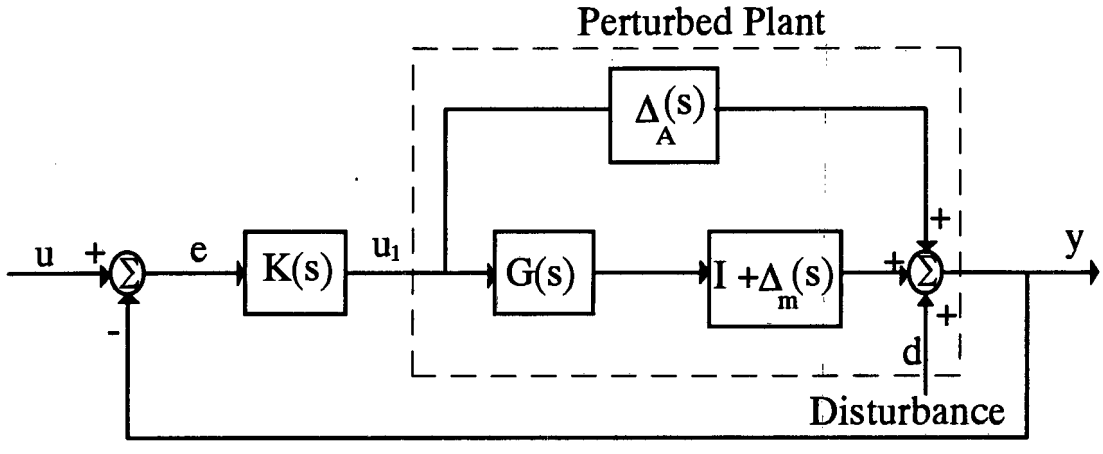

Figure 4.1: Nominal Plant with Perturbations and Controller

The closed loop performance is specified by three frequency dependent weighting functions, W1, W2, W3. In order to minimize the effects of disturbances on the plant output y, we specify that:

$$\sigma_{\max}(S(j\omega)) \leq \left|W1^{-1}(j\omega)\right|$$

Furthermore, in order to ensure robust performance under plant variations, we specify that:

$$\sigma_{\max}(R(j\omega)) \leq \left|\Delta_A(j\omega)\right| = \left|W2^{-1}(j\omega)\right|$$

$$\sigma_{\max}(T(j\omega)) \leq \left|\Delta_M(j\omega)\right| = \left|W3^{-1}(j\omega)\right|$$

where $\sigma_{\max}$ is the frequency dependent maximum singular value.

These requirements are simultaneously satisfied by the following inequality:

$$\left\| \begin{matrix} W1(j\omega)S(j\omega) \\ W2(j\omega)R(j\omega) \\ W3(j\omega)T(j\omega) \end{matrix} \right\|_\infty \leq 1 \qquad (4.8)$$

where $\|G(j\omega)\|_\infty = \sup_\omega(\sigma_{\max}(G(j\omega))$ denotes the $H\infty$ norm of the system. Thus the weighting functions are used as constraints to guide the search for an appropriate controller. The actual values of the parameters of the weighting functions depend on the closed loop specifications of the plant. The weighting functions are adjusted by a parameter γ_w in order to obtain the optimal weighting functions. The controller which corresponds to

these weighting functions is the optimal H_∞ controller. In this chapter we make use of the algorithm described in [16] to synthesize these optimal H_∞ controllers.

4.3.2.2 Calculating the Robust Stability Margin

Once the $H\infty$ controller has been synthesized, the robust stability margin of the closed loop system needs to be investigated. The robust stability margin is a measure of the maximum amount of perturbation that a control system can be subjected to while still remaining stable.

In order to determine the robust stability margin we could make use of eigenvalue techniques [17]. By repeatedly varying the operating point of the plant and calculating the eigenvalues we can determine the operating point at which the system becomes unstable. The *'distance'* between the initial operating point and the point at which instability occurs, would provide a measure of the robust stability margin. This approach is, however, computationally very intensive since it requires repeated calculation of the eigenvalues.

In this section we present a new method to determine the robustness of a power system *without* requiring repeated eigenvalue calculations. The details of this method can be found in Section C.1 of *Appendix C*. (*Appendix C* also provides a detailed discussion of the classes of perturbation that a power system can be subjected to).

For calculating the robust stability margin for the *ith* subsystem, we require information about the perturbations $E_{ii}(t)$ only. Thus, we make use of system V which is given by:

$$V = \{V_i\} = \{\dot{x}_i\} = \begin{Bmatrix} (A_{ii}^0 + E_{ii}(t))x_i(t) \\ y_i = C_i x + D_i u_i \end{Bmatrix} \tag{4.9}$$

For determining the robust stability margin, we assume A_{ii}^0 to be asymptotically stable. We further assume that the perturbations $E_{ii}(t)$ are structured (see *Appendix C* for a classification of perturbations). Since the perturbations are structured, we know the following:

$$\varepsilon^{k,l} \stackrel{\Delta}{=} \left| E^{k,l} \right| \quad \text{and} \quad \varepsilon \stackrel{\Delta}{=} \max_{k,l} \varepsilon^{k,l}$$

We can now state the following Lemma:

The perturbed system is stable i.e. $\mathrm{Re}(\lambda_i(A_{ii}^0 + E_{ii})) < 0,\ i = 1,...n$ if

$$\varepsilon < \frac{\sigma_{\min}(Q_{ii})}{\sigma_{\max}(P_{ii}U_{ii})} = \alpha_{ii} \tag{4.10}$$

where:

$$U_{ii}^{k,l} = \frac{\varepsilon^{k,l}}{\varepsilon} \tag{4.11}$$

P_{ii} satisfies the steady state Lyapunov equation $\left(A_{ii}^0\right)^T P_{ii} + P_{ii}\left(A_{ii}^0\right) + 2Q_{ii} = 0$

Q_{ii} is a positive definite matrix which we specify.

From equation (4.11), we note that matrix U_{ii} is obtained from a knowledge of each element in matrix E i.e. we assume that the perturbation is highly structured. In *Appendix C* we discuss ways of obtaining matrix U_{ii} for highly structured and weakly structured perturbations using power applications software (PAS).

The value α_{ii} is a measure of the amount of perturbation that the *ith* subsystem can be subjected to without becoming unstable. A large α_{ii} indicates that the subsystem has a large robust stability margin (it is difficult to destabilize the system), whereas a small α_{ii} indicates that the subsystem has a small robust stability margin (it is easy to destabilize the system).

We made use of α_{ii} to compare the robust stability margins of suboptimal H_∞ controllers with those of the CPSS and optimal H_∞ controllers. The robust stability margins for the case study is provided in Table 4.1 and will be discussed later.

4.3.3 Controller Order Reduction

This section addresses requirement (4) of the design strategy namely, the need for low order controllers.

Typically, the order of a generator subsystem, including AVR and governor modeling, is greater than eight [14]. The standard H_∞ optimal control method is known to obtain controllers of the same order as that of the open loop plant [5]. Thus, if the full model of the generator is used, the controller order will be unacceptably high.

In this section we obtain low order controllers by first reducing the order of the open loop system. The H_∞-based method of synthesizing the controllers is applied to the reduced model resulting in low order controllers.

The model reduction is applied only to the generator subsystems. Since the interactions and perturbations are not used in the decentralized design, system R is used in this section.

In order to reduce the order of the open loop system, we make use of the method of balanced truncation. In the following section, we describe this method for reducing the model of subsystem R_i. Subsystem R_i can be expressed as follows (for the sake of clarity the subscripts i and j are omitted):

$$R_i \triangleq \begin{Bmatrix} \dot{x} = Ax + Bu \\ y = Cx + Du \end{Bmatrix} \tag{4.12}$$

In model reduction, we would like to reduce the system order while preserving the input-output behavior. The modes that are uncontrollable or unobservable affect only the *internal* behavior of the system, not the *input-output* behavior. Therefore, the uncontrollable or unobservable modes can be removed without loss in modeling accuracy. The modes which are weakly controllable and weakly observable can be identified using a *transformation for balanced realization*. The method of obtaining this transformation is described in Section L of *Preliminaries*.

Assume that the *ith* subsystem is stable and that all uncontrollable and unobservable modes have been removed.

The Controllability Grammian P and Observability Grammian Q are defined as follows:

$$P = \int_0^\infty e^{At} BB^T e^{A^T t} dt \quad \text{and} \quad Q = \int_0^\infty e^{A^T t} C^T C e^{At} dt \tag{4.13}$$

We calculate P and Q from the following Lyapunov equations:

$$AP + PA^T + BB^T = 0. \tag{4.14}$$

$$A^T Q + QA + C^T C = 0. \tag{4.15}$$

From P and Q, the Hankel singular values can be calculated. The Hankel singular values $\sum$ are defined as follows:

$$\sum = \sqrt{\lambda(PQ)} \tag{4.16}$$

where λ (PQ) denotes the eigenvalues of PQ.

Let $x = Tx_b$. (4.17)

where T is a transformation for balanced realization (see Section L of *Preliminaries*)

x_b is the vector of transformed states (b denotes balanced).

We substitute equation (4.17) into equation (4.12) which transform subsystem R_i into the following balanced subsystem:

$$\begin{aligned} \dot{x}_b &= A_b x_b + B_b u \\ y_b &= C_b x_b + D_b u \end{aligned} \tag{4.18}$$

We use the transformation for balanced realization because the controllability and observability Grammians (P and Q) of the balanced system are equal and diagonal. Furthermore, the diagonal elements of P and Q are the Hankel singular values i.e. $P = Q = \sum^{\frac{1}{2}}$.

In the balanced form of equation (4.18), the last elements of the vector x_b are associated with the least controllable or least observable modes in the system model for a given set of inputs $u(t)$ and outputs $y(t)$.

By partitioning the state vector x_b into two parts $\begin{bmatrix} x_{b1} & x_{b2} \end{bmatrix}^T$, equation (4.18) becomes:

$$\begin{bmatrix} \dot{x}_{b1} \\ \dot{x}_{b2} \end{bmatrix} = \begin{bmatrix} A_{b11} & A_{b12} \\ A_{b21} & A_{b22} \end{bmatrix} \begin{bmatrix} x_{b1} \\ x_{b2} \end{bmatrix} + \begin{bmatrix} B_{b1} \\ B_{b2} \end{bmatrix}$$
$$y_b = \begin{bmatrix} C_{b1} & C_{b2} \end{bmatrix} \begin{bmatrix} x_{b1} \\ x_{b2} \end{bmatrix} + [D]u \tag{4.19}$$

where x_{b2} contains the number of states that we wish to remove.

The Controllability and Observability Grammians satisfy the following Lyapunov equations:

$$\begin{bmatrix} A_{b11} & A_{b12} \\ A_{b21} & A_{b22} \end{bmatrix} \Sigma + \Sigma \begin{bmatrix} A_{b11} & A_{b12} \\ A_{b21} & A_{b22} \end{bmatrix}^T + \begin{bmatrix} B_{b1}B_{b1}^T & B_{b1}B_{b2}^T \\ B_{b2}B_{b1}^T & B_{b2}B_{b2}^T \end{bmatrix} = 0 \tag{4.20}$$

$$\begin{bmatrix} A_{b11} & A_{b12} \\ A_{b21} & A_{b22} \end{bmatrix}^T \Sigma + \Sigma \begin{bmatrix} A_{b11} & A_{b12} \\ A_{b21} & A_{b22} \end{bmatrix} + \begin{bmatrix} C_{b1}^T C_{b1} & C_{b1}^T C_{b2} \\ C_{b2}^T C_{b1} & C_{b2}^T C_{b2} \end{bmatrix} = 0 \tag{4.21}$$

where:

$\Sigma = \begin{bmatrix} \Sigma_{11} & 0 \\ 0 & \Sigma_{22} \end{bmatrix}$ is the matrix of Hankel singular values arranged in decreasing order on the diagonal.

The reduced model of subsystem R_i is obtained by removing the state x_{b2} from x_b, thus removing the least controllable and/or observable modes of the system. The reduced model is given by:

$$\dot{x}_{b1} = A_{b11}x_{b1} + B_{b1}u$$
$$y_b = C_{b1}x_{b1} + Du \tag{4.22}$$

The transfer function $G_r(s)$ of the reduced order model is given by the following:

$$G_r(s) = C_{b1}(sI - A_{b11})^{-1}B_{b1} + D \tag{4.23}$$

Once the reduced order model has been obtained by eliminating the least controllable and least observable modes of the system, the reduced model can be further adjusted to achieve improved model matching. We can obtain better matching between the reduced order model and the full order model by adjusting the direct feedthrough term D in the reduced-

order model. For damping the electromechanical oscillations, it is important to obtain good model matching at discrete frequencies such as $\omega = 0$, $\omega = \infty$, and $\omega = \omega_m$ where ω_m is the electromechanical oscillation. To obtain a good approximation over a discrete set of frequencies ω_i, the direct feedthrough term of the reduced system D is set to be equal to D_r which is defined as follows:

$$D_r = \frac{1}{N_\omega} \sum_{i=1}^{N_\omega} \mathrm{Re}(G(j\omega_i) - C_{b1}(j\omega_i I - A_{b11})^{-1} B_{b1} \tag{4.24}$$

where:

N_ω is the number of discrete frequencies.

The error of the reduced order model has the following L_∞ bound:

$$\left\| G(j\omega) - G_r(j\omega) \right\|_{L_\infty} \leq 2\, Trace(\Sigma_{22}) \tag{4.25}$$

We apply the model reduction procedure to all the generator subsystems for R_i. The results of the model reduction technique as applied to the nine-bus system is provided in *Appendix F*.

4.3.4 Improving the Damping of Weakly Damped Modes

In this section we address the requirement (5) as outlined in section 4.2, namely that the closed loop system should have satisfactory damping. We first discuss the effect of the standard optimal H_∞ control on the damping. We outline the shortcomings of the standard optimal H_∞ control methodology for damping electromechanical oscillations. Thereafter, we present a method of improving the damping of weakly damped modes by using a suboptimal H_∞ algorithm.

4.3.4.1 Effect of Optimal H_∞ Control on Damping

In this section we analyze the effect that the optimal H_∞ control methodology has on the damping of oscillations. The effect can be determined by investigating the manner in which the optimal H_∞ control achieves its design objectives.

The objective in optimal H_∞ control is to minimize the H_∞ norm of a disturbance-related transfer function. For stable, minimum-phase systems, the optimal solution is found when the controller dynamics cancel the plant dynamics. For unstable, non-minimum-phase systems, the optimal solution is found by reflecting the unstable dynamics of the plant (about the $j\omega$-axis) and then inverting the reflected unstable part of the open loop plant. Thus, the optimal H_∞ controller attempts to cancel undesirable plant dynamics by means of inverting the stable part of the open loop plant while inverting the *reflected* unstable part of the open loop plant.

Stated differently, the optimal H_∞ method achieves its design objectives by affecting the *observability* of the open loop poles. However, it does not improve the *damping factor* of these poles. Thus, if the system operating point changes, the (initially unobservable) weakly damped poles will move away from the zeros. The weakly damped poles will therefore begin to dominate the performance of the closed loop under such changing operating conditions.

It may appear, therefore, that the H_∞ method of pole-zero cancellation explored above does not offer a solution to damping of power oscillations since only the observability of the voltage loop poles are affected. The poles of the power loop remain unaffected. In the next section however, we describe a technique for improving the damping of the voltage *and* power loop while still making use of excitation control only.

4.3.4.2 Effect of Suboptimal H_∞ Control on Damping

In this section we describe a well-known method of improving the damping of weakly damped modes using H_∞ control [17]. In particular, we are concerned with damping the power oscillations while restricting the control to the voltage loop. We impose this

restriction because fast control through the power loop is mechanically stressful on the valves and therefore undesirable.

Figure 4.2 illustrates the procedure that was used to improve the power loop damping through voltage loop control. The procedure is applied to the reduced order model of each subsystem. In Figure 4.2a the pole-zero plot of the generator subsystem voltage loop given by $G_i(s) = C_i(sI - A_{ii}^0)^{-1}B_i + D_i$ is shown (only weakly damped poles and critical zeros are shown).

By means of a bilinear transformation, the open loop poles can be shifted past the axis of the electromechanical eigenvalues i.e. let $\bar{s} = s + p$ where p is the horizontal shift of the jω axis. The constant matrices of the transformed state space description of the system is given by the following:

$$\begin{bmatrix} A_{iib} & B_{ib} \\ C_{ib} & D_{ib} \end{bmatrix} = \begin{bmatrix} (A_{ii}^0 - pI) & B_i \\ C_i & D_i \end{bmatrix} \tag{4.26}$$

where:

$A_{iib}, B_{ib}, C_{ib}, D_{ib}$ are the matrices of transformed system

If p is chosen such that $p > \mathrm{Re}\{\max \lambda(A_{ii})\}$, the transformation creates a fictitious unstable plant $G_i'(s)$ shown in Figure 4.3b. The standard H_∞ algorithm is then applied to $G_i'(s)$.

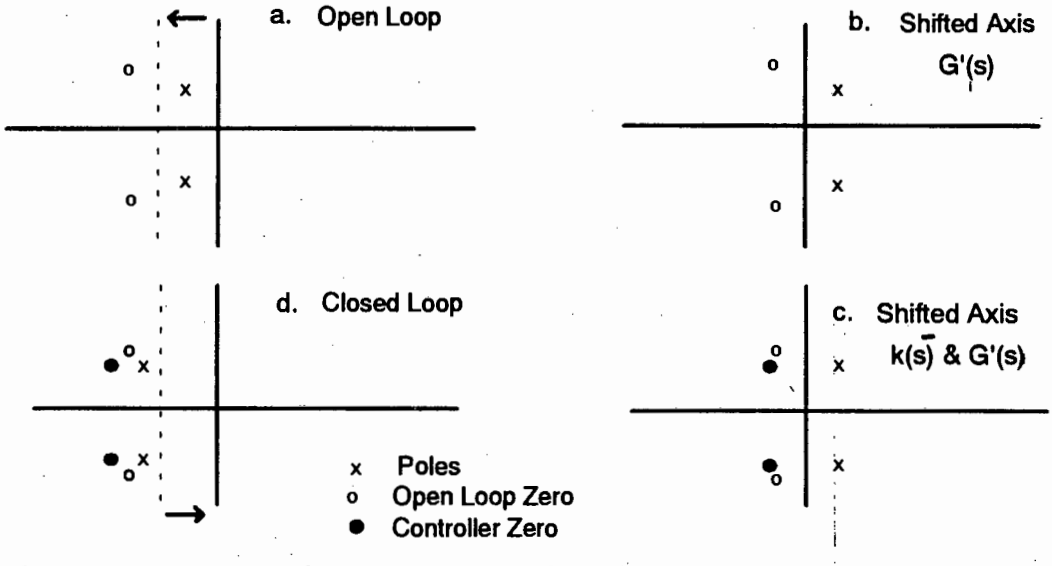

Figure 4.2: Pole-Zero Plot Demonstrating the Shifting of the jω-Axis to Improve Damping

The zeros of the H_∞ controller $k_i(s)$ that correspond to the unstable poles of $G_i'(s)$ are placed at the reflected positions about the jω-axis (Figure 4.3c). The closed loop pole-zero plot (Figure 4.2d) shows the shift in the unstable eigenvalue past the jω axis of $G_i'(s)$.

Thus, $G_i'(s)$ is stabilized and the damping of the poles of $G_i(s)$ is improved. The resulting controller is optimal for $G_i'(s)$ but suboptimal for the actual generator subsystem $G_i(s)$. Note that the robust stability margin of $G_i(s)$ is improved by the suboptimal controller since the weakly damped poles are shifted away from the jω axis. Thus, by applying this simple technique to each subsystem, the damping of the electromechanical oscillations can be enhanced via excitation control.

From Figure 4.2 it is observed that the amount of damping that can be achieved by shifting the axis is limited by the pole-zero pattern of the voltage loop. If the jω axis is shifted past the zeros, then $G_i'(s)$ will become an unstable non-minimum-phase plant i.e. it will have poles and zeros in the right-half plane. For such plants, it is only possible to find a stable controller if the open loop plant is Strongly Stabilizable (SS), or equivalently, if the plant satisfies the Parity Interlacing Principle (PIP) (see Section O of *Preliminaries*). Briefly, PIP states that there exists a stable controller only if between all non-minimum-phase zeros, either all the (unstable) poles occur in odd numbers or they all occur in even numbers [12].

For unstable non-minimum-phase plants, the H_∞ algorithm often provides unstable controllers even in cases when the system is Strongly Stabilizable. However, it has been shown that the selection of high order weights together with a suboptimal γ_w search ensures a stable controller [8].

Figure 4.3 illustrates the overall design procedure which satisfies all the requirements outlined in Section 4.2. The dashed lines in Figure 4.3 illustrates the standard optimal H_∞ procedure while the solid lines show the improvements that we propose for excitation control.

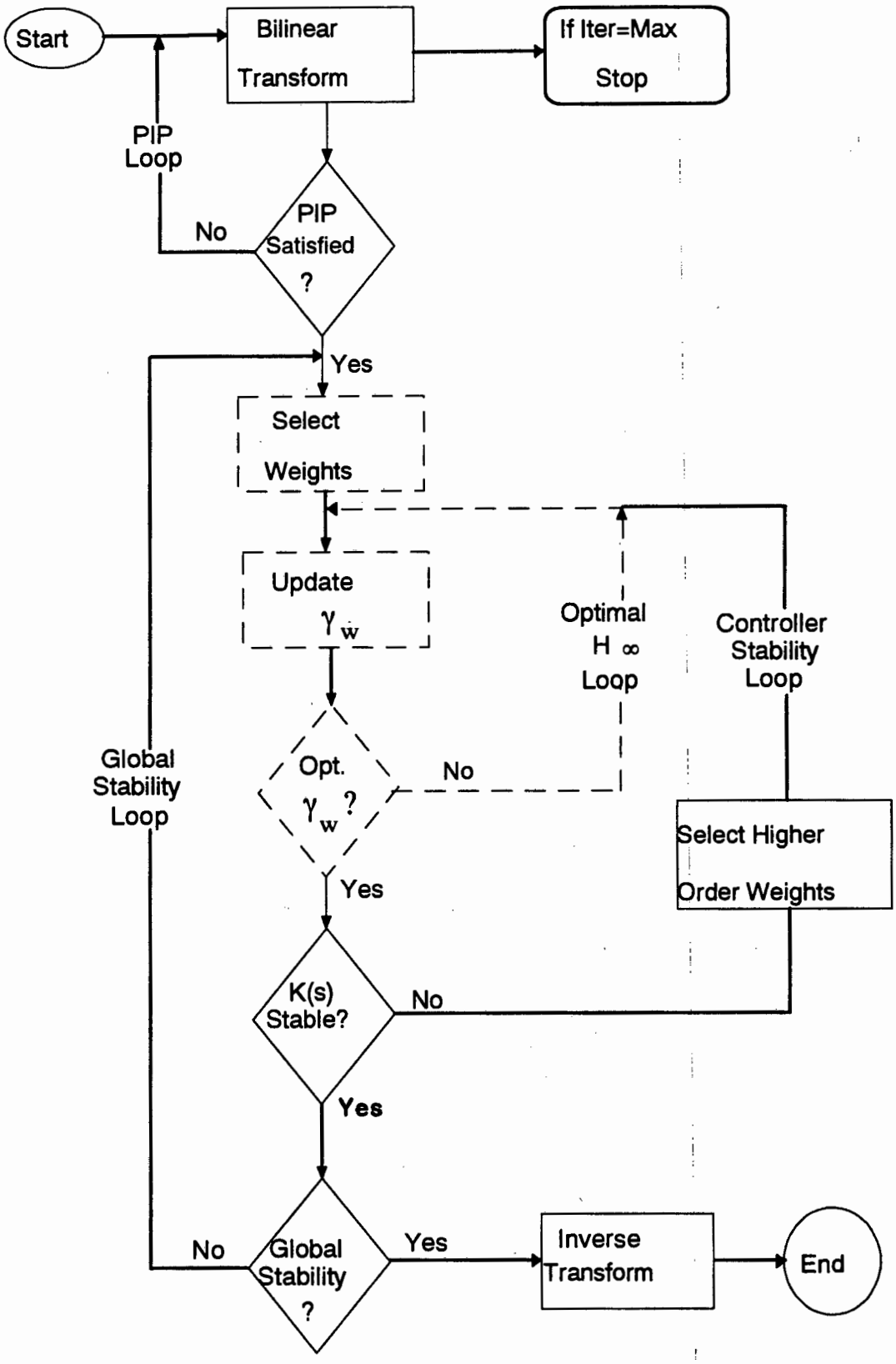

Figure 4.3: Flowchart Showing the Suboptimal Design Procedure

First, a bilinear transformation is applied to the reduced order model. The resulting system is then tested to determine if it is Strongly Stabilizable. If it is not, additional transformations need to be applied in order to satisfy this condition. If the PIP condition is satisfied, the weights (W1, W2 and W3) are selected based on desired closed loop performance and robustness characteristics. Then the optimal $H\infty$ loop begins with the search for the optimal γ_w. Once an optimal controller has been found, the controller is checked for stability. If it is unstable, higher order weights are selected. If the controller is stable the global system stability is verified. If the system is not globally stable, the weights are adjusted and a new controller is calculated. If however, the global system is stable, the inverse bilinear transform is used to obtain the controller for the generator subsystem. The resulting controller is suboptimal. This procedure was applied to the nine-bus system which is investigated in the next section.

4.4 Case Study

Appendix E gives the impedance diagram and load flow diagram of the nine-bus system under investigation. The power system consists of three generators and three loads. Each generator control system is modeled with a 6th order generator model and a 2nd order excitation system model. The loads are modeled as constant impedance loads and the network is modeled by algebraic equations. The generator control system for each subsystem is of 8th order. We applied the method of balanced truncation to each of the three subsystems. The models for subsystems 1 and 2 were reduced to 5th order models. The model for subsystem 3 was reduced to a 6th order model. The results of the model reduction procedure are given in *Appendix F*.

We specify the required response of the voltage loop as follows:

- The closed loop time constant must be equal to or slightly less than one second.
- The bandwidth of the closed loop system should be limited so as to avoid amplification of high frequency noise signals. We select the frequency bandwidth as $\omega_{bw} \leq 1000$ rad/sec.
- The steady-state error must be less than two percent.

The voltage loop specifications can be translated into frequency domain constraints in the form of the weighting functions. The details of the choice of weighting functions are provided in *Appendix H.*

The standard optimal $H\infty$ algorithm as outlined in Section 4.3.2 was used to synthesize controllers satisfying the constraints of the weighting functions. The optimal solution of the one-parameter (γ_w) search was obtained by the method of bisection. The results obtained for the optimal (γ_w) search for voltage loop control are shown in *Appendix H.*

From inspection of the poles and zeros of the open loop system and the poles and zeros of the optimal $H\infty$ controllers, the following observations are made (see *Appendix H*):

- The poles of the optimal $H\infty$ controllers are almost equal to the minimum phase zeros of the open loop plant thus canceling the effect of the open loop zeros.
- The zeros of the $H\infty$ controllers are almost equal to the stable poles of the open loop thus canceling the open loop poles.

Table 4.1 shows a comparison of the robust stability margins α_{ii} of the three control structures under investigation. The values in Table 4.1 were obtained using *Lemma 4.1.* These values were obtained for the closed loop system of each subsystem using CPSS, optimal $H\infty$ and suboptimal $H\infty$ controllers. Recall that the larger the value of α_{ii}, the larger the robust stability margin.

From column 1 of Table 4.1, we note that the suboptimal $H\infty$ control system has the largest robust stability margin (2.7>1.8>1.6). The optimal $H\infty$ controller has a larger robustness margin than the CPSS (1.8>1.6) for subsystem 1. For subsystem 2 (column 2), the robust stability margin of the suboptimal control system is the largest (2.8) with the CPSS having the smallest value (1.4). For subsystem 3, the suboptimal $H\infty$ control system has the largest robust stability margin. In this case however, the closed loop with the CPSS has a larger robust stability margin than the optimal $H\infty$ control system (1.8>1.2). This is due to the fact that the optimal $H\infty$ controller relies on pole-zero cancellation whereas the CPSS improves the damping of the electromechanical modes.

Controller	Gen1	Gen2	Gen3
CPSS	1.6	1.4	**1.8**
Opt. H_∞	1.8	1.7	**1.2**
Subopt H_∞	2.7	2.8	2.9

Table 4.1: Values of α_{ii} for CPSS, Optimal H_∞ Controller and Suboptimal H_∞ Controller.

Figures 4.4 to 4.10 illustrate the time domain performance for the closed loop system for different loading conditions. We consider three different loading conditions viz., nominal loading (Case A), high loading (Case B) and low loading (Case C). The loading conditions for Case A are those given in Figure E2 in *Appendix E*. The loading conditions for Case B is obtained by increasing the Case A loading by 20 percent for each load. The loading conditions for Case C is obtained by decreasing the nominal loading by 20 percent for each load.

The controllers $k_i(s)$ were designed for the generator subsystems under Case A loading (P_{nom}). Once these controllers were obtained, the robustness of the closed loop was investigated. This was done by performing step tests on Case B and Case C using the same controllers $k_i(s)$ to obtain the closed loop.

Figure 4.4 illustrates the step response of the generator terminal voltage deviation $(\Delta V_T = V_T - V_p)$ for Case A loading conditions. These oscillations are the deviations from the pre-disturbance terminal voltage V_p. Thus ΔV_T represents the change in terminal voltage of the generator after a step in V_{ref}. The closed loop with the optimal H_∞ controller has the fastest response in the voltage loop with the smallest voltage overshoot. The CPSS controller causes a large overshoot in the terminal voltage. The settling time of the optimal H_∞ controller is less than one second.

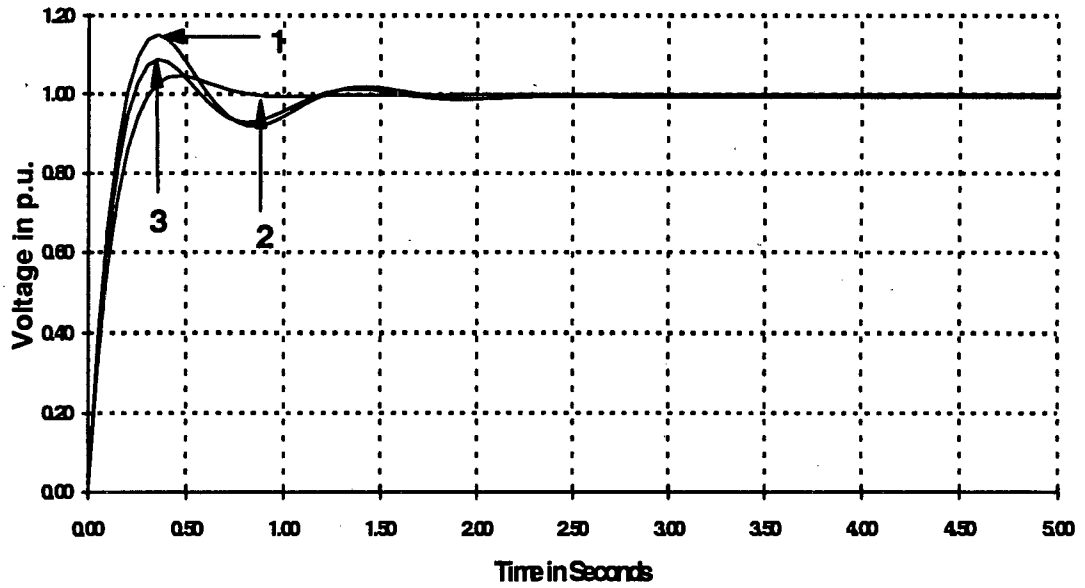

Figure 4.4: Voltage Response of Generator1 For Case A Load (Step in V_{ref})

1 - Conventional Power System Stabilizers (CPSS)

2 - Standard Optimal H_∞ Controllers

3 - Suboptimal H_∞ Controllers

Figure 4.5 illustrates the step response of the electrical power deviations ($\Delta P_{el} = P_{el} - P_{nom}$) for Case A loading conditions. These oscillations are the deviations from the initial electrical power and thus represent the change in electrical power delivered by the generator after a 1 p.u. step in mechanical power. The closed loop with the optimal H_∞ controller has very weak damping with the ΔP_{el} oscillations persisting after seven seconds. The reason for the weak damping is that in the optimal H_∞ methodology, the damping of the electromechanical mode in the power loop remains unaffected by the pole-zero cancellation in the voltage loop. On the other hand, both the CPSS and suboptimal H_∞ controllers add adequate damping to the power loop with oscillations settling after 3 seconds.

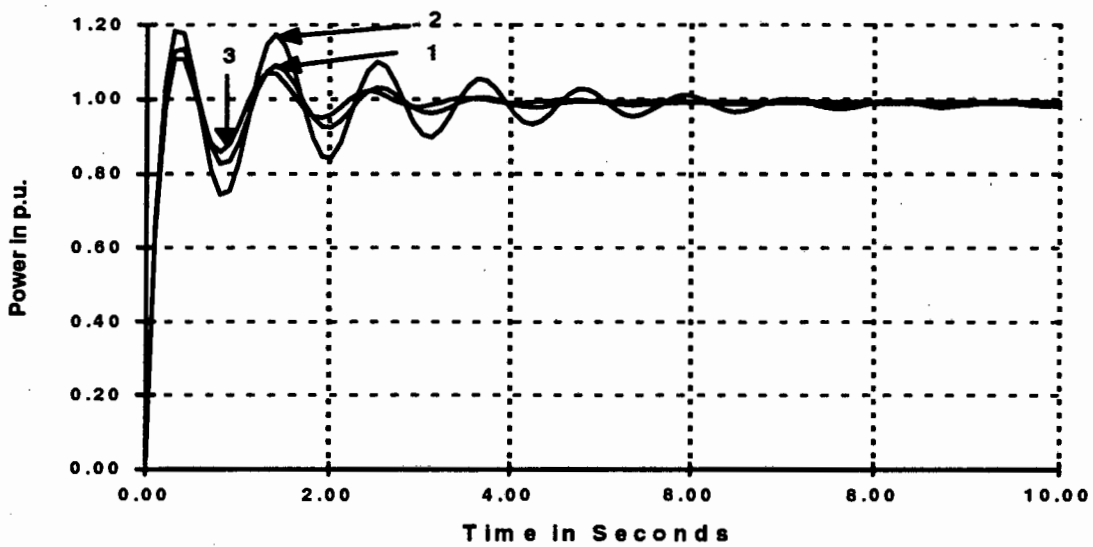

Figure 4.5: Closed Loop Power Deviation of Generator 1 for Case A Load (Step in Mechanical Power)

1 - Conventional Power System Stabilizers (CPSS)

2 - Standard Optimal H_∞ Controllers

3 - Suboptimal H_∞ Controllers

Figure 4.6 illustrates the ΔP_{el} oscillations for Case B loading conditions after a step in mechanical power of generator 2. In this case, the closed loop with the CPSS has the weakest damping in ΔP_{el}. Thus, even though the CPSS provides adequate damping under nominal operating conditions, its performance drastically deteriorates when the operating point is changed i.e. the CPSS on generator 2 has weak robustness properties. The suboptimal H_∞ controller adds the largest damping to the ΔP_{el} oscillations under Case B loading. Note that the damping provided by the optimal H_∞ controller in Case B has remained relatively constant compared to Case A. This means that the robustness of the optimal H_∞ controller is better than that of CPSS. This substantiates the robustness values for subsystem 2 obtained from Table 4.1 i.e. 1.7>1.4 in column 2.

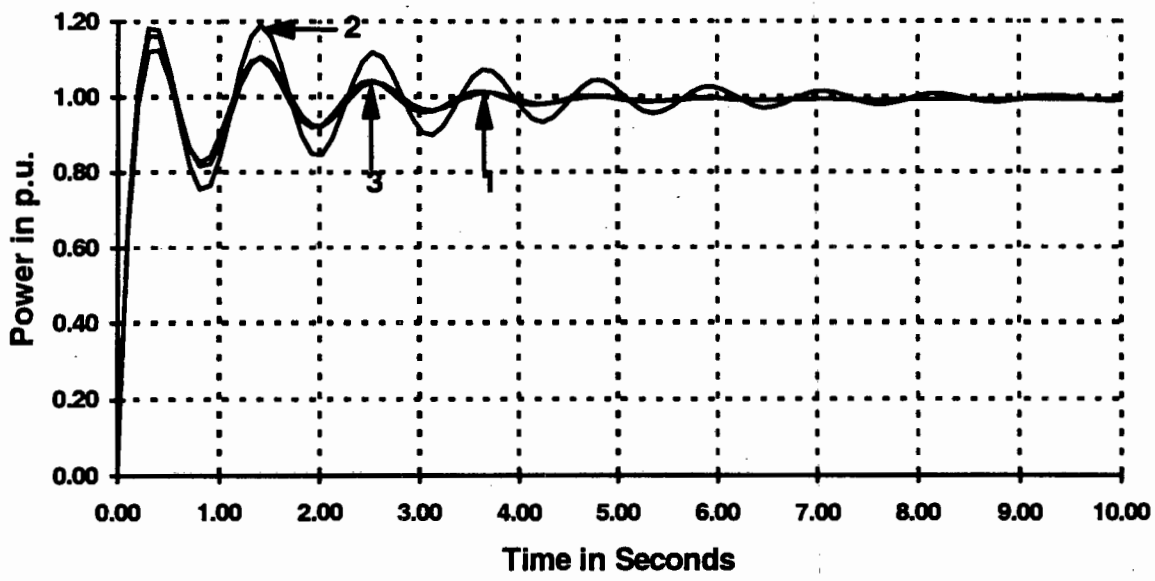

Figure 4.6: Closed Loop Power Deviation of Generator 2 for Case B Load (Step in Mechanical Power).

1 - Conventional Power System Stabilizers (CPSS)

2 - Standard Optimal H_∞ Controllers

3 - Suboptimal H_∞ Controllers

Figure 4.7 illustrates the ΔP_{el} oscillations for Case B loading conditions after a step in mechanical power of generator 3. In this case, the closed loop with the optimal H_∞ controller has the weakest damping in ΔP_{el}. The suboptimal H_∞ controller adds the largest damping to the ΔP_{el} oscillations under Case B loading. Note that the damping provided by the CPSS for generator 3 is larger than that of the optimal H_∞ controller. This substantiates the smaller value obtained in Table 4.1 for the robustness of the optimal H_∞ controller as compared to CPSS (1.2<1.8).

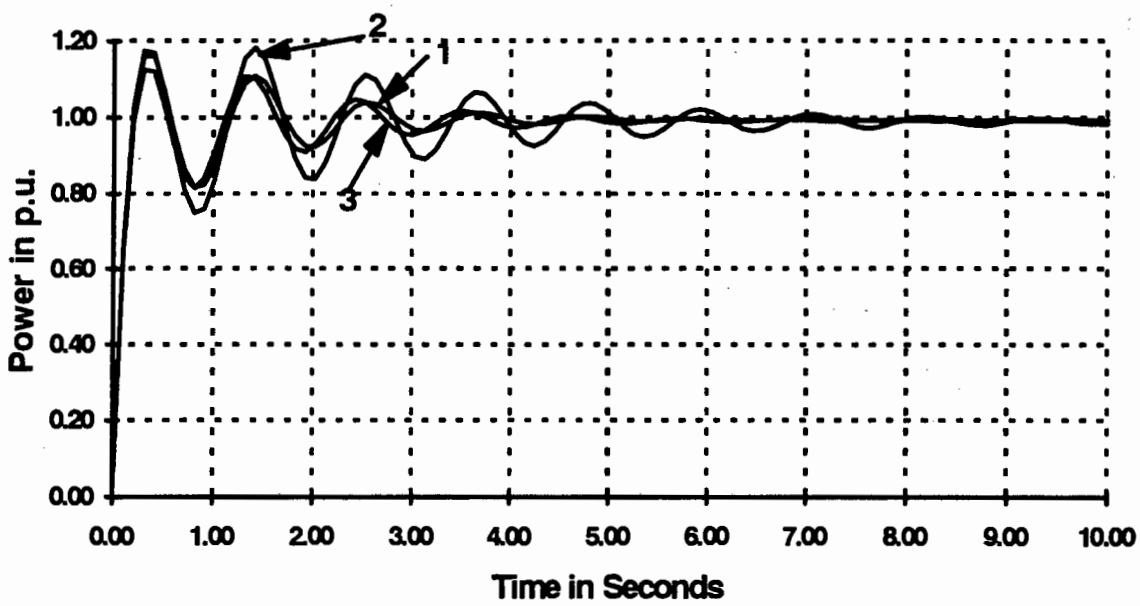

Figure 4.7: Closed Loop Power Deviation of Generator 3 for Case B Load (Step in Mechanical Power)

1 - Conventional Power System Stabilizers (CPSS)

2 - Standard Optimal H_∞ Controllers

3 - Suboptimal H_∞ Controllers

Figure 4.8 illustrates the voltage response of generator 1 due to a step in V_{ref} for Case B loading. The response indicates that the performance of the CPSS in the voltage loop has deteriorated as indicated by the large overshoot and long settling time as compared to optimal H_∞ and suboptimal H_∞ controllers.

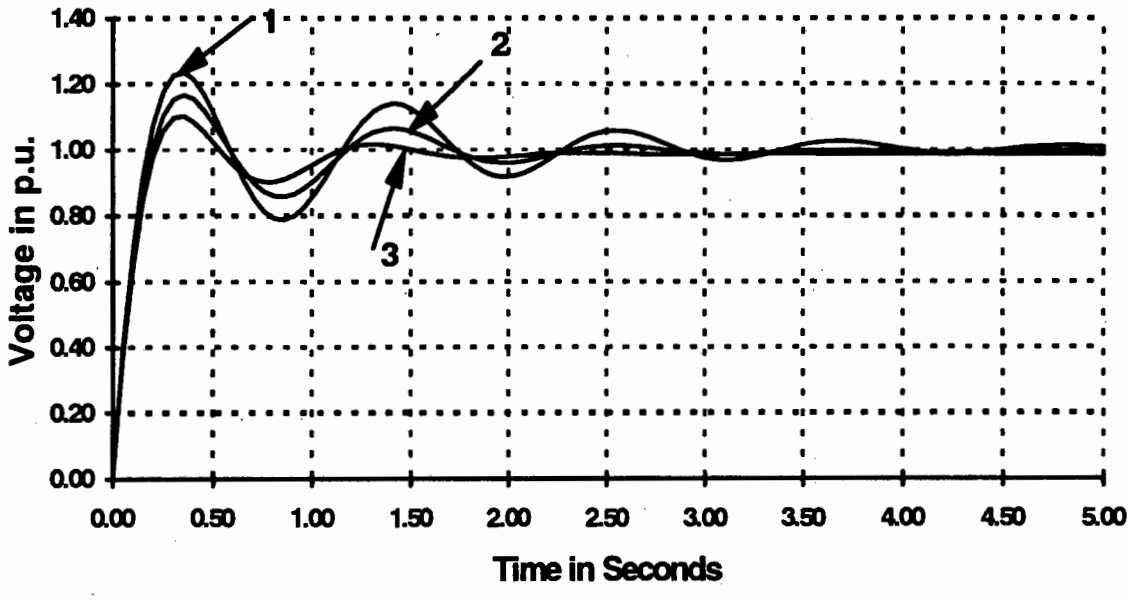

Figure 4.8: Closed Loop Voltage Deviation of Generator 1 for Case B Load (Step in V_{ref})

1 - Conventional Power System Stabilizers (CPSS)

2 - Standard Optimal H_∞ Controllers

3 - Suboptimal H_∞ Controllers

Figure 4.9 illustrates the rotor angle oscillations for Case C loading conditions after a step in V_{ref} of generator 3. The damping and overshoot of the closed loop with the suboptimal H_∞ is better than both CPSS and optimal H_∞. However, the closed loop with the CPSS has better damping than that of the optimal H_∞. Once again, this results from of the weaker robustness margin of the optimal H_∞ controller as compared to CPSS for Generator 3 (1.8>1.2 in column 3). In this case, since the plant model has changed, the weakly damped electromechanical modes move away from the zeros that made them unobservable in the nominal plant. Thus the electromechanical modes dominate the response in the system with the optimal H_∞ controller. The weak robustness properties of the optimal H_∞ controller for generator 3 is further illustrated in Figure 4.10.

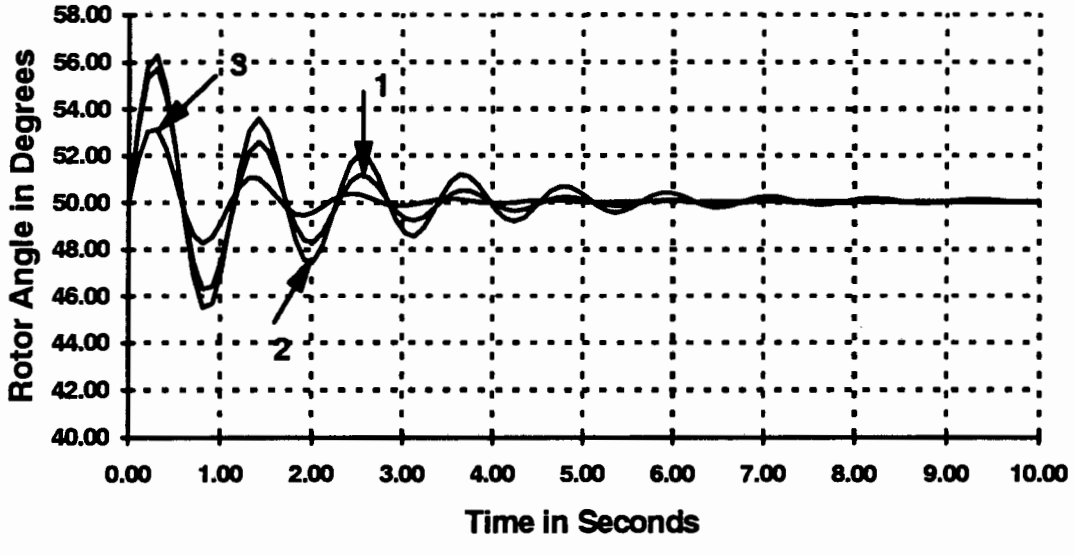

Figure 4.9: Closed Loop Rotor Angle Oscillations of Generator 3 for Case C Loading (Step in Reference Voltage)

1 - Conventional Power System Stabilizers (CPSS)

2 - Standard Optimal H_∞ Controllers

3 - Suboptimal H_∞ Controllers

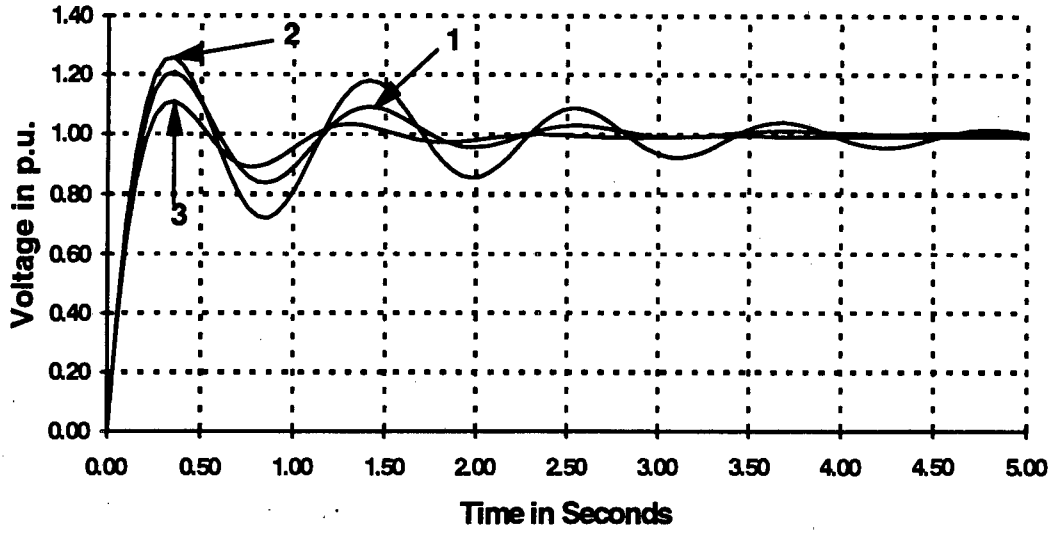

Figure 4.10: Closed Loop Voltage Deviation for Generator 3 for Case C Load (Step in Reference Voltage).

1 - Conventional Power System Stabilizers (CPSS)

2 - Standard Optimal H_∞ Controllers

3 - Suboptimal H_∞ Controllers

From the simulation results, we can conclude that for the nominal plant, the optimal H_∞ controller has better performance than the CPSS and the suboptimal H_∞ controller in the voltage loop. However, due the pole-zero cancellation, the optimal H_∞ controller does not improve the damping in the power loop. Furthermore, when the operating point changes, the performance of the optimal H_∞ controller deteriorates drastically even in the voltage loop. In the case of generator 3, the optimal H_∞ controller has weaker damping than both the CPSS and the suboptimal H_∞ controllers. The overall performance of the suboptimal H_∞ controllers is superior to that of both CPSS and optimal H_∞. The most significant feature is that the suboptimal H_∞ controllers posses superior robustness under changing load conditions.

4.5 Conclusions

In this chapter robust H_∞ controllers were designed for a multimachine system for damping electromechanical oscillations. The main features of the design are that the control is completely decentralized and that low order Dynamic Output Feedback controllers are obtained. In addition, stability of the interconnected power system is guaranteed by incorporating global stability constraints in the H_∞ algorithm. In order to improve the damping and the robust stability margin of the closed loop, it was necessary to make use of a bilinear transformation. This, in turn, necessitated the use of higher order weights to ensure the existence of stable controllers. The resulting decentralized controllers are suboptimal H_∞ controllers. The suboptimal controllers are always stable and have increased robust stability margins as compared to the optimal H_∞ controllers. The suboptimal H_∞ controller response was shown to be superior to that of the CPSS and optimal H_∞ under varying load conditions.

References

[1] Handschin E., Ahmed S. S. et. al., "A New Method of Excitation Control Based on Fuzzy Set Theory", *PICA* 1993, pp. 34-40

[2] Chow J. H. "Pole-Placement Designs of Power System Stabilizers", *IEEE Trans. on Power Systems*, Vol. 4, No. 1, February 1989, pp. 271-277.

[3] Lee K. C., "Analysis of PSS Application for Controlling Poorly Damped Oscillations in the Alcan/BC Hybrid System", *IEEE Trans. on Power Systems*, Vol. 8, No. 1, Feb. 1993, pp.255-63..

[4] Martins N., Lima L. T., "Determination of Suitable Location for Power System Stabilizers and Static Var Compensators for Damping Electromechanical Oscillations in Large Power Systems", *PICA 1989*, , pp. 74-82

[5] Maciejowski J. M., Multivariable Feedback Design, Cambridge University, Addison Wesley, 1989.

[6] Glover K., Doyle "State Space Formulae For All Stabilizing Controllers That Satisfy an H_∞ Norm Bound and Relation to Risk Sensitivity", *Systems & Control Letters*,, 1988, pp.167-72.

[7] Ohtsuka K., et. al., "An H_∞ Optimal Control Theory-Based Generator Control System", *IEEE Trans. on Energy Conversion*, Vol. 7, No 1, March 1992, pp. 108-113.

[8] Ito, H, Ohmori H, et. al., "Design of Stable Controllers Attaining Low H_∞ Weighted Sensitivity", *IEEE Trans. on Automatic Control,* Vol. 38, No. 3 March 1993.

[9] Kiffmeier U., Keuchel U., "Comparison of Classical PID and Modern H_∞-Control Concepts for Frequency and Voltage Control of Power Plants", *IFAC Symposium on Control of Power Plants and Power Systems,* Munich, Germany, 1992, pp. 97-102.

[10] Asgharian R. "A Robust H_∞ Power System Stabilizer With No Adverse Effect on Shaft Torsional Modes", *94WM 125-5 EC.*

[11] Yedavalli R. K., "Improved Measures of Robustness For Linear State Space Models ", *IEEE Trans. on Automatic Control,* Vol. AC-30, No. 6, June 1986, pp. 577-579.

[12] Youla D. C., Bongiorno B., et. al., "Single-Loop Feedback-Stabilization of Linear Multivariable Dynamical Plants", *Automatica,* Vol. 10, 1974, pp. 159-173.

[13] Safonov M. G., Chiang R. Y., " A Schur Method For Balanced Truncation Model Reduction", *IEEE Trans. on Automatic Control.*, Vol. 34, No. 6, June 1989, pp. 610-618.

[14] Ahmed S. S. Petroianu A. "A Coherent Procedure for Decentralized Excitation Control Via Power System Stabilizers", *Journal of the South African Institute of Electrical Engineers*, 1994, pp. 141-147.

[15] Ly U. L, *Linear Multivariable Control*, Department of Aeronautics and Astronautics, University of Washington (Seattle), Lecture notes, 1993

[16] Francis B., *A Course in H_∞ Control Theory, Lecture Notes in Control and Information Sciences*, Springer-Verlag, 1987.

[17] Craig I., "Sensitivity of H_∞ Controller Designs to Structured Uncertainty", Msc. Thesis, MIT, 1989.

[18] Taranto G., Chow J., Othman H., "Robust Redesign of Power System Damping Controllers", *Proceedings of the 32nd Conference on Decision and Control*, San Antonio, Texas, 1993.

[19] Ahmed S. S., Petroianu A., "Design of Decentralized Robust Excitation Controllers Based on $H\infty$ Control Theory", *Proceedings of the International Conference on Power System Technology*, Beijing, China, 1994.

[20] Ahmed S. S., Chen L., Petroianu A., "Design of Suboptimal $H\infty$-Based Excitation Controllers", Accepted for *PICA*, Salt Lake City, USA, 1995.

Chapter 5

Determination of the Parameters of Fixed Structure Power System Stabilizers

5.1 Introduction

This chapter deals with the determination of the parameters of fixed structure Power System Stabilizers (PSS). Figure (5.1) illustrates the contents of this chapter.

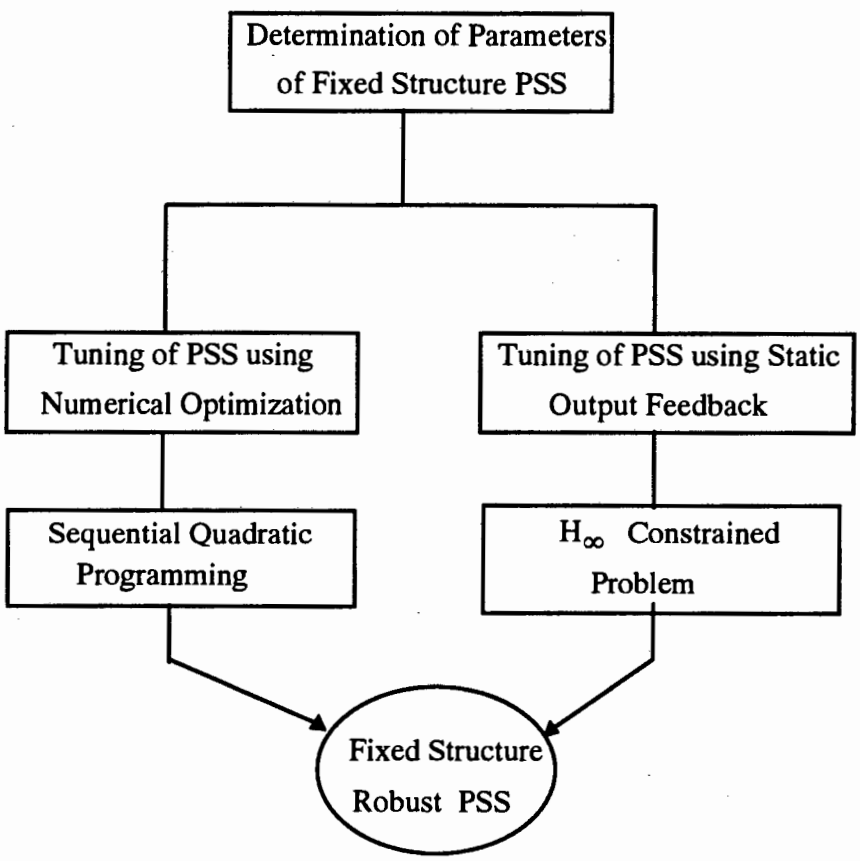

Figure 5.1: Outline of the Contents in Chapter 5

In Chapter 4, we synthesized H_∞ controllers using an existing Dynamic Output Feedback Ricatti-based algorithm (see Section 4.3.2.1). It was demonstrated that these controllers achieve superior robustness properties as compared to conventional lead-lag PSS. The performance of the closed loop was constrained by using the weighting functions W1, W2 and W3. Using this method, we obtained Dynamic Output Feedback controllers which were of the same order as that of the reduced open loop subsystem model.

In Chapter 4, we also described a two-stage procedure for designing robust decentralized controllers. In Stage 1, the controllers were designed for subsystems which were uncoupled and unperturbed. In this stage, the Dynamic Output Feedback Ricatti-based method was used to synthesize the controllers. In Stage 2, the global stability constraints were incorporated into the design procedure. In this chapter, we develop methods to tune the PSS for Stage 1 using a fixed structure PSS. This means that the methods developed in this chapter can replace the method described in Section 4.3.2.1 for each subsystem if we wish to retain the structure of existing PSS. Stage 2 in the design of robust decentralized controllers will follow the procedure outlined in Section 4.3.1.

In this chapter, we address two problems associated with the H_∞ synthesis methodology presented in Section 4.3.2.1.

The first problem relates to the high order of the controllers obtained using the methods described in Chapter 4. In power systems, the existing PSS are usually second order controllers [1]. Thus, if we wish to implement the H_∞ controllers, we would need to replace all existing PSS with new high order supplementary excitation controllers. This is not a practical solution to the problem of damping electromechanical oscillations. We need to develop a method to determine the parameters of robust controllers which have the existing PSS structure i.e. *tuning* existing PSS rather than *designing* new PSS.

The second problem associated with the synthesis method described in Section 4.3.2.1 is the manner in which the method achieves the design objectives. The optimal H_∞ controllers cancel the undesirable plant dynamics by inverting the stable part of the plant while inverting the reflected unstable part of the plant. Therefore, these controllers affect the

observability of the open loop poles while leaving the *damping* of these poles unaffected. The pole-zero cancellation associated with the Ricatti-based synthesis method (described in Section 4.3.2.1) degrade the internal dynamics of the system. We need to develop a method of improving the damping of the electromechanical oscillations while ensuring robust closed loop performance.

In this chapter we address these two problems associated with the synthesis method used in Chapter 4. We present two new methods of determining the parameters of the PSS, namely *tuning of PSS using numerical optimization* and *tuning of PSS using Static Output Feedback.*

The *tuning of PSS using numerical optimization* is based on formulating the PSS tuning problem as an optimization problem. In this formulation, the controller with the unknown PSS parameters is placed in a feedback control path with the open loop plant. The resulting closed loop system contains the unknown PSS parameters. The objective function of the optimization problem is the H_∞ norm of a closed loop disturbance-related transfer function. The constraints of the optimization problem are based on the stability of the controller, limits on the values of the parameters and the desired damping of the closed loop system. The PSS parameters are calculated using a numerical optimization technique based on a Sequential Quadratic Programming (SQP) algorithm (see Section Q of *Preliminaries*).

The *tuning of PSS using Static Output Feedback* is based on transforming the Dynamic Output Feedback problem into a Static Output Feedback problem. The fixed structure PSS is expressed in the controller canonical form. The PSS is augmented with the open loop plant such that the closed loop is in the form of a Static Output Feedback problem. The static gain matrix can be calculated using existing Static Output Feedback algorithms. The static gain matrix can then be used to obtain the parameters of the fixed structure PSS.

The main contributions in this chapter are the formulations of the robust tuning problem as *(a) a numerical optimization problem* and *(b) a Static Output Feedback problem,* while retaining the structure of the existing PSS. Thus, by using the methods described in this

chapter, we can tune the parameters of the existing PSS for robust closed loop performance rather than replace the existing PSS with new high order supplementary excitation controllers.

In this chapter we consider the following state space description of a power system:

$$\begin{aligned} \dot{x}(t) &= Ax(t) + B_1 w(t) + B_2 u(t) \\ \xi(t) &= C_1 x(t) + D_{11} w(t) + D_{12} u(t) \\ y(t) &= C_2 x(t) + D_{21} w(t) + D_{22} u(t) \end{aligned} \tag{5.1}$$

where:

$x(t) \in R^n$ is the state vector

$u(t) \in R^{m_2}$ is the input vector

$y(t) \in R^{p_2}$ is the output vector

$w(t) \in R^{m_1}$ is the disturbance input vector

$\xi(t) \in R^{p_1}$ is the performance output vector

n is the number of states of the plant

m_1 is the number of control inputs

m_2 is the number of disturbance inputs

p_1 is the number of performance outputs

p_2 is the number of sensor outputs

$A, B_1, B_2, C_1, C_2, D_{11}, D_{12}, D_{21}$ and D_{22} are constant matrices of appropriate dimensions.

We call $w(t)$ and $\xi(t)$ the disturbance-related variables. Both methods described in this chapter use the state space description given by equation (5.1).

In the next section, we present the method of *tuning the PSS using numerical optimization.* This method is tested on a SMIB system and the results are presented. Thereafter, we outline the method of *tuning the PSS by Static Output Feedback.* This method is described without applying it to a power system model.

5.2 Tuning the PSS using Numerical Optimization

In this section we present a new method of tuning existing PSS using numerical optimization for robust performance of the closed loop. The method ensures that the controllers have a fixed structure. In addition, the closed loop is guaranteed to have sufficient damping of the electromechanical oscillations. This means that robust damping of the electromechanical oscillations can be achieved without replacing the existing PSS hardware.

We wish to damp the oscillations in the electrical power output of the generator using control through the voltage loop. Figure 5.2 illustrates the control configuration under voltage loop feedback control.

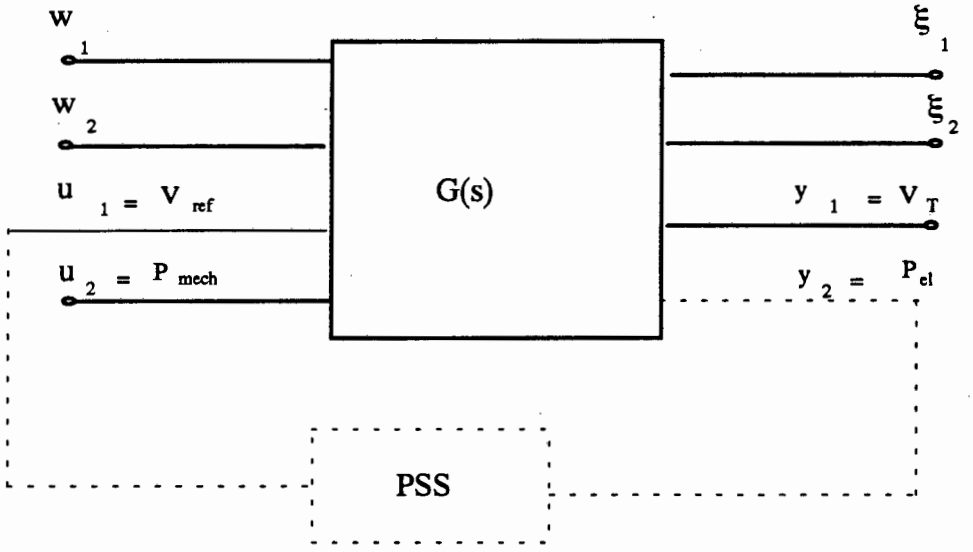

Figure 5.2: Control Configuration Under Voltage Loop Feedback Control.

In Figure 5.2, V_{ref} is the generator reference voltage, V_T is the generator terminal voltage, P_{mech} is the mechanical power and P_{el} the electrical power. The disturbance-related variables, (w_1,ξ_1) and (w_2,ξ_2), correspond to the voltage loop and power loop, respectively.

In the traditional formulation of the PSS tuning problem, we place a PSS between the output P_{el} and the input V_{ref} such that the damping of the oscillations in P_{el} is improved (see Figure 5.2) [1]. However, we wish to extend the traditional formulation of the PSS

tuning problem. In addition to improving the damping, we wish to maximize the robustness of the multivariable system while using a PSS of fixed structure.

For the 2-input, 2-output system illustrated in Figure (5.2), we rewrite the open loop state space description given by equation (5.1) as follows:

$$\begin{aligned} \dot{x} &= Ax + \begin{bmatrix} B_2^1 & B_2^2 \end{bmatrix} \begin{bmatrix} u_1 \\ u_2 \end{bmatrix} + B_1 w \\ \xi &= C_1 x + \begin{bmatrix} D_{12}^1 & D_{12}^2 \end{bmatrix} \begin{bmatrix} u_1 \\ u_2 \end{bmatrix} + D_{11} w \\ y &= \begin{bmatrix} C_2^1 \\ C_2^2 \end{bmatrix} x + D_{22} u + D_{21} w \end{aligned} \tag{5.2}$$

where:

B_2^1 is the coefficient vector associated with the reference voltage input V_{ref}

B_2^2 is the coefficient vector associated with the mechanical power input P_{mech}

C_2^1 is the coefficient (row) vector associated with the terminal voltage output

C_2^2 is the coefficient (row) vector associated with the electrical power output P_{el}

We make the assumption that the plant is strictly proper i.e. $D_{22} = 0$.

Consider the following state space description of the controller:

$$\begin{aligned} \dot{z} &= Ez + Fu_c \\ y_c &= Gz + Hu_c \end{aligned} \tag{5.3}$$

where:

$z \in R^{n_c}$ is the vector of controller states

$u_c \in R^{m_c}$ is the controller input

$y_c \in R^{p_c}$ is the controller output

n_c is the number of states of the controller

p_c is the number of outputs of the controller

m_c is the number of inputs of the controller

E, F, G and H are constant matrices of appropriate dimensions

The parameters of the controller are unknown and are contained in the matrices E, F, G and H.

In order to obtain the closed loop description of the system we have to connect the output of the plant y to the input of the controller u_c i.e.:

$$y = C_2 x + D_{21} w + D_{22} u = u_c \tag{5.4}$$

Thereafter we connect the input of the plant u to the output of the controller i.e.:

$$u = y_c = Gz + Hu_c . \tag{5.5}$$

The state space description of the closed loop system can be expressed as follows:

$$\begin{bmatrix} \dot{x} \\ \dot{z} \end{bmatrix} = \begin{bmatrix} \overline{A} \end{bmatrix} \begin{bmatrix} \dot{x} \\ \dot{z} \end{bmatrix} + \overline{B}_2 u_2 + \overline{B}_1 w$$

$$\xi = \overline{C}_1 \begin{bmatrix} \dot{x} \\ \dot{z} \end{bmatrix} + D_{12}^2 u_2 + \overline{D}_1 w \tag{5.6}$$

$$y = \begin{bmatrix} C_2^1 \\ C_2^2 \end{bmatrix} x + D_{21} w$$

where:

$$\overline{A} = \begin{bmatrix} A + B_2^1 H C_2^2 & B_2^1 G \\ F C_2^2 & E \end{bmatrix}$$

$$\overline{B}_2 = \begin{bmatrix} B_2^2 \\ 0 \end{bmatrix}$$

$$\overline{B}_1 = \begin{bmatrix} \overline{B}_1^1 & \overline{B}_1^2 \end{bmatrix} = \begin{bmatrix} B_2^1 H D_{21} + B_1 \\ F D_{21} \end{bmatrix}$$

$$\overline{C}_1 = \begin{bmatrix} \overline{C}_1 \\ \overline{C}_2 \end{bmatrix} = \begin{bmatrix} C_1 + D_{12}^1 H C_2^2 & D_{12}^1 G \end{bmatrix}$$

$$\overline{D}_1 = (D_{12}^1 H D_{21} + D_{11})$$

From the closed loop system given in equation (5.6), we define the transfer functions $H(s)$, $T_{11}(s)$, $T_{12}(s)$, $T_{21}(s)$, $T_{22}(s)$ and $T_1(s)$ as follows:

$$H(s) = C_2^2 (sI - \overline{A}) \overline{B}_2$$

$$T_{11}(s) = T_{w_1 z_1}(s) = \overline{C}_1^1 (sI - \overline{A})^{-1} \overline{B}_1^1 + \overline{D}_1^1 \tag{5.7}$$

$$T_{12}(s) = T_{w_1 z_2}(s) = \overline{C}_1^2 (sI - \overline{A})^{-1} \overline{B}_1^1 + \overline{D}_1^2 \tag{5.8}$$

$$T_{21}(s) = T_{w_2 z_1}(s) = \overline{C}_1^1 (sI - \overline{A})^{-1} \overline{B}_1^2 + \overline{D}_1^1 \tag{5.9}$$

$$T_{22}(s) = T_{w_2 z_2}(s) = \overline{C}_1^2 (sI - \overline{A})^{-1} \overline{B}_1^2 + \overline{D}_1^2 \tag{5.10}$$

$$T_1(s) = T_{w_1 (z_1 z_2)}(s) = \overline{C}_1 (sI - \overline{A})^{-1} \overline{B}_1^1 + \overline{D} \tag{5.11}$$

The transfer function $T_{ij}(s)$ $\left(i = \{1,2\}, j = \{1,2\}\right)$ gives the response of the performance variable ξ_j due to changes in the disturbance variable w_i. The two variables ξ_1 and w_1 are associated with the voltage loop. The two variables ξ_2 and w_2 are associated with the power loop.

The transfer function $T_1(s)$ gives the response of both performance variables ξ_1 and ξ_2 due to changes in the disturbance variable w_1.

We wish to address the problem of maximizing the robustness of the closed loop system to changes in the plant parameters. We consider five formulations of the H_∞ control problem. These can be stated as follows:

$$\underline{\text{Case 1}}: \underset{\chi}{Minimize}(J_1 = \|T_{11}\|_\infty) \tag{5.12}$$

$$\underline{\text{Case 2}}: \underset{\chi}{Minimize}(J_2 = \|T_{12}(s)\|_\infty) \tag{5.13}$$

$$\underline{\text{Case 3}}: \underset{\chi}{Minimize}(J_3 = \|T_{21}(s)\|_\infty) \tag{5.14}$$

$$\underline{\text{Case 4}}: \underset{\chi}{Minimize}(J_4 = \|T_{22}(s)\|_\infty) \tag{5.15}$$

$$\underline{\text{Case 5}}: \underset{\chi}{Minimize}(J_5 = \|T_1(s)\|_\infty = \|T_{11}(s) \quad T_{12}(s)\|_\infty) \tag{5.16}$$

Each objective function is subject to the following constraints:

$$\Psi_i(H(s)) \geq \Psi^0 \tag{5.17}$$

$$\gamma_i^{\min} \leq p_i \leq \gamma_i^{\max} \tag{5.18}$$

$$\mathrm{Re}(\lambda_i(k(s)) < 0 \quad \text{(internal stability)}$$

where:

χ is the set of parameters of the controller

p_i is the i*th* unknown parameter

$\gamma_i^{\min}$ is the lower limit of parameter p_i

$\gamma_i^{\max}$ is the upper limit of parameter p_i

$\Psi_i(H(s))$ is the damping factor of the i*th* mode of $H(s)$

Ψ^0 is the minimum damping

$\lambda_i(k(s))$ denotes the i*th* eigenvalue of the controller $k(s)$

By finding the optimal solution to each of these problems, we can obtain the optimal tuning of the PSS.

In Cases 1 to 4, the optimal PSS maximizes the robustness of the SISO transfer functions between the inputs (V_{ref} and P_{mech}) and the outputs (V_T and P_{el}) respectively.

In Case 5, the robustness requirement is expressed in terms of the transfer function matrix $T_1(s)$. In this case, the optimal PSS maximizes the robustness of the *multivariable system* between the input V_{ref} and the two outputs V_T and P_{el}. Thus, in this case we wish to determine how much robustness we can obtain for the *multivariable system* by using feedback through V_{ref} only.

In the formulation given by equations (5.12) to (5.18), the controller with the unknown parameters has been connected to the open loop plant to form the closed loop system. This means that the objective functions J_1 to J_5, contain these unknown parameters. Thus, (5.12) to (5.18) describe numerical optimization problems in the set of unknown PSS parameters.

To solve for the unknown parameters we make use of a numerical optimization algorithm. This algorithm is based on Sequential Quadratic Programming (SQP). The algorithm for SQP is described in Section Q of *Preliminaries.*

For each of the five cases, we obtain an optimal PSS which maximizes the robustness of the corresponding transfer function. For each PSS we have values for $\|T_{11}(s)\|_\infty$, $\|T_{12}(s)\|_\infty$, $\|T_{21}(s)\|_\infty$, $\|T_{22}(s)\|_\infty$ and $\|T_1(s)\|_\infty$. From these values, we need to determine the optimal robust excitation controller. We regard the optimal robust excitation controller as the one which minimizes the sensitivity of *both* output variables V_T and P_{el} to disturbances in the input variable V_{ref}.

We define the sensitivity measure SM_i^j between input i and outputs 1 and 2 as follows:

$$SM_i^j = \left\| \left[\|T_{i1}\|_\infty \quad \|T_{i2}\|_\infty \right] \right\|_1 = \sum_{j=1}^{2} T_{ij} \tag{5.19}$$

The optimal robust excitation controller is taken as the one which minimizes the sensitivity measure SM_i^j i.e.:

$$K_{opt}(s) = k(s): \min_K SM_i^j \tag{5.20}$$

where K is the set of controllers obtained from Case 1 to Case 5.

In the next section, we apply this method of tuning PSS for a SMIB system.

5.2.1 Case Study

In this section, we apply the method of *tuning the PSS using numerical optimization*. The method is applied to the SMIB illustrated in Figure 5.3.

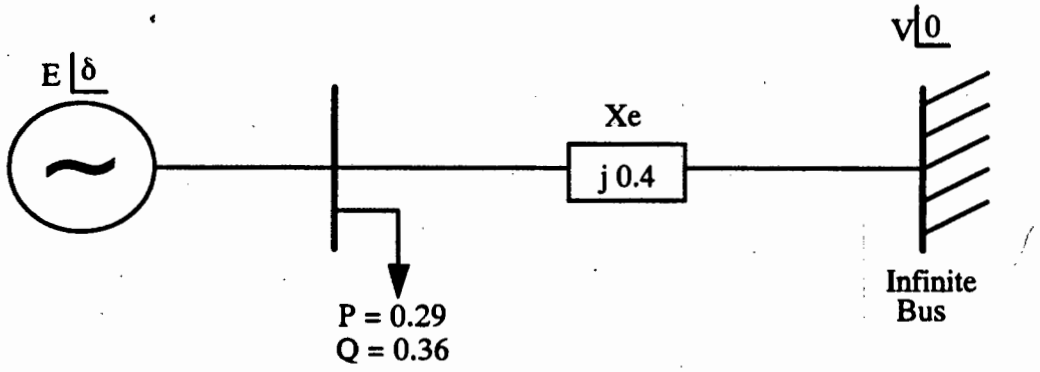

Figure 5.3: Diagrammatic Representation of SMIB System

The state space formulation of the SMIB system can be expressed as follows:

$$\begin{aligned} \dot{x}(t) &= Ax(t) + B_1 w(t) + B_2 u(t) \\ \xi(t) &= C_1 x(t) + D_{11} w(t) + D_{12} u(t) \\ y(t) &= C_2 x(t) + D_{21} w(t) + D_{22} u(t) \end{aligned} \tag{5.21}$$

where the matrices $A, B_1, B_2, C_1, C_2, D_{11}, D_{12}, D_{21}$ and D_{22} are given in *Appendix I.*

We wish to improve the damping of the electromechanical oscillations through supplementary excitation control using a fixed structure PSS. In order to do this, we need to determine the parameters of a 2nd order controller $K(s)$ of the following structure:

$$K(s) = \frac{a(s^2 + bs + c)}{(s^2 + ds + e)} \tag{5.22}$$

where a, b, c, d and e are the unknown controller parameters.

The method proposed in Section 5.2 was applied to a SMIB subsystem. The minimum damping Ψ^0 was taken as 0.2. The PSS parameters were obtained for the objective functions J_1 to J_5 using the SQP algorithm.

The PSS for Case 1 to Case 5 are as follows:

$$\text{Case 1: } PSS_1(s) = \frac{1.000(s^2 + 10.94s + 2.637)}{s^2 + 7.509s + 12.29} \tag{5.22a}$$

$$\text{Case 2: } PSS_2(s) = \frac{1.024(s^2 - 0.158s + 0.957)}{s^2 + 1.764s + 0.0771} \tag{5.22b}$$

$$\text{Case 3: } PSS_3(s) = \frac{2.308(s^2 - 0.702s + 1.790)}{s^2 + 2.203s + 2.874} \tag{5.22c}$$

$$\text{Case 4: } PSS_4(s) = \frac{2.109(s^2 + 0.991s + 2.0078)}{s^2 + 1.209s + 2.292} \tag{5.22d}$$

$$\text{Case 5: } PSS_5(s) = \frac{1.931(s^2 + 9.243s + 2.878)}{s^2 + 7.821s + 19.066} \tag{5.22e}$$

Table 5.1 provides the minimum H_∞ norms of the transfer functions under investigation. The H_∞ norms obtained from the SQP algorithm are compared to the H_∞ norms of a PSS

tuned using standard phase-compensation techniques [1]. The transfer function of the CPSS is given by:

$$K_{CPSS}(s) = \frac{2.180(s^2 + 11.760s + 34.570)}{(s^2 + 20.001s + 100.010)} \qquad (5.22f)$$

The highlighted values in Table 5.1 correspond to the optimal H_∞ norms of the transfer function that was optimized. For instance, in Case 1 the value of $\|T_{11}\|_\infty$ is minimized to a value of 13.196.

Case No	$\|T_{11}\|_\infty$	$\|T_{12}\|_\infty$	$\|T_{21}\|_\infty$	$\|T_{22}\|_\infty$
1	**13.196**	2.406	$7.206\text{x}10^{-10}$	44.160
2	43.211	**1.117**	$4.590\text{x}10^{-10}$	44.160
3	69.667	3.580	**$5.28\text{x}10^{-11}$**	44.160
4	52.160	4.546	$5.66\text{x}10^{-10}$	**44.160**
5	8.650	3.230	$7.40\text{x}10^{-11}$	44.160
CPSS	31.619	2.044	$1.94\text{x}10^{-10}$	44.160

Table 5.1: Values of Minimum H_∞-Norms of the Transfer Functions Under Investigation.

Note that for Case 1 to Case 4, the highlighted values are the smallest values in each column since these are the values that are minimized in the corresponding objective function. For instance, in column 1, 13.196<43.211<52.160<69.667. This means that for Case 1, the robustness of the SISO transfer function $T_{11}(s)$ is maximized if we use the PSS given in equation (5.22a). For Case 2, the robustness of the SISO transfer function $T_{12}(s)$ is maximized if we use the PSS in equation (5.22b). Similarly, for Case 3 and Case 4, the robustness of the SISO transfer functions $T_{21}(s)$ and $T_{22}(s)$ are maximized by selecting the PSS in equations (5.22c) and (5.22d), respectively.

For Case 5 the value that is minimized is the H_∞-norm of the one-input, 2-output transfer function $T_1(s)$. In this case, the value of $\|T_{11}\|_\infty$ is less than the corresponding value of Case 1 (8.650 < 13.196). This means that the robustness in the voltage loop will be better if we use the PSS given by equation (5.22e) instead of the PSS given by equation (5.22a). On

the other hand, for Case 5, the value of the $\|T_{12}\|_\infty$ is greater than the value corresponding to Case 2 (3.230 > 1.117). This means that the robustness in P_{el} due to disturbances in V_{ref} is maximized if we use the PSS given by equation (5.22c).

We wish to select the controller which maximizes the robustness of the output variables V_T *and* P_{el} due to disturbances in V_{ref}. From the foregoing discussion, we deduce that by using the values in Table 5.1, we are unable to determine which PSS needs to be selected since the PSS in Case 5 is the best for minimizing $\|T_{11}\|_\infty$ while the PSS in Case 2 is the best for minimizing $\|T_{12}\|_\infty$.

However, we can use equations (5.19) and (5.20) to select the controller which maximizes the robustness of the output variables V_T *and* P_{el} due to disturbances in V_{ref}. From equation (5.19), the sensitivity measures for Case 1 to Case 5 and CPSS are given in Table 5.2.

Case	Sensitivity Measure
Case 1	15.602
Case 2	44.328
Case 3	73.247
Case 4	56.706
Case 5	**11.880**
CPSS	33.663

Table 5.2: Sensitivity Measures for Case 1 to Case 6 Corresponding to V_{ref}

Using equation (5.20) we select the optimal controller K_{opt} as the one which minimizes the sensitivity of V_T and P_{el} to disturbances in V_{ref} (highlighted value in Table 5.2). Thus, the Optimal Robust PSS (RPSS) is chosen as the one corresponding to Case 5.

The results in Table 5.2 indicate that the controllers obtained using numerical optimization are effective for improving the robustness of the transfer functions between the input V_{ref} and the outputs V_T and P_{el}. This can be deduced from the small values of KM_i^j for Case 1, Case 2 and Case 5 (15.602), (44.328) and (11.880). Thus, we can increase the robustness of the $V_{ref} \rightarrow V_T$ and $V_{ref} \rightarrow P_{el}$ loops by using feedback into V_{ref} i.e. excitation control.

From Table 5.1 we can deduce that the H_∞-norms of the transfer functions corresponding to $P_{mech} \rightarrow V_{ref}$ and $P_{mech} \rightarrow P_{el}$ loops are not altered by excitation control. This is true even in Case 3 and Case 4 where the loops corresponding to $P_{mech} \rightarrow V_{ref}$ and $P_{mech} \rightarrow P_{el}$ are minimized respectively. In both these cases, the H_∞-norms remain at approximately the same at ~$5\text{x}10^{-10}$ and 44.16. Thus, excitation control as illustrated in Figure 5.2 does not affect the robustness of the $P_{mech} \rightarrow V_T$ and $P_{mech} \rightarrow P_{el}$ loops.

This means that we can use excitation control to damp the electromechanical oscillations in P_{el} as well as achieving robustness in V_T and P_{el} with respect to disturbances in V_{ref}. However, we cannot use supplementary excitation control to improve the robustness with respect to disturbances in P_{mech}. In order to achieve robustness with respect to disturbances in P_{mech} we would require power loop control through the governor [6].

Figures 5.4 illustrates the response of P_{el} to a step in V_{ref} for nominal loading conditions using the RPSS and the CPSS. From Figure 5.4 we note that the P_{el} oscillations for the open loop is weakly damped with oscillations persisting after 10 seconds. The closed loop system with the RPSS has significantly improved damping of the P_{el} oscillations. For the RPSS, the oscillations in P_{el} settle within 2 seconds as opposed to 3 seconds for the closed loop with the CPSS.

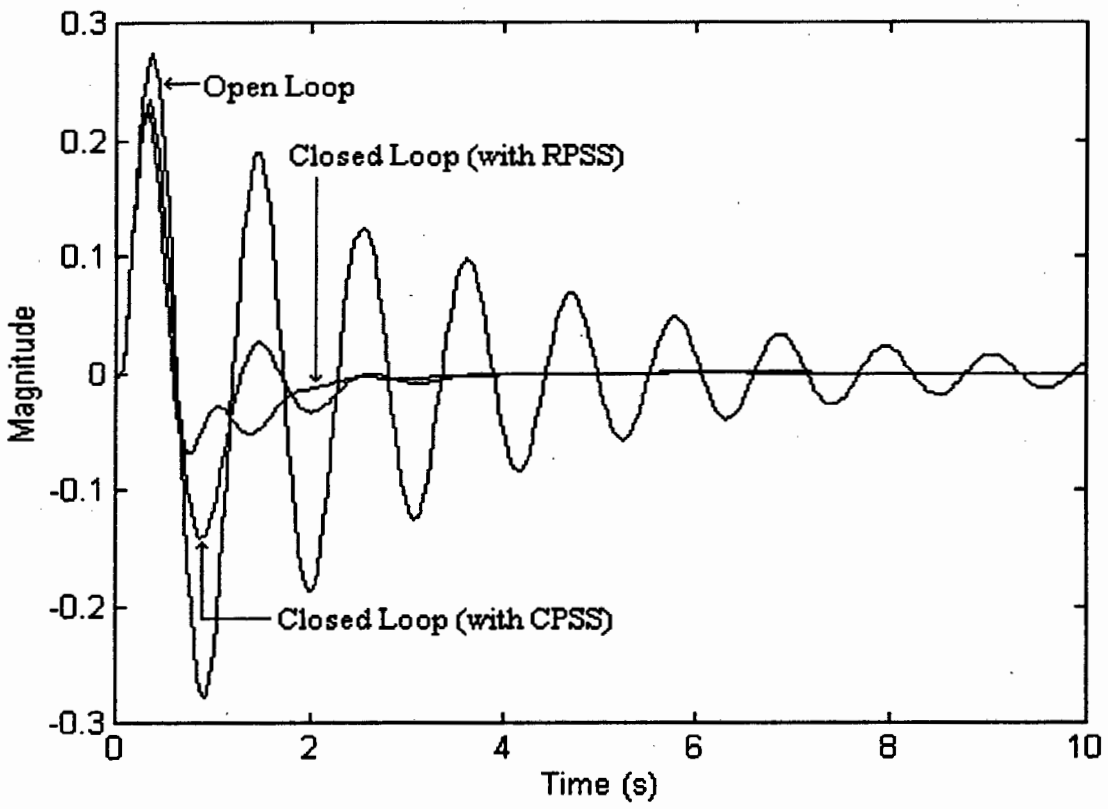

Figure 5.4: Responses of P_{el} Due to a Step in V_{ref} (Nominal Loading)

Figure 5.5 illustrates the magnitude plots of the transfer function between the output P_{el} and the input V_{ref} for nominal loading condition. The plots for the open loop, RPSS and CPSS are given. The peak value of each plot corresponds to the H_∞ norm of the transfer function between P_{el} and V_{ref}. From Figure 5.5 we note that the RPSS reduces the peak of the magnitude more than that of the CPSS. This means that the closed loop system with the RPSS has a lower H_∞ norm than that of the closed loop with the CPSS. Thus, the system with the RPSS has better robustness than the system with the CPSS.

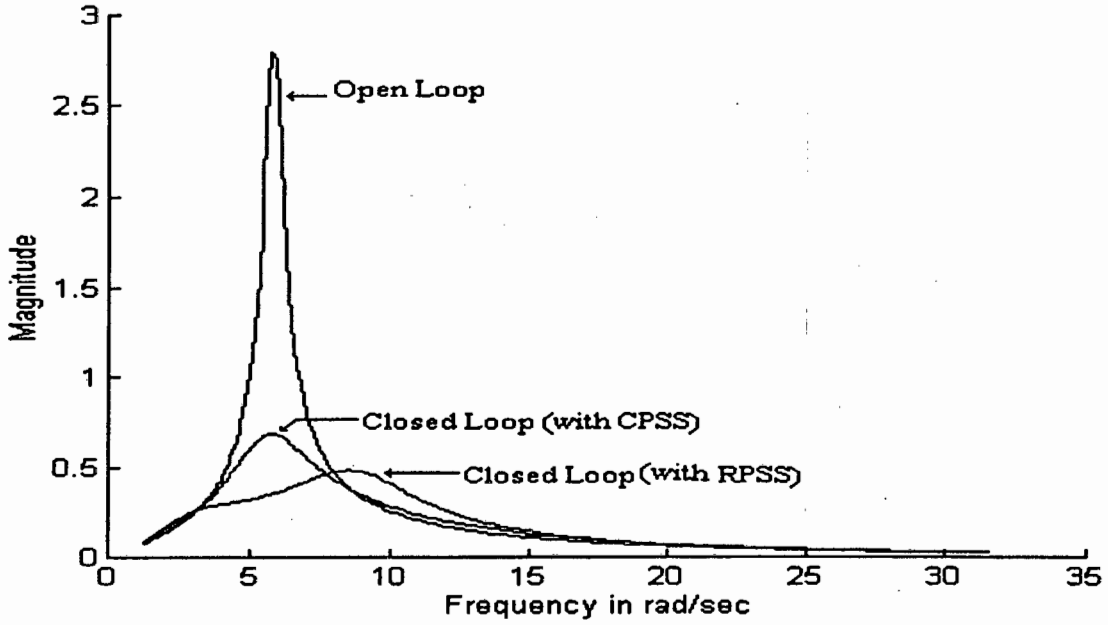

Figure 5.5: Magnitude Plots of the Transfer Function Between the Output P_{el} and the Input V_{ref} (Nominal Loading)

We wish to investigate the robustness properties of the RPSS and CPSS under different operating conditions. In order to do this, we change the loading conditions on the SMIB system and compare the responses of P_{el} due to a step in V_{ref}.

Figure 5.6 illustrates the responses of P_{el} due to a step in V_{ref} for the subsystem with a 20 percent increased loading (i.e. heavy loading). In this case, the oscillations in P_{el} settle within two seconds for the closed loop with the RPSS. On the other hand, the oscillations of the closed loop system with the CPSS persist after 3.5 seconds

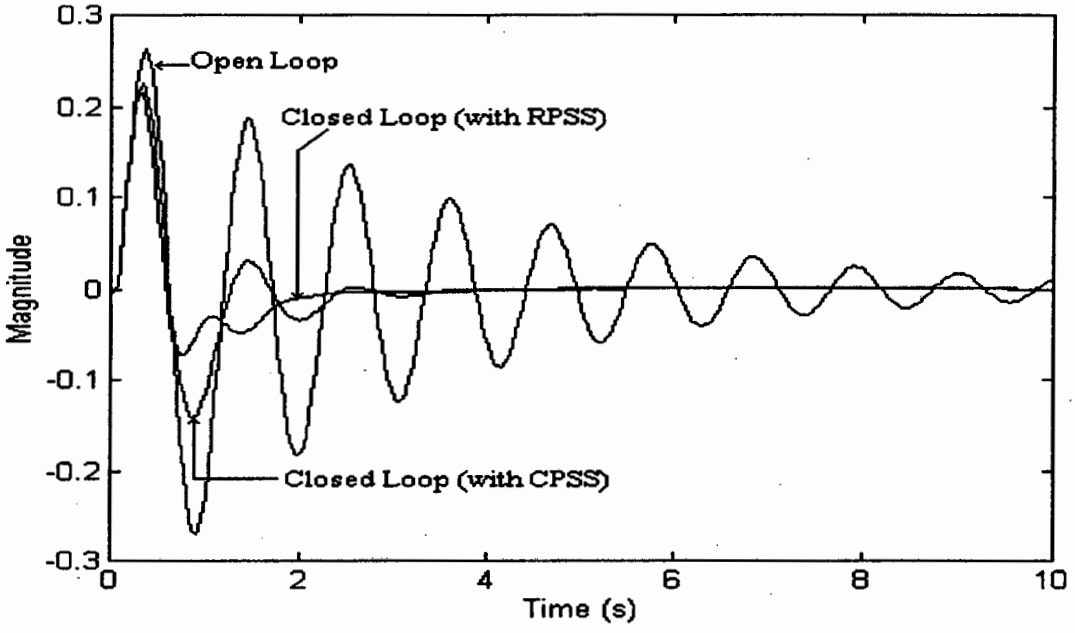

Figure 5.6: Responses of P_{el} Due to a Step in V_{ref} (Heavy Loading)

Figure 5.7 illustrates the responses of P_{el} due to a step in V_{ref} for the subsystem with a 20 percent decreased loading (i.e. light loading). In this case, the oscillations in P_{el} settle within two seconds for the closed loop with the RPSS. On the other hand, the oscillations of the closed loop system with the CPSS persist after 3.5 seconds

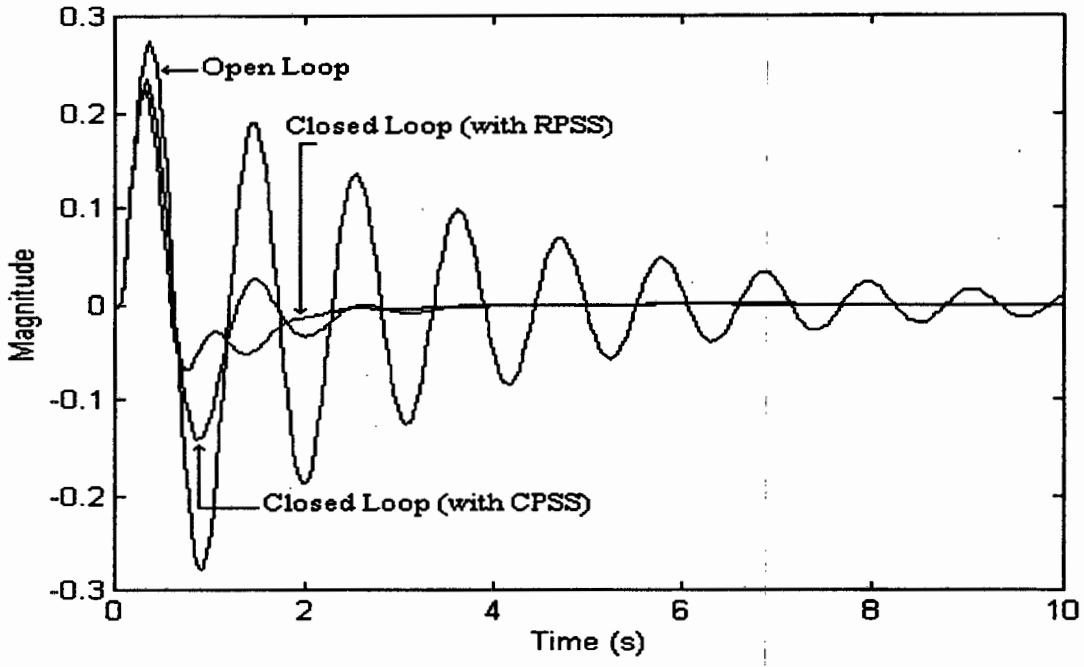

Figure 5.7: Responses of P_{el} Due to a Step in V_{ref} (Light Loading)

These results indicate that the procedure of tuning the PSS using numerical optimization provides damping controllers with robust closed loop performance.

In the next section we describe a procedure for tuning PSS using Static Output Feedback.

5.3 Tuning of PSS Using Static Output Feedback

In this section, we present a technique for determining the parameters of the PSS by making use of Static Output Feedback H_∞ control. The inputs to the PSS are output variables of the generator. This means that the PSS is a Dynamic Output Feedback controller. However, we show in this section that the parameters of the PSS can be obtained using Static Output Feedback methods. Thus, we can select the structure of the

controllers to correspond to existing PSS structures and obtain their optimal parameters for robust closed loop performance.

We wish to convert a *Dynamic Output Feedback* control problem into a *Static Output Feedback* control problem by making use of the method described in Section 3.2.3. In this section however, we wish to incorporate the effect of the disturbance input vector w(t) and the performance output vector $\xi(t)$. We make use of the lead-lag structure of the PSS. In doing so we are able to obtain robust controllers with a fixed structure. The development in this section is only conceptual. The method was not applied to a power system model.

In Section P of *Preliminaries* we outline the necessary conditions for the existence of a Static Output Feedback controller. These conditions are generally very difficult to satisfy (see Section P of *Preliminaries*). Our main contribution in this section is to demonstrate that by expressing the controller in the Controller Canonical Form and properly augmenting the controller to the plant, the necessary conditions for the existence of a Static Output Feedback controller are greatly simplified.

Assume that the structure of the controller is of the following form:

$$K_{co}'(s) = \frac{k(1+sT_1)(1+sT_3)}{(1+sT_2)(1+sT_4)} \tag{5.25}$$

where k, T_1, T_2, T_3 and T_4 are unknown parameters.

Assume further that the controller makes use of only output signals in order to effect control i.e. we have an Output Feedback problem. The aim in this section is to determine the values of T_1, T_2, T_3 and T_4 such that the closed loop robustness is maximized.

In order to determine the values of the unknown parameters, we transform the *Dynamic Output Feedback* problem into a *Static Output Feedback* problem using the technique described in Section (3.2.3). However, this technique requires that the controller be strictly proper i.e. that the number of poles must be strictly greater than the number of zeros. The lead-lag structure of the controller given by (5.25) does not satisfy this condition. In order to address this difficulty we let $T_3 = 0$. If T_3 cannot be set to zero, then one numerator

block can be absorbed into the plant, provided that the plant itself is strictly proper. This procedure is described in more detail in *Appendix B.*

Assume that the T_3 has been set to zero. Then the strictly proper controller, whose parameters need to be determined, can be expressed as follows:

$$K_{co}(s) = \frac{k(1+sT_1)}{(1+sT_2)(1+sT_4)} \tag{5.26}$$

The controller dynamics (in controller canonical form) is then expressed as follows:

$$\begin{aligned} \dot{z} &= P_c^0 z + N^0 u_{co} - N^0 u_c \\ u_{co} &= -P_c z \\ y_c &= -Hz + D_c u_c \end{aligned} \tag{5.27}$$

where:

$$P_c^0 = \begin{bmatrix} 0 & 1 \\ 0 & 0 \end{bmatrix}$$

$$N^0 = -\begin{bmatrix} 0 & 0 \\ 0 & 1 \end{bmatrix}$$

$$P_c = \begin{bmatrix} 0 & 0 \\ \dfrac{1}{T_2T_4} & \dfrac{T_2+T_4}{T_2T_4} \end{bmatrix}$$

$$H = -\begin{bmatrix} \dfrac{k(T_1T_4+T_2-T_1)}{T_2T_4} & \dfrac{kT_1}{T_2} \end{bmatrix}$$

$$D_c = \left[\frac{kT_1T_3}{T_2T_4}\right] = 0 \text{ since } T_3 = 0$$

The unknown parameters of the controller are contained in P_c and H. All the other matrices are known.

We wish to augment the controller dynamics with the dynamics of the open loop plant i.e. connect u_c to y ($u_c = y$). Thus, we can rewrite the state space description of the controller in controller canonical form as follows:

$$\dot{z} = P_c^0 z + N^0 u_{co} - N^0 y$$
$$u_{co} = -P_c z \qquad (5.28)$$
$$u = -Hz$$

The dynamics of the plant with the augmented controller are given by the following state space description:

$$\dot{x}' = A'x' + B_1' w + B_2' u' \qquad (5.29)$$
$$z = C_1' x + D_{11} w + D_{12}' u'$$
$$y' = C_2' x' + D_{21} w + D_{22}' u' \qquad (5.30)$$

where:

$$x' = \begin{bmatrix} x \\ z \end{bmatrix}$$

$$u' = \begin{bmatrix} u \\ u_{co} \end{bmatrix}$$

$$y' = z$$

$$A' = \begin{bmatrix} A & 0 \\ -N^0 C_2 & P_c^0 \end{bmatrix},$$

$$B_1' = \begin{bmatrix} B_1 \\ -N^0 D_{21} \end{bmatrix} w$$

$$B_2' = \begin{bmatrix} B_2 & 0 \\ -N^0 D_{22} & N^0 \end{bmatrix}$$

$$C_1' = \begin{bmatrix} C_1 & 0 \end{bmatrix}$$

$$C_2' = \begin{bmatrix} 0 & I_{nc} \end{bmatrix}$$

$$D_{22}' = \begin{bmatrix} 0 & 0 \\ 0 & 0 \end{bmatrix}$$

In order to find the closed loop system, we need to connect the output of augmented system to its input i.e.:

$$u' = -G' y' \qquad (5.31)$$

where:

$$G' = \begin{bmatrix} H \\ P_c \end{bmatrix}$$

The state equation of the closed loop system is given by the following:

$$\dot{x} = (A' - B_2' G' C_2')x \tag{5.32}$$

Matrix $K = G'C_2'$ can be calculated from a Static Output Feedback H_∞ algorithm. The Static Output Feedback H_∞ problem can be formulated as follows (see Section P of *Preliminaries*). Reference [7] provides a more detailed discussion of the Static Output Feedback algorithm that we use in this section.

Assume that (A, B_2) is stabilizable and that the pair (A, C_2) has no unobservable modes on the imaginary axis. Then we wish to obtain a stabilizing controller K which can be expressed as a static gain matrix. In addition to stabilizing the closed loop, we require that the closed loop transfer function $T_{w\xi}$ satisfies the following inequality:

$$\left\| T_{w\xi} \right\|_\infty < \gamma \tag{5.33}$$

where γ is a positive constant

The gain matrix K can be calculated by using a Static Output Feedback technique. The background to this technique is provided in Section P of *Preliminaries*.

The feedback law that we use is the following:

$$u(t) = -Ky(t) \tag{5.34}$$

where:

K is a gain matrix

$$K = W_2^T C_2^T (C_2 W_1 C_2^T)^{-1} C_2 = KC_2$$

$$\theta \stackrel{\Delta}{=} FW + WF^T + \gamma^{-2} WRW + Q \tag{5.35}$$

W is positive semi-definite, symmetric matrix

$$W = \begin{bmatrix} W_1 & W_2 \\ W_2^T & W_3 \end{bmatrix} \tag{5.36}$$

Q is a positive definite matrix

$v^T \theta v$ is negative semi-definite

$v \in nullspace(G^T)$

$W_1 \in R^{n \times n}$, $W_2 \in R^{n \times m}$ and $W_3 \in R^{m \times m}$

W_1 is positive definite

The uncertain system described by (5.1) is stabilizable by Static Output Feedback if and only there exists a matrix E which satisfies the following conditions:

$$(1)\ T \stackrel{\Delta}{=} \begin{bmatrix} C_2 \\ E^T \end{bmatrix} \in R^{n \times n} \text{ is full rank} \tag{5.37}$$

$$(2)\ C_\infty(E) \stackrel{\Delta}{=} C_\infty \cap \left\{ W : \begin{bmatrix} C_2 & 0 \\ 0 & I \end{bmatrix} W \begin{bmatrix} E \\ 0 \end{bmatrix} = 0 \right\} \neq 0 \tag{5.38}$$

Thus, in order to guarantee that the constant gain matrix exists, we need to find matrix E which satisfies these conditions. The determination of matrix E is generally a difficult task.

In this section, we present a method that allows us to evaluate matrix E, thus ensuring the existence of a stabilizing gain matrix K. The method makes use of the Controller Canonical Form of the augmented plant and controller. Using this formulation, the determination of matrix E is greatly simplified.

We partition the matrices W_1, W_2 and W_3 as follows:

$$W_1 = \begin{bmatrix} W_1^1 & W_1^2 \\ \left(W_1^2\right)^T & W_1^3 \end{bmatrix}_{n \times n} \tag{5.39}$$

$$W_2 = \begin{bmatrix} W_2^1 & W_2^2 \\ \left(W_2^2\right)^T & W_2^3 \end{bmatrix}_{n \times m} \tag{5.40}$$

$$W_3 = \begin{bmatrix} W_3^1 & W_3^2 \\ \left(W_3^2\right)^T & W_3^3 \end{bmatrix}_{m \times m} \tag{5.41}$$

where:

$W_1^1 \in R^{n_c \times n_c}$,

$W_1^2 \in R^{n_c \times (n - n_c)}$

$W_1^3 \in R^{(n-n_c)}$

$W_2^1 \in R^{n_c \times (m-n_c)}$

$W_2^2 \in R^{n_c \times n_c}$

$W_2^3 \in R^{(n-n_c)\times n_c}$

$W_3^1 \in R^{(m-n_c)\times(m-n_c)}$

$W_3^2 \in R^{(m-n_c)\times n_c}$

$W_3^3 \in R^{n_c \times n_c}$

n_c is the number of states of the controller

Using the above partitioning of matrix W, we can find matrix E which satisfies the two conditions as follows:

Condition 1

We need:

$$T \stackrel{\Delta}{=} \begin{bmatrix} 0_{n_c\times(n-n_c)} & I_{n_c\times n_c} \\ E_1^T & E_2^T \end{bmatrix}_{n\times n} \tag{5.42}$$

to have full rank.

By choosing matrix E to be the following:

$$E = \begin{bmatrix} I_{(n-n_c)\times(n-n_c)} \\ 0_{n_c\times(n-n_c)} \end{bmatrix} \tag{5.43}$$

we obtain the following for matrix T:

$$T = \begin{bmatrix} 0_{n_c\times(n-n_c)} & I_{n_c\times n_c} \\ I_{(n-n_c)\times(n-n_c)} & 0_{n_c\times(n-n_c)} \end{bmatrix}_{n\times n} \tag{5.44}$$

Thus, T is of full rank.

Note that the simple structure of T is as a result of expressing the controller in the Controller Canonical Form.

Condition 2

We need to ensure that:

$$C_\infty(E) \overset{\Delta}{=} C_\infty \cap \left\{ W : \begin{bmatrix} C_2 & 0 \\ 0 & I \end{bmatrix} W \begin{bmatrix} E \\ 0 \end{bmatrix} = 0 \right\} \tag{5.45}$$

is a non-empty set.

We consider the matrix equation:

$$\begin{bmatrix} C_2 & 0 \\ 0 & I \end{bmatrix} \begin{bmatrix} W_1 & W_2 \\ W_2^T & W_3 \end{bmatrix} \begin{bmatrix} E \\ 0 \end{bmatrix} = 0 \tag{5.46}$$

Thus, in order to satisfy *Condition 2* the following two equations must be satisfied:

$$C_2 W_1 E = 0 \tag{5.47}$$

$$E^T W_2 = 0 \tag{5.48}$$

From equation (5.47) we know that:

$$\begin{bmatrix} 0_{n_c \times (n-n_c)} & I_{n_c \times n_c} \end{bmatrix} \begin{bmatrix} W_1^1 & W_1^2 \\ \left(W_1^2\right)^T & W_1^3 \end{bmatrix}_{n \times n} \begin{bmatrix} I_{(n-n_c)\times(n-n_c)} \\ 0_{n_c \times (n-n_c)} \end{bmatrix} = 0 \tag{5.49}$$

Thus:

$$W_1^2 = \left(W_1^2\right)^T = 0 \tag{5.50}$$

From equation (5.48) we require that:

$$\begin{bmatrix} I_{(n-n_c)\times(n-n_c)} & 0_{(n-n_c)\times n_c} \end{bmatrix} \begin{bmatrix} W_2^1 & W_2^2 \\ \left(W_2^2\right)^T & W_2^3 \end{bmatrix}_{n \times m} = 0 \tag{5.51}$$

Thus, we require that:

$$\begin{aligned} W_2^1 &= 0 \\ W_2^2 &= 0 \end{aligned} \tag{5.52}$$

The equations in (5.51) and (5.52) are restrictions on the choice of matrix W. In addition to these restrictions, we also require that $W_1 > 0$ (positive definite) and $W = W^T$ (symmetric).

A necessary condition for the existence of E is that (see Section P of *Preliminaries*):

$$AW_1 - B_2 W_2^T + W_1 A^T - W_2 B_2^T + B_1 B_1^T \leq 0 \tag{5.53}$$

If we let $W_2 = 0$, the conditions given by (5.52) are satisfied. Substituting $W_2 = 0$ into (5.53) gives the following:

$$AW_1 + W_1A^T + B_1B_1^T \leq 0 \qquad (5.54)$$

If we consider the case when $AW_1 + W_1A^T + B_1B_1^T = 0$, the inequality in (5.53) becomes the steady state Lyapunov equation. The matrix W can be obtained from a solution of the Lyapunov matrix equation. If A is stable, the solution W_1 is positive definite and symmetric as required. If we choose $W_2^1 = W_2^2 = 0$ and $W_3 = I$ all the requirements for the existence of matrix K are met.

A choice of matrix W which satisfies all the conditions is as follows:

$$W = \left[\begin{array}{cc:cc} W_1^1{}_{n_c\times n_c} & 0 & 0_{n_c\times(m-n_c)} & 0 \\ 0 & W_1^3{}_{(n-n_c)\times(n-n_c)} & 0 & I_{(n-n_c)\times n_c} \\ \hdashline 0_{(m-n_c)\times n_c} & 0 & I_{m-n_c} & 0 \\ 0 & 0_{n_c\times(n-n_c)} & 0 & I_{n_c\times n_c} \end{array}\right] \qquad (5.55)$$

The controller transfer function K_{co} is then obtained from the following:

$$K_{co}(s) = H(sI - P_{co})^{-1}N^0 \qquad (5.56)$$

where:

$$P_{co} = P_c^0 - N^0P_c$$

Thus, we can obtain the parameters of the PSS which will provide robust performance of the closed loop.

5.4 Conclusions

In this chapter two new methods for determining the parameters of fixed structure PSS were presented, namely *tuning of PSS using numerical optimization* and *tuning of PSS using Static Output Feedback*. The tuning of PSS using numerical optimization is based on formulating the PSS tuning problem as an optimization problem. The objective function was taken as the H_∞ norm of a closed loop disturbance-related transfer function. We demonstrated that the H_∞ controller obtained using the numerical optimization formulation has better robustness properties than that of a PSS tuned using standard phase-compensation techniques.

The method based on Static Output Feedback made use of the transformation of a Dynamic Output Feedback problem into a Static Output Feedback problem. This was achieved by augmenting the controller (in Controller Canonical Form) to the open loop plant dynamics such that the resulting closed loop was in the form of a Static Output Feedback problem. The resulting static gain matrix can then be calculated from existing Static Output Feedback algorithms.

5.6 References

[1] Anderson P., Fouad A., *Power System Control and Stability*, Iowa State University Press, Ames, Iowa, 1977.

[2] Ahmed S. S., Petroianu A., "Design of Decentralized Robust Excitation Controllers Based on H_∞ Control Theory", *Proceedings of the International Conference on Power System Technology*, Beijing, China, October 1994.

[3] Bambang R., Shimemura E., Uchida K., "Mixed H_2/H_∞ Control of Uncertain Systems", *Proceedings of the American Control Conference*, San Francisco, USA, June 1993, pp. 245-247.

[4] Maciejowski J.M., *Multivariable Feedback Design*, Cambridge University, Addison Wesley, 1989.

[5] Fletcher R., *Practical Methods of Optimization*, Vol. 1 and Vol. 2, John Wiley and Sons, 1980.

[6] Ahmed S. S., Chen L., Petroianu A., "Robust H_∞ Tuning of Power System Stabilizers", accepted for *Stockholm Power Technologies Conference*, Stockholm, 1995

[7] Peres P. L., "H_∞ Robust Control By Static Output Feedback", *Proceedings of the American Control Conference*, San Francisco, California, June 1993.

Chapter 6

Conclusions

6.1 Overview

This thesis addressed the damping of electromechanical oscillations in electric power systems using Power System Stabilizers (PSS). We focused on three problems associated with damping the oscillations, namely the determination of the optimal locations of the PSS, the determination of the best control structure of the PSS and the design of robust PSS.

In *Chapter 2*, we addressed the problem of determining the optimal locations of the PSS. We introduced two new methods for the determination of the optimal PSS locations. These two methods were based on Total Modified Coupling Factors (TMC) and optimization by Simulated Annealing (SA) respectiveky.

The TMC is a measure of the damping influence of each machine pair on several power system modes. In order to take into account the effect of the performance and the type of excitation system, we incorporated an exciter penalty factor in the TMC. The method based on TMC was tested on a nine-bus benchmark network.

In the method based on SA, we formulated the placement problem as a discrete nonlinear optimization problem. The objective function was taken as the minimum damping of the electromechanical modes. In this method, the PSS placement can be performed simultaneously for all the PSS. In addition, only generators with acceptable excitation systems were included in the optimization search space, thus ensuring that the performance and the type of exciter is taken into account. Using the method based on SA, we obtained a placement scheme which ensured that the undesired poles were controlled with the available finite control energy. Since we used a discrete nonlinear optimization formulation, the nonlinear nature of the placement problem was taken into account. However, as a result of the nonlinear formulation, the method was computationally more intensive than the

method based on TMC. The method of SA was tested on two networks namely, a seven-bus network and a 35-bus equivalent of the Eskom network.

In *Chapter 3,* we addressed the problem of determining the control structure of PSS. Three aspects of the control structure were addressed, namely the *type of feedback*, the *type of signal* and the *type of control* to be used for damping electromechanical oscillations.

The type of feedback refers to whether State Feedback or Output Feedback is to be used. We used Output Feedback for damping electromechanical oscillations so as to reduce the number of feedback signals that need to be measured for control. However, Output Feedback requires that the controller be a dynamic controller. The order of the Dynamic Output Feedback controller is usually excessively high. In order to overcome this problem, we presented a new method of obtaining Output Feedback controllers of fixed structure. We achieved this by transforming the Dynamic Output Feedback problem into a Static Output Feedback problem using the Controller Canonical Form of the controller. In this way we can obtain the parameters of the PSS for the damping electromechanical oscillations.

The *type of signal* refers to the determination of the best output signals that are to be used for damping of the electromechanical oscillations. We presented two new methods for determining the best output signals. These methods were based on two measures of the contribution of the electromechanical oscillations to the outputs. The first measure, the *Centralized Modal Observer Measure (CMOM),* is based on the centralized observability of the electromechanical modes. The *CMOM* requires only the calculation of the right and left eigenvectors and is thus not computationally intensive. However, the *CMOM* does not take into account the existence of fixed modes in a system under decentralized control. The second measure, the *Decentralized Modal Observer Measure (DMOM)* takes into account the existence of decentralized fixed modes. The DMOM is based on the decentralized observability of the electromechanical modes. The CMOM and DMOM were tested on a seven-bus benchmark network.

The third aspect of the control structure that we addressed was whether centralized, decentralized or hierarchical control is to be used. We developed a new approach for designing decentralized controllers. For this approach, we derived new sufficient conditions for ensuring that the system under decentralized control remains globally stable. In addition, we presented an approach for the hierarchical control of power systems. For this approach, we derived new sufficient conditions for ensuring that the time-varying power system remains globally stable. We also proposed that these conditions be incorporated in the dynamic security assessment of the power system.

In *Chapters 4* and *5* we addressed the problem of designing robust PSS for damping the electromechanical oscillations. Chapter 4 focused on synthesizing H_∞-based controllers with structures which are different from those of existing PSS. On the other hand, Chapter 5 focuses on the determination of the parameters of existing PSS.

In *Chapter 4*, we developed a new procedure for designing suboptimal decentralized H_∞ controllers for damping electromechanical oscillations. The global stability of the interconnected power system was guaranteed by incorporating the sufficient conditions (derived in *Chapter 3*) in the design procedure. These sufficient conditions were used in a new two-stage method for designing decentralized controllers.

In order to evaluate the robustness of the controllers, we introduced a Lyapunov-based robust stability margin. We used this margin to compare the robustness of three controllers, namely Conventional PSS (CPSS), optimal H_∞ and suboptimal H_∞ controllers. In order to ensure that low order controllers are obtained, the method of balanced truncation was used to reduce the order of the open loop subsystems. The model reduction technique was applied to the generator subsystems which ensured that the order of the controllers was less than that of the open loop subsystems. We made use of an existing Dynamic Output Feedback Ricatti-based method to synthesize the H_∞ controllers. In addition, we outlined the major shortcomings of the standard optimal H_∞ control algorithms as applied to power systems and developed techniques for overcoming these. We used a bilinear transformation in order to improve the damping of the electromechanical oscillations. The design procedure was tested on nine-bus benchmark network. The results demonstrated that the

suboptimal H_∞ controllers possess superior robustness properties as compared to the optimal H_∞ and CPSS.

In *Chapter 5* we addressed the problem of determining the parameters of fixed structure PSS. We proposed two new methods for obtaining the parameters of the PSS, namely, *tuning of PSS using numerical optimization* and *tuning of PSS tuning using Static Output Feedback.* The tuning of PSS using numerical optimization was based on fromulating the tuning problem as an optimization problem. We calculated the PSS parameters for a SMIB system using a Sequential Quadratic Programming (SQP) algorithm. The tuning by Static Output Feedback was based on transforming the Dynamic Output Feedback problem into a Static Output Feedback problem. The static gain matrix can be calculated using an existing Static Output Feedback algorithm. The static gain matrix can then be used to calculate the parameters of the PSS.

6.2 Contributions of the Thesis

The thesis makes several contributions to the area of damping electromechanical oscillations using PSS. The following sections in the thesis are the *major* contributions:

Section 2.3: Placement of PSS using Total Modified Coupling Factors (TMC)
TMC incorporates the influence of the *type* of exciter and the *performance* of the excitation system in the optimal placement of the PSS. The TMC also considers the damping effect of each PSS under simultaneous excitation of several modes.

Section 2.5: Application of Simulated Annealing to Optimal PSS Placement
The PSS placement was formulated as a discrete nonlinear optimization problem. By doing this, the nonlinear nature of the placement problem is taken into account. Furthermore, simultaneous placement of PSS is obtained. The influence of non-minimum-phase zeros and uncontrollable modes are taken into account. No existing PSS placement method can achieve this.

Section 3.4.2.1: Global Stability of the Interconnected System

In this section we obtained new sufficient conditions for global stability of an interconnected system. Using these conditions, we can design decentralized controllers (using the two-stage procedure) while ensuring global stability. Only an upper bound for the interactions are required in designing the decentralized controllers. This is an improvement over existing global stability conditions which require detailed on-line measurements of the interactions.

Section 3.4.3: Hierarchical Control

In this section, we proposed the use of hierarchical control for damping of electromechanical oscillations using PSS. The hierarchical control was composed of two levels of controllers. Level 1 consisted of the decentralized controllers which operate autonomously under normal operating condition. Under alert conditions, the Level 2 controller is acomes into play by adjusting the parameters of the Level 1 controllers. The Level 2 controller monitors the operating state of the power system from measurements of the upper bound of the interaction. We developed new sufficient conditions for ensuring that the global system under hierarchical control remains stable. This approach of hierarchical excitation control incorporating the global stability constraints has not been previously developed for power systems.

Chapter 4 Design of H_∞-Based Robust Supplementary Excitation Controllers

In this chapter we developed a procedure for the design of decentralized robust supplementary excitation controllers. The procedure incorporated a model reduction technique, a Ricatti-based synthesis method and a bilinear transformation to improve the damping of the electromechanical modes. In addition, global stability constraints were incorporated into the design procedure. Such a coherent procedure for decentralized robust PSS design of multimachine power systems has not been developed up to now.

Chapter 5: Determination of Parameters of Fixed Structure PSS

In this chapter we presented two new methods of tuning robust fixed structure PSS namely, tuning of PSS using numerical optimization and tuning of PSS using Static Output Feedback. Up to now these methdos have not been applied to power systems.

6.3 Limitations of the Thesis

The major limitations of the thesis are:

- The procedures described in Chapter 4 and Chapter 5 do not incorporate the effect of Gaussian noise in the controller design.

- The global stability margins derived in Appendix C are based on Lyapunov stability criteria and are thus conservative. This means that the controllers which ensure global stability of the interconnected system, are not optimal.

- The method of tuning the PSS using numerical optimization was not tested on a multimachine power system model.

- The Static Output Feedback technique described in Chapter 5 was not tested on a power system model.

6.4 Future Work

The following are suggestions for future work:

- Develop a procedure for controllers based on a mixed H_2/H_∞ formulation to incorporate the influence of Gaussian white noise in robust control design.
- Develop less conservative measures of robustness.
- Develop less conservative conditions for global stability.
- Implementation of hierarchical control structure on a power system modeled as a time-varying system.
- Develop a description of the power system based on *Descriptor Systems* to avoid the ill-condition state space formulation.
- Develop and implement a fixed order Static Output Feedback H_∞ algorithm which can incorporate both an improper plant and an improper controller on a power system model.
- Incorporate the governor in the optimization formulation for a coordinated robust tuning of both the power loop and the voltage loop.

- Apply the methods developed in Chapter 5 to a multimachine system.

Appendices

Appendix A

Numerical Problems Associated with the State Space Formulation of Power Systems

In this section, we discuss the numerical problems associated with the state space formulation of power systems. We focus on the problems associated with the calculation of eigenvalues. The concepts developed in this Appendix are used throughout the thesis in obtaining a well-conditioned state space description. The new contribution in Appendix A is the development of a method of dealing with ill-conditioned eigenvalues by using a bilinear transformation.

Consider an LTI system given by the following state space description:

$$\begin{aligned} \dot{x} &= Ax + Bu \\ y &= Cx + Du \end{aligned} \tag{A1}$$

The linearized system of equations allows the use of powerful techniques based on eigenvalue and frequency domain analysis. From these, a variety of system attributes such as modal frequencies, damping factors, residues, sensitivities and the time domain step response can readily be computed. These techniques are used extensively and are considered as indispensable in modern software packages for small signal analysis of power systems.

The calculation of the eigenvalues of a system does, however, pose numerical difficulties. There are several very reliable routines for calculating the eigenvalues of a matrix A [1]. Due to the limitations of finite precision arithmetic, these routines cannot produce the exact eigenvalues of the given A matrix. However, the numbers which are computed by these routines are always very close to the eigenvalues of another matrix A_e which is given by the following:

$$A_e = A + \Delta A \tag{A2}$$

where ΔA is not unique

If some eigenvalues of A are very sensitive to changes in the elements of A, the corresponding eigenvalues of A_e will be very different from those of A. This means that the highly sensitive eigenvalues (or ill-conditioned eigenvalues) of A cannot be accurately approximated by these routines.

The problems associated with ill--conditioned eigenvalues is particularly pronounced in the state space formulation of power systems. The calculation of the state space matrices for power systems is carried out in terms of absolute rotor speed and absolute rotor angle. However, if no infinite bus is modelled, the actual states of the power system is defined in terms of relative values of speed and angle rather than absolute values. The A-matrix (if exactly calculated) will possess a non-maximal rank. Therefore at least one eigenvalue of the exact A-matrix will be zero.

Due to power flow mismatch errors, the A-matrix obtained by computer simulation software will be inexact i.e. we obtain matrix A_e instead of A. The eigenvalue(s) of A_e that corresponds to the zero eigenvalue(s) of matrix A, can now lie within an unacceptably large region around the complex plane origin. Thus a power system that is in fact stable may be calculated to have at least one eigenvalue with a positive real part.

In general, near-singularity (ill-conditioning for inversion) of a matrix A does not imply that the eigenvalues will be very sensitive to changes in the elements of A. Therefore, the usual condition-number for matrix inversion cannot be used as an accurate index for measuring the conditioning of a matrix for eigenvalue calculations. In this section we present a method of calculating the ill-conditioning of the eigenvalues using the left and right eigenvectors of a real matrix A. Furthermore, we present two methods of dealing with the eigenvalue ill-conditioning. The first method improves the eigenvalue conditioning by making use of a reference generator to express all absolute speed and angle quantities as relative speed and angle quantities. The second method retains the absolute speed and angle quantities by making use of a bilinear transformation to shift the $j\omega$ axis.

A1 Calculating the Condition Numbers of Eigenvalues

Consider a matrix $A \in R^{n \times n}$ which has no repeated eigenvalues. For any eigenvalue λ of A there exists a column vector x (right eigenvector) and a row vector y^H (left eigenvector) such that:

$$Ax = \lambda x \tag{A3}$$

$$y^H A = \lambda y^H \tag{A4}$$

where y^H is the conjugate transpose of y.

We define the condition number of eigenvalue λ as the acute angle θ between eigenvectors x and y i.e.:

$$cond(\lambda) = \sec ant\theta = \left(\frac{\|y\| \cdot \|x\|}{|y^H x|} \right) \tag{A5}$$

where $\|\cdot\|$ denotes the Euclidean norm.

The condition number as defined in equation (A5) is invariant under a unitary transformation. This property can be formally stated in the following Lemma [2]:

Lemma A1: If U is unitary then $cond(\lambda, UAU^H) = cond(\lambda, A)$

Proof: From equations (A3) and (A4):

$$Ax = \lambda x$$

$$y^H A = \lambda y^H$$

Then

$$\begin{aligned} (UAU^H)(Ux) &= \lambda(Ux) \\ (y^H U^H)(UAU^H) &= \lambda(y^H U^H) \end{aligned} \tag{A6}$$

$$\begin{aligned} cond(\lambda, UAU^H) &= \left(\frac{\|y^H U^H\| \cdot \|Ux\|}{|(y^H U^H)(Qx)|} \right) \\ &= \left(\frac{\|y^H\| \cdot \|x\|}{|y^H x|} \right) \end{aligned} \tag{A7}$$

which gives the result $cond(\lambda, UAU^H) = cond(\lambda, A)$.

If the eigenvectors x and y^H are normalized such that $\|y^H\| = \|x\| = 1$ then the condition number is given by:

$$cond(\lambda) = \left(\frac{1}{|y^H x|} \right) \tag{A8}$$

This definition of the eigenvalue condition number in equation (A7) is given in terms of the right and left eigenvectors of matrix A. These eigenvectors can easily be calculated using the procedure illustrated in Figure A1. First, the matrix is transformed to matrix H in Hessenberg form via a unitary transformation. Thereafter, matrix H is transformed to matrix S in the Schur triangular form. The eigenvectors of S are then calculated by back-substitution [2].

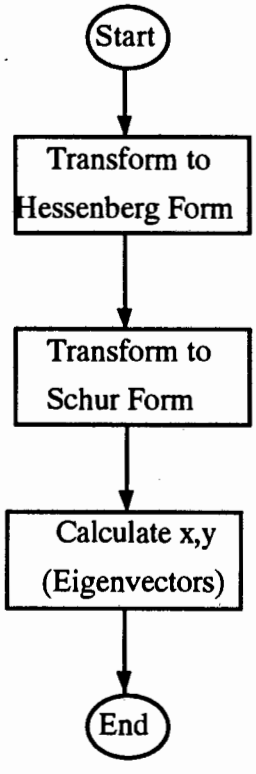

Figure A1: Flowchart Showing the Procedure of Calculating the Eigenvectors

A2.1 Selecting a Reference Machine

Consider an n-machine system in linearized state space form . Assume without loss of generality that the order of each generator is k. The state space description can be expressed in terms of absolute rotor angles and absolute rotor speeds given by equation (A1).

The state equation can be expressed as follows:

$$
\begin{bmatrix}
\dot{x}_1^1 \\ \dot{x}_2^1 \\ \vdots \\ \dot{\delta}_k^1 \\ \dot{\omega}_k^1 \\ \vdots \\ \dot{x}_1^r \\ \dot{x}_2^r \\ \vdots \\ \dot{\delta}_k^r \\ \dot{\omega}_k^r \\ \vdots \\ \dot{x}_1^n \\ \dot{x}_2^n \\ \vdots \\ \dot{\delta}_k^n \\ \dot{\omega}_k^n
\end{bmatrix}
=
\begin{bmatrix}
A_{11}^1 & A_{12}^1 & \cdots & & & & & \cdots & & A_{1n}^1 \\
A_{21}^1 & & & & & & & \cdots & & A_{2n}^1 \\
\vdots & & & & & & & \cdots & & \\
0 & \cdots & 0 & \omega_b & \cdots & 0 & 0 \cdots & & 0 & 0 \\
A_{k1}^1 & A_{K2}^1 & \cdots & -\dfrac{D^1}{M^1} & \cdots & & \cdots & & \cdots & A_{kn}^1 \\
\vdots & & & & & & \cdots & & & \\
\vdots & & & & & & \cdots & & & \\
 & & & & & & \cdots & & & \\
 & & & & & & \cdots & & & \\
0 & \cdots & 0 & & \cdots & & \omega_b & & 0 & 0 \\
A_{k1}^r & A_{k2}^r & \cdots & & & & -\dfrac{D^r}{M^r} & & & \\
 & & & & & & \cdots & & & \\
 & & & & & & \cdots & & & \\
 & & & & & & & & & \\
0 & \cdots & & & & & & & & \omega_b \\
A_{k1}^n & A_{k2}^n & \cdots & & & & & & & -\dfrac{D^n}{M^n}
\end{bmatrix}
\begin{bmatrix}
x_1^1 \\ x_2^1 \\ \vdots \\ \delta^1 \\ \omega^1 \\ \vdots \\ x_1^r \\ x_2^r \\ \vdots \\ \delta^r \\ \omega^r \\ \vdots \\ x_1^n \\ x_2^n \\ \vdots \\ \delta^n \\ \omega^n
\end{bmatrix}
+ Bu
\qquad \text{(A9)}
$$

where:

D^i is the damping of machine i

M^i is the inertia of machine i

ω_b is the synchronous speed

δ^i is the rotor angle of machine i

ω^i is the rotor speed of machine i

Consider the case where $\frac{D^i}{M^i} \neq D$ for all $i = 1,\ldots,n$. The system of equations given by (A9) is expressed in terms of absolute rotor angles. The state coefficient matrix A of (A9) is non-minimal since all the power flow equations require only relative rotor angles with respect to a reference machine. Thus, the rank of the state coefficient matrix is $n-1$. This means that the state coefficient matrix contains a zero eigenvalue. This zero eigenvalue is ill-conditioned for eigenvalue calculation.

The zero eigenvalue can be removed from the system by making the following substitution:

$$\Delta\dot{\delta}^{ir} = \Delta\dot{\delta}^i - \Delta\dot{\delta}^r = \Delta\omega^i - \Delta\omega^r \qquad \text{(A10)}$$

$$\Delta\delta^r = 0$$

where:

δ^r is the reference machine rotor angle

ω^r is the reference machine speed

Consider the case where $\frac{D^i}{M^i} = D$ for all i, then $rank(A) = n-2$

$$\Delta\dot{\delta}^{ir} = \Delta\dot{\delta}^i - \Delta\dot{\delta}^r = \Delta\omega^i - \Delta\omega^r \qquad \text{(A11)}$$

$$\Delta\dot{\omega}^{ir} = \Delta\dot{\omega}^i - \Delta\dot{\omega}^r \qquad \text{(A12)}$$

$$\Delta\delta^r = 0 \qquad \text{(A13)}$$

$$\Delta\omega^r = 0 \qquad \text{(A14)}$$

The method of eliminating the ill-conditioning of the A-matrix is to select one machine as a reference and to express quantities in terms of relative angular position and relative speed [3]. This method has the drawback that information about the absolute angle and speed is lost. This poses problems in systems in which no infinite bus is modelled, especially when the governor control needs to be analysed.

Using this technique, we also find that the eigenvalues change as the reference machine is changed [3]. This reflects a need to develop a satisfactory method of eliminating the ill-conditioning of the A-matrix without the selection of a machine as reference. In the next section, we describe two methods of dealing with the numerical problems associated with the state space formulation of power systems. The first method makes use of a reference machine in order to eliminate the zero eigenvalue(s). By eliminating the zeros eigenvalue(s) the information about the absolute rotor angle and absolute speed deviations is lost. The second method retains the information absolute rotor angles and speed deviations by making use of a bilinear transformation.

Example A1

Consider the nine-bus system described in *Appendix E*. We model the three generators with the second order swing equation i.e. each generator is modeled as a constant voltage behind a transient impedance. The state coefficient matrix A is given by the following.

MATRIX A

-.15480	-.08667	0.00000	0.04935	0.000000	0.03734
314.160	0.00000	0.00000	0.00000	0.000000	0.00000
0.00000	0.11000	-.29985	-.20268	0.000000	0.09286
0.00000	0.00000	314.160	0.00000	0.000000	0.00000
0.00000	0.18363	0.00000	0.20307	-0.41548	-.38654
0.00000	0.00000	0.00000	0.00000	314.1600	0.00000

The eigenvalues are calculated to be as follows:

$\lambda_1 = +0.0768$

$\lambda_2 = -0.3032$

$\lambda_3 = -0.1268 + 8.1567i$

$\lambda_4 = -0.1268 - 8.1567i$

$\lambda_5 = -0.1951 + 12.0734i$

$\lambda_6 = -0.1951 - 12.0734i$

The eigenvalue λ_1 has been calculated to have a positive real part, which suggests that the system is unstable. However, the system is not in fact unstable. Eigenvalue λ_1 has a positive real part because λ_1 is ill-conditioned.

The left eigenvector y_1 associate with λ_1 is:

$y_1 = [-0.8973$

-0.0007

-0.4017

-0.0005

-0.1831

$-0.0003]$

The right eigenvector x_1 associated with λ_1 is:

$x_1 = [-0.0001$

-0.5772

-0.0001

-0.5775

-0.0001

$-0.5774]$

The condition number associated with λ_1 is equal to 966.2698.

By selecting machine 2 as a reference, we can eliminate the 'unstable' eigenvalue λ_1.

We construct a matrix A_S given by the following:

$$A_S = \begin{bmatrix} 0 & 0 & 0 & 0 & 0 & 0 \\ 0 & 0 & -314.16 & 0 & 0 & 0 \\ 0 & 0 & 0 & 0 & 0 & 0 \\ 0 & 0 & -314.16 & 0 & 0 & 0 \\ 0 & 0 & 0 & 0 & 0 & 0 \\ 0 & 0 & -314.16 & 0 & 0 & 0 \end{bmatrix}$$

Thus $A + A_S$ equals the following:

$$A + A_S = \begin{bmatrix} -0.1548 & -0.0867 & 0 & 0.0493 & 0 & 0.0373 \\ 314.16 & 0 & -314.16 & 0 & 0 & 0 \\ 0 & 0.1100 & -0.2999 & -0.2027 & 0 & 0.0929 \\ 0 & 0 & 0 & 0 & 0 & 0 \\ 0 & 0.1836 & 0 & 0.2031 & -0.4155 & -0.3865 \\ 0 & 0 & -314.16 & 0 & 314.16 & 0 \end{bmatrix}$$

We now eliminate row 4 and column 4. This gives the following reduced matrix:

$$A_r = \begin{bmatrix} -0.1548 & -0.0867 & 0 & 0 & 0.0373 \\ 314.1600 & 0 & -314.1600 & 0 & 0 \\ 0 & 0.1100 & -0.2999 & 0 & 0.0929 \\ 0 & 0.1836 & 0 & -0.4155 & -0.3865 \\ 0 & 0 & -314.1600 & 314.1600 & 0 \end{bmatrix}$$

The eigenvalues of A_r are:

$\lambda_1 = -0.2263$

$\lambda_2 = -0.1268 + 8.1588i$

$\lambda_3 = -0.1268 - 8.1588i$

$\lambda_4 = -0.1951 + 12.0733i$

$\lambda_5 = -0.1951 - 12.0733$

Thus the 'unstable' eigenvalue has been removed from the system by selecting the rotor angle of machine 2 as a reference.

A2.2 Shifting the jω-Axis

In this section we present a new method of dealing with the ill-conditioned eigenvalue while still retaining information about absolute speed and absolute rotor angle. If we wish to do this we cannot eliminate the zero eigenvalue(s). Instead of selecting a reference machine, we adjust the ill-conditioned eigenvalues by using a bilinear transformation. The bilinear transformation that we use shifts the jω axis so that the resulting system has the zero eigenvalue.

The general bilinear transformation is given by the following:

$$\begin{bmatrix} A_b & B_b \\ C_b & D_b \end{bmatrix} = \begin{bmatrix} (\beta A - \delta i)(\alpha i - \gamma A)^{-1} & (\alpha\beta - \gamma\delta)(\alpha I - \gamma A)^{-1}B \\ C(\alpha I - \gamma A)^{-1} & D + \gamma C(\alpha I - \gamma A)^{-1}B \end{bmatrix} \tag{A17}$$

For a shift in the jω axis the following transformation is required:

$$\bar{s} = s + p \tag{A18}$$

where $p = \mathrm{Re}(\varepsilon) > 0$

$\varepsilon = \lambda^i(A)$ is the unstable ill-conditioned eigenvalue of A

Thus the following values for the transform parameters need to be selected::

$\beta = 1, \delta = p, \alpha = 1, \gamma = 0$

This results in the following state space description:

$$\begin{bmatrix} A_b & B_b \\ C_b & D \end{bmatrix} = \begin{bmatrix} (A - pI) & B \\ C & D \end{bmatrix} \tag{A19}$$

where $\dim(A_b) = n-1$

The procedure is described in Figure (A2). First we calculate the system eigenvalues and determine the amount of shift p that is required. Thereafter, we apply the bilinear transformation to the state space description.. The resulting state space description contains information about the absolute rotor angle and absolute speed deviations.

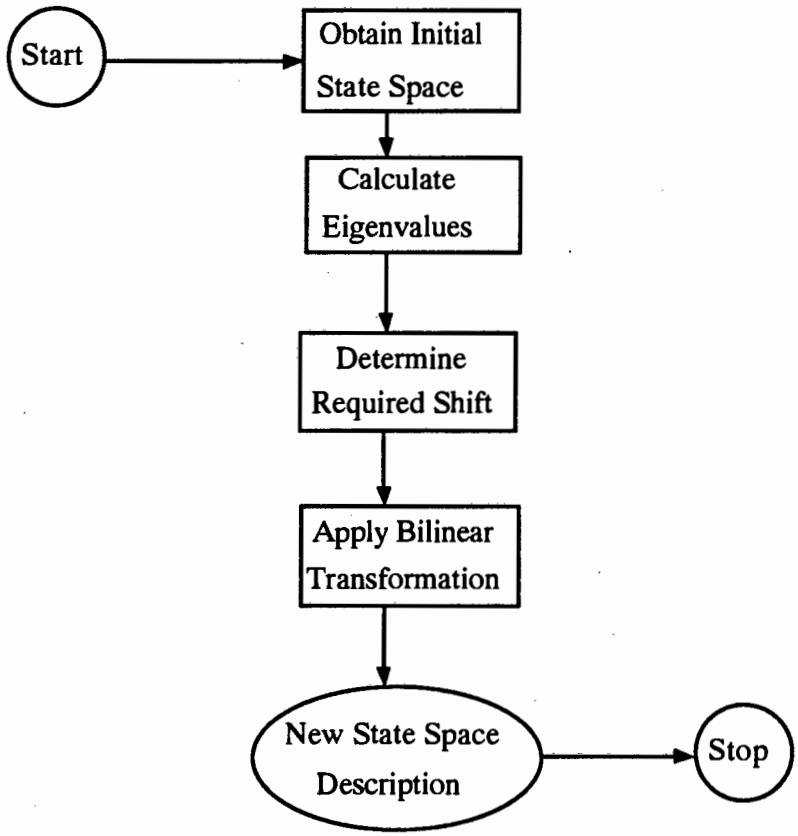

Figure A2: Flowchart Showing the Procedure for Shifting the jω-axis

We apply the method of shifting the $j\omega$ -axis to the nine-bus system.

The amount of shift in the $j\omega$ -axis which is required in order to stabilize the system is given by the real part of λ. i.e. $p = 0.0768$.

By applying the bilinear transformation to the nine-bus system, we obtain the following state coefficient matrix.

$$An = \begin{bmatrix} -0.2316 & -0.0867 & 0 & 0.0493 & 0 & 0.0373 \\ 314.1600 & -0.0768 & 0 & 0 & 0 & 0 \\ 0 & 0.1100 & -0.3767 & -0.2027 & 0 & 0.0929 \\ 0 & 0 & 314.16 & -0.0768 & 0 & 0 \\ 0 & 0.1836 & 0 & 0.2031 & -0.4923 & -0.3865 \\ 0 & 0 & 0 & 0 & 314.1600 & -0.0768 \end{bmatrix}$$

The eigenvalues of the transformed matrix are:

$\lambda_1 = 0.0000$

$\lambda_2 = -0.3800$

$\lambda_3 = -0.2036 + 8.1567i$

$\lambda_4 = -0.2036 - 8.1567i$

$\lambda_5 = -0.2719 + 12.0734i$

$\lambda_6 = -0.2719 - 12.0734i$

Therefore, the real part of all the eigenvalues are less than or equal to zero. Note the zero eigenvalue λ_1 has been retained in the transformed A matrix.

References

[1] Wilkinson, J. H. *The Algebraic Eigenvalue Problem*, Clarendon Press, Oxford, 1975

[2] Chan S. P., Feldman R., Parlett B. N., "A Program for Computing the Condition Numbers of Matrix Eigenvalues Without Computing Eigenvectors", *ACM Transactions on Mathematical Software*, Vol. 3, No. 2, June 1977, pp. 186-203.

[3] Anderson P., Fouad A., *Power System Control and Stability*. Vol. 1 , Iowa State University Press, Iowa, USA, 1977.

Appendix B

Controller Canonical Form of Lead-Lag Controller

In this section, we transform the state space description of a lead-lag controller to a controller canonical form. We consider only first and second order controllers.

We recommend that this section should be read in conjunction with Section M of *Preliminaries*. The results of *Appendix B* are relevant to Section 3.2.3 and Section 5.3.

First Order Lead/Lag

Consider a first order lead-lag controller given by the following transfer function:

$$K(s) = \frac{k(1+sT_1)}{1+sT_2} \tag{B1}$$

We decompose the system into two parts; one part consisting of the denominator polynomial and the other consisting of the numerator polynomial. This decomposition is illustrated in Figure B1.

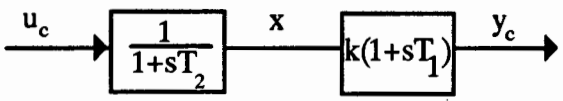

Figure B1: Decomposition of Lead/Lag Transfer Function

From Figure B1, the following two equations can be obtained:

$$u_c = x + T_2\dot{x} \tag{B2}$$

$$y_c = kx + k\dot{x}T_1 \tag{B3}$$

By rearranging equation (B2), we obtain the following state equation:

$$\dot{x} = -\frac{1}{T_2}x + \frac{1}{T_2}u_c \tag{B4}$$

By substituting equation (B4) into equation (B3) we get the following output equation:

$$y_c = k(1-\frac{T_1}{T_2})x + \frac{kT_1}{T_2}u_c \tag{B5}$$

Equations (B4) and (B5) are the equation for the state space description of the lead/lag controller.

The characteristic polynomial *D(s)* of the system given by equations (B4) and (B5) is given by:

$$D(s) = \det(sI - A) = s + \frac{1}{T_2} \tag{B6}$$

By applying the transformation T (such that $x = Tz$ as described in Section M of *Preliminaries*), we can obtain the following *controller canonical form* for the first order lead-lag controller:

$$\begin{aligned} \dot{z} &= -\frac{1}{T_2} z + 1 u_c \\ y_c &= \frac{k(T_2 - T_1)}{T_2^2} z + \frac{kT_1}{T_2} u_c \end{aligned} \tag{B7}$$

Second Order Lead-Lag

Consider a second order lead-lag controller given by the following transfer function:

$$K(s) = \frac{k(1 + sT_1)}{(1 + sT_2)} \frac{(1 + sT_3)}{(1 + sT_4)} \tag{B8}$$

We decompose the system into two first order lead/lag blocks. This decomposition is illustrated in Figure B2.

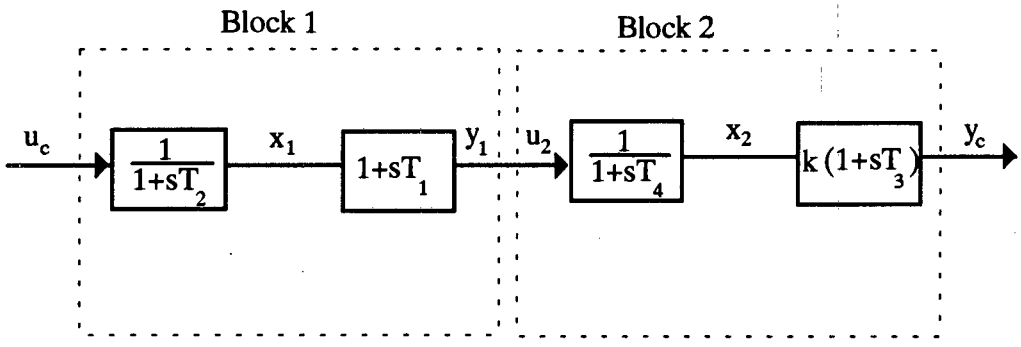

Figure B2: Decomposition of Second Order Lead-Lag Transfer Function

We can express the state and output equations form each block as follows:

Block 1

$$\dot{x}_1 = -\frac{1}{T_2} x_1 + \frac{1}{T_2} u_c \tag{B9}$$

$$y_1 = (1 - \frac{T_1}{T_2})\dot{x}_1 + \frac{T_1}{T_2}u_c \tag{B10}$$

Block 2

$$\dot{x}_1 = -\frac{1}{T_4}x_1 + \frac{1}{T_4}u_2 \tag{B11}$$

$$y_c = k(1 - \frac{T_3}{T_4})\dot{x}_1 + \frac{kT_3}{T_4}u_2 \tag{B12}$$

We wish to obtain the state space description in terms of input u_c and y_c. only. In order to do this we substitute the equation $y_1 = u_2$ into equations (B9) to (B12). This results in the following state space equations:

$$\dot{x}_1 = -\frac{1}{T_2}x_1 + \frac{1}{T_2}u_c \tag{B13}$$

$$\dot{x}_2 = -\frac{1}{T_2}x_2 + \frac{1}{T_4}\left\{\left(1 - \frac{T_1}{T_2}\right)\dot{x}_1 + \frac{T_1}{T_2}u_c\right\} \tag{B14}$$

$$y_c = k(1 - \frac{T_3}{T_4})x_2 + \frac{kT_3}{T_4}\left\{\left(1 - \frac{T_1}{T_2}\right)x_1 + \frac{T_1}{T_2}u_c\right\} \tag{B15}$$

In matrix form, the state space equations (B13) to (B15) can be rewritten as follows:

$$\begin{bmatrix}\dot{x}_1 \\ \dot{x}_2\end{bmatrix} = \left[\begin{array}{c:c} -\frac{1}{T_2} & 0 \\ \hdashline \frac{1}{T_4}\left(1 - \frac{T_1}{T_2}\right) & -\frac{1}{T_4}\end{array}\right]\begin{bmatrix}x_1 \\ x_2\end{bmatrix} + \begin{bmatrix}\frac{1}{T_2} \\ \frac{T_1}{T_2}\end{bmatrix}u_c \tag{B16}$$

$$y_c = \begin{bmatrix}\frac{kT_3}{T_4}\left(1 - \frac{T_1}{T_2}\right) & k(1 - \frac{T_3}{T_4})\end{bmatrix}\begin{bmatrix}x_1 \\ x_2\end{bmatrix} + \begin{bmatrix}\frac{kT_1T_3}{T_2T_4}\end{bmatrix}u \tag{B17}$$

We wish to transform the system given by (B16) and (B17) into the controller canonical form. In order to do this, we need to calculate the characteristic polynomial and the controllability matrix.

The characteristic polynomial $D(s) = \det(sI - A)$ can be expressed as follows:

$$D(s) = s^2 + \left(\frac{1}{T_4} + \frac{1}{T_2}\right)s + \frac{1}{T_2T_4} \tag{B18}$$

From the characteristic polynomial D(s) we construct matrix W (see Section M of *Preliminaries*) which can be expressed as follows:

$$W = \begin{bmatrix} \frac{1}{T_4} + \frac{1}{T_2} & 1 \\ 1 & 0 \end{bmatrix} \tag{B19}$$

The controllability matrix $\vartheta = \begin{bmatrix} B & AB \end{bmatrix}$ can be expressed as follows:

$$\vartheta = \begin{bmatrix} \frac{1}{T_2} & -\frac{1}{T_2^2} \\ \frac{T_1}{T_2} & \frac{T_1 - T_2 + T_1 T_2}{T_4 T_2^3} \end{bmatrix} \tag{B20}$$

The transformation that we require is defined as the product of matrices W and ϑ i.e.:

$$T = \vartheta W = \begin{bmatrix} \frac{1}{T_2 T_4} & \frac{1}{T_2} \\ \frac{T_1 T_4 + T_2 - T_1}{T_4 T_2^2} & \frac{T_1}{T_2} \end{bmatrix} \tag{B21}$$

The controller canonical form has the following state space description:

$$\begin{aligned} \dot{z} &= A_c z + B_c u_c \\ y_c &= C_c + D_c u_c \end{aligned} \tag{B22}$$

where:

$$A_c = \begin{bmatrix} 0 & 1 \\ -\frac{1}{T_2 T_4} & -\frac{T_2 + T_4}{T_2 T_4} \end{bmatrix}$$

$$B_c = \begin{bmatrix} 0 \\ 1 \end{bmatrix}$$

$$C_c = \begin{bmatrix} \frac{k(T_1 T_4 + T_2 - T_1 - T_1 T_3)}{T_2 T_4} & \frac{(kT_3 T_2 - T_3 T_1 + T_1 T_2 T_4 - T_1 T_2 T_3)}{T_4 T_2^2} \end{bmatrix}$$

$$D_c = \begin{bmatrix} \frac{kT_1 T_3}{T_2 T_4} \end{bmatrix}$$

The controller canonical form can be rewritten in the following form:

$$\begin{aligned} \dot{z} &= P_c^0 z + N^0 u_{co} - N^0 u_c \\ u_{co} &= -P_c z \\ y_c &= -Hz + D_c u_c \end{aligned} \tag{B23}$$

where:

$$P_c^0 = \begin{bmatrix} 0 & 1 \\ 0 & 0 \end{bmatrix},$$

$$N^0 = \begin{bmatrix} 0 & 0 \\ 0 & 1 \end{bmatrix}$$

$$P_c = \begin{bmatrix} 0 & 0 \\ \dfrac{1}{T_2T_4} & \dfrac{T_2+T_4}{T_2T_4} \end{bmatrix},$$

$$H = -\begin{bmatrix} \dfrac{k(T_1T_4+T_2-T_1-T_1T_3)}{T_2T_4} & \dfrac{k(T_3T_2-T_3T_1+T_1T_2T_4-T_1T_2T_3)}{T_4T_2^2} \end{bmatrix}$$

Lead-lag controllers are not strictly proper since the number of zeros equals the number of poles. This poses some problems when using lead-lag controllers for controlling a plant that is also not strictly proper.

The state space description of a strictly proper plant can be expressed as follows:

$$\begin{aligned} \dot{x} &= Ax + Bu \\ y &= Cx + Du \end{aligned} \qquad \text{(B24)}$$

where $D = 0$

If the plant is strictly proper (number of poles is greater than number of zeros or equivalently $D = 0$) then we can augment one zero block $(1+sT_3)$ to the plant. This is illustrated in Figure (B3) for a second order lead lag block. The zero block $(1+sT_3)$ is removed from the second order controller and augmented to the plant.

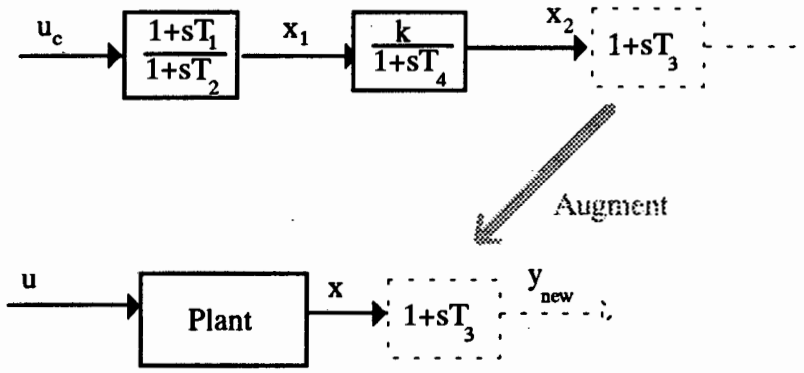

Figure B3: Augmenting a Zero Block to a Strictly Proper Plant

Note that the augmentation procedure requires that a value of T_3 be selected before the block $(1+sT_3)$ is augmented to the plant The augmentation does not affect the dimension of the plant or the controller. The resulting controller is strictly proper and of the following form:

$$K(s) = \frac{k(1+sT_1)}{(1+sT_2)(1+sT_4)} \tag{B25}$$

The dynamics of the plant and the zero block can be obtained as follows:

$$y_{new} = y + T_3\dot{y} \tag{B26}$$

Since

$$\dot{y} = C\dot{x} = C(Ax + Bu) \tag{B27}$$

the expression for y_{new} can be expressed as follows:

$$y_{new} = (C + T_3CA)x + T_3CBu \tag{B28}$$

The state space description of the plant with the augmented zero block then becomes:

$$\dot{x} = Ax + Bu \tag{B29}$$

$$y_{new} = (C + T_3CA)x + T_3CBu \tag{B30}$$

Note that if T_3 is chosen to be zero then the plant remains unaffected since the controller K(s) would then be strictly proper.

Appendix C

Determination of the Robust Stability Margin

In this section, we address the problem of determining the robust stability margin of systems described by state space models. We obtain upper bounds on the perturbations that asymptotically stable linear systems can withstand while maintaing stability. The results in this section are used in Section 4.3.2.2 in determining the robust stability margin.

Consider the state equation of an LTI system which can be expressed as follows:

$$\dot{x} = Ax + E(x,t) + Bu \qquad \text{(C1)}$$

where:

$A \in R^{n \times n}$ is the unperturbed state coefficient matrix

$E(x,t) : R^n \rightarrow R^n$ is the nonlinear time-varying perturbation

We define the *structure* of a matrix as the pattern of zero and non-zero elements in the matrix. For instance, the matrix $J = \begin{bmatrix} 0.12 & -1.0 \\ 1.0 & 0 \end{bmatrix}$ will have a *structure* of $\begin{bmatrix} \times & \times \\ \times & 0 \end{bmatrix}$.

It is convenient to distinguish between different types of perturbations as follows:

(a) *Structured Perturbations*: These perturbations are of two types namely, highly structured perturbations and weakly structured perurbations. These are defined as follows:

(a.1) Highly Structured Perturbations:

These include perturbations for which both the structure of the perturbation matrix E and the bounds on each element $E^{i,j}$ is known. This means that we know which elements in the perturbation matrix are affected and we know the upper bound on the value of each component in E. If two perturbation matrices E and $\overline{E}$ have the same perturbation matrix structure as well as the same

bounds on individual elements i.e. *i.e.* $\|E^{ij}\| \leq \gamma^{h}$ and $\|\overline{E}^{ij}\| \leq \gamma^{h}$ where λ^{h} is the upper bound, then E and $\overline{E}$ are said to belong to the same class of highly structured perturbations. Highly structured perturbations define the smallest class of perturbations that we consider.

(a.2) *Weakly Structured Perturbations*

These include perturbations for which the structure of the perturbation is known but only a upper bound on the perturbation matrix E is known. The bounds on the individual elements need not be known.. If two perturbation matrices E and $\overline{E}$ have the same perturbation matrix structure as well as the same matrix bounds *i.e.* $\|E\| \leq \gamma^{w}$ and $\|\overline{E}\| \leq \gamma^{w}$ where λ^{w} is the upper bound, then E and $\overline{E}$ are said to belong to the same class of weakly structured perturbations. Weakly structured perturbations define a broader class of perturbations than highly structured perturbations.

(b) *Unstructured Perturbations*: These include perturbations for which both the structure of the perturbation and the bounds on individual elements are unknown. Only an upper bound on the total perturbation is known. If two perturbation matrices E and E' have the same matrix bounds ($\|E\| \leq \gamma^{u}$ and $\|\overline{E}\| \leq \gamma^{u}$) where γ^{u} is the upper bound, then E and $\overline{E}$ are said to belong to the same class of unstructured perturbations. Unstructured perturbations define the broadest class of perturbations that we consider.

Figure C1 is a diagrammatic representation of a Single Machine Infinite Bus System (SMIB). The system consists of a generator connected to an infinite bus via two parallel transmission lines. The external impedance of the line X_e is an equivalent of an external network connected to the generator. The equivalent of the loads is obtained by modelling the loads as constant impedance loads.

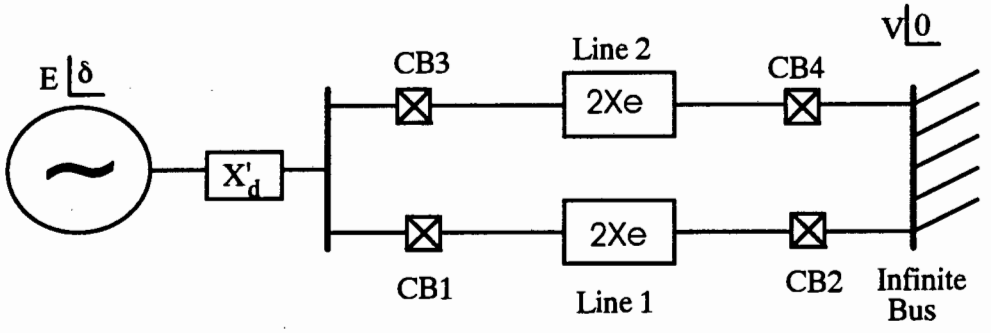

Figure C1: Diagrammatic Representation of a SMIB System

The second order swing equation for the SMIB system can be expressed as follows:

$$M\frac{\partial^2\delta}{\partial t^2} - D\omega = \frac{EV}{X_e + X_d^{'}}\sin(\delta) - P_{mech} \tag{C2}$$

where:

M is the inertia constant of the generator

D is the damping

$X_d^{'}$ is the transient reactance of the generator

By making use of Taylor series expansion,we can express the swing equation around an operating point $[\omega_0 \quad \delta_0]^T$ as follows:

$$\text{Let } F(\omega,\delta) = \begin{bmatrix} f_1 \\ f_2 \end{bmatrix}\begin{bmatrix} \dot{\omega} \\ \dot{\delta} \end{bmatrix} \tag{C3}$$

Then

$$F(\omega_0 + \Delta\omega, \delta_0 + \Delta\delta) - F(\omega_0,\delta_0) = \begin{bmatrix} \frac{\partial f_1}{\partial \omega} & \frac{\partial f_1}{\partial \delta} \\ \frac{\partial f_2}{\partial \omega} & \frac{\partial f_2}{\partial \delta} \end{bmatrix}\begin{bmatrix} \Delta\omega \\ \Delta\delta \end{bmatrix} + \Theta(\omega,\delta) \tag{C4}$$

where:

$\Theta(\omega,\delta)$ are the higher order terms

The linearized state equations equations can be expressed as follows:

$$\begin{bmatrix} \Delta\dot{\omega} \\ \Delta\dot{\delta} \end{bmatrix} = \begin{bmatrix} \frac{D}{M} & \frac{EV}{M(X_e + X_d^{'})}(Cos(\delta_0)) \\ 1 & 0 \end{bmatrix}\begin{bmatrix} \Delta\omega \\ \Delta\delta \end{bmatrix} - \frac{1}{M}P_{mech} \tag{C5}$$

We now consider some of the perturbations that can influence the system in Figure C1.

Assume that we have a line outage on Line 1 (CB1 and CB2 are open), possibly due to a short circuit. The external impedance will now have the value $2X_e$. Thus, the perturbation matrix will have the following structure.

$$E = \begin{bmatrix} 0 & \times \\ 0 & 0 \end{bmatrix} \tag{C6}$$

where × denotes a non-zero element

Now assume that the load of the system is changed. Since X_e is the equivalent impedance of the external system including the loads, the change in load results in a change in X_e. Thus, the structure of the perurbation matrix E will be the same as that given in equation (C6).

Thus, for the system in Figure C1, we can say that a loss of line and a change in load result in the same perturbation matrix structure. Furthermore, since we know the structure of the perturbation due to loss of a line and load changes, we consider such perturbations as structured. In power systems, the loss of a line and changes in load will be structured perturbations since the structure of the perturbation can be readily determined using simulation models. Structured perturbation also include uncertainty in the parameters of the system. For instance, uncertainty in the values of the generator parameter $X_d^{'}$ and M will be considered as structured perturbations.

Note however, that since the structured perturbations are defined in terms of the *structure* of perturbation matrix, it applies specifically to the linearized system of equations.

In the case of unstructured perturbations, we only have knoweldge about an upper bound to the perturbation. Perturbations which result from complex modeling inaccuracies in the power system will be unstructured perturbations. These modelling inaccuracies could be due to:

- Simplification in the model of the system, such as modeling the generator by a second order model, modeling the transmission line by a lumped model and modeling the external system by an impedance and an infinite bus.
- An unknown model of the system, such as in modeling the behaviour of dynamic loads.
- Higher order effects being neglected in the linearization when the state space model is obtained
- The influence of process noise (such as vibrations in a power plant) and sensor noise emanating from measurement devices.

All the above unstructured perturbations influence the SMIB system of Figure C1. We do not however, model these effects in the linearized state space model of the system. We consider these effects as perturbations on the linearized state space model in equation C5. We cannot obtain the exact structure of the perturbation matrix as in the case of structured perturbations. Since these perturbations are regarded as unstructured perturbations, we need to know only an upper bound μ to the perturbation i.e. $\|E(x,t)\| \leq \mu$. This is usually not difficult to estimate. For instance, in order to estimate the upper bound of the error associated with linearization we investigate the higher order terms $\Theta(\omega,\delta)$ in the Taylor series expansion.

$$\Theta = \frac{1}{(2)!}\left(\Delta\omega\frac{\partial}{\partial\omega} + \Delta\delta\frac{\partial}{\partial\delta}\right)^2 F(\omega_0 + \varepsilon\Delta\omega, \delta_0 + \varepsilon\Delta\delta), \qquad 0 < \varepsilon < 1 \qquad \text{(C7)}$$

From equation (C7) we can determine upper bound on the error in the linearization.

In the next section we will develop robustness margins for a decentralized system under both structured and unstructured perturbations.

C1. Robust Stability Margin For Highly Structured Perturbations

Consider the interconnected system described by the following:

$$S \triangleq \{S_i\} \triangleq \begin{Bmatrix} \dot{x}_i = (A_{ii}^0 + E_{ii}(t))x_i + B_i u_i + \sum_{\substack{j=1 \\ j \neq i}}^{m} (A_{ij}^0 + E_{ij}(t))x_j \\ y_i = C_i x + D_i u_i \end{Bmatrix}$$

In this section, we determine the robust stability margin for the uncoupled subsystems under the influence of structured perturbations:

For calculating the robust stability margin for subsystem *i*, we require information about the uncoupled subsystems A_{ii}^0 perturbations $E_{ii}(t)$ only. By ignoring the interactions $(A_{ij}^0 = 0)$ and the interaction perturbations $(E_{ij} = 0)$ in system S, we obtain *system V* which is defined as follows:

$$V = \{V_i\} = \{\dot{x}_i\} = \begin{Bmatrix} (A_{ii}^0 + E_{ii}(t))x_i(t) \\ y_i = C_i x + D_i u_i \end{Bmatrix} \tag{C8}$$

System V describes a fictitious power system where the subsystems are disconnected from each other i.e. there is no coupling between the generator subsystems $(A_{ij}^0 = 0)$. The power system is subjected to structured perturbations $(E_{ii} \neq 0)$.

For determining the robust stability margin, we assume A_{ii}^0 to be asymptotically stable. Since the perturbations are highly structured, we assume that $E_{ii}(t) = E_{ii}$ is a matrix of constants and the elements of E_{ii} are bounded as follows:

$$E_{ii}^{k,l} \leq \max_{k,l} \left| E_{ii}^{k,l} \right| \tag{C9}$$

where (k,l) are matrix indices

We define the following:

$$\varepsilon_{ii} = \max_{k,l} \left| E_{ii}^{k,l} \right| \tag{C10}$$

The value of ε_{ii} is the maximum element of the perturbation matrix E_{ii}. We use ε_{ii} as a normalization constant to define matrix U_{ii} as follows:

$$U_{ii}^{k,l} = \frac{\left|E_{ii}^{k,l}\right|}{\varepsilon_{ii}} \tag{C11}$$

where *(k,l)* are matrix indices

We consider system V in terms of the normalized matrix U_{ii} as follows:

$$V = \{V_i\} = \{\dot{x}_i\} = \begin{Bmatrix} (A_{ii}^0 + \varepsilon_{ii} U_{ii}) x_i(t) \\ y_i = C_i x + D_i u_i \end{Bmatrix} \tag{C12}$$

We can state the following lemma:

Lemma C1: The system described by equation (C8) is stable i.e. $\mathrm{Re}(\lambda(A_{ii}^0 + E_{ii})) < 0$ if

$$\varepsilon_{ii} \le \sigma_{\max}(P_{ii} U_{ii}) = \alpha_{ii}$$

where:

P_{ii} satisfies the following steady state Lyapunov equation:

$$(A_{ii}^0)^T P_{ii} + P_{ii} (A_{ii}^0)^T + 2Q_{ii} = 0 \tag{C13}$$

$\sigma_{\max}$ denotes the maximum singular value

Q_{ii} is a positive definite matrix

Proof: We choose a Lyapunov function for subsystem V_i as:

$$V_i(x) = x_i^T P_{ii} x_i \tag{C14}$$

The system is stable where $V_i > 0$ and $\dot{V}_i \le 0$ i.e.:

(a) $V_i(x) = x_i^T P_{ii} x_i$ is positive for all $x \ne 0$ since P_{ii} is positive definite (C15)

(b) $\dot{V}_i(x) = \dot{x}_i^T P_{ii} x_i + x_i^T P_{ii} \dot{x}_i \le 0$ (C16)

Substituting equation (C12) into (C16) we obtain the following:

$$\dot{V}_i(x) = \left((A_{ii}^0 + \varepsilon_{ii} U_{ii}) x_i\right)^T P_{ii} x_i + x_i^T P_{ii} (A_{ii}^0 + \varepsilon_{ii} U_{ii}) x_i \tag{C17}$$

$$\dot{V}_i(x) = x_i^T (A_{ii}^0)^T P_{ii} x_i + x^T \varepsilon_{ii} U_{ii}^T P_{ii} x_i + x_i^T P_{ii} (A_{ii}^0) x_i + x_i^T P_{ii} \varepsilon_{ii} U_{ii} x_i \tag{C18}$$

$$\dot{V}_i(x) = x_i^T \left((A_{ii}^0)^T P_{ii} + P_{ii} A_{ii}^0\right) x_i + x_i^T \left(\varepsilon_{ii} U_{ii}^T P_{ii} + P_{ii} \varepsilon_{ii} U_{ii}\right) x_i \tag{C19}$$

Substituting equation (C13) into equation (C19) gives the following:

$$\dot{V}_i(x) = x_i^T(-2Q_{ii})x_i + \varepsilon_{ii}x_i^T(U_{ii}^T P_{ii} + P_{ii}U_{ii})x_i \tag{C20}$$

For stability we need $\dot{V}_i(x) \leq 0$ i.e.:

$$x_i^T \varepsilon_{ii}(U_{ii}^T P_{ii} + P_{ii}U_{ii})x_i \leq x_i^T(2Q_{ii})x_i \tag{C21}$$

Consider the following inequality:

$$\varepsilon_{ii} \leq \frac{\sigma_{\min}(Q_{ii})}{\sigma_{\max}(P_{ii}U_{ii})} \tag{C22}$$

We wish to show that if the inequality in (C22) is satisfied, then the inequality in (C21) is satsified.

From (C22), we know that:

$$\sigma_{\max}(2\varepsilon_{ii}P_{ii}U_{ii}) \leq \sigma_{\min}(2Q_{ii}) \tag{C23}$$

Since we know that the singular values of a matrix and its transpose are equal we can rewrite equation (C23) as follows:

$$\sigma_{\max}(\varepsilon_{ii}P_{ii}U_{ii} + \varepsilon_{ii}(P_{ii}U_{ii})^T) \leq \sigma_{\min}(2Q_{ii}) \tag{C24}$$

From Rayleigh's principle, we know that:

$$\sigma_{\max}(\varepsilon_{ii}P_{ii}U_{ii} + \varepsilon_{ii}U_{ii}^T P_{ii}^T)x_i^T x_i \geq x_i^T(\varepsilon_{ii}P_{ii}U_{ii} + \varepsilon_{ii}U_{ii}^T P_{ii}^T)x_i \tag{C25}$$

$$\sigma_{\min}(2Q_{ii})x_i^T x_i \leq x_i^T(2Q_{ii})x_i \tag{C26}$$

Substituting equations (C25) and (C26) into equation (C24) gives the following:

$$x_i^T(\varepsilon_{ii}P_{ii}U_{ii} + \varepsilon U_{ii}^T P_{ii}^T)x_i \leq x_i^T(2Q_{ii})x_i \tag{C27}$$

Since $P_{ii} = P_{ii}^T$, we can rewrite (C27) as follows:

$$x_i^T \varepsilon_{ii}(U_{ii}^T P_{ii} + P_{ii}U_{ii})x_i \leq x_i^T(2Q_{ii})x_i$$

which is the same as the inequality in (C21).

Therefore the system described by (C12) is stable if the following condition holds:

$$\varepsilon_{ii} \leq \frac{\sigma_{\min}(Q_i)}{\sigma_{\max}(P_i U_{ii})} \tag{C29}$$

The matrix Q_i can be selected to be any positive definite matrix. If we choose $Q_i = I$, then $\sigma_{\min}(Q_i) = 1$. Therefore, (C29) becomes:

$$\varepsilon_{ii} \leq \frac{1}{\sigma_{\max}(P_i U_{ii})} \tag{C30}$$

This means that the system described by equation (C12) is stable if the

$$\varepsilon_{ii} \leq \frac{1}{\sigma_{\max}(P_{ii} U_{ii})} = \alpha_{ii} \tag{C31}$$

The value α_{ii} is a measure of the amount of perturbation E_{ii} that the subsystem i can be subjected to without becoming unstable. A large α_{ii} indicates that the subsystem has a large robust stability margin (it is difficult to destabilize the system), whereas a small α_{ii} indicates that the system has a small robust stability margin (it is easy to destabilize the system).

There are two problems associated with the use of α_{ii} as a robust stability margin.

Firstly, it can be seen from equation (C11), that the robust stability margin α_{ii} is dependent on the perturbation matrix of E_{ii} of subsystem i. This means that we need to know E_{ii} exactly in order to calculate α_{ii}. For a different perturbation matrix $E_{ii}^{'} \neq E_{ii}$, the robust stability margin $\alpha_{ii}^{'}$ will be different from α_{ii}. Thus α_{ii}, as defined in equation (C11), is only a good measure of the robust stability margin for the specific perturbation E_{ii} i.e. for highly structured perturbations.

The second problem in using α_{ii} is that the perturbation matrix applies only to a very narrow class of perturbations. In complex dynamical systems such as power systems, the exact values of the perturbation matrix is usually unknown.

In the next section, develop a robust stability measure for a more general class of perturbations, namely weakly structured perturbations.

C2. Calculating the Robust Stability Margin for Weakly Structured Perturbations

In order to develop a robust stability margin for a more general class of perturbations, we can modify the definition of matrix U_{ii} in equation (C11). Instead of making use of the actual values of E_{ii} in calculating α_i, we define the matrix W_{ii} as follows:

$$W_{ii}^{k,l} = \begin{cases} 0 & \text{if} \quad U_{ii}^{k,l} \le e_{tol} \\ 1 & \text{if} \quad U_{ii}^{k,l} > e_{tol} \end{cases} \tag{C32}$$

where e_{tol} is a tolerance value.

Thus W_{ii} is a boolean version of matrix U_{ii}. Matrix W_{ii} considers the family of perturbations which have a significant effect on the states which correspond to the ones in W_{ii}. By using W_{ii} instead of U_{ii}, the robust stability margin for weakly structured perturbations α_{ii}^{w} becomes:

$$\alpha_{ii}^{w} = \frac{1}{\sigma_{\max}(W_{ii}P_{ii})} \tag{C33}$$

The robust stability margin obtained when using W_{ii} is more conservative than the robust stability margin obtained when using U_{ii} i.e. $\alpha_{ii}^{W} \le \alpha_{ii}^{U}$. However, α_{i}^{W} represents the robust stability margin for a more general family of perturbations than α_{i}^{U} .In order to calculate the robust stability margin for the most general class of perturbations, we let W_{ii} equal a matrix of ones, i.e.:

$$W_{ii} = \begin{bmatrix} 1 & \cdots & 1 \\ \vdots & \ddots & \vdots \\ 1 & \cdots & 1 \end{bmatrix} \tag{C34}$$

C3. Calculating the Robust Stability Margin for Unstructured Perturbations

In this section we present a method of determining the robust stability margin for perturbation in which only an upper bound on the perturbation is known i.e. unstructured perturbations.

We consider the system described by the following:

$$V = \{V_i\} = \{\dot{x}_i\} = \begin{Bmatrix} (A_{ii}^0 x_i + E_{ii}(x,t) \\ y_i = C_i x + D_i u_i \end{Bmatrix} \quad \text{(C35)}$$

Note that the perturbation $E_{ii}(t)$ can be a nonlinear time-varying function.

Lemma C2: The system described by equation (C35) is stable if

$$\|E_{ii}(t)\|_2 \leq \frac{\sigma_{\min}(Q_{ii})}{\sigma_{\max}(P_{ii})} = \alpha_{ii}$$

where:

P_{ii} satisfies the following steady state Lyapunov equation:

$$(A_{ii}^0)^T P_{ii} + P_{ii}(A_{ii}^0)^T + 2Q_{ii} = 0 \quad \text{(C36)}$$

$\sigma_{\max}$ denotes the maximum singular value

Q_{ii} is a positive definite matrix

We choose a Lyapunov function for subsystem V_i as:

$$V_i(x) = x_i^T P_i x_i$$

The system is stable where $V_i > 0$ and $\dot{V}_i \leq 0$ i.e.:

(a) $V_i(x) = x_{ii}^T P_{ii} x_i$ is positive for all $x \neq 0$ since P is positive definite

(b) $\dot{V}_i(x) = \dot{x}_i^T P_{ii} x_i + x_i^T P_{ii} \dot{x}_i \leq 0$ (C37)

Substituting equation (C35) into (C37) we obtain the following:

$$\dot{V}_i(x) = \left((A_{ii}^0 x_i + E_{ii}(x_i,t))\right)^T P_{ii} x_i + x_i^T P_{ii}(A_{ii}^0 x_i + E_{ii}(x_i,t))$$

$$\dot{V}_i(x) = x_i^T (A_{ii}^0)^T P_{ii} x_i + E_{ii}^T(x_i,t) P_{ii} x_i + x_i^T P_{ii}(A_{ii}^0) x_i + x_i^T P_{ii} E_{ii}(x_i,t) \quad \text{(C38)}$$

$$\dot{V}_i(x) = x_i^T \left((A_{ii}^0)^T P_i + P_i A_{ii}^0\right) x_i + E_{ii}^T(x_i,t) P_{ii} x_i + x_i^T P_{ii} E_{ii}(x_i,t)) \quad \text{(C39)}$$

Substituting equation (C36) into equation (C39) gives the following:

$$\dot{V}_i(x) = x_i^T(-2Q_i)x_i + E_{ii}^T(x_i,t)P_{ii}x_i + x_i^T P_{ii}E_{ii}(x_i,t) \tag{C40}$$

For stability we need $\dot{V}(x) \le 0$ i.e.:

$$E_{ii}^T(x_i,t)P_{ii}x_i + x_i^T P_{ii}E_{ii}(x_i,t) \le x_i^T(2Q_i)x_i \tag{C41}$$

Consider the following inequality:

$$\|E_{ii}(x_i,t)\|_2 \le \frac{\sigma_{\min}(Q_{ii})}{\sigma_{\max}(P_{ii})} \tag{C42}$$

We wish to show that if the inequality in (C42) is satisfied, then the inequality in (C41) is also satisfied. From (C42) we know that:

$$2\|E_{ii}(x_i,t)\|_2 \sigma_{\max}(P_{ii})x_i^T x_i \le \sigma_{\min}(2Q_{ii})x_i^T x_i \tag{C43}$$

We know that:

$$2\|E_{ii}(x_i,t)x_i\sigma_{\max}(P_{ii})\| \le \|E_{ii}(x_i,t)\|\sigma_{\max}(P_{ii})x_i^T x_i \tag{C44}$$

Substituting (C44) into (C43) we obtain the following:

$$2\|E_{ii}(x_i,t)x_i\sigma_{\max}(P_{ii})\| \le \sigma_{\min}(Q_{ii})x_i^T x_i \tag{C45}$$

We also know that:

$$E_{ii}^T(x_i,t)P_{ii}x_i + (E^T(x_i,t)P_{ii}x_i)^T \le 2\|E_{ii}(x_i,t)x_i\sigma_{\max}(P_{ii})\| \tag{C46}$$

Substituting (C46) into (C45), we obtain the following:

$$E_{ii}^T(x_i,t)P_{ii}x_i + (E^T(x_i,t)P_{ii}x_i)^T \le \sigma_{\min}(Q_{ii})x_i^T x_i \tag{C47}$$

From Rayleigh's principle, we know that:

$$x_i^T Q_{ii} x_i \ge \sigma_{\min}(Q_{ii})x_i^T x_i \tag{C48}$$

Substituting (C48) into (C47) we obtain the following:

$$E_{ii}^T(x_i,t)(P_{ii})x_i + x_i^T(P_{ii})(E_{ii}(x_i,t)) \le x^T(2Q_{ii})x_i$$

which is the inequality in (C41).

The matrix Q_i can be selected to be any postive definite matrix. If we choose $Q_i = I$, then $\sigma_{\min}(Q_i) = 1$. Therefore, the system given by (C35) is stable if the following condition is met:

$$\|E_{ii}(t)\|_2 \le \frac{1}{\sigma_{\max}(P_{ii})} \tag{C49}$$

In the next section we present a procedure for calculating the perturbation matrix by using off-line Power System Application Software (PAS).

C4. Obtaining the Perturbation Matrix

In this section we present the procedure for determining the perturbation matrix E_{ii} for structured perturbations. This procedure is illustrated in Figure C2:

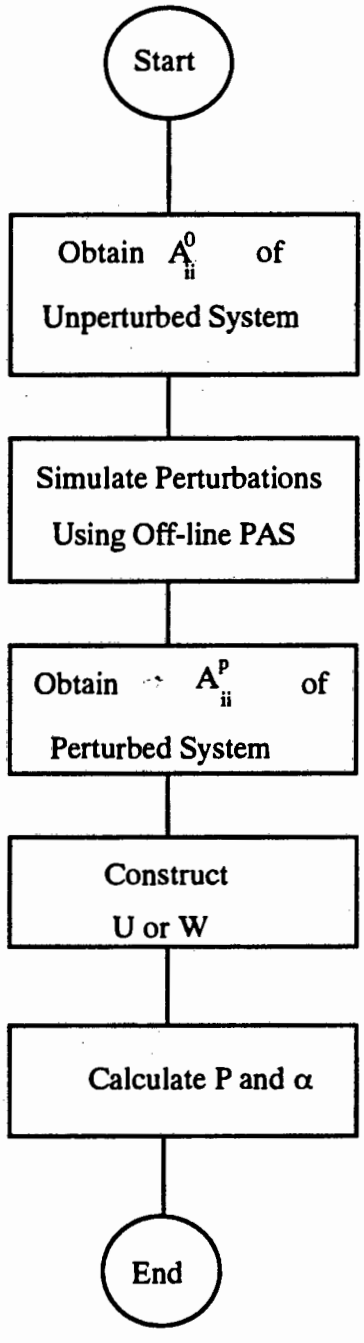

Figure C2: Procedure for Calculating the Robust Stability Margin for Perturbations in Power Systems.

First, the state coefficient matrix (A_{ii}^{0}) of the unperturbed and uncoupled subsystem is obtained. Thereafter, the perturbation is simulated off-line using existing Power Application Software (PAS). This perturbation can be in the form of a loss of line, loss of generation, increase in load, etc.. From the (PAS) simulation, the state coefficient matrix of the perturbed plant (A_{ii}^{P}) can be obtained. The perturbation matrix E_{ii} can then be calculated using $E_{ii} = A_{ii}^{P} - A_{ii}^{0}$. Once matrix E_{ii} has been calculated, the normalized matrix U_{ii} can be constructed using equation (C11). Thereafter, matrix P_i and the robust stability index is calculated.

Example C1

In this example, we apply the procedure for obtaining the perturbation matrix for a power system under perturbations of load changes. Figure C2 is a diagrammatic representation of a SMIB system. We make use of the *Power System Simulator for Engineers (PSS/e)* in order to obatin a state space model of the system in Figure C2..We model Generator 1 with a sixth order model and the excitation system with a second order model.

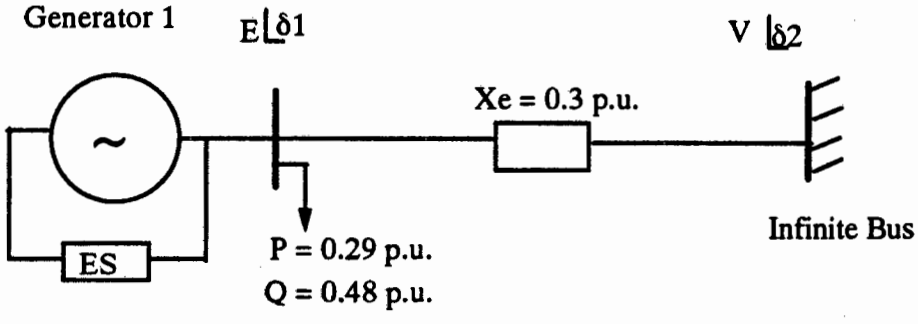

Figure C3: Diagrammatic Representation of SMIB System

The state coefficient matrix A_1 for the system is given by the following:

A_1 =

1.0e+003 *

[-0.0036	0.0000	0.0031	-0.0001	0	0.0001	0	0.0002
0.0002	-0.0013	-0.0007	0.0001	0	0.0000	0	0
0.0199	0.0000	-0.0223	-0.0004	0	-0.0014	0	0
-0.0004	0.0078	0.0014	-0.0149	0	0.0043	0	0
0.0000	0.0000	-0.0002	0.0001	-0.0001	-0.0001	0	0
0	0	0	0	0.3770	0	0	0
0.0000	0.0000	-0.0001	0.0000	0	0.0000	-0.0001	0
0.0509	0.0031	-0.1674	-0.0564	0	0.0161	2.0000	-0.0200]

We perturb the system by increasing the load at generator 1 to $P = 0.36$ p.u., $Q = 0.57$ p.u. The state space model of the perturbed system is then obtained from PSS/E The state coefficient matrix of the perturbed system A_2 is given by:

A_2 =

1.0e+003 *

[-0.0036	0.0000	0.0031	-0.0001	0	0.0001	0	0.0002
0.0002	-0.0013	-0.0006	0.0001	0	0.0000	0	0
0.0199	0.0000	-0.0224	-0.0004	0	-0.0014	0	0
-0.0004	0.0078	0.0015	-0.0150	0	0.0044	0	0
0.0000	0.0000	-0.0001	0.0001	-0.0001	-0.0001	0	0
0	0	0	0	0.3770	0	0	0
0.0000	0.0000	-0.0001	0.0000	0	0.0000	-0.0001	0
0.0511	0.0029	0.1680	0.0530	0	0.0150	2.0000	-0.0200]

The perturbation matrix $E = A_1 - A_2$ is given by the following;

E =

[-0.0081	0.0002	0.0269	-0.0036	0	0.0044	0	0
0.0034	-0.0004	-0.0116	0.0061	0	0.0003	0	0
-0.0140	-0.0021	0.0480	0.0192	0	-0.0754	0	0
0.0232	-0.0097	-0.0770	0.1040	0	-0.0595	0	0
0.0003	0.0001	-0.0010	-0.0008	0	0.0002	0	0
0	0	0	0	0	0	0	0
-0.0001	0.0001	0.0002	-0.0016	0	0.0005	0	0
-0.1700	0.2354	0.5500	-3.4590	0	1.1040	0	0]

The maximum element in matrix $|E|$ is 3.459. Thus, the normalized perturbation matrix U is given by:

U =

[0.0023	0.0001	0.0078	0.0010	0	0.0013	0	0
0.0010	0.0001	0.0033	0.0017	0	0.0001	0	0
0.0040	0.0006	0.0139	0.0055	0	0.0218	0	0
0.0067	0.0028	0.0223	0.0301	0	0.0172	0	0
0.0001	0.0000	0.0003	0.0002	0	0.0000	0	0
0	0	0	0	0	0	0	0
0.0000	0.0000	0.0001	0.0005	0	0.0001	0	0
0.0491	0.0681	0.1590	1.0000	0	0.3192	0	0]

If we choose a tolerance value of $\varepsilon_{tol} = 0.005$, we obtain a perturbation matrix for a more general class of perturbations.

W =

[1	0	1	0	0	0	0	0
0	0	1	1	0	0	0	0
1	0	1	1	0	1	0	0
1	1	1	1	0	1	0	0
0	0	0	0	0	0	0	0
0	0	0	0	0	0	0	0
0	0	0	0	0	0	0	0
1	1	1	1	0	1	0	0]

C5. Calculating the Structured Robust Stability Margin Including Interaction Perturbations

In this section we obtain the robust stability margin for structured perturbator in a decentralized system. For calculating the robust stability margin for subsystem i, we require information about the uncoupled subsystems A_{ii}^0 and the perturbations $E_{ii}(t)$ and $E_{ij}(t)$. By ignoring only the interactions $(A_{ij}^0 = 0)$ in system S, we obtain *system T* which is defined as follows:

$$T = \{T_i\} = \{\dot{x}_i\} = \begin{Bmatrix} (A_{ii}^0 + E_{ii}(t))x_i(t) \\ y_i = C_i x + D_i u_i \end{Bmatrix} \qquad \text{(C50)}$$

System T describes a fictitious power system where the subsystems are disconnected from each other. The power system is subjected to time-varying perturbations $(E_{ii} \neq 0, E_{ij} \neq 0)$.

System T can be rewritten as follows:

$$T \overset{\Delta}{=} \{T\} \overset{\Delta}{=} \{\dot{x}\} = \{A_{ii} + E'_{ii} + E'_{ij}\}x \qquad \text{(C51)}$$

where:

$$E'_{ij} = \begin{bmatrix} 0 & \dots & 0 & \dots & 0 \\ \vdots & & \vdots & & \vdots \\ E_{i1} & \cdot & 0 & \cdot & E_{im} \\ \vdots & & \vdots & & \vdots \\ 0 & \dots & 0 & \dots & 0 \end{bmatrix}_{n \times n}$$

$$E'_{ii} = \begin{bmatrix} 0 & \dots & 0 & \dots & 0 \\ \vdots & & \vdots & & \vdots \\ 0 & \cdot & E_{ii} & \cdot & 0 \\ \vdots & & \vdots & & \vdots \\ 0 & \dots & 0 & \dots & 0 \end{bmatrix}_{n \times n}$$

$$A_{ii} = \begin{bmatrix} 0 & \dots & 0 & \dots & 0 \\ \vdots & & \vdots & & \vdots \\ 0 & \cdot & A^0_{ii} & \cdot & 0 \\ \vdots & & \vdots & & \vdots \\ 0 & \dots & 0 & \dots & 0 \end{bmatrix}_{n \times n}$$

$$x = \begin{bmatrix} x_i & \dots & x_m \end{bmatrix}$$

Equation (C51) can be rewritten as follows:

$$V \overset{\Delta}{=} \{V\} \overset{\Delta}{=} \{\dot{x}\} = \{A_{ii} + E_i\}x \qquad \text{(C52)}$$

where:

$$E_i = \begin{bmatrix} 0 & \dots & 0 \\ E_{i1} & \dots & E_{ii} & \dots & E_{im} \\ 0 & \dots & 0 \end{bmatrix}$$

For determining the robust stability margin, we assume A_{ii} to be stable. We further assume that the perturbation matrices E_{ii} and E_{ij} are bounded i.e:

$$E_i^{k,l} \leq \left| E_i^{k,l} \right|_{\max} \qquad \text{(C53)}$$

We define the following:

$$\varepsilon_i = \max_{k,l} \left| E_i^{k,l} \right| \tag{C54}$$

The value of ε_i is the maximum element of the perturbation matrix E_i. We use ε_i as a normalization constant to define matrix $U_i^{k,l}$ as follows:

$$U_i^{k,l} = \frac{\left| E_i^{k,l} \right|}{\varepsilon_i} \tag{C55}$$

where *(k,l)* are matrix indices

We define system T in terms of the normalized matrix U_i as follows:

$$T = \{T_i\} = \{\dot{x}_i\} = \begin{Bmatrix} (A_{ii}^0 + \varepsilon_i U_i) x_i(t) \\ y_i = C_i x + D_i u_i \end{Bmatrix} \tag{C56}$$

We can state the following lemma:

Lemma C3: The system described by equation (C56) is stable i.e. $\mathrm{Re}(\lambda(A_{ii} + E_i)) < 0$ if

$$\varepsilon_i \le \frac{\sigma_{\min}(Q_{ii})}{\sigma_{\max}(P_{ii})\sigma_{\max}(U_i)} = \alpha_i$$

where

P_{ii} satisfies the steady state Lyapunov equation $(A_{ii})^T P_{ii} + P_{ii}(A_{ii})^T + 2Q_{ii} = 0$

$\sigma_{\max}$ denotes the maximum singular value

Q_{ii} is a positive definite matrix

Proof:

Since A_{ii}^o is asymptotically stable, it satisfies the following steady state Lyapunov equation:

$$(A_{ii}^0)P_{ii} + P_{ii}(A_{ii}^0)^T = -2Q_{ii} \tag{C57}$$

The solution to equation (C57), P_{ii}, is a symmetric, positive semi-definite matrix i.e. $P_{ii}^T = P_{ii}$ and $x_i^T P_{ii} x_i > 0$. Matrix Q_{ii} is positive definite i.e. $x_i^T Q_{ii} x > 0$.

We construct two matrices P_i and Q_i as follows:

$$P_i = \begin{bmatrix} 0 & \cdots & 0 \\ \vdots & [P_{ii}] & \vdots \\ 0 & \cdots & 0 \end{bmatrix}_{n \times n} \tag{C58}$$

$$Q_i = \begin{bmatrix} 0 & \cdots & 0 \\ \vdots & [Q_{ii}] & \vdots \\ 0 & \cdots & 0 \end{bmatrix}_{n \times n} \tag{C59}$$

Matrix P_i is symmetric, positive semi-definite and satisfies the following Lyapunov equation:

$$A_{ii}^T P_i + P_i A_{ii} = -2Q_i \tag{C60}$$

Matrix Q_i is a positive *semi-definite* matrix

We choose a Lyapunov function for subsystem V_i as:

$$V_i(x) = x_i^T P_i x_i \tag{C61}$$

The system is stable where $V_i > 0$ and $\dot{V}_i \leq 0$ i.e.:

(a) $V_i(x) = x_i^T P_i x_i$ is positive for all $x \neq 0$ since P_i is positive semi-definite (C62)

(b) $\dot{V}_i(x) = \dot{x}_i^T P_i x_i + x_i^T P_i \dot{x}_i \leq 0$ (C63)

Substituting equation (C56) into (C63) we obtain the following:

$$\dot{V}_i(x) = \left((A_{ii}^0 + \varepsilon_i U_i)x_i\right)^T P_i x_i + x_i^T P_i (A_{ii}^0 + \varepsilon_i U_i)x_i \tag{C64}$$

$$\dot{V}_i(x) = x_i^T (A_{ii}^0)^T P_i x_i + x^T \varepsilon_i U_i^T P_i x_i + x_i^T P_i (A_{ii}^0)x_i + x_i^T P_i \varepsilon_i U_i x_i \tag{C65}$$

$$\dot{V}_i(x) = x_i^T \left((A_{ii}^0)^T P_i + P_i A_{ii}^0\right)x_i + x_i^T \left(\varepsilon_i U_i^T P_i + P_i \varepsilon_i U_i\right)x_i \tag{C66}$$

Substituting equation (C60) into equation (C66) gives the following:

$$\dot{V}_i(x) = x_i^T (-2Q_i)x_i + \varepsilon_i x_i^T (U_i^T P_i + P_i U_i)x_i \tag{C67}$$

For stability we need $\dot{V}_i(x) \leq 0$ i.e.:

$$x_i^T \varepsilon_i (U_i^T P_i + P_i U_i)x_i \leq x_i^T (2Q_i)x_i \tag{C68}$$

Consider the following inequality:

$$\varepsilon_i \le \frac{\sigma_{\min}(Q_{ii})}{\sigma_{\max}(P_{ii})\sigma_{\max}(U_i)} \tag{C69}$$

We wish to show that if the inequality in (C69) is satisfied, then the inequality in (C68) is satsified.

From (C69), we know that:

$$\sigma_{\max}(2\varepsilon_i P_{ii})\sigma_{\max}(U_i) \le \sigma_{\min}(2Q_{ii}) \tag{C70}$$

From the definition of P_i and Q_i in (C58), we know that:

$$\sigma_{\max}(2\varepsilon_i P_{ii}) = \sigma_{\max}(2\varepsilon_i P_i) \tag{C71}$$

Furthermore we know that:

$$\sigma_{\max}(2\varepsilon_i P_i)\sigma_{\max}(U_i) \ge \sigma_{\max}(2\varepsilon_i P_i U_i) \tag{C72}$$

Substituting (C71) and (C72) into (C70) we get the following:

$$\sigma_{\max}(2\varepsilon_i P_i U_i) \le \sigma_{\min}(2Q_i) \tag{C73}$$

Since we know that the singular values of a matrix and its transpose are equal we can rewrite equation (C73) as follows:

$$\sigma_{\max}(\varepsilon_i P_i U_i + \varepsilon_i (P_i U_i)^T) \le \sigma_{\min}(2Q_i) \tag{C74}$$

From Rayleigh's principle, we know that:

$$\sigma_{\max}(\varepsilon_i P_i U_i + \varepsilon_i U_i^T P_i^T) x_i^T x_i \ge x_i^T (\varepsilon_i P_i U_i + \varepsilon_i U_i^T P_i^T) x_i \tag{C75}$$

$$\sigma_{\min}(2Q_i) x_i^T x_i \le x_i^T (2Q_i) x_i \tag{C76}$$

Substituting equations (C75) and (C76) into equation (C74) gives the following:

$$x_i^T (\varepsilon_i P_i U_i + \varepsilon U_i^T P_i^T) x_i \le x_i^T (2Q_i) x_i \tag{C77}$$

Since $P_i = P_i^T$, we can rewrite (C77) as follows:

$$x_i^T \varepsilon_i (U_i^T P_i + P_i U_i) x_i \le x_i^T (2Q_i) x_i \tag{C78}$$

which is the same as the inequality in (C68).

Therefore the system described by (C56) is stable if the following condition holds:

$$\varepsilon_i \le \frac{\sigma_{\min}(Q_{ii})}{\sigma_{\max}(P_{ii})\sigma_{\max}(U_i)} = \alpha_i \tag{C79}$$

The matrix Q_{ii} can be selected to be any positive definite matrix. If we choose $Q_{ii} = I$, then $\sigma_{\min}(Q_{ii}) = 1$. Therefore, (C79) becomes:

$$\varepsilon_i \leq \frac{1}{\sigma_{\max}(P_{ii})\sigma_{\max}(U_i)} \tag{C80}$$

Appendix D

Global Stability of the Interconnected System Under the Influence of Structured Perturbations

In this section, we present a method to guarantee global stability of the interconnected system. The global stability is guaranteed for a family of perturbations. The results of this section are used in Section 3.4.3 in developing a hierarchical control strategy.

When we investigate the global stability of the interconnected system, we consider information about the uncoupled subsystems A_{ii}^0, the interactions between subsystem A_{ij}^0, as well as the perturbations $E_{ii}(t)$ and $E_{ij}(t)$. Thus we consider system S which is expressed as follows:

$$S = \{S_i\} = \{\dot{x}_i\} = \begin{Bmatrix} (A_{ii}^0 + E_{ii}(t))x_i(t) + \sum_{\substack{j=1 \\ j \neq i}}^{m} (A_{ij}^0 + E_{ij}(t))x_j \\ y_i = C_i x + D_i u_i \end{Bmatrix} \qquad \text{(D1)}$$

where:

$x_i \in R^{n_i}$ and $u_i \in R$ are the state and input vectors respectively corresponding to subsystem S_i

$x = [x_1 \quad \dots \quad x_m]$ is the state vector of S

$A_{ii}^0 \in R^{n_i \times n_i}$ is the square diagonal block i of the nominal plant A matrix relating $\dot{x}_i$ to x_i

$A_{ij}^0 \in R^{n_j \times n_j}$ is the off-diagonal interaction block *(i,j)* of the nominal plant A matrix relating $\dot{x}_i$ to x_j

$E_{ii}(t) \in R^{n_i \times n_i}$ is the linear time-varying perturbation matrix function relating $\dot{x}_i$ to x_i

$E_{ij}(t) \in R^{n_j \times n_j}$ is the linear time-varying interaction perturbation matrix function relating $\dot{x}_i$ to x_i

$B_i \in R^{n_i \times 1}$ is the constant input coefficient vector relating $\dot{x}_i$ to u_i

$C_i \in R^{p_i \times n_i}$ is the constant vector relating the output y_i to the state vector x

$D_i \in R$ is the direct feedthrough term relating the output y_i to the input u_i

n_i is the number of states in vector x_i and $\sum_{i=1}^{m} n_i = n$

System S can be rewritten as follows:

$$S \overset{\Delta}{=} \{S\} \overset{\Delta}{=} \{\dot{x}\} = \left\{A_{ii} + E'_{ii} + E'_{ij} + A_{ij}\right\}x \qquad \text{(D2)}$$

where:

$$A_{ii} = \begin{bmatrix} 0 & . & 0 & . & 0 \\ . & . & . & . & . \\ 0 & . & A_{ii} & . & 0 \\ . & . & . & . & . \\ 0 & . & 0 & . & 0 \end{bmatrix}$$

$$A_{ij} = \begin{bmatrix} 0 & \dots & 0 & \dots & 0 \\ . & . & . & . & . \\ A^0_{i1} & \dots & 0 & \dots & A^0_{im} \\ . & . & . & . & . \\ 0 & \dots & 0 & \dots & 0 \end{bmatrix}_{n \times n}$$

$$E'_{ij} = \begin{bmatrix} 0 & \dots & 0 & \dots & 0 \\ . & . & . & . & . \\ E_{i1} & . & 0 & . & E_{im} \\ . & . & . & . & . \\ 0 & \dots & 0 & \dots & 0 \end{bmatrix}_{n \times n}$$

$$E'_{ii} = \begin{bmatrix} 0 & \dots & 0 & \dots & 0 \\ . & . & . & . & . \\ 0 & . & E_{ii} & . & 0 \\ . & . & . & . & . \\ 0 & \dots & 0 & \dots & 0 \end{bmatrix}_{n \times n}$$

$$x = \begin{bmatrix} x_i & \dots & x_m \end{bmatrix}$$

We define matrix A^E_{ij}, which constains the interaction and perturbation terms for subsystem i, as follows:

$$A^E_{ij} = \begin{bmatrix} 0 & \dots & 0 & & 0 \\ \vdots & & \vdots & & \vdots \\ A^0_{i1} + E_{i1} & \dots & E_{ii} & \dots & A^0_{im} + E_{im} \\ \vdots & & \vdots & & \vdots \\ 0 & \dots & 0 & \dots & 0 \end{bmatrix} \qquad \text{(D3)}$$

Equation (D2) can be rewritten as follows:

$$S \triangleq \{S\} \triangleq \{\dot{x}\} = \left\{A_{ii} + A_{ij}^{E}\right\}x \tag{D4}$$

We consider the related system which has the following state space description:

$$S \triangleq \{S\} \triangleq \{\dot{x}\} = \left\{A_{ii} + A_{ij}^{U}\right\}x \tag{D5}$$

$$A_{ij}^{U} = A_{ij}^{0} + \varepsilon_{ij}U_{ij} + \varepsilon_{ii}U_{ii} = \begin{bmatrix} 0 & \cdots & 0 & & 0 \\ \vdots & & \vdots & & \vdots \\ A_{i1}^{0} + \varepsilon_{i1}U_{i1} & \cdots & \varepsilon_{ii}U_{ii} & \cdots & A_{im}^{0} + \varepsilon_{im}U_{im} \\ \vdots & & \vdots & & \vdots \\ 0 & \cdots & 0 & \cdots & 0 \end{bmatrix} \tag{D6}$$

where:

$$U_{ii}^{k,l} = \frac{\left|E_{ii}^{k,l}\right|}{\varepsilon_{ii}}$$

$$U_{ij}^{k,l} = \frac{\left|E_{ij}^{k,l}\right|}{\varepsilon_{i}}$$

$$\varepsilon_{ii} = \max_{k,l}\left|E_{ii}^{k,l}\right|$$

$$\varepsilon_{ij} = \max_{k,l}\left|E_{ij}^{k,l}\right|$$

k,l are matrix indices.

Assume that the uncoupled and unperturbed subsystems are asymptotically stable i.e. $\mathrm{Re}(\lambda_k(A_{ii}^{0})) < 0, \quad k = 1,\ldots,n$ for all k. If $\mathrm{Re}(\lambda_k(A_{ii}^{0})) \geq 0$ for any k, then we apply feedback control in order to stabilize A_{ii}^{0}.

We can now state the following Lemma:

Lemma D1: *The interconnected system described by equation (D1) is globally stabilizable by completely decentralized feedback if the following condition is met:*

$$\sigma_{\max}(A_{ij}^{0}) + \varepsilon_{ij}\sigma_{\max}(U_{ij}) + \varepsilon_{ii}\sigma_{\max}(U_{ii}) \leq \frac{1}{\sigma_{\max}(P_{ii})} \text{ for all } i=1,..m:$$

where:

P_{ii} *is the solution to the Lyapunov equation* $(A_{ii}^0)P_{ii} + P_{ii}(A_{ii}^0)^T = -2Q_{ii}$

Q_{ii} *is a positive semi-definite matrix*

$\sigma_{\max}$ *denotes the maximum singular value*

Proof: Since A_{ii}^o is asymptotically stable, it satisfies the following steady state Lyapunov equation:

$$(A_{ii}^0)P_{ii} + P_{ii}(A_{ii}^0)^T = -2Q_{ii} \tag{D7}$$

The solution to equation (D7), P_{ii}, is a symmetric, positive semi-definite matrix i.e. $P_{ii}^T = P_{ii}$ and $x_i^T P_{ii} x_i \geq 0$. Matrix Q_{ii} is positive definite i.e. $x_i^T Q_{ii} x > 0$.

We construct two matrices P_i and Q_i as follows:

$$P_i = \begin{bmatrix} 0 & \cdots & 0 \\ \vdots & [P_{ii}] & \vdots \\ 0 & \cdots & 0 \end{bmatrix}_{n \times n} \tag{D8}$$

$$Q_i = \begin{bmatrix} 0 & \cdots & 0 \\ \vdots & [Q_{ii}] & \vdots \\ 0 & \cdots & 0 \end{bmatrix}_{n \times n} \tag{D9}$$

Matrix P_i is symmetric, positive semi-definite and satisfies the following Lyapunov equation:

$$A_{ii}^T P_i + P_i A_{ii} = -2Q_i \tag{D10}$$

We can choose a Lyapunov function for subsystem i as:

$$V_i(x) = x^T P_i x \tag{D11}$$

The system is stable where (a) $V_i(x)$ is positive semi-definite and (b) $\dot{V} \leq 0$.

(a) $V_i(x) = x^T P_i x$ is positive semi-definite for all x since P_i is positive semi-definite

Thus, to obtain the stability region we need to determine the region where:

$$\text{(b) } \dot{V}_i(x) = \dot{x}^T P_i x + x^T P_i \dot{x} \leq 0 \tag{D12}$$

Substituting equation (D5) into (D12) we obtain the following:

$$\dot{V}_i(x) = \left((A_{ii} + A_{ij}^U)x\right)^T P_i x + x^T P_i (A_{ii} + A_{ij}^U)x \tag{D13}$$

$$\dot{V}_i(x) = x^T (A_{ii})^T P_i x + x^T (A_{ij}^U) P_i x + x^T P_i (A_{ii}) x + x^T P_i A_{ij}^U x \tag{D14}$$

$$\dot{V}_i(x) = x^T \left((A_{ii})^T P_i + P_i A_{ii}\right) x + x^T \left((A_{ij}^U)^T P_i + P_i A_{ij}^U\right) x \tag{D15}$$

Substituting equation (D10) into equation (D15) gives the following:

$$\dot{V}_i(x) = x^T (-2Q_i)x + x^T ((A_{ij}^U)^T P_i + P_i A_{ij}^U)x \tag{D16}$$

For stability, we need $\dot{V}(x) \le 0$ i.e.:

$$x^T ((A_{ij}^U)^T P_i + P_i A_{ij}^U)x \le x^T (2Q_i)x \tag{D17}$$

Since $((A_{ij}^U)^T P_i)^T = P_i A_{ij}^U$ we can rewrite equation (D17) as follows:

$$x^T P_i (A_{ij}^U)^T x + x^T (P_i (A_{ij}^U)^T)^T x \le x^T (2Q_i)x \tag{D18}$$

Consider the following inequality:

$$\sigma_{\max}(A_{ij}^0) + \varepsilon_{ij}\sigma_{\max}(U_{ij}) + \varepsilon_{ii}\sigma_{\max}(U_{ii}) \le \frac{\sigma_{\max}(Q_{ii})}{\sigma_{\max}(P_{ii})} \tag{D19}$$

We need to show that if the inequality in (D19) is satisfied, then the inequality in (D18) is satisfied.

From (D19), we know that

$$2\sigma_{\max}(P_{ii})(\sigma_{\max}(A_{ij}^0) + \varepsilon_{ij}\sigma_{\max}(U_{ij}) + \varepsilon_{ii}\sigma_{\max}(U_{ii})) \le \sigma_{\max}(2Q_{ii}) \tag{D20}$$

$$2\sigma_{\max}\left(P_{ii}(A_{ij}^0 + \varepsilon_{ij}U_{ij} + \varepsilon_{ii}U_{ii})\right) \le \sigma_{\max}(2Q_{ii}) \tag{D21}$$

From the definition of A_{ij}^U in equation (D6), we can rewrite (D21) as follows:

$$2\sigma_{\max}\left(P_{ii}A_{ij}^U\right) \le \sigma_{\max}(2Q_{ii}) \tag{D22}$$

Therefore:

$$\sigma_{\max}\left(P_{ii}A_{ij}^U + \left(P_{ii}A_{ij}^U\right)^T\right) \le \sigma_{\max}(2Q_{ii}) \tag{D23}$$

We also know that:

$$\sigma_{\max}\left(P_{ii}A_{ij}^U + \left(P_{ii}A_{ij}^U\right)^T\right) = \sigma_{\max}\left(P_i A_{ij}^U + \left(P_i A_{ij}^U\right)^T\right)$$

Therefore:

$$\sigma_{\max}\left(P_i A_{ij}^U + \left(P_i A_{ij}^U\right)^T\right)x^T x \le \sigma_{\max}(2Q_i)x^T x \tag{D24}$$

From Rayleigh's Principle we know that:

$$\sigma_{\max}(P_i A_{ij}^U)x^T x \ge x^T(P_i A_{ij}^U)x \tag{D25}$$

and

$$\sigma_{\min}(2Q_i)x^T x \le x^T(2Q_i)x \tag{D26}$$

Substituting (D25) and D(26) into (D24) gives the following:

$$x^T\left(P_i A_{ij}^U + \left(P_i A_{ij}^U\right)^T\right)x \le x^T(2Q_i)x \tag{D27}$$

which is the inequality in (D18)

If we choose $Q_{ii} = I$ then condition for stability becomes:

$$\sigma_{\max}(A_{ij}^0) + \varepsilon_{ij}\sigma_{\max}(U_{ij}) + \varepsilon_{ii}\sigma_{\max}(U_{ii}) \le \frac{1}{\sigma_{\max}(P_{ii})} \tag{D28}$$

Equation (D28) gives us the condition which guarantees global stability with the contribution of the interaction terms A_{ij}^0, the interaction perturbation terms U_{ij} and the diagonal perturbation terms U_{ii}.

If the values of $\sigma_{\max}(A_{ij}^0)$ and the perturbations E_{ii} and E_{ij} are known, we can obtain decentralized controllers which, in addition to ensuring global stability, also ensure a robust stability margin of the closed loop. This is achieved by selecting controllers such that the state coefficient matrix of the closed loop A_{ii}^{cl} satisfies the Lyapunov equation:

$$A_{ii}^{cl}P_{ii} + P_{ii}A_{ii}^0 + 2Q_i = 0 \tag{D29}$$

and P_{ii} satisfies the inequality:

$$\sigma_{\max}(A_{ij}^0) + \varepsilon_{ij}\sigma_{\max}(U_{ij}) + \varepsilon_{ii}\sigma_{\max}(U_{ii}) \le \frac{1}{\sigma_{\max}(P_{ii})} \text{ for } i = 1,\ldots,m$$

Appendix E

State Space Description of the Nine-Bus System

The nine-bus system described in this appendix was used for two case studies. In Section 2.4, we used the nine-bus system for determining the optimal locations of PSS. In section 4.5, we used the nine-bus system to design robust H_∞-based controllers.

Figure E1 is a one-line impedance diagram of the nine-bus system. All the impedances are in per unit on a 100 MVA base. Figure E2 is a load flow diagram showing the nominal operating conditions of the power system.

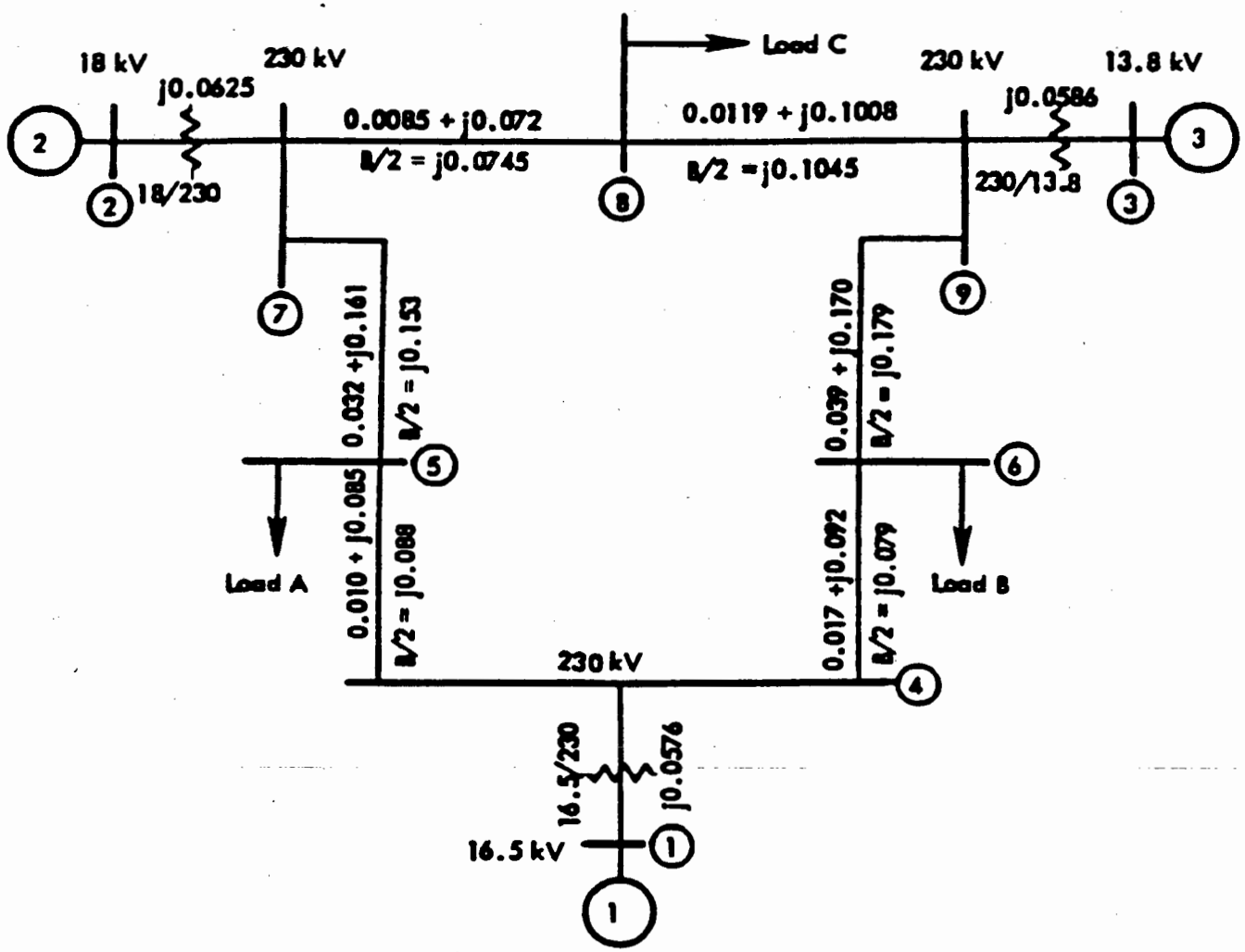

Figure E1: Impedance Diagram of the Nine-Bus System

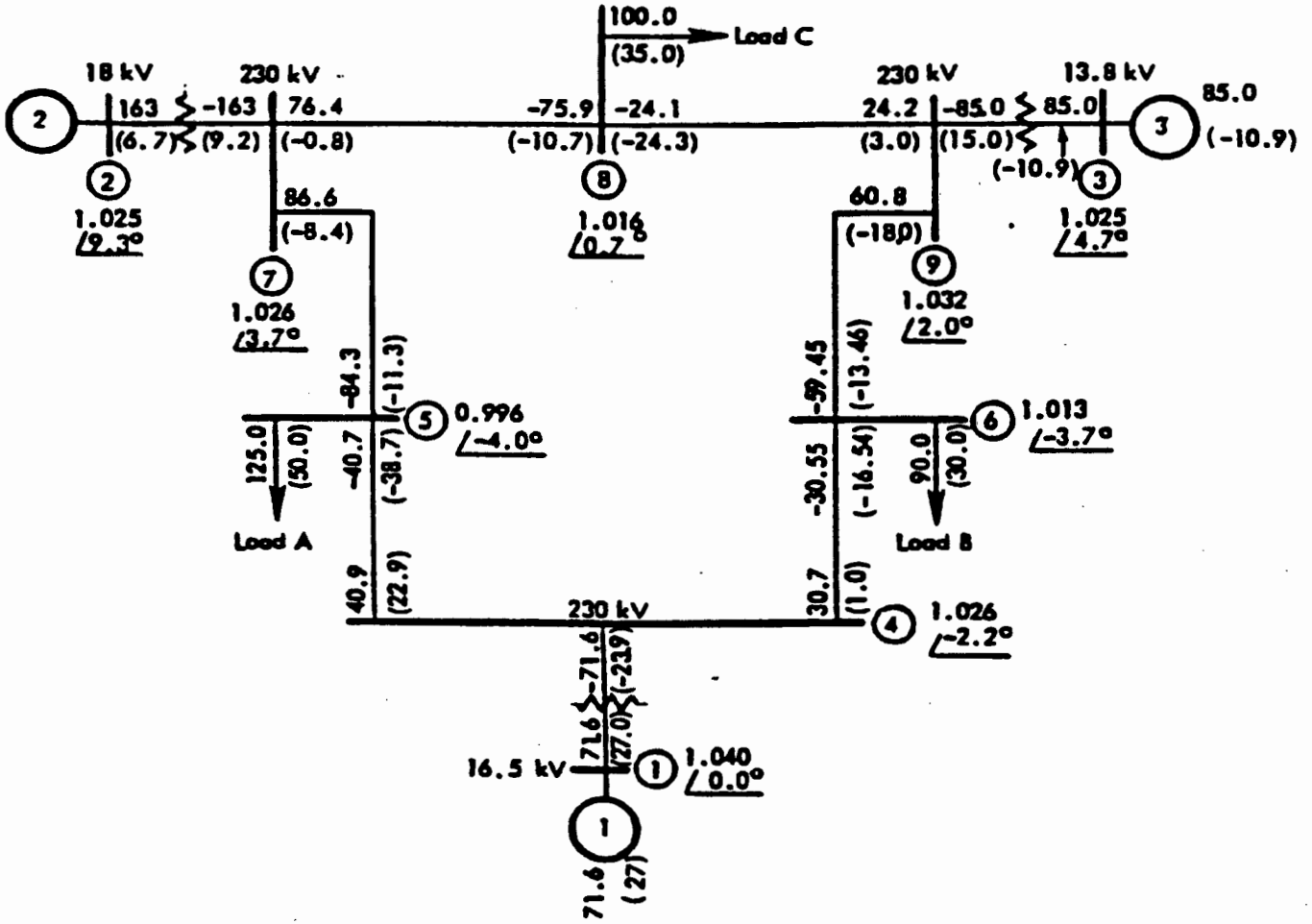

Figure E2: Load Flow Diagram of the Nine-Bus System

The generator parameters are provided in Table E1.

Parameters	Gen1	Gen2	Gen3
T'_{d0}	5.390	5.900	5.890
T''_{d0}	0.053	0.033	0.034
T'_{q0}	1.500	0.535	0.600
T''_{q0}	0.135	0.078	0.080
H	6.396	3.302	2.383
X_d	1.581	1.651	1.680
X_q	1.531	1.590	1.690
X'_d	0.380	0.232	0.232
X'_q	0.955	0.380	0.320
X''_d	0.252	0.171	0.171
X_l	0.291	0.102	0.091
S(1.0)	0.095	0.105	0.121
S(1.2)	0.345	0.477	0.610

Table E1: Generator Data for the Nine-Bus System

The state space description of the nine-bus system is expressed as follows:

$$\dot{x} = Ax + Bu$$
$$y = Cx + Du$$

where the matrices A, B, C and D are as follows:

MATRIX A COLUMNS STARTING AT 1

1	-3.7351	0.38569E-02	3.4202	-.70553E-01	0.00000	0.67644E-01	-.31549E-01	-.11081E-02	-.27893E-01	-.33412E-02
2	0.14581	-1.2648	-.48950	0.35457	0.00000	-.20889E-01	0.54725E-03	-.34080E-02	0.48453E-03	-.10320E-01
3	19.783	0.29238E-01	-21.871	-.52683	0.00000	-1.1634	0.54259	0.19028E-01	0.47970	0.57461E-01
4	-.63872	7.7663	2.0958	-13.882	0.00000	4.5558	-.11907	0.74323	-.10526	2.2509
5	0.43605E-01	-.30228E-02	-.14374	0.54445E-01	-.47041E-01	-.95959E-01	0.13333E-01	-.11241E-01	0.11787E-01	-.34048E-01
6	0.00000	0.00000	0.00000	0.00000	314.16	0.00000	0.00000	0.00000	0.00000	0.00000
7	-.32937E-01	0.28856E-02	0.10810	-.52375E-01	0.00000	0.82760E-01	-1.2478	-.43341E-01	0.68248	-.13193
8	-.95354E-01	-.19593E-01	0.31291	0.35000	0.00000	-.22797	-.67636	-8.5624	-.59690	4.3579
9	-1.0165	0.89128E-01	3.3361	-1.6163	0.00000	2.5540	27.073	-.29798	-33.159	-.90313
10	-.60538	-.12403	1.9867	2.2221	0.00000	-1.4474	0.57696	11.454	0.51010	-16.960
11	-.46328E-02	0.65237E-02	0.15212E-01	-.11732	0.00000	0.11413	-.14412	0.15823E-01	-.12739	0.47804E-01
12	0.00000	0.00000	0.00000	0.00000	0.00000	0.00000	0.00000	0.00000	0.00000	0.00000
13	-.47726E-01	0.29725E-02	0.15662	-.54834E-01	0.00000	0.10024	0.81369E-01	-.39030E-02	0.71934E-01	-.11811E-01
14	-.12088	-.34446E-01	0.39657	0.61391	0.00000	-.44792	0.44352E-01	0.20261	0.39215E-01	0.61370
15	-1.4101	0.87942E-01	4.6274	-1.6201	0.00000	2.9617	2.4041	-.11525	2.1254	-.34895
16	-.46811	-.13318	1.5359	2.3776	0.00000	-1.7347	0.17180	0.78472	0.15189	2.3768
17	-.18424E-01	0.10853E-01	0.60480E-01	-.19545	0.00000	0.20117	0.68852E-01	-.50704E-01	0.60868E-01	-.15357
18	0.00000	0.00000	0.00000	0.00000	0.00000	0.00000	0.00000	0.00000	0.00000	0.00000
19	0.24408E-01	0.16259E-02	-.80216E-01	-.29269E-01	0.00000	0.19312E-02	-.58851E-02	-.20591E-02	-.52008E-02	-.62393E-02
20	54.241	3.6146	-178.26	-65.041	0.00000	4.2915	-13.078	-4.5757	-11.557	-13.865
21	0.46269E-02	0.14720E-03	-.15189E-01	-.26374E-02	0.00000	-.23148E-02	-.25983E-01	-.11149E-01	-.22963E-01	-.33806E-01
22	10.282	0.32711	-33.752	-5.8608	0.00000	-5.1439	-57.739	-24.775	-51.030	-75.123
23	0.56370E-02	0.27432E-03	-.18499E-01	-.47086E-02	0.00000	-.14229E-02	-.72096E-02	-.26966E-02	-.63730E-02	-.81694E-02
24	12.527	0.60962	-41.109	-10.464	0.00000	-3.1619	-16.021	-5.9925	-14.162	-18.154

MATRIX A COLUMNS STARTING AT 11

1	0.00000	-.34998E-01	-.27647E-01	0.27607E-03	-.22194E-01	0.54763E-03	0.00000	-.32006E-01	0.00000	0.18553
2	0.00000	0.11868E-01	-.10459E-03	-.38860E-02	-.82558E-04	-.76208E-02	0.00000	0.91340E-02	0.00000	0.00000
3	0.00000	0.60190	0.47546	-.47846E-02	0.38168	-.94464E-02	0.00000	0.55043	0.00000	0.00000
4	0.00000	-2.5879	0.23029E-01	0.84798	0.18518E-01	1.6625	0.00000	-1.9919	0.00000	0.00000
5	0.00000	0.53263E-01	0.96881E-02	-.13385E-01	0.77764E-02	-.26244E-01	0.00000	0.42838E-01	0.00000	0.00000
6	0.00000	0.00000	0.00000	0.00000	0.00000	0.00000	0.00000	0.00000	0.00000	0.00000
7	0.00000	-.16592	0.50447E-01	-.10564E-01	0.40482E-01	-.20738E-01	0.00000	0.82360E-01	0.00000	0.00000
8	0.00000	0.45709	0.76419E-01	0.13513	0.61282E-01	0.26479	0.00000	-.23477	0.00000	0.00000
9	0.00000	-5.1204	1.5568	-.32606	1.2493	-.63996	0.00000	2.5416	0.00000	0.00000
10	0.00000	2.9021	0.48525	0.85790	0.38917	1.6812	0.00000	-1.4905	0.00000	0.00000
11	-.12728	-.22883	0.22355E-01	-.37810E-01	0.17947E-01	-.74120E-01	0.00000	0.11531	0.00000	0.00000
12	314.16	0.00000	0.00000	0.00000	0.00000	0.00000	0.00000	0.00000	0.00000	0.00000

13	0.00000	0.11243	-1.2512	-.66991E-01	0.57265	-.13186	0.00000	-.21423	0.00000	0.00000
14	0.00000	-.61151	-.68641	-8.9778	-.54936	4.3932	0.00000	1.0506	0.00000	0.00000
15	0.00000	3.3220	24.770	-.42931	-33.138	-.84141	0.00000	-6.3295	0.00000	0.00000
16	0.00000	-2.3682	0.49180	10.527	0.39463	-16.368	0.00000	4.0689	0.00000	0.00000
17	0.00000	0.25090	-.24113	0.74689E-01	-.19351	0.14633	-.13795	-.45155	0.00000	0.00000
18	0.00000	0.00000	0.00000	0.00000	0.00000	0.00000	314.16	0.00000	0.00000	0.00000
19	0.00000	-.44531E-03	-.54714E-02	-.20483E-02	-.43927E-02	-.40168E-02	0.00000	-.13345E-02	-.10000	0.00000
20	0.00000	-.98931	-12.158	-4.5519	-9.7615	-8.9263	0.00000	-2.9653	2000.0	-20.000
21	0.00000	0.46075E-02	-.57012E-02	-.18171E-02	-.45738E-02	-.35607E-02	0.00000	-.21487E-02	0.00000	0.00000
22	0.00000	10.239	-12.669	-4.0380	-10.164	-7.9127	0.00000	-4.7749	0.00000	0.00000
23	0.00000	0.16759E-04	-.24869E-01	-.12577E-01	-.19956E-01	-.24677E-01	0.00000	0.15926E-02	0.00000	0.00000
24	0.00000	0.37242E-01	-55.264	-27.949	-44.346	-54.838	0.00000	3.5392	0.00000	0.00000

MATRIX A COLUMNS STARTING AT 21

1	0.00000	0.00000	0.00000	0.00000
2	0.00000	0.00000	0.00000	0.00000
3	0.00000	0.00000	0.00000	0.00000
4	0.00000	0.00000	0.00000	0.00000
5	0.00000	0.00000	0.00000	0.00000
6	0.00000	0.00000	0.00000	0.00000
7	0.00000	0.16949	0.00000	0.00000
8	0.00000	0.00000	0.00000	0.00000
9	0.00000	0.00000	0.00000	0.00000
10	0.00000	0.00000	0.00000	0.00000
11	0.00000	0.00000	0.00000	0.00000
12	0.00000	0.00000	0.00000	0.00000
13	0.00000	0.00000	0.00000	0.16978
14	0.00000	0.00000	0.00000	0.00000
15	0.00000	0.00000	0.00000	0.00000
16	0.00000	0.00000	0.00000	0.00000
17	0.00000	0.00000	0.00000	0.00000
18	0.00000	0.00000	0.00000	0.00000
19	0.00000	0.00000	0.00000	0.00000
20	0.00000	0.00000	0.00000	0.00000
21	-.10000	0.00000	0.00000	0.00000
22	2000.0	-20.000	0.00000	0.00000
23	0.00000	0.00000	-.10000	0.00000
24	0.00000	0.00000	2000.0	-20.000

MATRIX B

1	0.00000	0.00000	0.00000
2	0.00000	0.00000	0.00000
3	0.00000	0.00000	0.00000
4	0.00000	0.00000	0.00000
5	0.00000	0.00000	0.00000

```
 6 0.00000      0.00000      0.00000
 7 0.00000      0.00000      0.00000
 8 0.00000      0.00000      0.00000
 9 0.00000      0.00000      0.00000
10 0.00000      0.00000      0.00000
11 0.00000      0.00000      0.00000
12 0.00000      0.00000      0.00000
13 0.00000      0.00000      0.00000
14 0.00000      0.00000      0.00000
15 0.00000      0.00000      0.00000
16 0.00000      0.00000      0.00000
17 0.00000      0.00000      0.00000
18 0.00000      0.00000      0.00000
19 0.90000E-01 0.00000      0.00000
20  200.00      0.00000      0.00000
21 0.00000      0.90000E-01 0.00000
22 0.00000       200.00      0.00000
23 0.00000      0.00000      0.90000E-01
24 0.00000      0.00000       200.00
```

MATRIX C COLUMNS STARTING AT 1

```
 1 -.27120      -.18066E-01 0.89129      0.32521      0.00000      -.21458E-01 0.65390E-01 0.22879E-01 0.57787E-01 0.69326E-01
 2 -.51410E-01 -.16356E-02 0.16876      0.29304E-01 0.00000      0.25720E-01 0.28870      0.12387      0.25515      0.37562
 3 -.62633E-01 -.30481E-02 0.20554      0.52317E-01 0.00000      0.15810E-01 0.80106E-01 0.29962E-01 0.70811E-01 0.90771E-01
```

MATRIX C COLUMNS STARTING AT 11

```
 1 0.00000      0.49479E-02 0.60793E-01 0.22759E-01 0.48807E-01 0.44631E-01 0.00000      0.14828E-01 0.00000      0.00000
 2 0.00000      -.51195E-01 0.63346E-01 0.20190E-01 0.50820E-01 0.39564E-01 0.00000      0.23874E-01 0.00000      0.00000
 3 0.00000      -.18621E-03 0.27632      0.13975      0.22173      0.27419      0.00000      -.17696E-01 0.00000      0.00000
```

MATRIX C COLUMNS STARTING AT 21

```
 1 0.00000      0.00000      0.00000      0.00000
 2 0.00000      0.00000      0.00000      0.00000
 3 0.00000      0.00000      0.00000      0.00000
```

MATRIX D

```
 1 0.00000      0.00000      0.00000
 2 0.00000      0.00000      0.00000
 3 0.00000      0.00000      0.00000
```

Nine Bus System with Machine 1 Taken as Reference

By taking the rotor angle deviation of machine 1 as a reference, the transformation described in Appendix A is used to obtain reduced matrices. These are given by the following:

MATRIX A COLUMNS STARTING AT 1

1	-3.7351	0.38241E-02	3.4202	-.70558E-01	0.00000	-.31550E-01	-.11081E-02	-.27897E-01	-.33476E-02	0.00000
2	0.14581	-1.2648	-.48950	0.35456	0.00000	0.54492E-03	-.34098E-02	0.48065E-03	-.10324E-01	0.00000
3	19.783	0.29632E-01	-21.871	-.52683	0.00000	0.54260	0.19016E-01	0.47978	0.57552E-01	0.00000
4	-.63864	7.7670	2.0959	-13.882	0.00000	-.11907	0.74327	-.10506	2.2511	0.00000
5	0.43605E-01	-.30257E-02	-.14374	0.54445E-01	-.47041E-01	0.13333E-01	-.11242E-01	0.11786E-01	-.34049E-01	0.00000
6	-.32947E-01	0.28981E-02	0.10810	-.52403E-01	0.00000	-1.2478	-.43333E-01	0.68249	-.13193	0.00000
7	-.95397E-01	-.19593E-01	0.31290	0.34985	0.00000	-.67638	-8.5624	-.59684	4.3579	0.00000
8	-1.0167	0.89269E-01	3.3360	-1.6171	0.00000	27.073	-.29794	-33.159	-.90313	0.00000
9	-.60562	-.12403	1.9866	2.2212	0.00000	0.57685	11.454	0.51030	-16.960	0.00000
10	-.46311E-02	0.65237E-02	0.15213E-01	-.11731	0.00000	-.14412	0.15822E-01	-.12739	0.47803E-01	-.12728
11	0.00000	0.00000	0.00000	0.00000	-314.16	0.00000	0.00000	0.00000	0.00000	314.16
12	-.47725E-01	0.29788E-02	0.15662	-.54834E-01	0.00000	0.81371E-01	-.38974E-02	0.71944E-01	-.11791E-01	0.00000
13	-.12087	-.34446E-01	0.39658	0.61391	0.00000	0.44363E-01	0.20261	0.39279E-01	0.61382	0.00000
14	-1.4101	0.88078E-01	4.6273	-1.6201	0.00000	2.4042	-.11517	2.1256	-.34837	0.00000
15	-.46811	-.13341	1.5358	2.3776	0.00000	0.17178	0.78462	0.15206	2.3772	0.00000
16	-.18424E-01	0.10872E-01	0.60480E-01	-.19545	0.00000	0.68854E-01	-.50694E-01	0.60867E-01	-.15357	0.00000
17	0.00000	0.00000	0.00000	0.00000	-314.16	0.00000	0.00000	0.00000	0.00000	0.00000
18	0.24408E-01	0.16192E-02	-.80216E-01	-.29266E-01	0.00000	-.58851E-02	-.20591E-02	-.52022E-02	-.62409E-02	0.00000
19	54.241	3.5982	-178.26	-65.036	0.00000	-13.078	-4.5757	-11.561	-13.869	0.00000
20	0.46279E-02	0.14720E-03	-.15188E-01	-.26325E-02	0.00000	-.25981E-01	-.11149E-01	-.22965E-01	-.33807E-01	0.00000
21	10.284	0.32711	-33.750	-5.8494	0.00000	-57.736	-24.775	-51.033	-75.127	0.00000
22	0.56370E-02	0.27432E-03	-.18499E-01	-.47086E-02	0.00000	-.72096E-02	-.26966E-02	-.63744E-02	-.81709E-02	0.00000
23	12.526	0.60813	-41.109	-10.464	0.00000	-16.022	-5.9929	-14.166	-18.158	0.00000

MATRIX A COLUMNS STARTING AT 11

1	-.34999E-01	-.27652E-01	0.27607E-03	-.22194E-01	0.54763E-03	0.00000	-.32005E-01	0.00000	0.18553	0.00000
2	0.11866E-01	-.10700E-03	-.38896E-02	-.86428E-04	-.76238E-02	0.00000	0.91340E-02	0.00000	0.00000	0.00000
3	0.60190	0.47554	-.47972E-02	0.38168	-.94464E-02	0.00000	0.55041	0.00000	0.00000	0.00000
4	-2.5879	0.23162E-01	0.84809	0.18576E-01	1.6625	0.00000	-1.9918	0.00000	0.00000	0.00000
5	0.53263E-01	0.96875E-02	-.13388E-01	0.77758E-02	-.26244E-01	0.00000	0.42836E-01	0.00000	0.00000	0.00000
6	-.16592	0.50434E-01	-.10580E-01	0.40482E-01	-.20744E-01	0.00000	0.82351E-01	0.00000	0.00000	0.00000
7	0.45710	0.76352E-01	0.13507	0.61311E-01	0.26474	0.00000	-.23480	0.00000	0.00000	0.00000
8	-5.1203	1.5563	-.32651	1.2493	-.64020	0.00000	2.5413	0.00000	0.00000	0.00000
9	2.9023	0.48476	0.85748	0.38920	1.6810	0.00000	-1.4908	0.00000	0.00000	0.00000
10	-.22883	0.22360E-01	-.37808E-01	0.17946E-01	-.74120E-01	0.00000	0.11531	0.00000	0.00000	0.00000
11	0.00000	0.00000	0.00000	0.00000	0.00000	0.00000	0.00000	0.00000	0.00000	0.00000
12	0.11244	-1.2512	-.66993E-01	0.57265	-.13186	0.00000	-.21422	0.00000	0.00000	0.00000

13	-.61150	-.68638	-8.9779	-.54934	4.3932	0.00000	1.0507	0.00000	0.00000	0.00000
14	3.3220	24.770	-.42921	-33.138	-.84140	0.00000	-6.3294	0.00000	0.00000	0.00000
15	-2.3682	0.49182	10.527	0.39463	-16.368	0.00000	4.0689	0.00000	0.00000	0.00000
16	0.25090	-.24114	0.74697E-01	-.19351	0.14633	-.13795	-.45154	0.00000	0.00000	0.00000
17	0.00000	0.00000	0.00000	0.00000	0.00000	314.16	0.00000	0.00000	0.00000	0.00000
18	-.44531E-03	-.54726E-02	-.20483E-02	-.43927E-02	-.40168E-02	0.00000	-.13345E-02	-.10000	0.00000	0.00000
19	-.98931	-12.161	-4.5519	-9.7615	-8.9263	0.00000	-2.9653	2000.0	-20.000	0.00000
20	0.46075E-02	-.56986E-02	-.18152E-02	-.45752E-02	-.35591E-02	0.00000	-.21473E-02	0.00000	0.00000	-.10000
21	10.239	-12.663	-4.0333	-10.167	-7.9088	0.00000	-4.7715	0.00000	0.00000	2000.0
22	0.16759E-04	-.24869E-01	-.12577E-01	-.19956E-01	-.24677E-01	0.00000	0.15926E-02	0.00000	0.00000	0.00000
23	0.36976E-01	-55.265	-27.950	-44.346	-54.838	0.00000	3.5392	0.00000	0.00000	0.00000

MATRIX A COLUMNS STARTING AT 21

1	0.00000	0.00000	0.00000
2	0.00000	0.00000	0.00000
3	0.00000	0.00000	0.00000
4	0.00000	0.00000	0.00000
5	0.00000	0.00000	0.00000
6	0.16949	0.00000	0.00000
7	0.00000	0.00000	0.00000
8	0.00000	0.00000	0.00000
9	0.00000	0.00000	0.00000
10	0.00000	0.00000	0.00000
11	0.00000	0.00000	0.00000
12	0.00000	0.00000	0.16978
13	0.00000	0.00000	0.00000
14	0.00000	0.00000	0.00000
15	0.00000	0.00000	0.00000
16	0.00000	0.00000	0.00000
17	0.00000	0.00000	0.00000
18	0.00000	0.00000	0.00000
19	0.00000	0.00000	0.00000
20	0.00000	0.00000	0.00000
21	-20.000	0.00000	0.00000
22	0.00000	-.10000	0.00000
23	0.00000	2000.0	-20.000

MATRIX B

1	0.00000	0.00000	0.00000
2	0.00000	0.00000	0.00000
3	0.00000	0.00000	0.00000
4	0.00000	0.00000	0.00000
5	0.00000	0.00000	0.00000
6	0.00000	0.00000	0.00000
7	0.00000	0.00000	0.00000
8	0.00000	0.00000	0.00000

```
  9 0.00000      0.00000      0.00000
 10 0.00000      0.00000      0.00000
 11 0.00000      0.00000      0.00000
 12 0.00000      0.00000      0.00000
 13 0.00000      0.00000      0.00000
 14 0.00000      0.00000      0.00000
 15 0.00000      0.00000      0.00000
 16 0.00000      0.00000      0.00000
 17 0.00000      0.00000      0.00000
 18 0.90000E-01  0.00000      0.00000
 19  200.00      0.00000      0.00000
 20 0.00000      0.90000E-01  0.00000
 21 0.00000       200.00      0.00000
 22 0.00000      0.00000      0.90000E-01
 23 0.00000      0.00000       200.00

MATRIX C COLUMNS STARTING AT  1
  1 -.27120      -.17991E-01 0.89129      0.32518      0.00000      0.65390E-01 0.22879E-01 0.57802E-01 0.69343E-01 0.00000
  2 -.51421E-01  -.16356E-02 0.16875      0.29250E-01  0.00000      0.28868      0.12387      0.25517      0.37564      0.00000
  3 -.62633E-01  -.30481E-02 0.20554      0.52317E-01  0.00000      0.80106E-01  0.29962E-01  0.70827E-01  0.90788E-01  0.00000

MATRIX C COLUMNS STARTING AT  11
  1 0.49479E-02  0.60807E-01 0.22759E-01  0.48807E-01  0.44631E-01  0.00000      0.14828E-01  0.00000      0.00000      0.00000
  2 -.51195E-01  0.63317E-01 0.20169E-01  0.50835E-01  0.39546E-01  0.00000      0.23859E-01  0.00000      0.00000      0.00000
  3 -.18621E-03  0.27632      0.13975      0.22173      0.27419      0.00000      -.17696E-01  0.00000      0.00000      0.00000

MATRIX C COLUMNS STARTING AT  21
  1 0.00000      0.00000      0.00000
  2 0.00000      0.00000      0.00000
  3 0.00000      0.00000      0.00000

MATRIX D
  1 0.00000      0.00000      0.00000
  2 0.00000      0.00000      0.00000
  3 0.00000      0.00000      0.00000
```

Table E2 gives the eigenvalues and associated damping factors of the nine-bus system.

Eigenvalue	Damping
-0.0806	1.0000
-0.3490 + 0.4395i	0.6219
-0.3490 - 0.4395i	0.6219
-0.4683 + 0.5369i	0.6573
-0.4683 - 0.5369i	0.6573
-0.7852 + 7.2328i	0.1079
-0.7852 - 7.2328i	0.1079
-1.0549	1.0000
-1.0935 + 0.6626i	0.8552
-1.0935 - 0.6626i	0.8552
-1.2758 +12.0864i	0.1050
-1.2758 -12.0864i	0.1050
-3.0569	1.0000
-5.2229	1.0000
-12.4694	1.0000
-16.1346	1.0000
-18.0498	1.0000
-18.9625	1.0000
-20.5065	1.0000
-21.7751	1.0000
-27.7914	1.0000
-32.8788	1.0000
-35.1025	1.0000

Table E2: Eigenvalues of the Nine-Bus System

The right eigenvectors of the nine-bus system are:

Columns 1 through 3

-1.4012e-004	-1.7065e-003	-1.2287e-002
4.4753e-005	2.6420e-004	7.9660e-004
1.1321e-003	1.5154e-002	3.7142e-002
-2.1080e-003	-1.9162e-003	-3.7760e-003
3.4859e-005	1.5883e-004	1.8089e-004
8.4577e-003	6.4744e-003	-2.3282e-003
-7.2593e-003	-4.9629e-003	2.3785e-003
-2.6856e-001	-1.4265e-001	2.2633e-002
2.7836e-003	1.0855e-002	-1.0523e-002
-9.9185e-004	-4.3053e-004	4.4855e-005
9.1888e-003	5.6314e-003	1.5378e-003
-7.9553e-003	8.3049e-003	-3.0817e-003
8.2465e-003	-6.3590e-003	1.5798e-003
3.0910e-001	-2.1600e-001	3.0333e-002
-4.0767e-003	6.0707e-003	-5.6679e-003
1.8216e-003	-8.8002e-004	1.3536e-005
-1.5991e-002	9.9264e-003	1.8919e-003
-4.2727e-007	-9.8241e-006	1.1956e-004
-2.1545e-003	-5.4042e-002	9.1362e-001
-1.3227e-004	-1.0674e-004	3.0402e-005
-6.6371e-001	-5.8712e-001	2.3230e-001
1.2465e-004	-1.3901e-004	4.3044e-005
6.2545e-001	-7.6464e-001	3.2891e-001

Columns 4 through 6

1.2225e-004	-5.0447e-004	-1.8057e-003
1.9330e-004	-2.6763e-004	-3.1614e-005
1.6275e-003	-3.1588e-003	-4.7424e-003
-8.2099e-003	9.6520e-003	-3.9767e-003
8.0769e-005	-1.0050e-004	-1.7392e-005
-6.9751e-003	2.5496e-003	7.0436e-003
-1.7639e-002	4.8329e-003	-9.6286e-004
-1.9888e-002	7.8799e-003	1.3592e-002
5.0679e-002	-1.0980e-002	5.2568e-003
-3.1026e-004	2.4809e-005	1.0228e-004
5.6416e-003	-1.9198e-003	-2.0830e-003
1.9566e-003	7.3855e-003	5.7935e-003

```
 8.6506e-003   1.7522e-002  -1.1664e-003
 5.3142e-003   1.9406e-002   1.1656e-002
-2.7406e-002  -4.0828e-002   4.9797e-003
 3.8546e-004   3.6512e-004   9.0021e-005
-4.3960e-003  -7.1334e-003  -1.8696e-003
-1.8103e-006   1.2958e-006  -1.1843e-005
-4.7081e-002   1.1088e-001   2.3009e-001
 3.6881e-005  -3.8909e-006   3.8748e-005
 9.5923e-001  -3.3299e-001  -7.5279e-001
-1.0413e-005  -1.0925e-005   3.1724e-005
-2.7084e-001  -9.3491e-001  -6.1633e-001
```

Columns 7 through 9

```
-4.4489e-006  -4.2635e-003   7.6821e-004- 2.0219e-003i
 3.2562e-005  -1.1088e-003  -9.4715e-004+ 1.5382e-003i
 2.6736e-004  -2.0636e-002   9.2457e-003+ 7.0271e-003i
-1.1869e-003   1.9825e-002  -4.1526e-002- 3.4238e-002i
 9.5145e-006  -2.0481e-004   1.4741e-003- 1.3261e-004i
-5.4117e-003  -5.1763e-003   8.9417e-003- 5.5459e-003i
-8.4828e-004   1.7305e-003  -4.7220e-002+ 1.1255e-002i
-9.3060e-003  -1.4654e-002   6.4843e-002+ 6.6316e-002i
-7.8226e-004  -5.3204e-003  -8.6124e-002- 3.8635e-002i
-8.4464e-005  -3.8198e-007   1.0391e-002- 2.8208e-003i
 1.5570e-003  -3.9805e-003  -9.3301e-002- 2.2194e-001i
 7.3250e-003  -5.0545e-003  -1.6591e-002+ 1.4477e-002i
 4.1598e-004   1.3951e-003   1.1592e-001- 2.3679e-002i
 1.1924e-002  -1.5773e-002  -1.1685e-001- 1.1396e-001i
 2.8742e-003  -4.6197e-003   1.9181e-001+ 5.9488e-002i
 1.4560e-004   4.3333e-005  -2.9141e-002+ 7.1909e-003i
-2.2546e-003  -4.8317e-003   2.7133e-001+ 7.6712e-001i
 1.2861e-007  -7.6490e-005  -3.2623e-005+ 2.2389e-006i
-4.9406e-003   6.6554e-001  -2.2866e-002- 3.2103e-002i
-1.5586e-005  -6.1108e-005  -2.1832e-004- 1.2890e-005i
 5.9969e-001   5.3169e-001  -1.2440e-001- 2.3244e-001i
 2.0793e-005  -6.0042e-005   1.7548e-004+ 2.0088e-004i
-8.0001e-001   5.2242e-001  -9.5764e-002+ 3.0696e-001i
```

Columns 10 through 12

```
 7.6821e-004+ 2.0219e-003i-1.2477e-002   1.1103e-002- 1.2084e-002i
-9.4715e-004- 1.5382e-003i 1.4431e-003  -7.0974e-003+ 6.3352e-003i
 9.2457e-003- 7.0271e-003i-2.0938e-002   2.5595e-002+ 1.6774e-002i
-4.1526e-002+ 3.4238e-002i-7.0345e-002  -1.1371e-001- 1.4437e-001i
```

```
 1.4741e-003+ 1.3261e-004i-5.8946e-006    6.5566e-003- 7.2606e-004i
 8.9417e-003+ 5.5459e-003i-2.8107e-003   -9.3980e-003+ 4.0907e-003i
-4.7220e-002- 1.1255e-002i 1.3139e-002    4.0046e-002+ 8.2113e-003i
 6.4843e-002- 6.6316e-002i-2.7195e-003   -2.7338e-002- 5.1088e-002i
-8.6124e-002+ 3.8635e-002i-6.2443e-003    4.9927e-002+ 4.0547e-002i
 1.0391e-002+ 2.8208e-003i-5.8140e-004   -1.0013e-002+ 8.9122e-004i
-9.3301e-002+ 2.2194e-001i 1.4499e-002    1.4665e-001+ 7.0380e-001i
-1.6591e-002- 1.4477e-002i-2.9422e-003   -3.6568e-003+ 1.9782e-003i
 1.1592e-001+ 2.3679e-002i 1.3695e-002    2.0874e-002+ 2.4963e-003i
-1.1685e-001+ 1.1396e-001i-6.3346e-003   -1.4743e-002- 2.5708e-002i
 1.9181e-001- 5.9488e-002i-3.1688e-003    2.6416e-002+ 1.3510e-002i
-2.9141e-002- 7.1909e-003i-7.9559e-004   -6.6088e-003+ 9.3654e-004i
 2.7133e-001- 7.6712e-001i 1.9896e-002    1.3273e-001+ 5.5743e-001i
-3.2623e-005- 2.2389e-006i-2.8088e-004    1.9928e-004- 1.6144e-004i
-2.2866e-002+ 3.2103e-002i 9.5065e-001    1.7627e-001+ 9.6354e-002i
-2.1832e-004+ 1.2890e-005i-5.6753e-005    2.5554e-004+ 1.0774e-004i
-1.2440e-001+ 2.3244e-001i 1.9208e-001   -2.0175e-003+ 2.1720e-001i
 1.7548e-004- 2.0088e-004i-6.7851e-005    1.7658e-004+ 4.7808e-005i
-9.5764e-002- 3.0696e-001i 2.2965e-001    1.7903e-002+ 1.4215e-001i
```

Columns 13 through 15

```
 1.1103e-002+ 1.2084e-002i 2.5773e-003    3.5329e-002
-7.0974e-003- 6.3352e-003i-4.8279e-004   -3.6318e-003
 2.5595e-002- 1.6774e-002i 2.4759e-003    3.5976e-002
-1.1371e-001+ 1.4437e-001i 8.7290e-003    6.1836e-002
 6.5566e-003+ 7.2606e-004i 2.0537e-004    3.3652e-003
-9.3980e-003- 4.0907e-003i 3.5666e-002    4.1255e-002
 4.0046e-002- 8.2113e-003i 1.4363e-001    5.2263e-002
-2.7338e-002+ 5.1088e-002i 1.9897e-002    4.2082e-002
 4.9927e-002- 4.0547e-002i 1.2561e-001    6.7530e-002
-1.0013e-002- 8.9122e-004i-2.3406e-004    4.0102e-003
 1.4665e-001- 7.0380e-001i 2.6432e-002   -6.6285e-002
-3.6568e-003- 1.9782e-003i-3.8322e-002    4.3431e-002
 2.0874e-002- 2.4963e-003i-1.6473e-001    5.7774e-002
-1.4743e-002+ 2.5708e-002i-4.1228e-003    4.4242e-002
 2.6416e-002- 1.3510e-002i-1.5131e-001    7.1933e-002
-6.6088e-003- 9.3654e-004i 1.4844e-003    3.9576e-003
 1.3273e-001- 5.5743e-001i-7.6935e-002   -6.0880e-002
 1.9928e-004+ 1.6144e-004i 1.0172e-004    1.8798e-003
 1.7627e-001- 9.6354e-002i-6.4599e-002   -5.0714e-001
 2.5554e-004- 1.0774e-004i 1.1552e-003    2.1765e-003
-2.0175e-003- 2.1720e-001i-7.3366e-001   -5.8716e-001
```

```
 1.7658e-004- 4.7808e-005i-9.4647e-004                2.2252e-003
 1.7903e-002- 1.4215e-001i 6.0106e-001               -6.0032e-001

  Columns 16 through 18
-1.0874e-001- 4.8941e-002i-1.0874e-001+ 4.8941e-002i-2.4569e-001
 1.2010e-002- 3.1290e-002i 1.2010e-002+ 3.1290e-002i-4.9438e-001
-1.0663e-001- 4.2204e-002i-1.0663e-001+ 4.2204e-002i-2.0784e-001
-4.4508e-002- 3.2723e-002i-4.4508e-002+ 3.2723e-002i-5.0990e-001
-7.8689e-003- 9.4273e-003i-7.8689e-003+ 9.4273e-003i-3.6472e-002
-8.2516e-002- 4.9495e-003i-8.2516e-002+ 4.9495e-003i-4.9275e-002
-6.4622e-003- 1.1992e-002i-6.4622e-003+ 1.1992e-002i-1.1758e-001
-8.8503e-002- 4.0943e-003i-8.8503e-002+ 4.0943e-003i-5.3112e-002
-2.5819e-002- 1.7407e-002i-2.5819e-002+ 1.7407e-002i-1.7029e-001
-8.2039e-003- 9.2863e-003i-8.2039e-003+ 9.2863e-003i-3.7619e-002
 8.8374e-002+ 1.3019e-002i 8.8374e-002- 1.3019e-002i 3.4155e-001
-8.0021e-002- 4.0865e-003i-8.0021e-002+ 4.0865e-003i-4.2971e-002
-5.2933e-003- 1.5330e-002i-5.2933e-003+ 1.5330e-002i-1.4170e-001
-8.9288e-002- 4.0144e-003i-8.9288e-002+ 4.0144e-003i-5.4301e-002
-2.0709e-002- 2.0203e-002i-2.0709e-002+ 2.0203e-002i-1.8907e-001
-8.1906e-003- 9.2807e-003i-8.1906e-003+ 9.2807e-003i-3.7555e-002
 8.6270e-002+ 1.0148e-002i 8.6270e-002- 1.0148e-002i 3.2247e-001
-4.7608e-003- 6.6123e-003i-4.7608e-003+ 6.6123e-003i-2.8914e-002
 5.5617e-001- 3.1758e-001i 5.5617e-001+ 3.1758e-001i 1.8624e-001
-4.4903e-003- 4.6257e-003i-4.4903e-003+ 4.6257e-003i-1.5878e-002
 3.9863e-001- 3.1284e-001i 3.9863e-001+ 3.1284e-001i 1.0222e-001
-4.3636e-003- 4.6980e-003i-4.3636e-003+ 4.6980e-003i-1.7014e-002
 4.0325e-001- 3.0233e-001i 4.0325e-001+ 3.0233e-001i 1.0965e-001

Columns 19 through 21
-8.0944e-002- 1.0337e-001i-8.0944e-002+ 1.0337e-001i-3.1669e-002- 2.0039e-003i
 7.5008e-002+ 8.3991e-003i 7.5008e-002- 8.3991e-003i 1.6439e-002- 9.7063e-003i
-8.4390e-002- 9.8221e-002i-8.4390e-002+ 9.8221e-002i-3.1270e-002- 7.8096e-004i
 8.0222e-002+ 4.9460e-002i 8.0222e-002- 4.9460e-002i 2.8252e-002- 4.6126e-003i
-2.8141e-003+ 1.6586e-004i-2.8141e-003- 1.6586e-004i 1.4866e-004+ 1.7172e-003i
 8.4898e-002+ 1.3484e-001i 8.4898e-002- 1.3484e-001i-8.6853e-002- 3.7316e-002i
-6.1924e-002- 6.4292e-002i-6.1924e-002+ 6.4292e-002i 5.7091e-002+ 1.7063e-002i
 9.1545e-002+ 1.3813e-001i 9.1545e-002- 1.3813e-001i-8.8999e-002- 3.5823e-002i
-6.5699e-002- 6.7152e-002i-6.5699e-002+ 6.7152e-002i 6.2928e-002+ 1.9898e-002i
-2.0118e-003+ 1.8954e-004i-2.0118e-003- 1.8954e-004i 1.9716e-005+ 1.7572e-003i
-2.2468e-001- 2.7348e-001i-2.2468e-001+ 2.7348e-001i 6.2401e-002+ 4.2615e-002i
 1.4884e-002+ 7.7970e-002i 1.4884e-002- 7.7970e-002i 2.4357e-001+ 6.6970e-002i
-1.9876e-002- 4.5618e-002i-1.9876e-002+ 4.5618e-002i-1.7652e-001- 2.5535e-002i
```

```
 1.8313e-002+ 8.1383e-002i 1.8313e-002- 8.1383e-002i 2.5049e-001+ 6.0896e-002i
-2.1323e-002- 4.7475e-002i-2.1323e-002+ 4.7475e-002i-1.9155e-001- 2.9481e-002i
-2.2497e-003+ 2.4134e-004i-2.2497e-003- 2.4134e-004i 6.4604e-004+ 1.2904e-003i
-1.3853e-001- 2.0946e-001i-1.3853e-001+ 2.0946e-001i-3.6025e-001- 6.9449e-002i
 1.5591e-003- 5.4996e-003i 1.5591e-003+ 5.4996e-003i-5.5348e-004- 9.3710e-004i
 4.2342e-001- 2.4910e-001i 4.2342e-001+ 2.4910e-001i 3.6765e-003- 9.6575e-002i
-4.0038e-003+ 5.5104e-003i-4.0038e-003- 5.5104e-003i 5.1719e-005- 3.0373e-003i
-5.7595e-001+ 1.0460e-001i-5.7595e-001- 1.0460e-001i 1.4975e-001- 2.2437e-001i
-2.9540e-003+ 1.8921e-003i-2.9540e-003- 1.8921e-003i 9.8224e-004+ 8.2831e-003i
-2.9588e-001- 5.7848e-002i-2.9588e-001+ 5.7848e-002i-3.2448e-001+ 6.6585e-001i
```

Columns 22 through 23

```
-3.1669e-002+ 2.0039e-003i 2.2711e-002
 1.6439e-002+ 9.7063e-003i-3.9545e-002
-3.1270e-002+ 7.8096e-004i 3.7557e-002
 2.8252e-002+ 4.6126e-003i-1.0521e-001
 1.4866e-004- 1.7172e-003i-4.6451e-001
-8.6853e-002+ 3.7316e-002i-1.4834e-002
 5.7091e-002- 1.7063e-002i 3.3028e-002
-8.8999e-002+ 3.5823e-002i-3.4964e-002
 6.2928e-002- 1.9898e-002i 4.3421e-002
 1.9716e-005- 1.7572e-003i-4.6459e-001
 6.2401e-002- 4.2615e-002i 3.1953e-001
 2.4357e-001- 6.6970e-002i-3.2388e-002
-1.7652e-001+ 2.5535e-002i 5.0142e-002
 2.5049e-001- 6.0896e-002i-5.1564e-002
-1.9155e-001+ 2.9481e-002i 6.0762e-002
 6.4604e-004- 1.2904e-003i-4.6460e-001
-3.6025e-001+ 6.9449e-002i 3.2720e-001
-5.5348e-004+ 9.3710e-004i-1.8087e-003
 3.6765e-003+ 9.6575e-002i-1.8551e-001
 5.1719e-005+ 3.0373e-003i 2.1041e-003
 1.4975e-001+ 2.2437e-001i 2.1582e-001
 9.8224e-004- 8.2831e-003i 1.7838e-003
-3.2448e-001- 6.6585e-001i 1.8297e-001
```

The left eigenvectors of the nine-bus system are:

Columns 1 through 3

```
-9.8379e-003              -2.4532e-001              -4.3061e-001
 2.0971e-003               5.0636e-003              -2.2092e-002
 1.3387e-002               3.2006e-001               5.0069e-001
```

```
-7.9123e-003              -1.8243e-002               6.8670e-002
-6.4366e-002              -5.1888e-001              -6.0388e-002
 2.8247e-001               2.7597e-001              -2.6488e-002
 6.7691e-003               9.2019e-003              -8.9742e-004
-3.7568e-001              -3.1092e-001               2.0598e-002
-3.1072e-002              -3.3957e-002               2.0191e-003
 5.9135e-001               2.4099e-001               3.3824e-002
-6.5835e-002              -2.5124e-002              -2.9785e-003
-1.7070e-001               2.2454e-001              -2.0532e-002
-4.7540e-004               3.0210e-003              -7.0771e-004
 2.5340e-001              -2.7663e-001               1.6871e-002
 1.1759e-002              -3.1090e-002               2.4877e-003
-5.2700e-001               2.7925e-001               2.6749e-002
 5.8652e-002              -2.9103e-002              -2.3546e-003
-6.9055e-003              -2.1563e-001              -7.4057e-001
 1.2086e-004               3.5341e-003               1.0254e-002
 1.8113e-001               2.2160e-001              -4.1616e-002
-3.1701e-003              -3.6318e-003               5.7621e-004
-1.0965e-001               1.8061e-001              -3.2313e-002
 1.9190e-003              -2.9601e-003               4.4740e-004
```

Columns 4 through 6

```
-1.4597e-003+ 1.2610e-003i-1.4597e-003- 1.2610e-003i 1.6855e-002
 1.6442e-003- 2.4111e-003i 1.6442e-003+ 2.4111e-003i-1.4109e-002
-8.9479e-004- 1.4157e-003i-8.9479e-004+ 1.4157e-003i-1.6292e-002
 3.8135e-003+ 3.1870e-003i 3.8135e-003- 3.1870e-003i 3.5294e-002
 1.5419e-002+ 1.7171e-001i 1.5419e-002- 1.7171e-001i 2.6166e-001
-1.6312e-002+ 7.3963e-003i-1.6312e-002- 7.3963e-003i 2.1044e-002
 7.7238e-003- 2.0379e-003i 7.7238e-003+ 2.0379e-003i 3.0667e-001
-2.1636e-003- 2.5667e-003i-2.1636e-003+ 2.5667e-003i-1.0400e-002
 6.2621e-003+ 3.0400e-003i 6.2621e-003- 3.0400e-003i-3.6603e-001
 1.7282e-001+ 5.7969e-001i 1.7282e-001- 5.7969e-001i-6.6478e-001
-2.2934e-002+ 4.5296e-003i-2.2934e-002- 4.5296e-003i 4.5808e-002
 2.3905e-002- 1.0032e-002i 2.3905e-002+ 1.0032e-002i 8.1960e-003
-9.5030e-003+ 1.5100e-003i-9.5030e-003- 1.5100e-003i-9.9438e-002
 2.9943e-003+ 3.6746e-003i 2.9943e-003- 3.6746e-003i-4.1772e-003
-7.2126e-003- 3.0357e-003i-7.2126e-003+ 3.0357e-003i 1.3511e-001
-1.8648e-001- 7.5183e-001i-1.8648e-001+ 7.5183e-001i 4.0235e-001
 2.9600e-002- 4.4512e-003i 2.9600e-002+ 4.4512e-003i-2.7711e-002
 2.5981e-003+ 4.9461e-004i 2.5981e-003- 4.9461e-004i 1.6256e-001
-4.5164e-006+ 1.5410e-005i-4.5164e-006- 1.5410e-005i-1.7617e-003
 1.9951e-002+ 1.0259e-002i 1.9951e-002- 1.0259e-002i 1.8541e-001
```

```
-7.3724e-005+ 1.1454e-004i -7.3724e-005- 1.1454e-004i -2.0094e-003
-2.8495e-002- 1.5688e-002i -2.8495e-002+ 1.5688e-002i  7.2334e-002
 1.1156e-004- 1.6298e-004i  1.1156e-004+ 1.6298e-004i -7.8393e-004
```

Columns 7 through 9

```
-5.3996e-003   6.7007e-002  -1.2437e-001
 3.2842e-002  -1.0026e-002   5.1883e-002
 4.9772e-003  -5.5243e-002   9.2673e-002
-7.7721e-002   2.1107e-002  -9.7897e-002
-5.6981e-001   1.1241e-001  -4.9978e-001
-6.8788e-003  -5.4734e-002  -2.6780e-002
-1.2829e-001  -1.2326e-001   1.1661e-002
 3.0713e-003   1.9863e-002   8.1585e-003
 1.3106e-001   8.9438e-002  -6.0951e-003
 4.7433e-002  -7.0955e-002   2.9074e-001
-3.0769e-003   4.0479e-003  -1.4814e-002
-8.9049e-003  -3.9422e-002  -1.5173e-002
-2.8598e-001  -9.0933e-002   1.3722e-002
 4.0629e-003   1.4550e-002   4.6793e-003
 3.1559e-001   6.4250e-002  -6.3342e-003
 5.2489e-001  -4.1985e-002   2.1168e-001
-3.4031e-002   2.3938e-003  -1.0779e-002
-1.9383e-001  -7.1027e-001   7.4456e-001
 1.9777e-003   6.3746e-003  -5.9694e-003
-2.2558e-001   5.3002e-001   1.4646e-001
 2.3017e-003  -4.7568e-003  -1.1742e-003
-2.9253e-001   3.8240e-001   8.3124e-002
 2.9847e-003  -3.4320e-003  -6.6643e-004
```

Columns 10 through 12

```
-3.8755e-003  -5.2539e-002  -2.9061e-003- 7.2797e-003i
-1.4389e-003  -8.3646e-002   4.8255e-003+ 7.8517e-003i
 3.3344e-003   3.0347e-002   3.8422e-003- 1.9772e-003i
 3.1361e-003   1.2211e-001  -8.0403e-003+ 5.0121e-003i
 2.3749e-002   7.6515e-001  -7.7772e-001+ 2.5710e-002i
-3.7432e-002  -3.3499e-002   4.6388e-004+ 2.0506e-002i
-7.4328e-002  -6.4830e-002  -1.3330e-004- 4.5577e-004i
 1.4700e-002   6.9337e-003  -2.2249e-003+ 7.3598e-004i
 6.1728e-002   1.2373e-002   7.6177e-005- 3.1885e-004i
 6.3520e-002  -4.5675e-001   5.9808e-001- 1.1206e-002i
-3.8083e-003   1.7944e-002  -9.9447e-004+ 1.3793e-002i
 4.1932e-002  -3.2451e-002   1.0720e-004+ 9.0892e-003i
```

```
 1.0648e-001              -4.6655e-002              -3.8963e-004+ 1.0910e-003i
-1.6790e-002               6.7452e-003              -9.6516e-004+ 3.1033e-004i
-8.9602e-002               4.6648e-003              -5.3392e-004+ 5.6997e-004i
-8.7420e-002              -3.1365e-001               1.8074e-001- 5.7092e-003i
 5.2383e-003               1.2311e-002              -2.4091e-004+ 4.1728e-003i
 7.3486e-002               2.0929e-001              -1.3098e-002+ 1.4445e-002i
-6.9306e-004              -1.2944e-003              -4.7752e-005- 5.2315e-005i
 6.4841e-001               1.2191e-001               4.1408e-002- 2.1404e-002i
-6.1153e-003              -7.5395e-004               6.3220e-005+ 1.5708e-004i
-7.2760e-001               1.1829e-001               1.8484e-002- 9.3022e-003i
 6.8622e-003              -7.3161e-004               2.7308e-005+ 7.0032e-005i
```

Columns 13 through 15

```
-2.9061e-003+ 7.2797e-003i 3.1693e-003               1.1579e-001
 4.8255e-003- 7.8517e-003i 3.2446e-003               7.3569e-002
 3.8422e-003+ 1.9772e-003i-5.4421e-004              -2.9750e-003
-8.0403e-003- 5.0121e-003i-1.7698e-003              -1.8612e-002
-7.7772e-001- 2.5710e-002i 4.0485e-002               2.7782e-001
 4.6388e-004- 2.0506e-002i-8.5484e-002              -1.8637e-002
-1.3330e-004+ 4.5577e-004i-1.1323e-001              -8.5362e-002
-2.2249e-003- 7.3598e-004i 4.6639e-003               3.1391e-004
 7.6177e-005+ 3.1885e-004i-3.5290e-002              -3.6946e-002
 5.9808e-001+ 1.1206e-002i-5.7634e-001              -8.2203e-002
-9.9447e-004- 1.3793e-002i 9.3482e-003               7.6656e-004
 1.0720e-004- 9.0892e-003i 9.7235e-002              -4.3509e-002
-3.8963e-004- 1.0910e-003i 9.5971e-002              -7.0252e-002
-9.6516e-004- 3.1033e-004i-5.3166e-003               7.6096e-004
-5.3392e-004- 5.6997e-004i 3.5490e-002              -3.3110e-002
 1.8074e-001+ 5.7092e-003i 5.3634e-001              -2.0397e-001
-2.4091e-004- 4.1728e-003i-8.6812e-003               1.8951e-003
-1.3098e-002- 1.4445e-002i-1.5535e-002              -8.5761e-001
-4.7752e-005+ 5.2315e-005i 3.9792e-005               1.2679e-003
 4.1408e-002+ 2.1404e-002i 3.8278e-001               1.2610e-001
 6.3220e-005- 1.5708e-004i-9.8048e-004              -1.8643e-004
 1.8484e-002+ 9.3022e-003i-4.3615e-001               2.9489e-001
 2.7308e-005- 7.0032e-005i 1.1172e-003              -4.3599e-004
```

Columns 16 through 18

```
-5.4779e-002+ 1.3447e-002i-5.4779e-002- 1.3447e-002i-2.4789e-002- 6.5416e-004i
-3.6114e-002- 1.4784e-002i-3.6114e-002+ 1.4784e-002i-2.1733e-003- 9.5804e-003i
-7.1671e-003- 1.2090e-003i-7.1671e-003+ 1.2090e-003i-4.1176e-003- 1.1652e-003i
 6.3107e-004- 3.7062e-003i 6.3107e-004+ 3.7062e-003i 4.9670e-004- 1.2226e-003i
```

```
 7.7631e-003+ 1.1326e-002i 7.7631e-003- 1.1326e-002i 5.5127e-002- 1.8393e-002i
-1.8425e-002+ 1.1825e-002i-1.8425e-002- 1.1825e-002i 2.4341e-002+ 4.6396e-003i
 4.5537e-004- 8.1936e-003i 4.5537e-004+ 8.1936e-003i-2.4327e-003+ 3.0480e-003i
-3.9330e-004- 1.5369e-005i-3.9330e-004+ 1.5369e-005i 5.5360e-004+ 3.1121e-004i
 5.1140e-004- 4.3615e-003i 5.1140e-004+ 4.3615e-003i-1.4521e-003+ 1.6576e-003i
-4.6955e-003+ 7.8994e-004i-4.6955e-003- 7.8994e-004i-4.8136e-002+ 1.1319e-002i
 1.2775e-005- 1.2333e-005i 1.2775e-005+ 1.2333e-005i 3.2905e-005- 9.4551e-005i
-1.0475e-002+ 3.7135e-003i-1.0475e-002- 3.7135e-003i 5.4713e-003+ 4.1307e-003i
 4.5737e-004- 6.2053e-003i 4.5737e-004+ 6.2053e-003i-1.2826e-003+ 7.4487e-004i
-1.7979e-004- 5.5188e-005i-1.7979e-004+ 5.5188e-005i 9.2547e-005+ 1.3836e-004i
 4.1433e-004- 3.4211e-003i 4.1433e-004+ 3.4211e-003i-7.5545e-004+ 4.0380e-004i
-3.0222e-003- 1.3171e-002i-3.0222e-003+ 1.3171e-002i-1.2826e-002+ 2.2863e-003i
 3.6972e-005+ 3.3688e-005i 3.6972e-005- 3.3688e-005i 9.5795e-006- 2.4324e-005i
 8.8159e-001+ 2.8476e-001i 8.8159e-001- 2.8476e-001i 4.0980e-001+ 5.9600e-001i
-5.3227e-004+ 1.5061e-004i-5.3227e-004- 1.5061e-004i-2.3546e-004+ 2.5856e-007i
 3.2845e-001- 5.7196e-003i 3.2845e-001+ 5.7196e-003i-2.8145e-001- 5.9727e-001i
-1.6126e-004+ 1.1166e-004i-1.6126e-004- 1.1166e-004i 2.1217e-004+ 3.4429e-005i
 1.6329e-001+ 3.5226e-002i 1.6329e-001- 3.5226e-002i 3.2852e-003- 1.8296e-001i
-9.2785e-005+ 3.6599e-005i-9.2785e-005- 3.6599e-005i 4.8510e-005+ 3.4573e-005i

  Columns 19 through 21
-2.4789e-002+ 6.5416e-004i-4.1001e-003- 4.6800e-003i-4.1001e-003+ 4.6800e-003i
-2.1733e-003+ 9.5804e-003i 1.3533e-003- 1.3050e-003i 1.3533e-003+ 1.3050e-003i
-4.1176e-003+ 1.1652e-003i-5.6118e-004- 9.7138e-004i-5.6118e-004+ 9.7138e-004i
 4.9670e-004+ 1.2226e-003i 2.5324e-004- 8.0183e-005i 2.5324e-004+ 8.0183e-005i
 5.5127e-002+ 1.8393e-002i 1.3099e-002+ 5.0411e-004i 1.3099e-002- 5.0411e-004i
 2.4341e-002- 4.6396e-003i-4.5745e-003- 1.4991e-002i-4.5745e-003+ 1.4991e-002i
-2.4327e-003- 3.0480e-003i 1.8409e-003+ 3.6077e-004i 1.8409e-003- 3.6077e-004i
 5.5360e-004- 3.1121e-004i-1.9686e-005- 4.2137e-004i-1.9686e-005+ 4.2137e-004i
-1.4521e-003- 1.6576e-003i 1.0421e-003+ 2.4453e-004i 1.0421e-003- 2.4453e-004i
-4.8136e-002- 1.1319e-002i 1.6450e-002+ 2.1098e-002i 1.6450e-002- 2.1098e-002i
 3.2905e-005+ 9.4551e-005i-4.1127e-005+ 8.1227e-006i-4.1127e-005- 8.1227e-006i
 5.4713e-003- 4.1307e-003i 8.3594e-003+ 2.2166e-002i 8.3594e-003- 2.2166e-002i
-1.2826e-003- 7.4487e-004i-3.8455e-003- 2.5675e-004i-3.8455e-003+ 2.5675e-004i
 9.2547e-005- 1.3836e-004i 6.2312e-005+ 6.0117e-004i 6.2312e-005- 6.0117e-004i
-7.5545e-004- 4.0380e-004i-2.2324e-003- 2.1300e-004i-2.2324e-003+ 2.1300e-004i
-1.2826e-002- 2.2863e-003i-3.0261e-002- 2.4368e-002i-3.0261e-002+ 2.4368e-002i
 9.5795e-006+ 2.4324e-005i 5.4423e-005- 2.5964e-005i 5.4423e-005+ 2.5964e-005i
 4.0980e-001- 5.9600e-001i-7.1709e-002+ 2.2118e-001i-7.1709e-002- 2.2118e-001i
-2.3546e-004- 2.5856e-007i-3.9678e-005- 4.3298e-005i-3.9678e-005+ 4.3298e-005i
-2.8145e-001+ 5.9727e-001i-3.5953e-001+ 3.9631e-001i-3.5953e-001- 3.9631e-001i
 2.1217e-004- 3.4429e-005i-4.2326e-005- 1.2835e-004i-4.2326e-005+ 1.2835e-004i
 3.2852e-003+ 1.8296e-001i 5.0456e-001- 6.3384e-001i 5.0456e-001+ 6.3384e-001i
```

```
4.8510e-005- 3.4573e-005i 7.6468e-005+ 1.8980e-004i 7.6468e-005- 1.8980e-004i
```

Columns 22 through 23

```
-4.8095e-002                5.9629e-004
-9.2280e-002               -7.2553e-005
-5.8848e-003                1.1280e-004
-2.4888e-003               -1.1954e-005
-3.5544e-003               -4.9770e-001
 6.0194e-003                5.1696e-004
-1.9746e-003               -1.5383e-005
 9.1573e-005                1.5513e-005
-1.0576e-003               -8.8253e-006
 5.1681e-003               -2.2542e-001
-1.5260e-005               -3.3510e-005
 3.0076e-003                4.5242e-004
-1.6295e-003               -1.6415e-005
 4.2217e-005                1.2871e-005
-9.0318e-004               -9.6820e-006
-1.3214e-003               -1.0744e-001
 3.8568e-006               -1.9620e-005
 9.8647e-001                5.7191e-001
-4.7099e-004                5.5538e-006
-1.1279e-001                4.5296e-001
 5.3852e-005                4.3987e-006
-5.6453e-002                3.9709e-001
 2.6953e-005                3.8561e-006
```

Appendix F

Model Reduction Using Balanced Truncation

In this section, we present the results of the model reduction procedure using the method of balanced truncation described in section 4.3.3. The reduced order models given in this appendix were used in Chapter 4 to design low order H_∞^--based controllers.

The model of the nine-bus system that we wish to reduce is given in *Appendix E*. The original system has 24 states. The system consists of three generator subsystems. Each generator subsystem has eight states. We apply the method of balanced truncation to each subsystem in order to obtain reduced models for the three subsystems. We demonstrate this procedure for each subsystem in the the next sections.

Generator Subsystem 1

The full-order model of subsystem 1 has eight states with the following state space description:

A =

1.0e+003 *

[-0.0037	0.0000	0.0034	-0.0001	0	0.0001	0	0.0002
0.0001	-0.0013	-0.0005	0.0004	0	0.0000	0	0
0.0198	0.0000	-0.0219	-0.0005	0	-0.0012	0	0
-0.0006	0.0078	0.0021	-0.0139	0	0.0046	0	0
0.0000	0.0000	-0.0001	0.0001	0.0000	-0.0001	0	0
0	0	0	0	0.3142	0	0	0
0.0000	0.0000	-0.0001	0.0000	0	0.0000	-0.0001	0
0.0542	0.0036	-0.1783	-0.0650	0	0.0043	2.0000	-0.0200]

B = [0

0

0

0

0

0

0.0900

200.0000]

C = [-0.2712 -0.01810.89130.3252 0 -0.0215 0 0]

D = [0]

The eigenvalues and damping of subsystem 1 are given in Table F1.

Eigenvalue	Damping
-3.7711e-001+ 4.8454e+000i	**7.7595e-002**
-3.7711e-001- 4.8454e+000i	**7.7595e-002**
-6.4220e-001+ 5.8664e-001i	7.3832e-001
-6.4220e-001- 5.8664e-001i	7.3832e-001
-1.1117e+000	1.0000e+000
-1.3254e+001	1.0000e+000
-1.6554e+001	1.0000e+000
-2.7941e+001	1.0000e+000

Table F1: Eigenvalues and Damping of Subsystem 1

From Table F1, we note that there is a weakly damped mode $\lambda = -3.7711e-01 \pm 4.8454$ with a damping of 7.7595e-002. This corresponds to the electromechanical mode of subsystem 1.

The zeros of subsystem 1 are given in Table F2.

Zeros
43.1436
-14.3042
-0.4060 + 4.6718i
-0.4060 - 4.6718i
-0.8515
-1.0000

Table F2: Zeros of Subsystem 1

Table F2 illustrates that subsystem 1 has a non-minimum-phase zero $z = 43.1436$. This zero in fact corresponds to a zero approaching infinity. The value of $z = 43.1436$ is obtained due to limitations in the algorithm used in calculating the zeros [1,2].

The transformation for balanced realization T is given by the following:

$T =$

1.8567	1.1113	-0.3566	-0.0612	0.4279	-1.0284	0.2930	0.2783
-0.2978	-1.1280	-0.3635	-0.0072	0.3014	-0.1461	-0.7078	0.1472
1.7351	1.4742	-0.5764	-0.6436	0.8494	0.1800	0.1735	0.7785
-0.6166	-1.4400	-0.9433	2.0594	-0.7467	0.2693	-0.3988	-1.9629
-0.0059	0.0196	0.0785	0.0136	0.0848	-0.0020	0.0047	0.0129
-2.0477	-2.6341	-0.5656	7.7999	-1.5906	0.6256	-0.4897	-0.1678
0.0782	-0.0538	-0.0088	0.0020	0.0142	-0.0018	-0.0037	0.0002
13.6893	-49.7137	88.4185	15.4943	-86.6276	114.0217	-14.9717	-45.7957

The hankel singular values (HSV) of subsystem 1 are given in Table F3.

HSV
0.6277
0.1178
0.0515
0.0443
0.0294
0.0038
0.0004
0.0000

Table F3: Hankel Singular Values for Subsystem 1

Removing three states from the system, we obtain the reduced model of subsystem 1. The reduced model of subsystem 1 is given by the following:

Ar = [

[0.9484	-1.7417	-37.4556	-2.0937	8.5774
0.8947	-3.8829	-70.6488	-12.8337	12.1372
-0.6702	1.0358	-2.7938	-1.2784	-1.5285
0.1671	-0.0415	13.7239	2.0618	-1.1850
-3.1563	2.5347	-16.3129	-8.7427	-6.5625]

Br = [1.4172
0.2362
2.1506
-1.7816
9.0144]

Cr = [0.3396 -0.2509 -0.3721 -0.1552 -0.0183]

Dr = [0]

The L_∞ error in the reduced order model is equal to0.0083

The poles of the reduced order model of subsystem 1 are:

Eigenvalue	Damping,
-0.5606 + 4.8429i	0.1150
-0.5606 - 4.8429i	0.1150
-0.6485 + 0.4935i	0.7958
-0.6485 - 0.4935i	0.7958
-7.8110	1.0000

Table F4: Eigenvalues and Damping of Reduced Model for Subsystem 1

The zeros of the reduced model are:

Zeros
33.6065
-0.5693 + 4.5637i
-0.5693 - 4.5637i
-0.6149

Table F5: Zeros of Reduced Model for Subsystem 1

Table F4 illustrates that the stability of the system is retained by the method of balanced truncation. However, the eigenvalues of the reduced system is different from the full order model. The damping of the electromechanical mode has been significantly increased in the reduced model; from 7.7595e-002 to 0.1150. Therefore, the reduced model would provide

results which are optimistic as compared to the full order model for the electromechanical mode damping.

Table F5 illustrates that the zeros of the reduced model is different from the zeros of the full model. However, the right-half-plane zero of the full model of subsystem 1 has been retained.

Figure F1 illustrates that the singular value plots of the full model and the reduced model match closely over the fequency range 0.01 to 100 radians per second. The accuracy of the reduced model is also illustrated in the time-domain simulation plot of Figure F2.

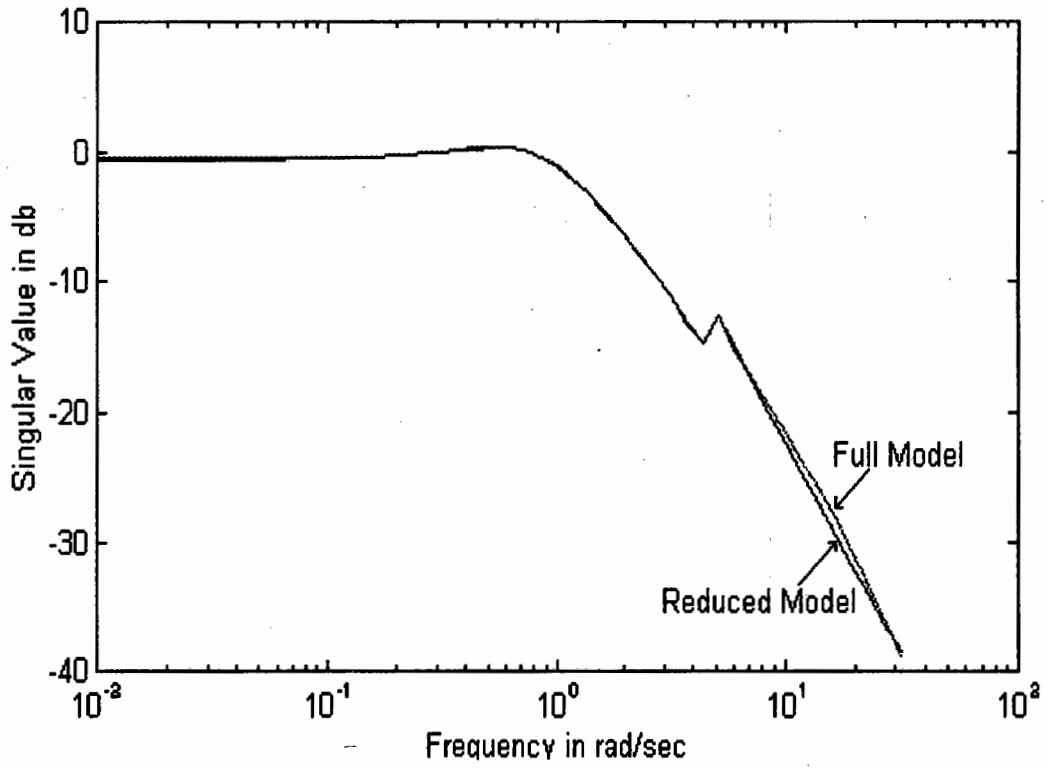

Figure F1: Singular Value Plots of Subsystem 1

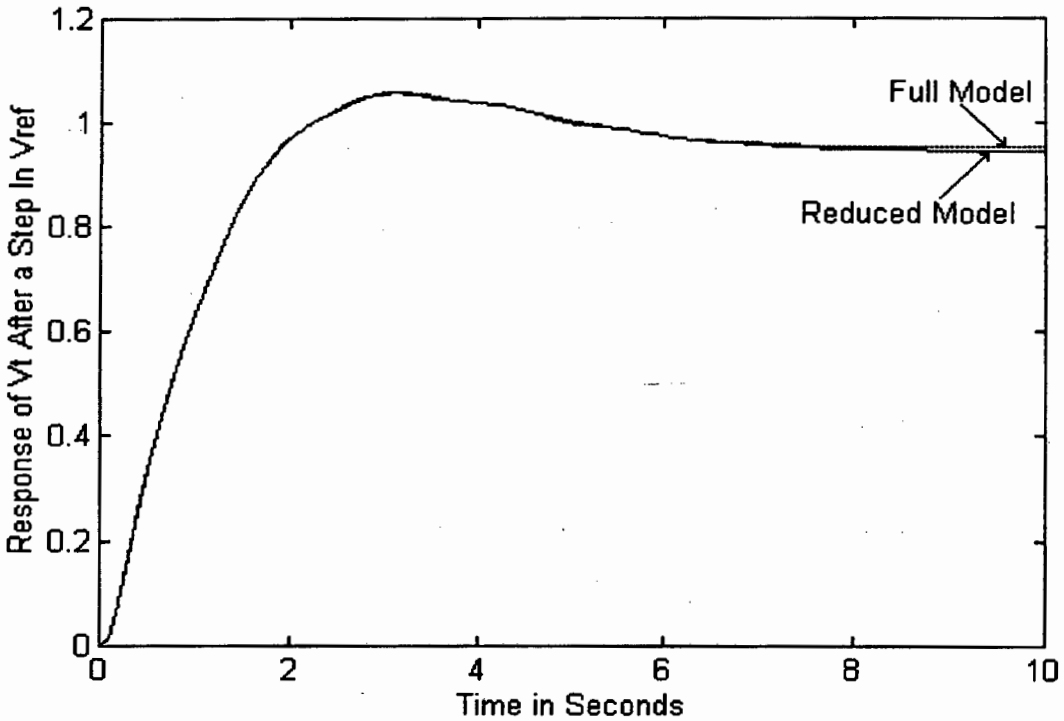

Figure F2: Step Response of Terminal Voltage After a Step in V_{ref} of Generator 1

Generator Subsystem 2

The full-order model of subsystem 2 has eight states with the following state space description:

A =

```
1.0e+003 *
 [-0.0012    ,0.0000    0.0007    -0.0001   0         -0.0002   0         0.0002
  -0.0007    -0.0086    -0.0006   0.0044    0         0.0005    0         0
  0.0271     -0.0003    -0.0332   -0.0009   0         -0.0051   0         0
  0.0006     0.0115     0.0005    -0.0170   0         0.0029    0         0
  -0.0001    0.0000     -0.0001   0.0000    -0.0001   -0.0002   0         0
  0          0          0         0         0.3142    0         0         0
  0.0000     0.0000     0.0000    0.0000    0         0.0000    -0.0001   0
  -0.0577    -0.0248    -0.0510   -0.0751   0         0.0102    2.0000    -0.0200 ]
```

```
B= [ 0
     0
     0
     0
     0
     0
    0.0900
    200.0000]
```

```
C = [ 0.28870.12390.25520.3756 0 -0.0512 0 0]
```

D = [0]

The eigenvalues of the subsystem 2 are:

Eigenvalue	Damping
-0.4419 + 8.0545i	0.0548
-0.4419 - 8.0545i	0.0548
-0.4754 + 0.6215i	0.6075
-0.4754 - 0.6215i	0.6075
-4.8158	1.0000
-18.1516	1.0000
-21.3616	1.0000
-33.9930	1.0000

Table F6: Eigenvalues and Damping of Subsystem 2

From Table F6, we note that there is a weakly damped mode $\lambda = -0.4419 \pm 8.0545i$ with a damping of 0.0548. This corresponds to the electromechanical mode of subsystem 2.

The zeros of subsystem 1 are given in Table F7.

Zeros
57.0873
-21.7474
-0.7813 + 8.4365i
-0.7813 - 8.4365i
-2.8003
-1.0000

Table F7: Zeros of Subsystem 2

Table F7 illustrates that subsystem 1 has a non-minimum-phase zero $z = 57.0873$. As in the case of subsystem 1, this zero corresponds to a zero approaching infinity.

The transformation for balanced realization T is given by the following:

$T =$

2.1374	1.3102	-0.3175	-0.5067	1.7273	-0.9569	-1.0551	-0.7294
-0.8123	-1.0547	-0.0839	1.0903	-0.6569	1.3944	0.1152	-0.9575
2.1472	1.5572	-0.9749	-1.4057	1.7463	-1.3047	1.2557	-2.3218
-0.8379	-1.0644	0.2057	1.5611	-0.4145	1.0719	0.3861	2.4831
-0.0074	0.0157	0.0853	-0.1203	0.0483	0.0201	-0.0088	-0.0204
-2.7368	-2.0270	4.6644	4.6088	0.8944	-0.1111	0.1013	0.3007
0.0765	-0.0649	-0.0005	0.0045	0.0004	0.0085	0.0006	0.0000
12.8774	-28.1644	57.5111	20.6174	-200.8426	88.7029	115.9683	90.8592

The hankel singular values (HSV) of subsystem 2 are given in Table F8.

HSV
0.6403
0.1544
0.0598
0.0586
0.0131
0.0110
0.0004
0.0000

Table F8: Hankel Singular Values for Subsystem 2

Removing three states from the system, we obtain the reduced model of subsystem 2. The reduced model of subsystem 2 is given by the following:

Ar =

[5.5580e+001	-9.7562e+000	-1.1174e+002	6.9574e+000	7.5810e+000
4.6639e+001	-8.3517e+000	-9.0230e+001	7.5830e+000	2.8435e+000
2.2804e+001	-3.8678e+000	-4.5275e+001	3.2839e+000	2.9789e+000
2.6383e+000	9.1850e-001	-1.3436e+001	-4.7713e+000	2.8294e+000
-2.4276e+001	-2.5646e+000	6.3504e+001	4.8262e+000	-1.7133e+001]

B_r =

[0.1031

-0.0291

0.2322

-3.2523

7.1732]

C_r = [0.3508 -0.3933 0.0841 0.0165 -0.0060]

D_r = [0]

The L_∞ error in the reduced order model is equal to 0.0227 The poles of the reduced order model of subsystem 2 are given in Table F10.

Eigenvalue	Damping
-4.7311e-001+ 5.1281e-001i	6.7808e-001
-4.7311e-001- 5.1281e-001i	6.7808e-001
-5.1433e-001+ 7.7966e+000i	6.5825e-002
-5.1433e-001- 7.7966e+000i	6.5825e-002
-1.7976e+001	1.0000e+000

Table F9: Eigenvalues and Damping of Reduced Model for Subsystem 2

The zeros of the reduced model are:

Zeros
4.4125e+002
-1.1858e+000+ 7.9644e+000i
-1.1858e+000- 7.9644e+000i
-5.9327e-001

Table F10: Zeros of Reduced Model for Subsystem 2

Table F9 illustrates that the stability of the subsystem 2 is retained by the method of balanced truncation. However, the eigenvalues of the reduced system is different from the full order model. The damping of the electromechanical mode has been increased only slightly in the reduced model; from 0.0548 to 0.0793.

Table F10 illustrates that the zeros of the reduced model is different from the zeros of the full model. However, the right-half-plane zero of the full model of subsystem 1 has been retained in the reduced model.

Figure F3 illustrates that the singular value plots of the full model and the reduced model match closely over the fequency range 0.01 to 100 radians per second. The accuracy of the reduced model is also illustrated in the time-domain simulation plot of Figure F2.

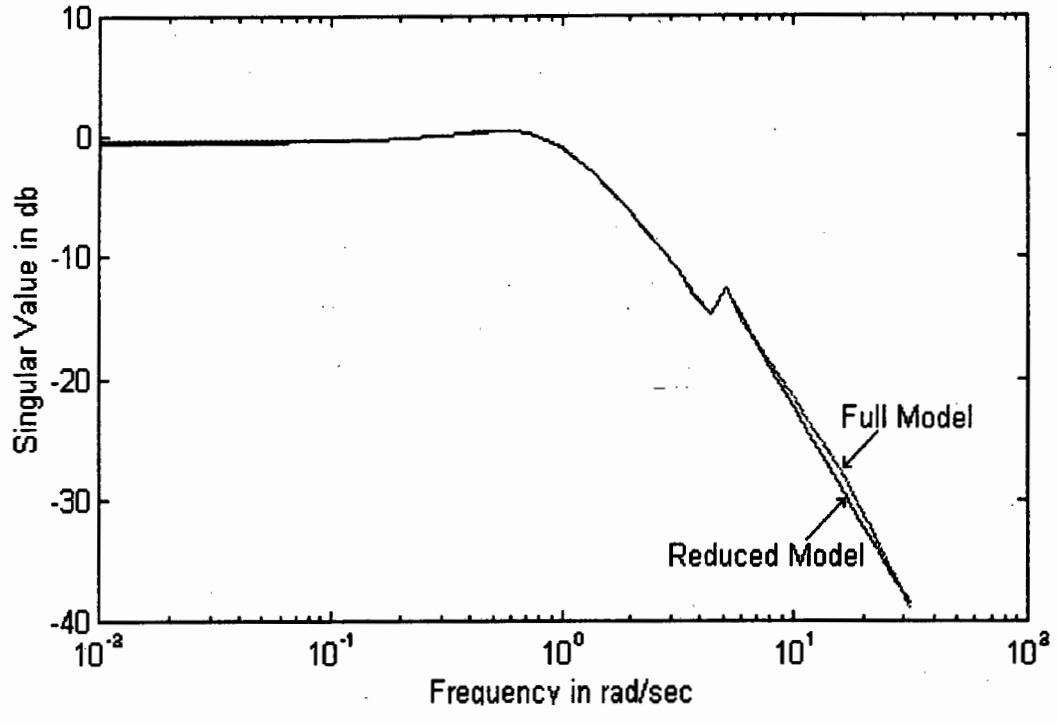

Figure F3: Singular Value Plots for Subsystem 2

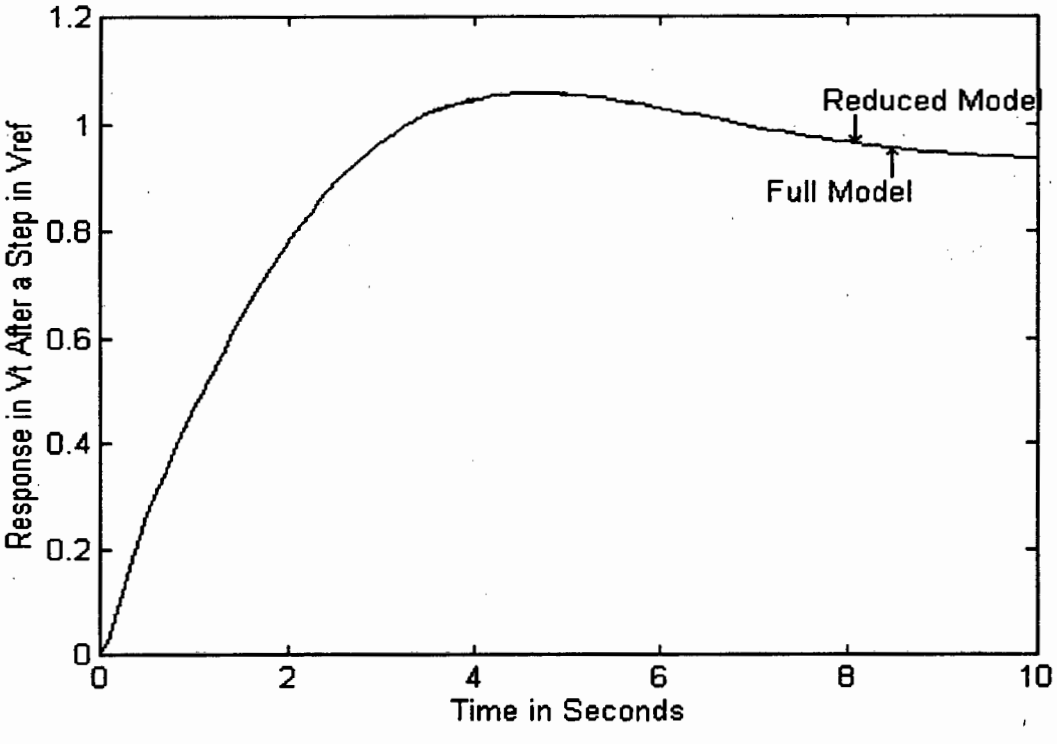

Figure F4: Step Response of Terminal Voltage After a Step in V_{ref} of Generator 2

Generator Subsystem 3

The model reduction of subsystem 3 follows that of subsystems 1 and 2. We therefore present the results without comments.

The full-order model of subsystem 3 has eight states with the following state space description:

A = [

1.0e+003 *

-0.0013	-0.0001	0.0006	-0.0001	0	-0.0002	0	0.0002
-0.0007	-0.0090	-0.0005	0.0044	0	0.0011	0	0.0000
0.0248	-0.0004	-0.0331	-0.0008	0	-0.0063	0	0.0000
0.0005	0.0105	0.0004	-0.0164	0	0.0041	0	0.0000
-0.0002	0.0001	-0.0002	0.0001	-0.0001	-0.0005	0	0.0000
0.0000	0.000	0.0000	0.0000	0.3142	0.0000	0	0.0000
0.0000	0.0000	0.0000	0.0000	0	0.0000	-0.0001	0.0000
-0.0553	-0.0280	-0.0443	-0.0548	0	0.0035	2.0000	-0.0200]

B = [0

0

0

0

0

0

0.0900

00.0000]

C = [

[0.2763 0.1398 0.2217 0.2742 0 -0.0177 0 0]

D = [0]

The eigenvalues of the subsystem 3 are:

Eigenvalue	Damping
-3.8925e-001+ 4.9850e-001i	6.1544e-001
-3.8925e-001- 4.9850e-001i	6.1544e-001
-9.0632e-001+ 1.1260e+001i	8.0228e-002
-9.0632e-001- 1.1260e+001i	8.0228e-002
-4.7089e+000	1.0000e+000
-1.8462e+001	1.0000e+000
-2.0544e+001	1.0000e+000
-3.3667e+001	1.0000e+000

Table F11: Eigenvalues and Damping for Subsystem 3

From Table F11, we note that there is a pair of weakly damped eigenvalues at $\lambda = -9.0632e-001 \pm 1.1260e+001i$ with a damping of 8.0228e-002. This corresponds to the electromechanical mode of subsystem 3.

The zeros of the subsystem 3 are given in Table F12.

Zeros
-5.3014e+001
-1.4401e+000+ 1.1526e+001i
-1.4401e+000- 1.1526e+001i
-2.0657e+001
-2.0878e+000
-1.0000e+000

Table F12: Zeros of Subsystem 3

The transformation for balanced realization T is given by the following:

T =

2.6728	1.8443	-1.1067	-0.9559	0.7154	1.6991	1.0643	-0.9827
-1.3828	-1.7809	2.0269	-0.0977	-1.0577	-1.0207	-0.1239	-1.7642
2.6279	2.1165	-2.2846	-1.3134	0.2571	1.6895	-1.4280	-2.6433
-1.4978	-1.8887	2.4785	-0.0196	-0.5331	-1.0148	-0.4075	4.0649
-0.0064	0.0167	-0.0940	0.1089	-0.0569	0.1339	0.0182	-0.0443
-3.2551	-2.8013	4.8336	3.0086	2.7126	0.5645	-0.4029	0.6847
0.0896	-0.0700	0.0096	0.0007	-0.0066	-0.0013	-0.0005	0.0000
14.2400	-26.139	78.616	125.578	-59.9114	-184.946	-115.958	120.237

The hankel singular values HSV of subsystem 3 are given in Table F13:

HSV
0.5961
0.1331
0.0287
0.0247
0.0114
0.0072
0.0003
0.0000

Table F13: Hankel Singular Values of Subsystem 3

The reduced model of subsystem3 is given by the following:

Ar = [

59.8871	22.0121	9.1893	19.0443	-119.7753	-9.1076
-19.3132	-15.5290	2.3111	-15.8784	35.4588	2.0066
-70.5357	-20.2531	-15.3047	-23.1445	140.8629	9.7505
-19.1411	-9.7454	-3.0185	-14.6763	36.1104	3.1041
21.3540	17.4347	-2.5638	19.1510	-39.1717	-3.1070
-55.2070	-172.4688	65.8433	-231.0179	48.9473	3.7777]

Br = [0.6826

-0.8097

0.3742

-0.7840

1.6296

-20.5187]

Cr =

[0.1124 0.3513 0.0494 -0.2655 0.0344 0.0047]

Dr = [0]

The L_∞ error in the reduced order model is equal to 0.0005

The poles of the reduced order model of subsystem 3 are given in Table F14.

Eigenvalue	Damping
-0.3894 + 0.4956i	0.6179
-0.3894 - 0.4956i	0.6179
-0.8906 +11.1938i	0.0793
-0.8906 -11.1938i	0.0793
-5.6429	1.0000
-12.8139	1.0000

Table F14: Eigenvalues and Damping of Subsystem 3

The zeros of the reduced model are given in Table F15.

Zeros (x1.0e+002)
559.11
-1.44 + 11.39i
-1.44 - 11.39i
-2.32
-0.96

Table F15: Zeros of the Reduced Order Model for Subsystem 3

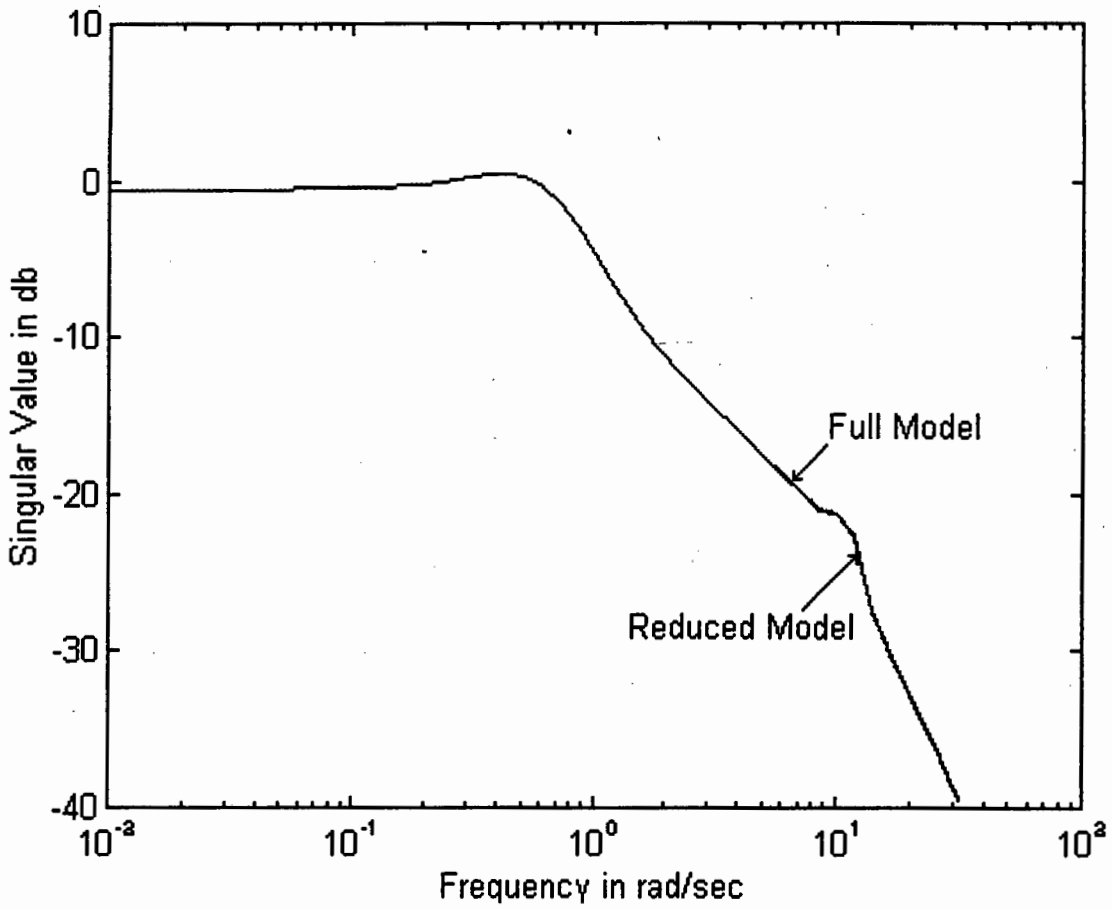

Figure F5: Singular Value Plots of Subsystem 3

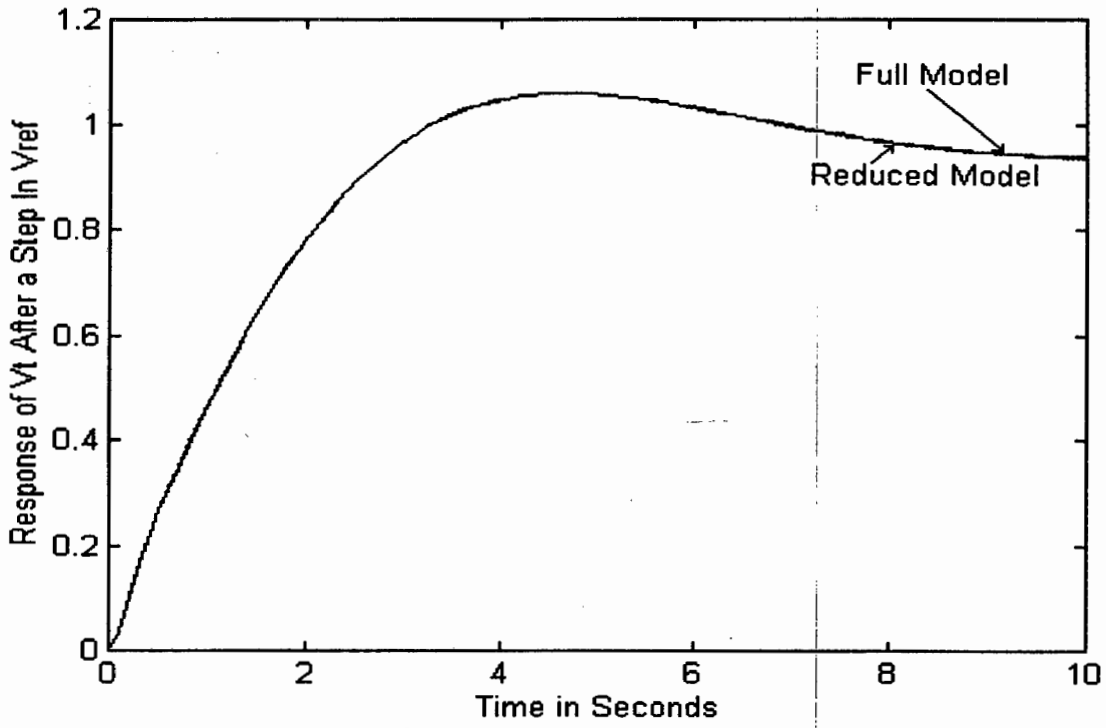

Figure F6: Step Response of Terminal Voltage After a Step in V_{ref} of Generator 3

References

[1] Dongarra J. J., Moler C. B., Bunch J. R., *Linpack User's Guide*, SIAM Philadelphia.

[2] Davidson E., "A Computational Method for Finding the Zeros of a Multivariable LTI System", *Automatica*, Vol., 6, pp., 481-484, May 1970.

Appendix G

State Space Description of the Seven-Bus System

In this section, we present the generator data and state space description of the seven-bus system. This system was used in Section 2.5.5 in determining the optimal PSS locations using simulated annealing.

Figure G1 is a diagrammatic representation of the seven-bus system.

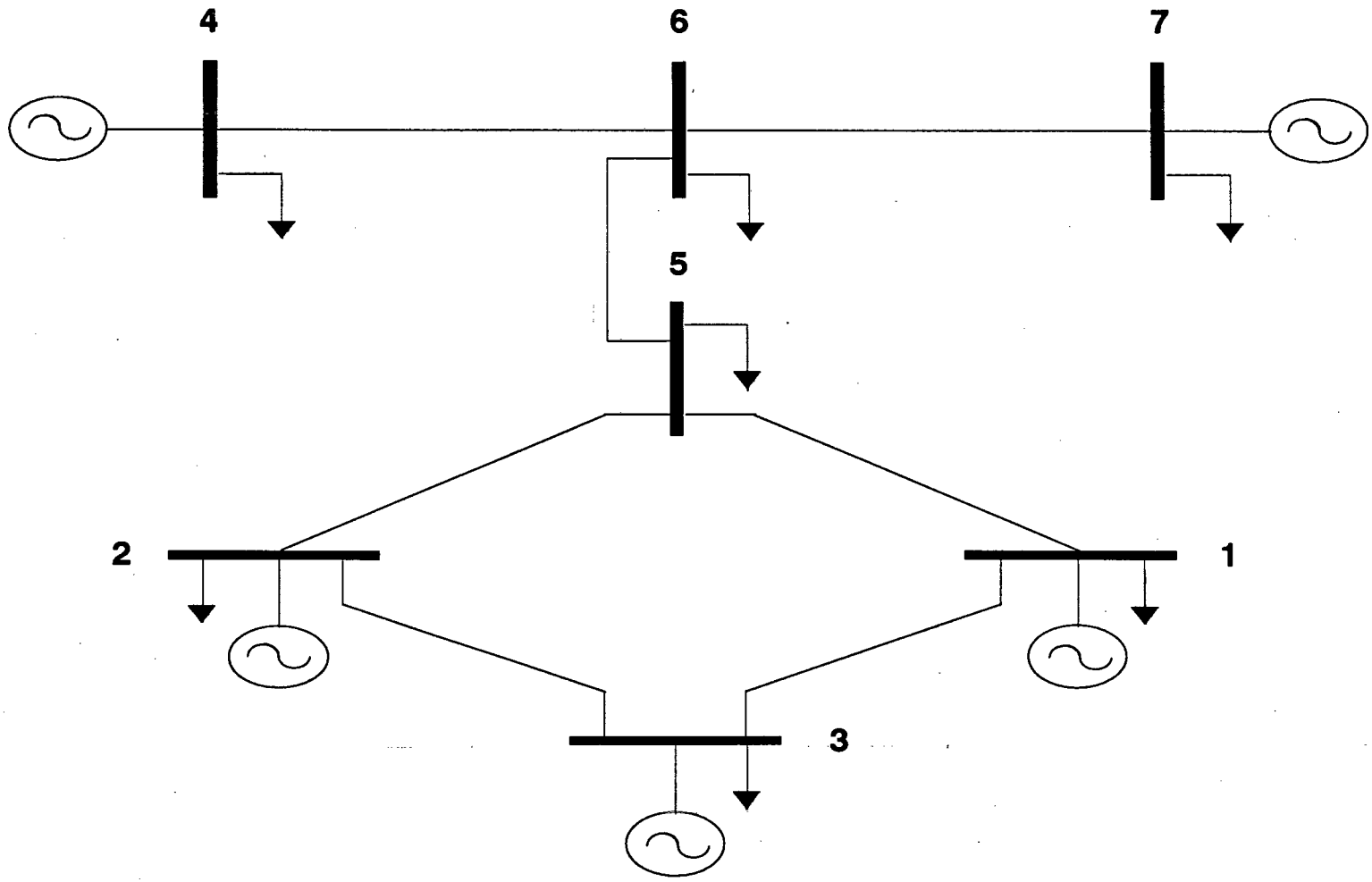

Figure G1: Network Diagram for the Seven-Bus System

The line data, bus data and load data are provided in Tables G1, G2 and G3 respectively.

From Bus	To Bus	R+jX (p.u.)
1	3	0.003 + j 0.038
2	3	0.005 + j 0.076
4	6	0.0029 + j 0.0734
5	1	0.019 + j 0.245
5	2	0.015 + j 0.225
6	5	0 + j 0.039
6	7	0.004 + j 0.057

Table G1: Line Data for the Seven-Bus System

Bus No	Voltage	Voltage	Generation	Generation
	Magnitude	Angle	MW	Mvar
1	1.03	24.5	1658	-412.0
2	1.03	27.2	1332	-200.1
3	1.029	26.6	1540	-446.5
4	1.039	48.5	6500	1958.6
5	0.998	21.2		
6	0.989	21.4		
7	0.966	0.0		

Table G2: Bus Data for the Seven-Bus System

Bus No	Real Load	Reactive Load	Shunt
	MW	Mvar	(p.u.)
1	2405	-467	0.1792
2	692.3	-184	0.1491
3	688.2	-235	0.1142
4	62.6	24.3	0.0368
5	845.8	-9.2	0.0330
6	-4.9	79.8	2.1420
7	2884	-196	0.0420

Table G3: Load Data for the Seven-Bus System

Table G4 presents the generator data for the seven-bus system:

Gen Bus No.	1	2	3	4	7
T'_{d0}	5.0	5.0	7.6	8.0	
T''_{d0}	0.053	0.053	0.06	0.09	0.09
T''_{q0}	0.123	0.123	0.09	0.19	0.2
H	4.5	4.5	4.5	5.07	5.0
X_d	0.85	0.85	0.88	0.9	1.0
X_q	0.7	0.7	0.69	0.68	0.7
X'_d	0.3	0.3	0.3	0.3	0.3
X''_d	0.2	0.2	0.2	0.24	0.25
X''_q	0.2	0.2	0.2	0.27	0.25
MVA	1900	1400	1944	6633	6000

Table G4: Generator Data for the Seven -Bus System

The state space description of the five-bus system is expressed as follows:

$\dot{x} = Ax + Bu$

$y = Cx + Du$

where the matrices A, B, C and D are as follows:

A MATRIX COLUMNS STARTING AT 1

1	-.55142	0.19858	-.18892E-01	0.00000	-.91251E-01	0.18449E-01	0.18451E-01	-.38524E-02	0.00000	0.18868E-01
2	13.624	-24.111	-1.2961	0.00000	-6.2608	1.2658	1.2659	-.26429	0.00000	1.2946
3	0.69822	0.69818	-19.427	0.00000	9.6591	0.14231	0.14264	2.7273	0.00000	-2.4216
4	-.12649	-.12649	0.23346	-.95999E-01	-.31707	0.11737E-01	0.11730E-01	-.71361E-01	0.00000	0.76168E-01
5	0.00000	0.00000	0.00000	376.99	0.00000	0.00000	0.00000	0.00000	0.00000	0.00000
6	0.24528E-01	0.24526E-01	-.11337E-01	0.00000	0.30286E-01	-.55634	0.19365	-.10471E-01	0.00000	-.10529
7	1.6828	1.6827	-.77782	0.00000	2.0779	13.287	-24.449	-.71848	0.00000	-7.2239
8	0.39010	0.39026	3.3784	0.00000	-2.7798	0.36045	0.36029	-18.780	0.00000	9.1099
9	0.10138E-01	0.10133E-01	-.10166	0.00000	0.10139	-.12532	-.12531	0.25055	-.10467	-.33738
10	0.00000	0.00000	0.00000	0.00000	0.00000	0.00000	0.00000	0.00000	376.99	0.00000
11	0.41774E-01	0.41775E-01	-.11989E-01	0.00000	0.44879E-01	0.26486E-01	0.26485E-01	-.28079E-02	0.00000	0.24548E-01
12	2.4008	2.4009	-.68903	0.00000	2.5793	1.5222	1.5222	-.16136	0.00000	1.4108
13	0.56229	0.56266	7.8428	0.00000	-6.7318	0.13179	0.13168	4.9726	0.00000	-4.5212
14	0.19777E-01	0.19770E-01	-.15617	0.00000	0.15918	0.16764E-01	0.16766E-01	-.95538E-01	0.00000	0.10284
15	0.00000	0.00000	0.00000	0.00000	0.00000	0.00000	0.00000	0.00000	0.00000	0.00000
16	0.28183E-02	0.28169E-02	-.30235E-02	0.00000	0.50578E-02	0.26549E-02	0.26526E-02	-.21659E-02	0.00000	0.42207E-02
17	0.11331	0.11328	-.12161	0.00000	0.20339	0.10673	0.10667	-.87102E-01	0.00000	0.16971
18	0.63443E-01	0.63332E-01	0.23634	0.00000	-.16500	0.45530E-01	0.45499E-01	0.22233	0.00000	-.16928
19	-.13749E-02	-.13704E-02	-.12613E-01	0.00000	0.10437E-01	-.63636E-03	-.63618E-03	-.11489E-01	0.00000	0.10171E-01
20	0.00000	0.00000	0.00000	0.00000	0.00000	0.00000	0.00000	0.00000	0.00000	0.00000
21	0.20554E-02	0.20579E-02	0.83643E-02	0.00000	-.60013E-02	0.14467E-02	0.14457E-02	0.78392E-02	0.00000	-.61074E-02
22	0.69606E-01	0.69686E-01	0.28322	0.00000	-.20322	0.48981E-01	0.48950E-01	0.26545	0.00000	-.20682
23	-.14338	-.14342	0.14128	0.00000	-.24576	-.13445	-.13443	0.99296E-01	0.00000	-.20372
24	0.56922E-02	0.56929E-02	-.88855E-02	0.00000	0.12761E-01	0.54893E-02	0.54887E-02	-.68640E-02	0.00000	0.10935E-01
25	-122.13	-122.12	-114.64	0.00000	5.2184	-35.751	-35.758	-37.952	0.00000	5.6427
26	-51.027	-51.024	-40.700	0.00000	-4.2364	-107.23	-107.23	-120.99	0.00000	23.186
27	-80.328	-80.325	-68.606	0.00000	-2.6302	-48.358	-48.360	-51.963	0.00000	8.1895
28	-8.3328	-8.3275	0.20916	0.00000	-6.9578	-7.4391	-7.4369	-1.3652	0.00000	-4.8952
29	-3.8103	-3.8121	-7.4471	0.00000	3.7314	-3.0523	-3.0517	-7.3464	0.00000	4.3130

A MATRIX COLUMNS STARTING AT 11

1	0.40412E-01	0.40411E-01	-.13220E-01	0.00000	0.42480E-01	0.15444E-01	0.66193E-02	0.26356E-02	0.00000	0.38199E-02
2	2.7727	2.7726	-.90707	0.00000	2.9146	1.0596	0.45416	0.18086	0.00000	0.26210
3	0.48851	0.48882	5.9733	0.00000	-5.1487	-.13624	-.58373E-01	1.6309	0.00000	-1.8341
4	0.21291E-01	0.21282E-01	-.16026	0.00000	0.16390	0.16208E-01	0.69465E-02	-.38580E-01	0.00000	0.49009E-01
5	0.00000	0.00000	0.00000	0.00000	0.00000	0.00000	0.00000	0.00000	0.00000	0.00000
6	0.34257E-01	0.34256E-01	-.13574E-01	0.00000	0.38194E-01	0.18827E-01	0.80679E-02	0.26961E-02	0.00000	0.52207E-02
7	2.3504	2.3503	-.93139	0.00000	2.6205	1.2917	0.55352	0.18487	0.00000	0.35818
8	0.46738	0.46730	4.7191	0.00000	-4.0065	-.12976	-.55579E-01	1.8528	0.00000	-2.0727
9	0.16271E-01	0.16273E-01	-.14008	0.00000	0.14151	0.19477E-01	0.83453E-02	-.48204E-01	0.00000	0.60897E-01
10	0.00000	0.00000	0.00000	0.00000	0.00000	0.00000	0.00000	0.00000	0.00000	0.00000
11	-.57337	0.20663	-.13658E-01	0.00000	-.96287E-01	0.14044E-01	0.60187E-02	0.29323E-02	0.00000	0.28874E-02
12	11.875	-21.458	-.78491	0.00000	-5.5337	0.80712	0.34591	0.16854	0.00000	0.16595
13	0.64071	0.64062	-26.764	0.00000	13.725	-.19274	-.82652E-01	1.8836	0.00000	-2.1339
14	-.11568	-.11567	0.26109	-.87149E-01	-.32801	0.13826E-01	0.59261E-02	-.33288E-01	0.00000	0.42219E-01
15	0.00000	0.00000	0.00000	376.99	0.00000	0.00000	0.00000	0.00000	0.00000	0.00000
16	0.25047E-02	0.25037E-02	-.26419E-02	0.00000	0.43180E-02	-.28131	0.10500	-.36447E-02	0.00000	-.48986E-01
17	0.10071	0.10067	-.10627	0.00000	0.17361	9.8520	-11.651	-.14653	0.00000	-1.9698
18	0.55422E-01	0.55395E-01	0.20987	0.00000	-.15213	0.10690	0.45787E-01	-7.1375	0.00000	0.47866
19	-.11774E-02	-.11767E-02	-.11176E-01	0.00000	0.94308E-02	-.71027E-01	-.30430E-01	0.16896E-01	-.95685E-01	-.49284E-01
20	0.00000	0.00000	0.00000	0.00000	0.00000	0.00000	0.00000	0.00000	376.99	0.00000
21	0.17961E-02	0.17951E-02	0.74278E-02	0.00000	-.55147E-02	0.32104E-03	0.13748E-03	0.45539E-01	0.00000	-.49440E-01
22	0.60820E-01	0.60780E-01	0.25154	0.00000	-.18674	0.10870E-01	0.46559E-02	1.5421	0.00000	-1.6741
23	-.12738	-.12737	0.12342	0.00000	-.20932	-1.0929	-.46836	0.16034E-01	0.00000	-.49057
24	0.50661E-02	0.50661E-02	-.78006E-02	0.00000	0.10995E-01	0.48230E-01	0.20668E-01	-.15073E-01	0.00000	0.37287E-01
25	-81.237	-81.237	-74.480	0.00000	7.5850	-25.728	-11.028	-31.615	0.00000	23.257
26	-69.872	-69.870	-60.901	0.00000	3.6331	-31.423	-13.469	-38.275	0.00000	28.005
27	-116.34	-116.34	-108.37	0.00000	12.224	-22.640	-9.7064	-26.753	0.00000	19.275
28	-7.3790	-7.3794	0.75442E-01	0.00000	-5.6161	-303.45	-130.00	-215.25	0.00000	99.406
29	-3.3517	-3.3521	-6.6389	0.00000	3.6154	-12.512	-5.3551	-48.898	0.00000	47.794

A MATRIX COLUMNS STARTING AT 21

1	-.64504E-03	-.21426E-03	-.24666E-01	0.00000	0.20000	0.00000	0.00000	0.00000	0.00000
2	-.44250E-01	-.14684E-01	-1.6924	0.00000	0.00000	0.00000	0.00000	0.00000	0.00000
3	1.3677	0.45599	-.63212E-01	0.00000	0.00000	0.00000	0.00000	0.00000	0.00000
4	-.34720E-01	-.11575E-01	-.18868E-01	0.00000	0.00000	0.00000	0.00000	0.00000	0.00000
5	0.00000	0.00000	0.00000	-377.00	0.00000	0.00000	0.00000	0.00000	0.00000
6	-.12165E-02	-.40738E-03	-.29976E-01	0.00000	0.00000	0.20000	0.00000	0.00000	0.00000
7	-.83472E-01	-.27968E-01	-2.0565	0.00000	0.00000	0.00000	0.00000	0.00000	0.00000
8	1.5488	0.51626	-.11202	0.00000	0.00000	0.00000	0.00000	0.00000	0.00000
9	-.43232E-01	-.14412E-01	-.22329E-01	0.00000	0.00000	0.00000	0.00000	0.00000	0.00000
10	0.00000	0.00000	0.00000	-377.00	0.00000	0.00000	0.00000	0.00000	0.00000
11	-.14580E-03	-.49069E-04	-.22525E-01	0.00000	0.00000	0.00000	0.20000	0.00000	0.00000
12	-.83760E-02	-.28203E-02	-1.2946	0.00000	0.00000	0.00000	0.00000	0.00000	0.00000
13	1.5859	0.52852	-.17278E-01	0.00000	0.00000	0.00000	0.00000	0.00000	0.00000
14	-.29925E-01	-.99734E-02	-.16038E-01	0.00000	0.00000	0.00000	0.00000	0.00000	0.00000
15	0.00000	0.00000	0.00000	-377.00	0.00000	0.00000	0.00000	0.00000	0.00000

```
16 -.51486E-02 -.17152E-02 -.34010E-01 0.00000      0.00000      0.00000      0.00000      0.13158      0.00000
17 -.20705     -.68983E-01 -1.3676     0.00000      0.00000      0.00000      0.00000      0.00000      0.00000
18  1.0688     0.35626     -.28766     0.00000      0.00000      0.00000      0.00000      0.00000      0.00000
19 -.52311E-01 -.17437E-01 -.55258E-02 0.00000      0.00000      0.00000      0.00000      0.00000      0.00000
20 0.00000     0.00000     0.00000     -377.00      0.00000      0.00000      0.00000      0.00000      0.00000
21 -.28039     0.94033E-01 -.24095E-01 0.00000      0.00000      0.00000      0.00000      0.00000      0.12500
22  9.5530     -11.631     -.81590     0.00000      0.00000      0.00000      0.00000      0.00000      0.00000
23 0.61973     0.20666     -7.1035     0.00000      0.00000      0.00000      0.00000      0.00000      0.00000
24 0.21396E-01 0.71775E-02 0.67009E-01 0.52217E-01 0.00000      0.00000      0.00000      0.00000      0.00000
25 -21.355     -7.1189      45.718     0.00000      -20.000      0.00000      0.00000      0.00000      0.00000
26 -25.788     -8.5957      55.773     0.00000      0.00000      -20.000      0.00000      0.00000      0.00000
27 -17.892     -5.9677      40.050     0.00000      0.00000      0.00000      -20.000      0.00000      0.00000
28 -18.818     -6.2631      86.874     0.00000      0.00000      0.00000      0.00000      -20.000      0.00000
29 -155.77     -51.896      102.74     0.00000      0.00000      0.00000      0.00000      0.00000      -10.000
```

B Matrix:

Columns 1 to 2 correspond to Vref at generators 3 and 4 respectively

```
        0.00000      0.00000
        0.00000      0.00000
        0.00000      0.00000
        0.00000      0.00000
        0.00000      0.00000
        0.00000      0.00000
        0.00000      0.00000
        0.00000      0.00000
        0.00000      0.00000
        0.00000      0.00000
        0.00000      0.00000
        0.00000      0.00000
        0.00000      0.00000
        0.00000      0.00000
        0.00000      0.00000
        0.00000      0.00000
        0.00000      0.00000
        0.00000      0.00000
        0.00000      0.00000
        0.00000      0.00000
        0.00000      0.00000
        0.00000      0.00000
        0.00000      0.00000
        0.00000      0.00000
         600.00      0.00000
        0.00000       600.00
        0.00000      0.00000 ];
```

C Matrix:

Row 1 corresponds to P_{el} at Generator 3

Row 2 corresponds to P_{el} at Generator 4

Row 3 corresponds to Q_{el} l at Generator 3

Row 4 corresponds to Q_{el} at Generator 4

Row 5 corresponds to ω at Generator 3

Row 6 corresponds to ω at Generator 4

Row 7 corresponds to V_T ω at Generator 3

Row 8 corresponds to V_T at Generator 4

C MATRIX COLUMNS STARTING AT 1

1	-.34601	-.34590	2.7324	0.00000	-2.7850	-.29331	-.29334	1.6715	0.00000	-1.7993
2	0.92418E-01	0.92169E-01	0.84804	0.00000	-.70191	0.42811E-01	0.42811E-01	0.77270	0.00000	-.68409
3	-1.3134	-1.3133	-1.5957	0.00000	0.38690	-.77701	-.77690	-1.1456	0.00000	0.41894
4	-.37386	-.37363	-.16477	0.00000	-.15286	-.32578	-.32549	-.21684	0.00000	-.68819E-01
5	0.13388	0.13387	0.11434	0.00000	0.43837E-02	0.80597E-01	0.80600E-01	0.86604E-01	0.00000	-.13649E-01
6	0.13888E-01	0.13879E-01	-.34861E-03	0.00000	0.11596E-01	0.12398E-01	0.12395E-01	0.22753E-02	0.00000	0.81586E-02
7	0.00000	0.00000	0.00000	0.00000	0.00000	0.00000	0.00000	0.00000	0.00000	0.00000
8	0.00000	0.00000	0.00000	0.00000	0.00000	0.00000	0.00000	0.00000	0.00000	0.00000

C MATRIX COLUMNS STARTING AT 11

1	2.0238	2.0238	-4.5681	0.00000	5.7389	-.24191	-.10368	0.58242	0.00000	-.73866
2	0.79154E-01	0.79222E-01	0.75165	0.00000	-.63433	4.7771	2.0466	-1.1365	0.00000	3.3148
3	2.3921	2.3918	2.7376	0.00000	-.70744	-.34726	-.14876	-.54586	0.00000	0.44291
4	-.33051	-.33034	-.15019	0.00000	-.10944	5.8608	2.5053	-.85076	0.00000	3.5414
5	0.19390	0.19390	0.18062	0.00000	-.20373E-01	0.37733E-01	0.16177E-01	0.44589E-01	0.00000	-.32124E-01
6	0.12298E-01	0.12299E-01	-.12574E-03	0.00000	0.93603E-02	0.50576	0.21666	0.35875	0.00000	-.16568
7	0.00000	0.00000	0.00000	1.0000	0.00000	0.00000	0.00000	0.00000	0.00000	0.00000
8	0.00000	0.00000	0.00000	0.00000	0.00000	0.00000	0.00000	0.00000	1.0000	0.00000

C MATRIX COLUMNS STARTING AT 21

1	0.52355	0.17451	0.28065	0.00000	0.00000	0.00000	0.00000	0.00000	0.00000	
2	3.5184	1.1727	0.37159	0.00000	0.00000	0.00000	0.00000	0.00000	0.00000	
3	-.38631	-.12866	0.63701	0.00000	0.00000	0.00000	0.00000	0.00000	0.00000	
4	-1.5228	-.50683	3.6248	0.00000	0.00000	0.00000	0.00000	0.00000	0.00000	
5	0.29819E-01	0.99462E-02	-.66751E-01	0.00000	0.00000	0.00000	0.00000	0.00000	0.00000	
6	0.31363E-01	0.10438E-01	-.14479	0.00000	0.00000	0.00000	0.00000	0.00000	0.00000	
7	0.00000	0.00000	0.00000	0.00000	0.00000	0.00000	0.00000	0.00000	0.00000	
8	0.00000	0.00000	0.00000	0.00000	0.00000	0.00000	0.00000	0.00000	0.00000	

D MATRIX

1	0.00000	0.00000	0.00000	0.00000
2	0.00000	0.00000	0.00000	0.00000
3	0.00000	0.00000	0.00000	0.00000
4	0.00000	0.00000	0.00000	0.00000
5	0.00000	0.00000	0.00000	0.00000
6	0.00000	0.00000	0.00000	0.00000
7	0.00000	0.00000	0.00000	0.00000
8	0.00000	0.00000	0.00000	0.00000

Table G5 illustrates that the system has a pair of unstable eigenvalues $\lambda = 5.4162e-001 \pm 5.5296e+000i$ (highlighetd values in Table G5).

Eigenvalue	Damping
5.4162e-001+ 5.5296e+000i	**-9.7483e-002**
5.4162e-001- 5.5296e+000i	**-9.7483e-002**
-4.4674e-002	1.0000e+000
-2.6026e-001+ 5.8626e+000i	4.4350e-002
-2.6026e-001- 5.8626e+000i	4.4350e-002
-8.1615e-001	1.0000e+000
-1.3979e+000	1.0000e+000
-1.9165e+000+ 9.2253e+000i	2.0340e-001
-1.9165e+000- 9.2253e+000i	2.0340e-001
-2.0638e+000+ 9.1521e+000i	2.1997e-001
-2.0638e+000- 9.1521e+000i	2.1997e-001
-3.3445e+000	1.0000e+000
-6.0192e+000+ 2.6602e+000i	9.1466e-001
-6.0192e+000- 2.6602e+000i	9.1466e-001
-6.2639e+000	1.0000e+000
-6.4948e+000+ 5.1709e+000i	7.8234e-001
-6.4948e+000- 5.1709e+000i	7.8234e-001
-8.1075e+000+ 7.7590e-001i	9.9545e-001
-8.1075e+000- 7.7590e-001i	9.9545e-001
-1.2755e+001	1.0000e+000
-1.2936e+001	1.0000e+000
-1.8292e+001+ 1.2507e+000i	9.9767e-001
-1.8292e+001- 1.2507e+000i	9.9767e-001
-1.8953e+001	1.0000e+000
-1.9079e+001	1.0000e+000
-2.3319e+001	1.0000e+000
-2.5512e+001	1.0000e+000
-2.6465e+001	1.0000e+000
-2.8975e+001	1.0000e+000

Table G5: Eigenvalues and Damping of the Seven-Bus System

Table G6 gives the zeros of the seven-bus system for each of the eight outputs with V_{ref} of the generator 3 as the input.

P_{el} (Gen 3)	Q_{el} (Gen 3)	ω (Gen3)	V_T (Gen 3)
-8.7267e-002	-4.4766e-002	-4.4533e-002	-9.0350e-001
-9.0135e-001	-1.3819e+000	-1.2535e+000	-1.2859e+000- 8.5679e-001i
-1.2874e+000- 8.5489e-001i	-3.3381e+000	-1.5317e+000	-1.2859e+000+ 8.5679e-001i
-1.2874e+000+ 8.5489e-001i	**5.9346e-001- 5.5571e+000i**	-3.3581e+000	-2.6962e+000- 2.1410e-001i
-2.6956e+000- 2.1361e-001i	**5.9346e-001+ 5.5571e+000i**	**4.9253e-001- 5.4759e+000i**	-2.6962e+000+ 2.1410e-001i
-2.6956e+000+ 2.1361e-001i	-5.5977e+000	**4.9253e-001+ 5.4759e+000i**	**5.4448e-001- 5.5141e+000i**
5.4448e-001- 5.5141e+000i	-2.0398e-001- 5.7833e+000i	-3.7604e-001- 5.9279e+000i	**5.4448e-001+ 5.5141e+000i**
5.4448e-001+ 5.5141e+000i	-2.0398e-001+ 5.7833e+000i	-3.7604e-001+ 5.9279e+000i	-5.4211e+000- 3.7442e+000i
-5.4211e+000- 3.7442e+000i	-6.4711e+000- 2.0587e+000i	-5.5144e+000- 3.3528e+000i	-5.4211e+000+ 3.7442e+000i
-5.4211e+000+ 3.7442e+000i	-6.4711e+000+ 2.0587e+000i	-5.5144e+000+ 3.3528e+000i	-6.9390e+000- 7.6735e-001i
-6.9390e+000- 7.6731e-001i	-6.3379e+000- 4.8409e+000i	-7.1707e+000	-6.9390e+000+ 7.6735e-001i
-6.9390e+000+ 7.6731e-001i	-6.3379e+000+ 4.8409e+000i	-7.6801e+000- 4.8603e-001i	-1.3886e+000- 6.9933e+000i
-1.3886e+000- 6.9933e+000i	-8.4214e+000- 8.7038e-001i	-7.6801e+000+ 4.8603e-001i	-1.3886e+000+ 6.9933e+000i
-1.3886e+000+ 6.9933e+000i	-8.4214e+000+ 8.7038e-001i	-1.8798e+000- 9.0715e+000i	-8.4013e+000
-8.4013e+000	-2.2040e+000- 9.0256e+000i	-1.8798e+000+ 9.0715e+000i	-1.9446e+000- 9.2191e+000i
-1.9446e+000- 9.2191e+000i	-2.2040e+000+ 9.0256e+000i	-2.0027e+000- 9.1853e+000i	-1.9446e+000+ 9.2191e+000i
-1.9446e+000+ 9.2191e+000i	-1.9296e+000- 9.2397e+000i	-2.0027e+000+ 9.1853e+000i	-1.0188e+001
-1.0188e+001	-1.9296e+000+ 9.2397e+000i	-1.2452e+001	-1.2865e+001
-1.2865e+001	-1.2848e+001	-1.2896e+001	-1.3317e+001
-1.3317e+001	-1.3094e+001	-1.7981e+001	-1.8310e+001- 1.2618e+000i
-1.8310e+001- 1.2618e+000i	-1.8302e+001- 1.2495e+000i	-1.8278e+001- 1.2373e+000i	-1.8310e+001+ 1.2618e+000i
-1.8310e+001+ 1.2618e+000i	-1.8302e+001+ 1.2495e+000i	-1.8278e+001+ 1.2373e+000i	-1.9079e+001
-1.9079e+001	-1.9079e+001	-1.9079e+001	-2.4931e+001
-2.4931e+001	-2.4970e+001	-2.6480e+001	-2.6466e+001
-2.6466e+001	-2.6462e+001	-2.7213e+001- 2.5408e-001i	-3.0709e+001
-3.0708e+001	-2.7493e+001	-2.7213e+001+ 2.5408e-001i	-3.3330e+001
-3.3332e+001	-3.3332e+001	-3.3333e+001	

Table G6: Zeros of the Seven-Bus System Corresponding to the Eight Candidate Outputs (V_{ref} of the Generator 3 as Input)

Table G7 gives the zeros of the seven-bus system for each of the eight outputs with V_{ref} of the generator 4 as the input. Table G6 and G7 illustrate that the seven-bus system has non-minimum phase-zeros for all eight outputs. These zeros are highlighted values in Table G6 and G7.

P_{el} (Gen 4)	Q_{el} (Gen 4)	ω (Gen 4)	V_T (Gen 4)
-9.5724e-002	-4.9295e-002	-4.4570e-002	-7.2076e-001
-7.2059e-001	-8.1807e-001	-8.1624e-001	-1.2264e+000- 6.2343e-002i
-1.2261e+000- 6.1617e-002i	-1.4017e+000	-1.3983e+000	-1.2264e+000+ 6.2343e-002i
-1.2261e+000+ 6.1617e-002i	**9.3743e-001- 3.2708e+000i**	-4.6244e+000	-1.6919e+000- 2.1096e+000i
-1.6922e+000- 2.1093e+000i	**9.3743e-001+ 3.2708e+000i**	-2.0546e-001- 5.9297e+000i	-1.6919e+000+ 2.1096e+000i
-1.6922e+000+ 2.1093e+000i	-5.2825e+000	-2.0546e-001+ 5.9297e+000i	**1.1884e-002- 5.8963e+000i**
1.1878e-002- 5.8963e+000i	-2.5385e-001- 5.8569e+000i	**5.8239e-001- 2.3010e+000i**	**1.1884e-002+ 5.8963e+000i**
1.1878e-002+ 5.8963e+000i	-2.5385e-001+ 5.8569e+000i	**5.8239e-001+ 2.3010e+000i**	-6.1843e+000- 2.0467e+000i
-6.1843e+000- 2.0467e+000i	-5.9816e+000- 2.6348e+000i	-2.4043e-001- 6.3998e+000i	-6.1843e+000+ 2.0467e+000i
-6.1843e+000+ 2.0467e+000i	-5.9816e+000+ 2.6348e+000i	-2.4043e-001+ 6.3998e+000i	-7.5696e+000
-7.5696e+000	-7.4269e+000	-7.3761e+000	-6.5258e+000- 4.5361e+000i
-6.5258e+000- 4.5361e+000i	-6.6665e+000- 5.3538e+000i	-6.6820e+000- 4.7437e+000i	-6.5258e+000+ 4.5361e+000i
-6.5258e+000+ 4.5361e+000i	-6.6665e+000+ 5.3538e+000i	-6.6820e+000+ 4.7437e+000i	-2.0625e+000- 9.1501e+000i
-2.0625e+000- 9.1501e+000i	-2.0641e+000- 9.1517e+000i	-2.0636e+000- 9.1527e+000i	-2.0625e+000+ 9.1501e+000i
-2.0625e+000+ 9.1501e+000i	-2.0641e+000+ 9.1517e+000i	-2.0636e+000+ 9.1527e+000i	-1.9166e+000- 9.2200e+000i
-1.9166e+000- 9.2200e+000i	-1.9173e+000- 9.2259e+000i	-1.9159e+000- 9.2253e+000i	-1.9166e+000+ 9.2200e+000i
-1.9166e+000+ 9.2200e+000i	-1.9173e+000+ 9.2259e+000i	-1.9159e+000+ 9.2253e+000i	-1.2763e+001
-1.2763e+001	-1.2758e+001	-1.2756e+001	-1.2861e+001
-1.2861e+001	-1.2881e+001	-1.2930e+001	-1.5872e+001
-1.5872e+001	-1.5863e+001	-1.5871e+001	-1.8293e+001- 1.2526e+000i
-1.8293e+001- 1.2526e+000i	-1.8290e+001- 1.2509e+000i	-1.8292e+001- 1.2508e+000i	-1.8293e+001+ 1.2526e+000i
-1.8293e+001+ 1.2526e+000i	-1.8290e+001+ 1.2509e+000i	-1.8292e+001+ 1.2508e+000i	-1.8960e+001
-1.8960e+001	-1.8952e+001	-1.8954e+001	-2.3317e+001
-2.3317e+001	-2.3314e+001	-2.3320e+001	-2.5519e+001
-2.5519e+001	-2.5492e+001	-2.5517e+001	-2.6465e+001
-2.6465e+001	-2.6464e+001	-2.6465e+001	-2.8968e+001
-2.8968e+001	-2.8976e+001	-2.8976e+001	

Table G7: Zeros of the Seven-Bus System Corresponding to the Eight Candidate Outputs (V_{ref} of the Generator 4 as Input).

Appendix H

H_∞ Controllers for the Nine-Bus System

In this section, we present the results of the H_∞ synthesis method applied in Chapter 4. Firstly, we give the frequency-dependent weighting functions that were selected for the generator subsystems. Thereafter, we present the controllers which are obtained from the optimal H_∞ and suboptimal H_∞ synthesis methods.

H.1 Optimal H_∞ Controller Design

For the optimal H_∞ controller design, we used the same weighting functions for all subsystems.

Figure H1 illustrates the weighting functions (W1, W3) that were selected for all three generator subsystems: The weighting function W2 was not used.

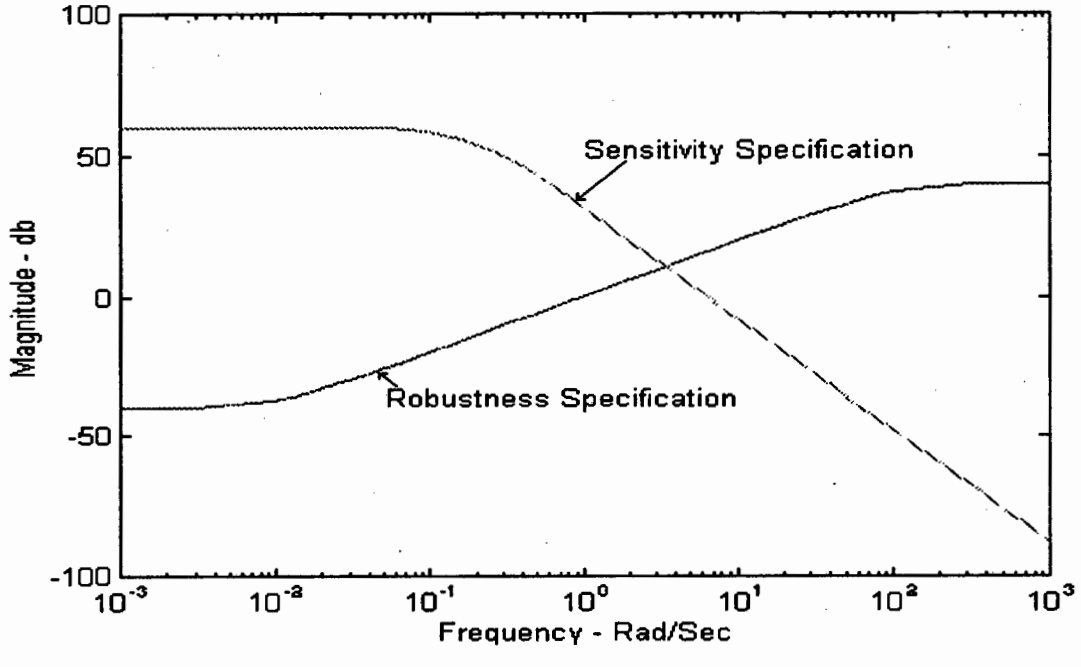

Figure H1: Magnitude Plot for Sensitivity Specification (1/W1) and Robustness Specification (1/W3).

The weighting functions W1 and W3 can be expressed as follows (W2 is ignored):

$$W1 = \frac{0.01s + 1}{s + 0.01}$$

$$W3 = \frac{(5s + 1)^2}{1000}$$

H.1.1 Subsystem 1

The state space description of the open loop augmented plant can be expressed as follows:

$$\dot{z} = A_a z + B_1 u_1 + B_2 u_2$$
$$y_1 = C_1 z + D_{11} u_1 + D_{12} u_2$$
$$y_2 = C_2 z + D_{21} u_2 + D_{22} u_2$$

where the matrices $A_a, B_1, B_2, C_1, C_2, D_{11}, D_{12}, D_{21}$ and D_{22} are as follows:

A_a =[9.4836e-001 -1.7417e+000 -3.7456e+001 -2.0937e+000 8.5774e+000 0
8.9470e-001 -3.8829e+000 -7.0649e+001 -1.2834e+001 1.2137e+001 0
-6.7024e-001 1.0358e+000 -2.7938e+000 -1.2784e+000 -1.5285e+000 0
1.6710e-001 -4.1513e-002 1.3724e+001 2.0618e+000 -1.1850e+000 0
-3.1563e+000 2.5347e+000 -1.6313e+001 -8.7427e+000 -6.5625e+000 0
-3.3962e-001 2.5091e-001 3.7215e-001 1.5524e-001 1.8335e-002 -1.0e-02]

B_1 = [0
0
0
0
0
1]

B_2 = [1.4172e+000
2.3619e-001
2.1506e+000
-1.7816e+000
9.0144e+000
0]

C_1 =

[-3.3962e-03 2.5091e-03 3.7215e-03 1.5524e-03 1.8335e-04 1.0
-1.0511e-01 1.4010e-01 1.3521e-01 -1.2901e-01 -2.9058e-01 0.0]

C_2 = [-3.3962e-01 2.5091e-01 3.7215e-01 1.5524e-01 1.8335e-02 0]

D_{11} = [1.0000e-002
0]

D_{12} = [0
2.7820e-001]

D_{21} = [1]

D_{22} = [0]

The eigenvalues of the augmented system are:

-1.0000e-002
-7.8110e+000
-5.6057e-001+ 4.8429e+000i
-5.6057e-001- 4.8429e+000i
-6.4850e-001+ 4.9346e-001i
-6.4850e-001- 4.9346e-001i

The transmission zeros of the augmented system are:

3.3606e+001
-5.6930e-001+ 4.5637e+000i
-5.6930e-001- 4.5637e+000i
-6.1487e-001
-1.0000e-002

Optimal H_∞ Controller for Subsystem 1

The state space description of the controller for subsystem 1 is given by the following:

$$\dot{z} = A_c z + B_c u_c$$
$$y_c = C_c z + D_c u_c$$

where the matrices A_c, B_c, C_c and D_c are as follows:

Matrix A_c

Columns 1 through 6

```
-1.9368e+000 -2.7822e-001  4.4078e-001  4.6304e+000 -1.5524e+001  6.2697e+004
 1.6752e+000 -1.9709e+000  2.3248e+000 -2.8948e+000 -1.1486e+001 -2.9039e+004
-7.8599e-001  2.5523e-001 -1.3512e+000  8.3034e-001 -5.7800e+000 -2.6024e+004
-1.1986e-001  7.2238e-001 -6.8303e-001 -1.6794e+000 -5.7425e-001 -5.5281e+004
 2.8300e-001  8.7001e-001  6.3818e-001  5.7043e-001 -9.4390e-001  4.0738e+003
-4.1414e+003  3.5810e+003 -6.1761e+003  2.4737e+003 -2.1326e+003 -9.9714e+007
```

Matrix A_c

Columns 7 through 9

```
 8.1588e-001  9.2608e-004 -4.8855e-004
-1.3599e+001 -1.5080e-002  3.9982e-003
-9.7831e+000 -4.8820e-003  1.4341e-003
 3.4968e+000  2.8123e-003 -3.6729e-004
-7.6302e+000 -6.1372e-003  1.6362e-003
 1.3870e+000  3.5321e-003 -9.3285e-004
-6.3255e-001 -3.5648e-004  9.9996e-005
-3.5405e+001 -3.4596e-002  1.1853e-002
-2.6301e+002 -2.4957e-001  8.7057e-002
```

Matrix B_c

```
[-5.5070e-003
  3.1053e-002
 -1.0135e-001
 -3.1099e-001
  2.2340e-001
  3.7518e+004 ]
```

Matrix C_c

Columns 1 through 6

```
4.2655e-001 -3.5593e-001 -5.6190e-002  2.1315e-001 -8.6344e-001  9.5480e+003
```

Matrix D_c

[0]

The eigenvalues of the controller are:

```
[-9.9714e+007
 -9.6278e+000
 -5.6150e-001+ 4.5770e+000i
 -5.6150e-001- 4.5770e+000i
 -1.0000e-002
 -6.1489e-001                ]
```

The transmission zeros of the controller are:

```
[-7.8110e+000
-5.6057e-001+ 4.8429e+000i
-5.6057e-001- 4.8429e+000i
-6.4850e-001+ 4.9346e-001i
-6.4850e-001- 4.9346e-001i]
```

The closed loop for subsystem 1 with the optimal H_∞ controller has the following state space description:

$$x_{cl} = A_{cl}x_{cl} + B_{cl}u_{cl}$$
$$y_{cl} = C_{cl}x_{cl} + D_{cl}u_{cl}$$

where the matrices A_{cl}, B_{cl}, C_{cl} and D_{cl} are given by the following:

Matrix A_{cl}

Columns 1 through 6

```
 9.4836e-001 -1.7417e+000 -3.7456e+001 -2.0937e+000  8.5774e+000            0
 8.9470e-001 -3.8829e+000 -7.0649e+001 -1.2834e+001  1.2137e+001            0
-6.7024e-001  1.0358e+000 -2.7938e+000 -1.2784e+000 -1.5285e+000            0
 1.6710e-001 -4.1513e-002  1.3724e+001  2.0618e+000 -1.1850e+000            0
-3.1563e+000  2.5347e+000 -1.6313e+001 -8.7427e+000 -6.5625e+000            0
-3.3962e-001  2.5091e-001  3.7215e-001  1.5524e-001  1.8335e-002 -1.0000e-002
 1.8703e-003 -1.3817e-003 -2.0494e-003 -8.5492e-004 -1.0097e-004            0
-1.0546e-002  7.7915e-003  1.1556e-002  4.8208e-003  5.6937e-004            0
 3.4422e-002 -2.5431e-002 -3.7719e-002 -1.5735e-002 -1.8584e-003            0
 1.0562e-001 -7.8030e-002 -1.1573e-001 -4.8279e-002 -5.7021e-003            0
-7.5871e-002  5.6052e-002  8.3137e-002  3.4681e-002  4.0961e-003            0
-1.2742e+004  9.4136e+003  1.3962e+004  5.8245e+003  6.8791e+002            0
```

Columns 7 through 12

```
 6.0451e-001 -5.0442e-001 -7.9634e-002  3.0208e-001 -1.2237e+000  1.3532e+004
 1.0075e-001 -8.4065e-002 -1.3271e-002  5.0343e-002 -2.0393e-001  2.2551e+003
 9.1733e-001 -7.6544e-001 -1.2084e-001  4.5839e-001 -1.8569e+000  2.0534e+004
```

```
-7.5994e-001  6.3412e-001  1.0011e-001 -3.7974e-001  1.5383e+000 -1.7011e+004
 3.8451e+000 -3.2084e+000 -5.0652e-001  1.9214e+000 -7.7834e+000  8.6069e+004
           0            0            0            0            0            0
-1.9368e+000 -2.7822e-001  4.4078e-001  4.6304e+000 -1.5524e+001  6.2697e+004
 1.6752e+000 -1.9709e+000  2.3248e+000 -2.8948e+000 -1.1486e+001 -2.9039e+004
-7.8599e-001  2.5523e-001 -1.3512e+000  8.3034e-001 -5.7800e+000 -2.6024e+004
-1.1986e-001  7.2238e-001 -6.8303e-001 -1.6794e+000 -5.7425e-001 -5.5281e+004
 2.8300e-001  8.7001e-001  6.3818e-001  5.7043e-001 -9.4390e-001  4.0738e+003
-4.1414e+003  3.5810e+003 -6.1761e+003  2.4737e+003 -2.1326e+003 -9.9714e+007
```

Matrix B_{cl}

```
[           0
            0
            0
            0
            0
  1.0000e+000
 -5.5070e-003
  3.1053e-002
 -1.0135e-001
 -3.1099e-001
  2.2340e-001
  3.7518e+004 ]
```

Matrix C_{cl} Columns 1 through 6

```
-1.1344e-002  8.3804e-003  1.2430e-002  5.1852e-003  6.1241e-004  3.3397e+000
-1.0511e-001  1.4010e-001  1.3521e-001 -1.2901e-001 -2.9058e-001            0
```

Columns 7 through 12

```
           0            0            0            0            0            0
 1.1867e-001 -9.9018e-002 -1.5632e-002  5.9298e-002 -2.4021e-001  2.6563e+003
```

Matrix D_{cl}

```
[  3.3401e-002
           0    ]
```

H.1.2 Subsystem 2

The state space description of the open loop augmented plant can be expressed as follows:

A_a =

```
[ 5.5580e+001 -9.7562e+000 -1.1174e+002  6.9574e+000  7.5810e+000            0
  4.6639e+001 -8.3517e+000 -9.0230e+001  7.5830e+000  2.8435e+000            0
  2.2804e+001 -3.8678e+000 -4.5275e+001  3.2839e+000  2.9789e+000            0
  2.6383e+000  9.1850e-001 -1.3436e+001 -4.7713e+000  2.8294e+000            0
 -2.4276e+001 -2.5646e+000  6.3504e+001  4.8262e+000 -1.7133e+001            0
 -3.5081e-001  3.9332e-001 -8.4105e-002 -1.6479e-002  6.0284e-003 -1.0000e-002]
```

B_1 =

```
  [        0
           0
           0
           0
           0
           1 ]
```

B_2 =

```
[ 1.0308e-001
 -2.9129e-002
  2.3223e-001
 -3.2523e+000
  7.1732e+000
            0 ]
```

C_1 =

```
[-3.5081e-003  3.9332e-003 -8.4105e-004 -1.6479e-004  6.0284e-005  9.9990e-001
 -1.7729e+000 -5.7604e-002  4.1844e+000  9.3539e-002 -8.5613e-001            0]
```

C_2 =

```
[-3.5081e-001  3.9332e-001 -8.4105e-002 -1.6479e-002  6.0284e-003            0]
```

D_{11} =

```
 [ 1.0000e-002
            0  ]
```

D_{12} =

```
 [          0
  3.3979e-001    ]
```

D_{21} = [1]

D_{22} = [0]

The eigenvalues of the augmented system are:

```
-1.0000e-002
-1.7976e+001
-5.1433e-001+ 7.7966e+000i
-5.1433e-001- 7.7966e+000i
-4.7311e-001+ 5.1281e-001i
-4.7311e-001- 5.1281e-001i
```

The transmission zeros of the augmented plant are:

```
 4.4125e+002
-1.1858e+000+ 7.9644e+000i
-1.1858e+000- 7.9644e+000i
-5.9327e-001
-1.0000e-002
```

Optimal H_∞ Controller for Subsystem 2

Matrix A_c Columns 1 through 7

```
 -2.0497e+000  3.4200e+000  4.0398e+000  1.8255e+000  2.3619e+001 -6.5018e+003
 -1.0403e-001 -3.3011e+000  4.7343e+000  3.5345e+000  1.0601e+001 -1.0628e+005
 -1.4229e+000 -1.4755e+000 -1.1572e+000 -3.4104e-001  1.5689e+001  8.7431e+004
  4.3553e-001 -1.5011e+000  1.3510e-001 -1.8543e+000  3.5535e+000  1.0541e+005
 -4.3729e-001 -7.8845e-001 -1.5606e+000 -2.7046e-001 -1.6184e+000 -7.5652e+003
 -5.8632e+003  9.8739e+003 -3.0210e+003  5.5081e+003  1.2368e+004 -2.9420e+008
```

Matrix B_c =

```
[ 1.4145e-002
 -1.5006e-002
  1.2603e-002
 -1.9973e-001
  1.1609e+000
 -5.2915e+004]
```

Matrix C_c =

```
[-1.5126e-001  1.8130e+00 -2.7049e-001  7.3851e-001  2.1774e+00 -1.6350e+004 ]
```

Matrix D_c =[0]

The eigenvalues of the controller for subsystem 2 are:

```
[ -2.9420e+008
  -9.7173e+000
  -1.1699e+000+ 7.9620e+000i
  -1.1699e+000- 7.9620e+000i
  -1.0000e-002
  -5.9327e-001]
```

The transmission zeros of the controller for subsystem 2 are:

```
-1.7976e+001
-5.1433e-001+ 7.7966e+000i
-5.1433e-001- 7.7966e+000i
-4.7311e-001+ 5.1281e-001i
-4.7311e-001- 5.1281e-001i
```

The closed loop state space description for subsystem 2 with the H_∞ controller is as follows:

Matrix A_{cl}

Columns 1 through 6

```
  5.5580e+001 -9.7562e+000 -1.1174e+002  6.9574e+000  7.5810e+000             0
  4.6639e+001 -8.3517e+000 -9.0230e+001  7.5830e+000  2.8435e+000             0
  2.2804e+001 -3.8678e+000 -4.5275e+001  3.2839e+000  2.9789e+000             0
  2.6383e+000  9.1850e-001 -1.3436e+001 -4.7713e+000  2.8294e+000             0
 -2.4276e+001 -2.5646e+000  6.3504e+001  4.8262e+000 -1.7133e+001             0
 -3.5081e-001  3.9332e-001 -8.4105e-002 -1.6479e-002  6.0284e-003 -1.0000e-002
 -4.9622e-003  5.5634e-003 -1.1897e-003 -2.3309e-004  8.5271e-005             0
  5.2641e-003 -5.9019e-003  1.2620e-003  2.4727e-004 -9.0460e-005             0
 -4.4213e-003  4.9570e-003 -1.0600e-003 -2.0768e-004  7.5977e-005             0
  7.0067e-002 -7.8556e-002  1.6798e-002  3.2912e-003 -1.2041e-003             0
 -4.0727e-001  4.5662e-001 -9.7641e-002 -1.9131e-002  6.9987e-003             0
  1.8563e+004 -2.0812e+004  4.4504e+003  8.7196e+002 -3.1899e+002             0
```

Columns 7 through 12

```
-1.5591e-002  1.8688e-001 -2.7881e-002  7.6123e-002  2.2444e-001 -1.6853e+003
 4.4059e-003 -5.2810e-002  7.8791e-003 -2.1512e-002 -6.3424e-002  4.7625e+002
-3.5126e-002  4.2103e-001 -6.2816e-002  1.7150e-001  5.0565e-001 -3.7968e+003
 4.9193e-001 -5.8963e+000  8.7971e-001 -2.4018e+000 -7.0813e+000  5.3173e+004
-1.0850e+000  1.3005e+001 -1.9403e+000  5.2975e+000  1.5619e+001 -1.1728e+005
           0             0             0             0             0             0
-2.0497e+000  3.4200e+000  4.0398e+000  1.8255e+000  2.3619e+001 -6.5018e+003
-1.0403e-001 -3.3011e+000  4.7343e+000  3.5345e+000  1.0601e+001 -1.0628e+005
-1.4229e+000 -1.4755e+000 -1.1572e+000 -3.4104e-001  1.5689e+001  8.7431e+004
 4.3553e-001 -1.5011e+000  1.3510e-001 -1.8543e+000  3.5535e+000  1.0541e+005
-4.3729e-001 -7.8845e-001 -1.5606e+000 -2.7046e-001 -1.6184e+000 -7.5652e+003
-5.8632e+003  9.8739e+003 -3.0210e+003  5.5081e+003  1.2368e+004 -2.9420e+008
```

Matrix B_{cl}

```
[            0
             0
             0
             0
             0
  1.0000e+000
  1.4145e-002
 -1.5006e-002
  1.2603e-002
 -1.9973e-001
  1.1609e+000
 -5.2915e+004 ]
```

Matrix C_{cl} Columns 1 through 7

```
-1.3958e-002  1.5649e-002 -3.3463e-003 -6.5563e-004  2.3985e-004  3.9783e+000
-1.7729e+000 -5.7604e-002  4.1844e+000  9.3539e-002 -8.5613e-001             0
```

Columns 7 through 12

```
            0             0             0             0             0             0
-5.1396e-002  6.1604e-001 -9.1911e-002  2.5094e-001  7.3985e-001 -5.5555e+003
```

Matrix D_{cl} = `[3.9787e-002`

```
                        0 ]
```

H.1.3 Subsystem 3

The state space description of the open loop augmented plant can be expressed as follows:

A_a =

```
-7.1618e+000 -1.1270e+001  7.9822e+000  7.3213e+000 -1.1943e+000             0
-2.8962e+000  1.0700e+001 -7.6788e+000 -5.5210e+000 -2.4164e+000             0
 2.6791e+000  4.1995e+001 -2.5204e+001 -2.8662e+001 -5.2030e+000             0
-8.7179e+000 -1.5730e+001  9.0191e+000  1.2163e+001 -8.4487e-001             0
-1.3090e+001 -4.7111e+001  3.1823e+001  2.8995e+001  3.6831e-001             0
 3.6262e-001 -2.2775e-001  1.1240e-001 -1.4668e-001  5.7533e-002 -1.0000e-002
```

B_1 =

```
[ 0
  0
  0
  0
  0
  1 ]
```

B_2 =

```
[ 5.9636e-001
  1.1913e+000
 -4.3904e-001
  1.9795e+000
  4.2567e+000
            0 ]
```

C_1 =

```
[ 3.6262e-003 -2.2775e-003  1.1240e-003 -1.4668e-003  5.7533e-004  9.9990e-001]
 -4.8339e-001 -2.2881e+000  1.3625e+000  1.6133e+000  1.5338e-001            0 ]
```

C_2 =

```
[ 3.6262e-001 -2.2775e-001  1.1240e-001 -1.4668e-001  5.7533e-002            0 ]
```

D_{11} = [1.0000e-002

```
                  0 ]
```

D_{12} =[0

```
      1.1509e-001 ]
```

D_{21} = [1]

D_{22} = [0]

The eigenvalues of the augmented system are:

```
-1.0000e-002
-3.9878e+000+ 1.0290e+001i
-3.9878e+000- 1.0290e+001i
-3.1136e-001+ 4.9569e-001i
-3.1136e-001- 4.9569e-001i
-5.3584e-001
```

The transmission zeros of the augmented system are:

```
-1.9256e+001+ 7.1927e+000i
-1.9256e+001- 7.1927e+000i
-4.6826e-001+ 3.4433e-001i
-4.6826e-001- 3.4433e-001i
-1.0000e-002
```

Optimal H_∞ Controller for Subsystem 3

The controller for subsystem 3 has the following state space description:

Matrix A_c Columns 1 through 6

```
 -5.9873e+000  2.8878e+000 -6.4513e+000 -5.8701e+000 -6.8713e+000  1.1249e+004
  1.4657e+000 -1.7597e+000  2.3429e+000 -4.6684e+000  2.2479e+000 -2.4312e+004
 -1.9201e-001  1.2698e+000 -3.6344e+000  6.7996e+000  2.2701e+000  2.7843e+004
  1.3106e+000  3.0286e-001 -3.0745e+000 -2.8044e+000  8.3704e-002 -2.0838e+004
 -1.0025e-001 -1.2643e-002 -7.2313e-002 -7.9398e-002 -5.8750e-001 -1.8652e+002
  3.0537e+003  7.5667e+002 -6.4349e+003 -7.1126e+002  2.0762e+003 -2.4629e+007
```

Matrix B_c

```
[ 2.7307e-003
 -5.1125e-004
 -4.5161e-002
 -2.8065e-001
 -6.9163e-001
  3.0334e+004 ]
```

Matrix C_c

```
[-1.8404e+000  7.0631e-001 -9.4227e-001 -1.0615e+000 -2.9368e+000  7.0468e+003]
```

Matrix D_c

```
 [ 0 ]
```

The eigenvalues of the controller of subsystem 3 are:

```
[  -2.4629e+007
   -9.9338e+000+ 3.9937e+000i
   -9.9338e+000- 3.9937e+000i
   -1.0000e-002
   -4.6827e-001+ 3.4433e-001i
   -4.6827e-001- 3.4433e-001i]
```

The transmission zeros of the controller of subsystem 3 are:

```
[ -3.9878e+000+ 1.0290e+001i
  -3.9878e+000- 1.0290e+001i
  -3.1136e-001+ 4.9569e-001i
  -3.1136e-001- 4.9569e-001i
  -5.3584e-001]
```

The closed loop of subsystem 3 with the optimal H_∞ controller has the following state space description:

Matrix A_{cl} Columns 1 through 6

```
-7.1618e+000 -1.1270e+001  7.9822e+000  7.3213e+000 -1.1943e+000            0
-2.8962e+000  1.0700e+001 -7.6788e+000 -5.5210e+000 -2.4164e+000            0
 2.6791e+000  4.1995e+001 -2.5204e+001 -2.8662e+001 -5.2030e+000            0
-8.7179e+000 -1.5730e+001  9.0191e+000  1.2163e+001 -8.4487e-001            0
-1.3090e+001 -4.7111e+001  3.1823e+001  2.8995e+001  3.6831e-001            0
 3.6262e-001 -2.2775e-001  1.1240e-001 -1.4668e-001  5.7533e-002 -1.0000e-002
 9.9022e-004 -6.2194e-004  3.0693e-004 -4.0055e-004  1.5711e-004            0
-1.8539e-004  1.1644e-004 -5.7464e-005  7.4992e-005 -2.9414e-005            0
-1.6376e-002  1.0285e-002 -5.0760e-003  6.6243e-003 -2.5982e-003            0
-1.0177e-001  6.3920e-002 -3.1545e-002  4.1167e-002 -1.6147e-002            0
-2.5080e-001  1.5752e-001 -7.7738e-002  1.0145e-001 -3.9792e-002            0
 1.1000e+004 -6.9086e+003  3.4095e+003 -4.4494e+003  1.7452e+003            0
```

Columns 7 through 12

```
-1.0975e+000  4.2122e-001 -5.6193e-001 -6.3305e-001 -1.7514e+000  4.2024e+003
-2.1925e+000  8.4144e-001 -1.1225e+000 -1.2646e+000 -3.4987e+000  8.3949e+003
 8.0800e-001 -3.1010e-001  4.1369e-001  4.6606e-001  1.2894e+000 -3.0938e+003
-3.6431e+000  1.3982e+000 -1.8652e+000 -2.1013e+000 -5.8135e+000  1.3949e+004
-7.8340e+000  3.0066e+000 -4.0110e+000 -4.5186e+000 -1.2501e+001  2.9996e+004
           0             0             0             0             0            0
-5.9873e+000  2.8878e+000 -6.4513e+000 -5.8701e+000 -6.8713e+000  1.1249e+004
 1.4657e+000 -1.7597e+000  2.3429e+000 -4.6684e+000  2.2479e+000 -2.4312e+004
-1.9201e-001  1.2698e+000 -3.6344e+000  6.7996e+000  2.2701e+000  2.7843e+004
 1.3106e+000  3.0286e-001 -3.0745e+000 -2.8044e+000  8.3704e-002 -2.0838e+004
-1.0025e-001 -1.2643e-002 -7.2313e-002 -7.9398e-002 -5.8750e-001 -1.8652e+002
 3.0537e+003  7.5667e+002 -6.4349e+003 -7.1126e+002  2.0762e+003 -2.4629e+007
```

Matrix B_{cl}

```
[           0
            0
            0
            0
            0
  1.0000e+000
  2.7307e-003
 -5.1125e-004
 -4.5161e-002
 -2.8065e-001
 -6.9163e-001
  3.0334e+004]
```

Matrix C_{cl}

Columns 1 through 6

```
  1.7423e-002 -1.0943e-002  5.4006e-003 -7.0479e-003  2.7644e-003  4.8044e+000
 -4.8339e-001 -2.2881e+000  1.3625e+000  1.6133e+000  1.5338e-001            0
```

Columns 7 through 12

```
            0            0            0            0            0            0
 -2.1180e-001  8.1286e-002 -1.0844e-001 -1.2217e-001 -3.3798e-001  8.1099e+002
```

Matrix D_{cl}

```
[ 4.8049e-002
            0 ]
```

H.2 Suboptimal H_∞ Controllers

H.2.1 Subsystem 1

The weighting functions that were selected for subsystem 1 are illustrated in Figure H2.

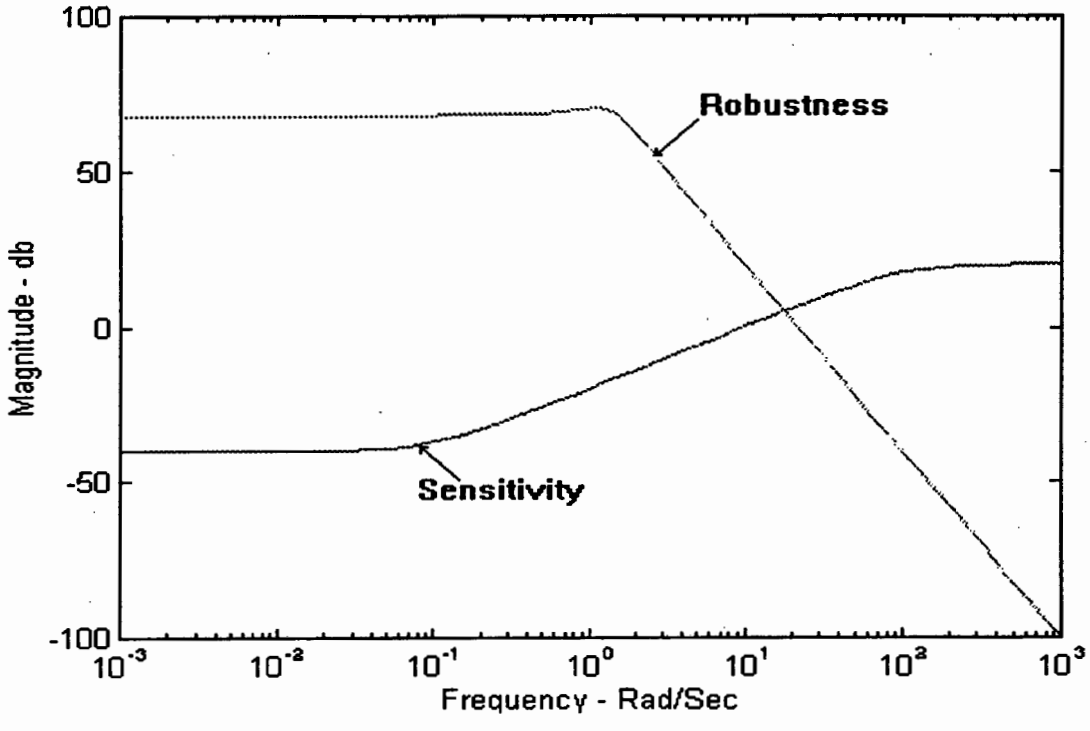

Figure H2: Weighting Functions for Subsystem 1

The weighting functions $W1$ and $W3$ can be expressed as follows:

$$W1 = \frac{as^3 + bs^2 + c}{ds^4 + es^3 + fs^2 + g}$$

$$W3 = \frac{s^3 + hs^2 + ks + m}{1000}$$

where:

$$a = 1.00 \times 10^{-3},\quad b = 1.00 \times 10^{-4},\quad c = 2.10 \times 10^{3},\quad d = 1.00 \times 10^{-1},\quad e = 1.24 \times 10^{-4},$$
$$f = 2.13,\quad g = 2.11 \times 10^{-1},\quad h = 3.0,\quad k = 4.0, m = 4$$

The state space model of the open loop augmented plant is as follows:

A_a =

Columns 1 through 6

```
  9.4836e-001 -1.7417e+000 -3.7456e+001 -2.0937e+000  8.5774e+000             0
  8.9470e-001 -3.8829e+000 -7.0649e+001 -1.2834e+001  1.2137e+001             0
 -6.7024e-001  1.0358e+000 -2.7938e+000 -1.2784e+000 -1.5285e+000             0
  1.6710e-001 -4.1513e-002  1.3724e+001  2.0618e+000 -1.1850e+000             0
 -3.1563e+000  2.5347e+000 -1.6313e+001 -8.7427e+000 -6.5625e+000             0
 -3.3962e-001  2.5091e-001  3.7215e-001  1.5524e-001  1.8335e-002 -1.2386e+000
            0             0             0             0             1.0000e+000
            0             0             0             0             0
```

Columns 7 through 8

```
            0             0
            0             0
            0             0
            0             0
            0             0
 -2.1266e+001 -2.1152e+000
            0             0
  1.0000e+000             0
```

B_1 =

```
[     0
      0
      0
      0
      0
      1
      0
      0 ]
```

B_2 =

```
[ 1.4172e+000
  2.3619e-001
  2.1506e+000
 -1.7816e+000
  9.0144e+000
            0
            0
            0 ]
```

C_1 =

Columns 1 through 6

```
         0         0         0         0         0  1.0000e-002
 2.4724e-002 -2.4614e-002 -1.0985e-001  1.5174e-002  7.7954e-002         0
```

Columns 7 through 8

```
 1.0000e-003  2.1000e+004
         0         0
```

C_2 =

Columns 1 through 6

```
-3.3962e-001  2.5091e-001  3.7215e-001  1.5524e-001  1.8335e-002         0
```

Columns 7 through 8

```
         0         0
```

D_{11} = [0
0]

D_{12} = [0]
- 6.0434e-002]

D_{21} = [1]

D_{22} = [0]

The eigenvalues and associated damping factors of the augmented plant are given in Table H1.

Eigenvalue	Damping
-1.0000e-001	1.0000e+000
-5.6057e-001+ 4.8429e+000i	1.1498e-001
-5.6057e-001- 4.8429e+000i	1.1498e-001
-5.6930e-001+ 4.5637e+000i	1.2378e-001
-5.6930e-001- 4.5637e+000i	1.2378e-001
-6.4850e-001+ 4.9346e-001i	7.9581e-001
-6.4850e-001- 4.9346e-001i	7.9581e-001
-7.8110e+000	1.0000e+000

Table H1: Eigenvalues and Damping of the Augmented Plant

The transmission zeros of the augmented plant are:

-1.0000e-001
 3.3606e+001
-5.6930e-001+ 4.5637e+000i
-5.6930e-001- 4.5637e+000i
-5.6930e-001+ 4.5637e+000i
-5.6930e-001- 4.5637e+000i
-6.1487e-001

Table H2 gives the controller eigenvalues and associated damping factors for subsystem 1.

Eigenvalue	Damping
-1.0000e-001	1.0000e+000
-6.1487e-001	1.0000e+000
-9.1866e+000+ 1.2499e+001i	5.9223e-001
-9.1866e+000 - 1.2499e+001i	5.9223e-001
-3.6233e+001	1.0000e+000
-5.0000e+002 + 1.3601e+003i	3.4503e-001
-5.0000e+002 - 1.3601e+003i	3.4503e-001

Table H2: Eigenvalues and Damping of Controller for Subsystem 1

The transmission zeros of the controller are:

-5.3347e-001+ 2.1875e+000i

-5.3347e-001- 2.1875e+000i

-6.4850e-001+ 4.9346e-001i

-6.4850e-001- 4.9346e-001i

-7.8110e+000

The closed loop eigenvalues and associated damping factors of subsystem 1 are given in Table H3.

Eigenvalue	Damping
-1.0000e-001	1.0000e+000
-6.1487e-001	1.0000e+000
-6.4850e-001+ 4.9346e-001i	7.9581e-001
-6.4850e-001- 4.9346e-001i	7.9581e-001
-1.2476e+000+ 4.6484e+000i	2.5923e-001
-1.2476e+000- 4.6484e+000i	2.5923e-001
-4.0717e+000+ 5.1636e+000i	6.1919e-001
-4.0717e+000- 5.1636e+000i	6.1919e-001
-7.5860e+000	1.0000e+000
-7.8110e+000	1.0000e+000
-3.3603e+001	1.0000e+000

Table H3: Eigenvalues and Damping of the Closed Loop for Subsystem 1

H.2.2 Subsystem 2

The weighting functions that were selected for subsystem 2 are illustrated in Figure H3.

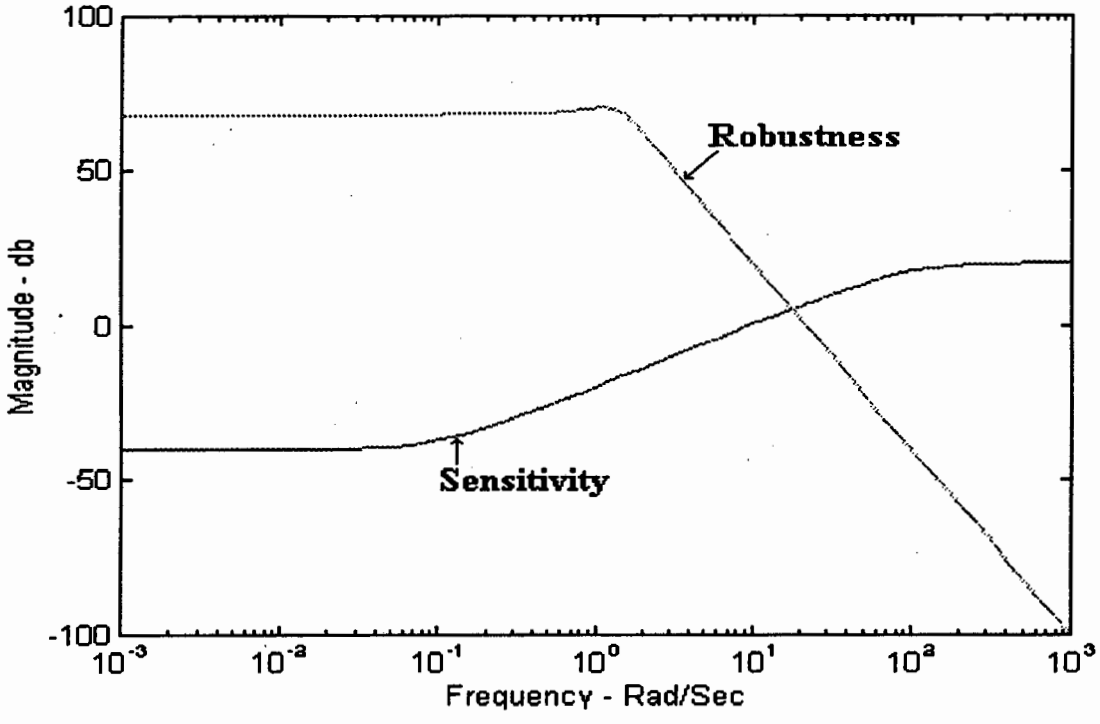

Figure H3: Weighting Functions for Subsystem 2

The weighting functions $W1$ and $W3$ can be expressed as follows:

$$W1 = \frac{0.01s + 1}{0.1s + 0.01}$$

$$W3 = \frac{s^3 + 3s^2 + 4s + 4}{10000}$$

The state space description of the augmented plant for subsystem 2 are as follows:

A_a =

```
 5.5580e+001 -9.7562e+000 -1.1174e+002  6.9574e+000  7.5810e+000             0
 4.6639e+001 -8.3517e+000 -9.0230e+001  7.5830e+000  2.8435e+000             0
 2.2804e+001 -3.8678e+000 -4.5275e+001  3.2839e+000  2.9789e+000             0
 2.6383e+000  9.1850e-001 -1.3436e+001 -4.7713e+000  2.8294e+000             0
-2.4276e+001 -2.5646e+000  6.3504e+001  4.8262e+000 -1.7133e+001             0
-3.5081e-001  3.9332e-001 -8.4105e-002 -1.6479e-002  6.0284e-003 -1.0000e-001
```

B_1 = [0
0
0
0
0
1]

C_1 =

```
[ -3.5081e-002  3.9332e-002 -8.4105e-003 -1.6479e-003  6.0284e-004  9.9900e+000
  4.3565e-002  1.4621e-002 -1.2591e-001 -1.3563e-002  4.6837e-002           0 ]
```

C_2 =

```
[-3.5081e-001 3.9332e-001 -8.4105e-002 -1.6479e-002  6.0284e-003       0 ]
```

D_{11} =

```
[ 1.0000e-001
            0 ]
```

D_{12} =

```
[           0
-1.9094e-002  ]
```

D_{21} = [1]

D_{22} = [0]

Table H4 gives the eiegenvalues and associated damping factors for the augmented plant.

Eigenvalue	Damping
-1.0000e-001	1.0000e+000
-4.7311e-001+5.1281e-001i	6.7808e-001
-4.7311e-001-5.1281e-001i	6.7808e-001
-5.1433e-001+7.7966e+000i	6.5825e-002
-5.1433e-001-7.7966e+000i	6.5825e-002
-1.7976e+001	1.0000e+000

Table H4: Eigenvalues and Damping of the Augmented Plant

The Transmission Zeros of the Augmented System

```
 4.4125e+002
-1.1858e+000+ 7.9644e+000i
-1.1858e+000- 7.9644e+000i
-5.9327e-001
-1.0000e-001
```

The eigenvalues and associated damping factors of the controller for subsystem 2 are given in Table H5.

Eigenvalue	Damping
-1.0000e-001	1.0000e+000
-5.9327e-0011.0000e+000	5.9327e-001
-1.1629e+000+7.9702e+000i	1.4438e-001
-1.1629e+000-7.9702e+000i	1.4438e-001
-4.8216e+001	1.0000e+000

Table H5: Eigenvalues and Damping of Controller for Subsystem 2

The transmission zeros of the controller are:

-1.7976e+001
-8.5760e-001+ 6.6497e+000i
-8.5760e-001- 6.6497e+000i
-4.7311e-001+ 5.1281e-001i
-4.7311e-001- 5.1281e-001i

The eigenvalues and associated damping factors of the closed loop for subsystem 2 are given in Table H6.

Eigenvalue	Damping
-1.0000e-001	1.0000e+000
-4.7311e-001+ 5.1281e-001i	6.7808e-001
-4.7311e-001- 5.1281e-001i	6.7808e-001
-5.9327e-001	1.0000e+000
-1.1846e+000+ 7.8459e+000i	1.4929e-001
-1.1846e+000- 7.8459e+000i	1.4929e-001
-1.5023e+000+ 7.9061e+000i	1.8667e-001
-1.5023e+000- 7.9061e+000i	1.8667e-001
-1.7976e+001	1.0000e+000
-2.0077e+001+ 1.6660e+001i	7.6955e-001
-2.0077e+001- 1.6660e+001i	7.6955e-001

Table H6: Eigenvalues and Damping of the Closed Loop for Subsystem 2

H.2.3 Subsystem 3

The weighting functions that were selected for subsystem 3 are illustrated in Figure H4.

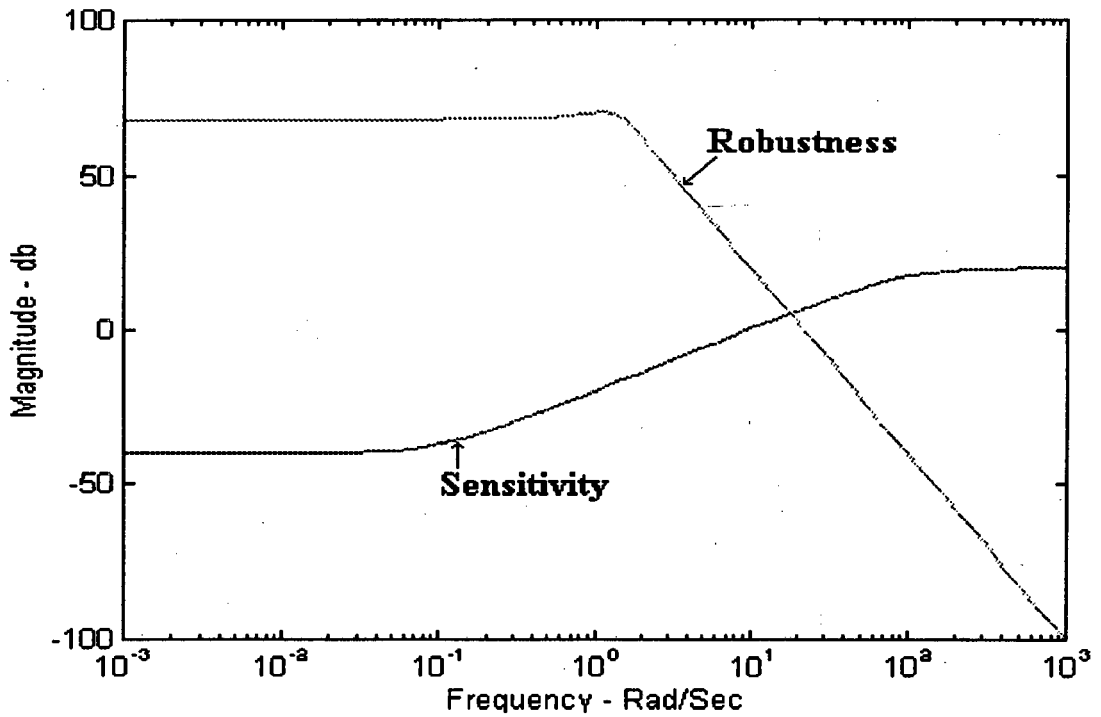

Figure H4: Weighting Functions for Subsystem 3

The weighting functions $W1$ and $W3$ can be expressed as follows:

$$W1 = \frac{0.01s + 1}{0.1s + 0.01}$$

$$W3 = \frac{s^3 + 3s^2 + 4s + 4}{10000}$$

A_a =

```
 Columns 1 through 6
-2.3350e+000 -1.2952e+002 -3.5289e+002 -2.0568e+003  8.4104e+003  1.1399e+004
 8.5628e-001 -8.0183e+000 -2.1923e+001 -1.2773e+002  5.2222e+002  7.0776e+002
-1.3366e-013  2.7915e+000  5.1371e+000  3.0502e+001 -1.2591e+002 -1.7125e+002
 1.1224e-013 -6.3093e-013  1.4749e+000  6.0984e+000 -2.7661e+001 -3.8194e+001
-7.6978e-018 -7.4322e-017 -9.4309e-016  4.9585e+000 -1.9587e+001 -2.7283e+001
-2.7119e-019  4.2151e-018  2.5257e-017 -2.2518e-017  7.8643e-001  6.8803e-001
 1.8971e-012  4.3581e-012  6.1331e-011  1.4147e-010  1.1575e-010 -8.1123e+005
```

```
  Column 7
            0
            0
            0
            0
            0
            0
 -1.0000e-001
```

B_1 =

```
[     0
      0
      0
      0
      0
      0
      1 ]
```

B_2 =

```
[-7.9144e-003
 -4.9142e-004
  1.1871e-004
  2.6295e-005
  1.8707e-005
 -2.5735e-008
            0 ]
```

C_1 =

```
  Columns 1 through 6
  1.8971e-013   4.3581e-013   6.1331e-012   1.4147e-011   1.1575e-011 -8.1123e+004
  3.5496e-011 -2.0055e-010   4.6657e+002 -3.1003e+003   1.0166e+004   1.5084e+004

  Column 7
  9.9900e+000
            0
```

C_2 =

```
  Columns 1 through 6
1.8971e-012   4.3581e-012   6.1331e-011   1.4147e-010   1.1575e-010 -8.1123e+005   0
```

D_{11} = [1.0000e-001

```
            0      ]
```

D_{12} = [0
-1.0626e-002]

D_{21} = [1]

D_{22} = [0]

Table H7 shows the eigenvalues and damping factors of the controller for subsystem 3.

Eigenvalue	Damping
-1.0000e-001	1.0000e+000
-9.5522e-001	1.0000e+000
-1.3999e+000+1.1375e+001i	1.2214e-001
-1.3999e+000-1.1375e+001i	1.2214e-001
-2.3239e+000	1.0000e+000
-5.2313e+001	1.0000e+000

Table H7: Eigenvalues and Damping of Controller for Subsystem 3

The transmission zeros of the controller are:

-3.8693e-001+ 1.0529e+001i
-3.8693e-001- 1.0529e+001i
-5.6429e+000
-3.8945e-001+ 4.9555e-001i
-3.8945e-001- 4.9555e-001i
-1.2814e+001

Table H8 gives the eigenvalues and associated damping factors of the closed loop for subsystem 3.

Eigenvalues	Damping
-1.0000e-001	1.0000e+000
-3.8945e-001+ 4.9555e-001i	6.1791e-001
-3.8945e-001- 4.9555e-001i	6.1791e-001
-6.2171e-001+ 1.1146e+001i	5.5693e-002
-6.2171e-001- 1.1146e+001i	5.5693e-002
-9.5521e-001	1.0000e+000
-1.4210e+000+ 1.1448e+001i	1.2318e-001
-1.4210e+000- 1.1448e+001i	1.2318e-001
-2.3241e+000	1.0000e+000
-5.6429e+000	1.0000e+000
-1.2814e+001	1.0000e+000
-2.3989e+001+ 1.9539e+001i	7.7535e-001
-2.3989e+001- 1.9539e+001i	7.7535e-001

Table H8: Eigenvalues and Damping of the Closed Loop for Subsystem 3

Appendix I

State Space Formulation of the SMIB System

In this section we present the state space matrices of the SMIB system used in Section 5.2.1. The state space description can be expressed as follows:

Consider the following state space description of a power system:

$$\begin{aligned} \dot{x}(t) &= Ax(t) + B_1 w(t) + B_2 u(t) \\ \xi(t) &= C_1 x(t) + D_{11} w(t) + D_{12} u(t) \\ y(t) &= C_2 x(t) + D_{21} w(t) + D_{22} u(t) \end{aligned} \tag{I.1}$$

where:

$x(t) \in R^n$ is the state vector

$u(t) \in R^{m_2}$ is the input vector

$y(t) \in R^{p_2}$ is the output vector

$w(t) \in R^{m_1}$ is the disturbance input vector

$\xi(t) \in R^{p_1}$ is the performance output vector

n is the number of states of the plant

m_1 is the number of control inputs

m_2 is the number of disturbance inputs

p_1 is the number of performance outputs

p_2 is the number of sensor outputs

$A, B_1, B_2, C_1, C_2, D_{11}, D_{12}, D_{21}$ and D_{22} are constant matrices of appropriate dimensions.

The matrices $A, B_1, B_2, C_1, C_2, D_{11}, D_{12}, D_{21}$ and D_{22} are given by the following:

$A =$

Columns 1 through 6

```
-3.6449e+000  6.5065e-003  3.1193e+000 -1.1680e-001            0  8.3733e-002
 1.9651e-001 -1.2531e+000 -6.5326e-001  1.4284e-001            0 -1.9934e-002
 1.9927e+001  1.8717e-002 -2.2343e+001 -3.5182e-001            0 -1.4401e+000
-4.2633e-001  7.8217e+000  1.3990e+000 -1.4900e+001            0  4.3474e+000
 4.5777e-002 -3.2881e-003 -1.5077e-001  5.9560e-002 -7.7400e-002 -1.1276e-001
           0            0            0            0  3.7699e+002            0
 2.2924e-002  1.4013e-003 -7.5338e-002 -2.5395e-002            0  7.2423e-003
 5.0943e+001  3.1140e+000 -1.6742e+002 -5.6434e+001            0  1.6094e+001
 2.5471e-001  1.5570e-002 -8.3708e-001 -2.8216e-001            0  8.0470e-002
           0            0            0            0            0            0
 5.8558e-001 -4.2326e-002 -1.9287e+000  7.6187e-001            0 -1.4425e+000
           0            0            0            0            0            0
-2.5471e-001 -1.5570e-002  8.3708e-001  2.8216e-001            0 -8.0470e-002
           0            0            0            0            0            0
-5.8558e-001  4.2326e-002  1.9287e+000 -7.6187e-001            0  1.4425e+000
           0            0            0            0            0            0
```

Columns 7 through 12

```
           0  1.8553e-001            0            0            0            0
           0            0            0            0            0            0
           0            0            0            0            0            0
           0            0            0            0            0            0
           0            0            0            0            0            0
           0            0            0            0            0            0
-1.0000e-001            0            0            0            0            0
 2.0000e+003 -2.0000e+001            0            0            0            0
           0            0 -4.3985e-001 -4.8367e-002            0            0
           0            0  1.0000e+000            0            0            0
           0            0            0            0 -4.3985e-001 -4.8367e-002
           0            0            0            0  1.0000e+000            0
           0            0            0            0            0            0
           0            0            0            0            0            0
           0            0            0            0            0            0
           0            0            0            0            0            0
```

Columns 13 through 16

0	0	0	0
0	0	0	0
0	0	0	0
0	0	0	0
0	0	0	0
0	0	0	0
0	0	0	0
0	0	0	0
0	0	0	0
0	0	0	0
0	0	0	0
0	0	0	0
-4.5351e+002	-5.1419e+004	0	0
1.0000e+000	0	0	0
0	0	-4.5351e+002	-5.1419e+004
0	0	1.0000e+000	0

$B_1 =$

0	0
0	0
0	0
0	0
0	0
0	0
0	0
0	0
1	0
0	0
0	1
0	0
0	0
0	0
0	0
0	0

$B_2 =$

```
                0                0
                0                0
                0                0
                0                0
                0   7.8174e-002
                0                0
   9.0000e-002                   0
   2.0000e+002                   0
                0                0
                0                0
                0                0
                0                0
                0                0
                0                0
                0                0
                0                0
```

$C_1 =$

Columns 1 through 6

```
   2.5546e-003    1.5616e-004   -8.3954e-003   -2.8299e-003                   0    8.0707e-004
   5.8730e-003   -4.2450e-004   -1.9344e-002    7.6411e-003                   0   -1.4467e-002
                0              0              0              0                0              0
                0              0              0              0                0              0
  -2.5471e+001   -1.5570e+000    8.3708e+001    2.8216e+001                   0   -8.0470e+000
  -5.8558e+001    4.2326e+000    1.9287e+002   -7.6187e+001                   0    1.4425e+002
```

Columns 7 through 12

```
                0              0    1.3886e+000    4.8367e+001                0              0
                0              0              0              0    1.3886e+000    4.8367e+001
                0              0              0              0                0              0
                0              0              0              0                0              0
                0              0              0              0                0              0
                0              0              0              0                0              0
```

Columns 13 through 16

```
                0              0              0              0
                0              0              0              0
                0              0              0              0
                0              0              0              0
  -4.4898e+004   -5.1414e+006                 0              0
                0              0   -4.4898e+004   -5.1414e+006
```

C_2 =

Columns 1 through 6

```
 2.5471e-001  1.5570e-002 -8.3708e-001 -2.8216e-001            0  8.0470e-002
 5.8558e-001 -4.2326e-002 -1.9287e+000  7.6187e-001            0 -1.4425e+000
```

Columns 7 through 12

```
     0     0     0     0     0     0
     0     0     0     0     0     0
```

Columns 13 through 16

```
          0           0           0           0
          0           0           0           0
```

D_{11} =

```
[ 1.0029e-002           0
          0  1.0029e-002
          0           0
          0           0
          0           0
          0           0   ]
```

D_{12} =

```
[         0           0
          0           0
  1.0000e-003         0
          0  1.0000e-003
          0           0
          0           0   ]
```

D_{21} =

```
[    1     0
     0     1   ]
```

D_{22} =

```
[    0     0
     0     0   ]
```